GAUGE AND HIGGS BOSONS

γ

$I(J^{PC}) = 0,1(1^{--})$

γ MASS

For a review of the photon mass, see BYRNE 77.

VALUE (eV)	CL%	DOCUMENT ID		TECN	COMMENT
$< 6 \times 10^{-17}$		[1] RYUTOV	97		MHD of solar wind
• • • We do not use the following data for averages, fits, limits, etc. • • •					
$< 7 \times 10^{-19}$		[2] LUO	03		Modulation torsion balance
$< 1 \times 10^{-17}$		[3] LAKES	98		Torque on toroid balance
$< 9 \times 10^{-16}$	90	[4] FISCHBACH	94		Earth magnetic field
$<(4.73\pm0.45) \times 10^{-12}$		[5] CHERNIKOV	92	SQID	Ampere-law null test
$<(9.0 \pm 8.1) \times 10^{-10}$		[6] RYAN	85		Coulomb-law null test
$< 3 \times 10^{-27}$		[7] CHIBISOV	76		Galactic magnetic field
$< 6 \times 10^{-16}$	99.7	DAVIS	75		Jupiter magnetic field
$< 7.3 \times 10^{-16}$		HOLLWEG	74		Alfven waves
$< 6 \times 10^{-17}$		[8] FRANKEN	71		Low freq. res. cir.
$< 1 \times 10^{-14}$		WILLIAMS	71	CNTR	Tests Gauss law
$< 2.3 \times 10^{-15}$		GOLDHABER	68		Satellite data
$< 6 \times 10^{-15}$		[8] PATEL	65		Satellite data
$< 6 \times 10^{-15}$		GINTSBURG	64		Satellite data

[1] RYUTOV 97 uses a magnetohydrodynamics argument concerning survival of the Sun's field to the radius of the Earth's orbit. "To reconcile observations to theory, one has to reduce [the photon mass] by approximately an order of magnitude compared with" DAVIS 75.

[2] LUO 03 determine a limit on $\mu^2 \boldsymbol{A} < 1.1 \times 10^{-11}$ T m/m^2 (with μ^{-1}=characteristic length for photon mass; $\boldsymbol{A}$=ambient vector potential) — similar to the LAKES 98 technique. Unlike LAKES 98 who used static, the authors used dynamic torsion balance. Assuming $\boldsymbol{A}$ to be 10^{12} T m, they obtain $\mu < 1.2 \times 10^{-51}$ g, equivalent to 6.7×10^{-19} eV. The rotating modified Cavendish balance removes dependence on the direction of $\boldsymbol{A}$. GOLDHABER 03 argue that because plasma current effects are neglected, the LUO 03 limit does not provide the best available limit on $\mu^2 \boldsymbol{A}$ nor a reliable limit at all on μ. The reason is that the $\boldsymbol{A}$ associated with cluster magnetic fields could become arbitrarily small in plasma voids, whose existence would be compatible with present knowledge. LUO 03B reply that fields of distant clusters are not accurately mapped, but assert that a zero $\boldsymbol{A}$ is unlikely given what we know about the magnetic field in our galaxy.

[3] LAKES 98 reports limits on torque on a toroid Cavendish balance, obtaining a limit on $\mu^2 \boldsymbol{A} < 2 \times 10^{-9}$ Tm/m^2 via the Maxwell-Proca equations, where μ^{-1} is the characteristic length associated with the photon mass and $\boldsymbol{A}$ is the ambient vector potential in the Lorentz gauge. Assuming $\boldsymbol{A} \approx 1 \times 10^{12}$ Tm due to cluster fields he obtains $\mu^{-1} > 2 \times 10^{10}$ m, corresponding to $\mu < 1 \times 10^{-17}$ eV. A more conservative limit, using $\boldsymbol{A} \approx (1\ \mu\text{G}) \times (600\ \text{pc})$ based on the galactic field, is $\mu^{-1} > 1 \times 10^{9}$ m or $\mu < 2 \times 10^{-16}$ eV.

[4] FISCHBACH 94 report $< 8 \times 10^{-16}$ with unknown CL. We report Bayesian CL used elsewhere in these Listings and described in the Statistics section.

[5] CHERNIKOV 92 measures the photon mass at 1.24 K, following a theoretical suggestion that electromagnetic gauge invariance might break down at some low critical temperature. See the erratum for a correction, included here, to the published result.

[6] RYAN 85 measures the photon mass at 1.36 K (see the footnote to CHERNIKOV 92).

[7] CHIBISOV 76 depends in critical way on assumptions such as applicability of virial theorem. Some of the arguments given only in unpublished references.

[8] See criticism questioning the validity of these results in GOLDHABER 71, PARK 71 and KROLL 71. See also review GOLDHABER 71B.

γ CHARGE

VALUE (e)	DOCUMENT ID		TECN	COMMENT
$<5 \times 10^{-30}$	[9] RAFFELT	94	TOF	Pulsar $f_1 - f_2$
• • • We do not use the following data for averages, fits, limits, etc. • • •				
$<8.5 \times 10^{-17}$	[10] SEMERTZIDIS	03		Laser light deflection in B-field
$<2 \times 10^{-28}$	[11] COCCONI	92		VLBA radio telescope resolution
$<2 \times 10^{-32}$	COCCONI	88	TOF	Pulsar $f_1 - f_2$ TOF

[9] RAFFELT 94 notes that COCCONI 88 neglects the fact that the time delay due to dispersion by free electrons in the interstellar medium has the same photon energy dependence as that due to bending of a charged photon in the magnetic field. His limit is based on the assumption that the entire observed dispersion is due to photon charge. It is a factor of 200 less stringent than the COCCONI 88 limit.

[10] SEMERTZIDIS 03 reports the first laboratory limit on the photon charge in the last 30 years. Straightforward improvements in the apparatus could attain a sensitivity of 10^{-20} e.

[11] See COCCONI 92 for less stringent limits in other frequency ranges. Also see RAFFELT 94 note.

γ REFERENCES

GOLDHABER	03	PRL 91 149101	A.S. Goldhaber, M.M. Nieto	
LUO	03	PRL 90 081801	J. Luo *et al.*	
LUO	03B	PRL 91 149102	J. Luo *et al.*	
SEMERTZIDIS	03	PR D67 017701	Y.K. Semertzidis, G.T. Danby, D.M. Lazarus	
LAKES	98	PRL 80 1826	R. Lakes	(WISC)
RYUTOV	97	PPCF 39 A73	D.D. Ryutov	(LLNL)
FISCHBACH	94	PRL 73 514	E. Fischbach *et al.*	(PURD, JHU+)
RAFFELT	94	PR D50 7729	G. Raffelt	(MPIM)
CHERNIKOV	92	PRL 68 3383	M.A. Chernikov *et al.*	(ETH)
Also	92B	PRL 69 2999 (erratum)	M.A. Chernikov *et al.*	(ETH)
COCCONI	92	AJP 60 750	G. Cocconi	(CERN)
COCCONI	88	PL B206 705	G. Cocconi	(CERN)
RYAN	85	PR D32 802	J.J. Ryan, F. Accetta, R.H. Austin	(PRIN)
BYRNE	77	Ast.Sp.Sci. 46 115	J. Byrne	(LOIC)
CHIBISOV	76	SPU 19 624	G.V. Chibisov	(LEBD)
DAVIS	75	PRL 35 1402	L. Davis, A.S. Goldhaber, M.M. Nieto	(CIT, STON+)
HOLLWEG	74	PRL 32 961	J.V. Hollweg	(NCAR)
FRANKEN	71	PRL 26 115	P.A. Franken, G.W. Ampulski	(MICH)
GOLDHABER	71	PRL 26 1390	A.S. Goldhaber, M.M. Nieto	(STON, BOHR, UCSB)
GOLDHABER	71B	RMP 43 277	A.S. Goldhaber, M.M. Nieto	(STON, BOHR, UCSB)
KROLL	71	PRL 26 1395	N.M. Kroll	(SLAC)
PARK	71	PRL 26 1393	D. Park, E.R. Williams	(WILC)
WILLIAMS	71	PRL 26 721	E.R. Williams, J.E. Faller, H.A. Hill	(WESL)
GOLDHABER	68	PRL 21 567	A.S. Goldhaber, M.M. Nieto	(STON)
PATEL	65	PL 14 105	V.L. Patel	(DUKE)
GINTSBURG	64	Sov. Astr. AJ7 536	M.A. Gintsburg	(ASCI)

g or gluon

$I(J^P) = 0(1^-)$

SU(3) color octet

Mass $m = 0$. Theoretical value. A mass as large as a few MeV may not be precluded, see YNDURAIN 95.

VALUE	DOCUMENT ID		TECN	COMMENT
• • • We do not use the following data for averages, fits, limits, etc. • • •				
	ABREU	92E	DLPH	Spin 1, not 0
	ALEXANDER	91H	OPAL	Spin 1, not 0
	BEHREND	82D	CELL	Spin 1, not 0
	BERGER	80D	PLUT	Spin 1, not 0
	BRANDELIK	80C	TASS	Spin 1, not 0

gluon REFERENCES

YNDURAIN	95	PL B345 524	F.J. Yndurain	(MADU)
ABREU	92E	PL B274 498	P. Abreu *et al.*	(DELPHI Collab.)
ALEXANDER	91H	ZPHY C52 543	G. Alexander *et al.*	(OPAL Collab.)
BEHREND	82D	PL B110 329	H.J. Behrend *et al.*	(CELLO Collab.)
BERGER	80D	PL B97 459	C. Berger *et al.*	(PLUTO Collab.)
BRANDELIK	80C	PL B97 453	R. Brandelik *et al.*	(TASSO Collab.)

graviton

$J = 2$

OMITTED FROM SUMMARY TABLE

graviton MASS

All of the following limits are obtained assuming Yukawa potential in weak field limit. VANDAM 70 argue that a massive field cannot approach general relativity in the zero-mass limit; however, see GOLDHABER 74 and references therein. h_0 is the Hubble constant in units of 100 km s^{-1} Mpc^{-1}.

VALUE (eV)	DOCUMENT ID		COMMENT
• • • We do not use the following data for averages, fits, limits, etc. • • •			
$<7.6 \times 10^{-20}$	[1] FINN	02	Binary Pulsars
	[2] DAMOUR	91	Binary pulsar PSR 1913+16
$< 2 \times 10^{-29}\ h_0^{-1}$	GOLDHABER	74	Rich clusters
$<7 \times 10^{-28}$	HARE	73	Galaxy
$<8 \times 10^{4}$	HARE	73	2γ decay

[1] FINN 02 analyze the orbital decay rates of PSR B1913+16 and PSR B1534+12 with a possible graviton mass as a parameter. The combined frequentist mass limit is at 90%CL.

[2] DAMOUR 91 is an analysis of the orbital period change in binary pulsar PSR 1913+16, and confirms the general relativity prediction to 0.8%. "The theoretical importance of the [rate of orbital period decay] measurement has long been recognized as a direct confirmation that the gravitational interaction propagates with velocity c (which is the immediate cause of the appearance of a damping force in the binary pulsar system) and thereby as a test of the existence of gravitational radiation and of its quadrupolar nature." TAYLOR 93 adds that orbital parameter studies now agree with general relativity to 0.5%, and set limits on the level of scalar contribution in the context of a family of tensor [spin 2]-biscalar theories.

graviton REFERENCES

FINN	02	PR D65 044022	L.S. Finn, P.J. Sutton	
TAYLOR	93	NAT 355 132	J.N. Taylor *et al.*	(PRIN, ARCBO, BURE+) J
DAMOUR	91	APJ 366 501	T. Damour, J.H. Taylor	(BURE, MEUD, PRIN)
GOLDHABER	74	PR D9 1119	A.S. Goldhaber, M.M. Nieto	(LANL, STON)
HARE	73	CJP 51 431	M.G. Hare	(SASK)
VANDAM	70	NP B22 397	H. van Dam, M. Veltman	(UTRE)

W $J = 1$

THE MASS OF THE W BOSON

Revised November 2003 by C. Caso (University of Genova) and A. Gurtu (Tata Institute).

Till 1995 the production and study of the W boson was the exclusive domain of the $\overline{p}p$ colliders at CERN and FNAL. W production in these hadron colliders is tagged by a high p_T lepton from W decay. Owing to unknown parton–parton effective energy and missing energy in the longitudinal direction, the experiments reconstruct only the transverse mass of the W and derive the W mass from comparing the transverse mass distribution with Monte Carlo predictions as a function of M_W.

Beginning 1996 the energy of LEP increased to above 161 GeV, the threshold for W–pair production. A precise knowledge of the e^+e^- center-of-mass energy enables one to reconstruct the W mass even if one of them decays leptonically. At LEP two methods have been used to obtain the W mass. In the first method the measured W–pair production cross sections, $\sigma(e^+e^- \rightarrow W^+W^-)$, have been used to determine the W mass using the predicted dependence of this cross section on M_W (see Fig. 1). At 161 GeV, which is just above the W–pair production threshold, this dependence is a much more sensitive function of the W mass than at the higher energies (172 to 208 GeV) at which LEP has run during 1996–2000. In the second method, which is used at the higher energies, the W mass has been determined by directly reconstructing the W from its decay products.

Each LEP experiment has combined their own mass values properly taking into account the common systematic errors. In order to compute the LEP average W mass each experiment has provided its measured W mass for the $qqqq$ and $qq\ell\nu$ channels at each center-of-mass energy along with a detailed break-up of errors (statistical and uncorrelated, partially correlated and fully correlated systematics [1]). These have been properly combined to obtain a *preliminary* LEP W mass = 80.412±0.042 GeV [2]. Errors due uncertainties in LEP energy (17 MeV) and possible effect of color reconnection (CR) and Bose–Einstein (BE) correlations between quarks from different W's are included. The mass difference between $qqqq$ and $qq\ell\nu$ final states (due to possible CR and BE effects) is $+22 \pm 43$ MeV.

The two Tevatron experiments have also carried out the exercise of identifying common systematic errors and averaging with CERN UA2 data obtain an average W mass [2]= 80.454±0.059 GeV.

Combining the above W mass values from LEP and hadron colliders, which are based on all published and unpublished results, and assuming no common systematics between them, yields an average W mass of 80.426 ± 0.034 GeV.

Finally a fit to this directly determined W mass together with measurements on the ratio of W to Z mass (M_W/M_Z) and on their mass difference ($M_Z - M_W$) yields a world average W-boson mass of 80.425 ± 0.033 GeV.

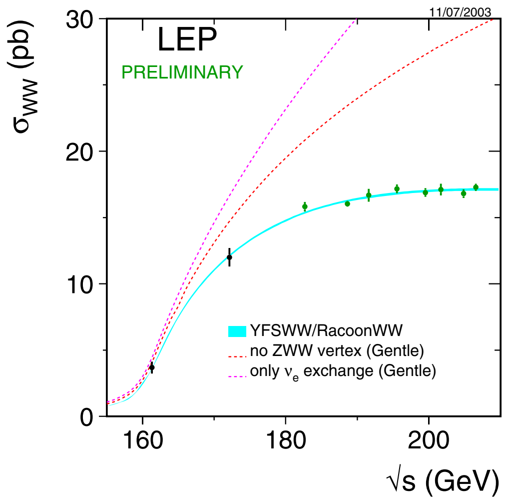

Figure 1: The W–pair cross section as a function of the center–of–mass energy. The data points are the LEP averages. The solid lines are predictions from different models of WW production. For comparison the figure contains also the cross section if the ZWW coupling did not exist (dashed line), or if only the t–channel ν_e exchange diagram existed (dotted-dashed line). (Figure from `http://lepewwg.web.cern.ch/LEPEWWG/lepww/4f/Summer03/wwxsec_nocouplings_2003.eps`)
See full-color version on color pages at end of book.

The Standard Model prediction from the electroweak fit, using Z-pole data plus $m_{\rm top}$ measurement, gives a W–boson mass of 80.378 ± 0.023 GeV [2].

OUR FIT in the listing below is obtained by combining only published LEP and p–$\overline{p}$ Collider results using the same procedure as above.

References

1. The LEP Collaborations: ALEPH, DELPHI, L3, OPAL, the LEP Electroweak Working Group, and the SLD Heavy Flavour Group, CERN-EP-2002-091, `hep-ex/0212036` (17 December 2002).
2. P. Wells, "Experimental Tests of the Standard Model," Int. Europhysics Conference on High-Energy Physics (Aachen, Germany, 17–23 July 2003).

W MASS

To obtain the world average, common systematics between experiments are properly taken into account. The procedure for averaging the LEP data is given in the note LEPEWWG/MASS/2002-01 (March 11, 2002), accessible at http://lepewwg.web.cern.ch/LEPEWWG/lepww/mw/pdg_2002/. The LEP average W mass based on published results is 80.400 ± 0.056 GeV. The combined $p\overline{p}$ collider data yields an average W mass of 80.454 ± 0.059 GeV (KOTWAL 02).

OUR FIT uses these average LEP and $p\overline{p}$ collider W mass values together with the Z mass, the W to Z mass ratio, and mass difference measurements.

VALUE (GeV)	*EVTS*	*DOCUMENT ID*	*TECN*	*COMMENT*
80.425± 0.038 OUR FIT				
80.41 ± 0.41 ±0.13	1101	[1] ABBIENDI 03C	OPAL	E^{ee}_{cm}= 183–207 GeV
80.483± 0.084	49247	[2] ABAZOV 02D	D0	$E^{p\overline{p}}_{cm}$= 1.8 TeV
80.432± 0.066±0.045	2789	[3] ABBIENDI 01F	OPAL	E^{ee}_{cm}= 161+172+183 +189 GeV
80.359± 0.074±0.049	3077	[4] ABREU 01K	DLPH	E^{ee}_{cm}= 161+172+183 +189 GeV
80.433± 0.079	53841	[5] AFFOLDER 01E	CDF	$E^{p\overline{p}}_{cm}$= 1.8 TeV
80.418± 0.061±0.047	2977	[6] BARATE 00T	ALEP	E^{ee}_{cm}= 161+172+183 +189 GeV
80.61 ± 0.15	801	[7] ACCIARRI 99	L3	E^{ee}_{cm}= 161+172+ 183 GeV
• • • We do not use the following data for averages, fits, limits, etc. • • •				
80.3 ± 2.1 ± 1.2 ± 1.0	645	[8] CHEKANOV 02C	ZEUS	$e^- p \to \nu_e X$, $\sqrt{s}$= 318 GeV
79.9 ± 2.2 ±2.3	700	[9] ADLOFF 01A	H1	$e^- p \to \nu_e X$, $\sqrt{s} \approx$ 320 GeV
80.482± 0.091	45394	[10] ABBOTT 00	D0	Repl. by ABAZOV 02D
80.9 ± 3.7 ±3.7	700	[11] ADLOFF 00B	H1	$e^+ p \to \overline{\nu}_e X$, $\sqrt{s} \approx$ 300 GeV
$81.4^{+2.7}_{-2.6} \pm 2.0^{+3.3}_{-3.0}$	1086	[12] BREITWEG 00D	ZEUS	$e^+ p \to \overline{\nu}_e X$, $\sqrt{s} \approx$ 300 GeV
80.38 ± 0.12 ±0.05	701	[13] ABBIENDI 99C	OPAL	Repl. by ABBIENDI 01F
80.270± 0.137±0.048	809	[14] ABREU 99T	DLPH	Repl. by ABREU 01K
80.423± 0.112±0.054	812	[15] BARATE 99	ALEP	Repl. by BARATE 00T
$80.80 ^{+0.48}_{-0.42} \pm 0.03$	20	[16] ACCIARRI 97	L3	Repl. by ACCIARRI 99
$80.5 ^{+1.4}_{-2.4} \pm 0.3$	94	[17] ACCIARRI 97M	L3	Repl. by ACCIARRI 99
$80.71 ^{+0.34}_{-0.35} \pm 0.09$	101	[18] ACCIARRI 97S	L3	Repl. by ACCIARRI 99
80.41 ± 0.18	8986	[19] ABE 95P	CDF	Repl. by AF-FOLDER 01E
80.84 ± 0.22 ±0.83	2065	[20] ALITTI 92B	UA2	See W/Z ratio below
80.79 ± 0.31 ±0.84		[21] ALITTI 90B	UA2	$E^{p\overline{p}}_{cm}$= 546,630 GeV
80.0 ± 3.3 ±2.4	22	[22] ABE 89I	CDF	$E^{p\overline{p}}_{cm}$= 1.8 TeV
82.7 ± 1.0 ±2.7	149	[23] ALBAJAR 89	UA1	$E^{p\overline{p}}_{cm}$= 546,630 GeV
$81.8 ^{+6.0}_{-5.3} \pm 2.6$	46	[24] ALBAJAR 89	UA1	$E^{p\overline{p}}_{cm}$= 546,630 GeV
89 ± 3 ±6	32	[25] ALBAJAR 89	UA1	$E^{p\overline{p}}_{cm}$= 546,630 GeV
81. ± 5.	6	ARNISON 83	UA1	E^{ee}_{cm}= 546 GeV
$80. ^{+10.}_{-6.}$	4	BANNER 83B	UA2	Repl. by ALITTI 90B

[1] ABBIENDI 03C determine the mass of the W boson using fully leptonic decays $W^+ W^- \to \ell \nu_\ell \ell' \nu_{\ell'}$. They use the measured energies of the charged leptons and an approximate kinematic reconstruction of the event (both neutrinos are assumed in the same plane as the charged leptons) to get a W pseudo-mass. All these variables are combined in a simultaneous maximum likelihood fit. The systematic error is dominated by the uncertainty on the lepton energy.

[2] ABAZOV 02D improve the measurement of the W-boson mass including $W \to e \nu_e$ events in which the electron is close to a boundary of a central electromagnetic calorimeter module. Properly combining the results obtained by fitting $m_T(W)$, $p_T(e)$, and $p_T(\nu)$, this sample provides a mass value of 80.574 ± 0.405 GeV. The value reported here is a combination of this measurement with all previous DØ W-boson mass measurements.

[3] ABBIENDI 01F obtain this value properly combining results obtained from a direct W mass reconstruction at 172, 183, and 189 GeV with that from measurement of the W-pair production cross section at 161 GeV. The systematic error includes ±0.017 GeV due to LEP energy uncertainty and ±0.028 GeV due to possible color reconnection and Bose-Einstein effects in the purely hadronic final state.

[4] ABREU 01K obtain this value properly combining results obtained from a direct W mass reconstruction at 172, 183, and 189 GeV with those from measurements of W-pair production cross sections at 161, 172, and 183 GeV. The systematic error includes ±0.017 GeV due to the beam energy uncertainty and ±0.033 GeV due to possible color reconnection and Bose-Einstein effects in the purely hadronic final state.

[5] AFFOLDER 01E fit the transverse mass spectrum of 30115 $W \to e \nu_e$ events (M_W= 80.473 ± 0.065 ± 0.092 GeV) and of 14740 $W \to \mu \nu_\mu$ events (M_W= 80.465 ± 0.100 ± 0.103 GeV) obtained in the run IB (1994-95). Combining the electron and muon results, accounting for correlated uncertainties, yields M_W= 80.470 ± 0.089 GeV. They combine this value with their measurement of ABE 95P reported in run IA (1992-93) to obtain the quoted value.

[6] BARATE 00T obtain this value properly combining results obtained from a direct W mass reconstruction at 172, 183, and 189 GeV with those from measurements of W-pair production cross sections at 161 and 172 GeV. The systematic error includes ±0.017 GeV due to LEP energy uncertainty and ±0.019 GeV due to possible color reconnection and Bose-Einstein effects in the purely hadronic final state.

[7] ACCIARRI 99 obtain this value properly combining results obtained from a direct W mass reconstruction at 172 and 183 GeV with those from the measurements of the total W-pair production cross sections at 161 and 172 GeV. The value of the mass obtained from the direct reconstruction at 172 and 183 GeV is $M(W)$= 80.58 ± 0.14 ± 0.08 GeV.

[8] CHEKANOV 02C fit the Q^2 dependence (200<Q^2 <60000 GeV^2) of the charged-current differential cross sections with a propagator mass fit. The last error is due to the uncertainty on the probability density functions.

[9] ADLOFF 01A fit the Q^2 dependence (150 < Q^2 < 30000 GeV^2) of the charged-current double-differential cross sections with a propagator mass fit. The second error includes 2.1 GeV due to the theoretical uncertainties.

[10] ABBOTT 00 use $W \to e \nu_e$ events to measure the W mass with a fit to the transverse mass distribution. The result quoted here corresponds to electrons detected both in the forward and in the central calorimeters for the data recorded in 1992–1995. For the large rapidity electrons recorded in 1994–1995, the analysis combines results obtained from m_T, $p_T(e)$, and $p_T(\nu)$.

[11] ADLOFF 00B fit the Q^2 dependence (300 < Q^2 < 15000 GeV^2) of the charged-current double-differential cross sections with a propagator mass fit. The second error is due to the theoretical uncertainties.

[12] BREITWEG 00D fit the Q^2 dependence (200 < Q^2 < 22500 GeV^2) of the charged-current differential cross sections with a propagator mass fit. The last error is due to the uncertainty on the probability density functions.

[13] ABBIENDI 99C obtain this value properly combining results from a direct W mass reconstruction at 172 and 183 GeV with that from the measurement of the total W-pair production cross section at 161 GeV. The systematic error includes an uncertainty of ±0.02 GeV due to the possible color-reconnection and Bose-Einstein effects in the purely hadronic final states and an uncertainty of ±0.02 GeV due to the beam energy.

[14] ABREU 99T obtain this value properly combining results obtained from a direct W mass reconstruction at 172 and 183 GeV with those from measurement of W-pair production cross sections at 161, 172, and 183 GeV. The systematic error includes ±0.021 GeV due to the beam energy uncertainty and ±0.030 GeV due to possible color reconnection and Bose-Einstein effects in the purely hadronic final state.

[15] BARATE 99 obtain this value properly combining results from a direct W mass reconstruction at 172 and 183 GeV with those from the measurements of the total W-pair production cross sections at 161 and 172 GeV. The systematic error includes ±0.023 GeV due to LEP energy uncertainty and ±0.021 GeV due to theory uncertainty on account of possible color reconnection and Bose-Einstein correlations.

[16] ACCIARRI 97 derive this value from their measured W-W production cross section $\sigma_{WW} = 2.89^{+0.81}_{-0.70} \pm 0.14$ pb using the Standard Model dependence of σ_{WW} on M_W at the given c.m. energy. Statistical and systematic errors are added in quadrature and the last error of ±0.03 GeV arises from the beam energy uncertainty. The same result is given by a fit of the production cross sections to the data.

[17] ACCIARRI 97M derive this value from their measured WW production cross section $\sigma_{WW} = 12.27^{+1.41}_{-1.32} \pm 0.23$ pb using the Standard Model dependence of σ_{WW} on M_W at the given c.m. energy. Combining with ACCIARRI 97 authors find $M(W) = 80.78^{+0.45}_{-0.41} \pm 0.03$ GeV where the last error is due to beam energy uncertainty.

[18] ACCIARRI 97S obtain this value from a fit to the reconstructed W mass distribution. The W width was taken as its Standard Model value at the fitted W mass. When both W mass and width are varied they obtain $M(W) = 80.72^{+0.31}_{-0.33} \pm 0.09$ GeV. The systematic error includes ±0.03 GeV due to the beam energy uncertainty and ±0.05 GeV due to the possible color reconnection and Bose-Einstein effects in the purely hadronic final state. Combining with ACCIARRI 97 and ACCIARRI 97M authors find: $M(W) = 80.75^{+0.26}_{-0.27} \pm 0.03$ (LEP) GeV.

[19] ABE 95P use 3268 $W \to \mu \nu_\mu$ events to find M = 80.310 ± 0.205 ± 0.130 GeV and 5718 $W \to e \nu_e$ events to find M = 80.490 ± 0.145 ± 0.175 GeV. The result given here combines these while accounting for correlated uncertainties.

[20] ALITTI 92B result has two contributions to the systematic error (±0.83); one (±0.81) cancels in m_W/m_Z and one (±0.17) is noncancelling. These were added in quadrature. We choose the ALITTI 92B value without using the LEP m_Z value, because we perform our own combined fit.

[21] There are two contributions to the systematic error (±0.84): one (±0.81) which cancels in m_W/m_Z and one (±0.21) which is non-cancelling. These were added in quadrature.

[22] ABE 89I systematic error dominated by the uncertainty in the absolute energy scale.

[23] ALBAJAR 89 result is from a total sample of 299 $W \to e \nu$ events.

[24] ALBAJAR 89 result is from a total sample of 67 $W \to \mu \nu$ events.

[25] ALBAJAR 89 result is from $W \to \tau \nu$ events.

W/Z MASS RATIO

The fit uses the W and Z mass, mass difference, and mass ratio measurements.

VALUE	*EVTS*	*DOCUMENT ID*	*TECN*	*COMMENT*
0.88197±0.00042 OUR FIT				
0.8821 ±0.0011 ±0.0008	28323	[26] ABBOTT 98N	D0	$E^{p\overline{p}}_{cm}$= 1.8 TeV
0.88114±0.00154±0.00252	5982	[27] ABBOTT 98P	D0	$E^{p\overline{p}}_{cm}$= 1.8 TeV
0.8813 ±0.0036 ±0.0019	156	[28] ALITTI 92B	UA2	$E^{p\overline{p}}_{cm}$= 630 GeV

[26] ABBOTT 98N obtain this from a study of 28323 $W \to e \nu_e$ and 3294 $Z \to e^+ e^-$ decays. Of this latter sample, 2179 events are used to calibrate the electron energy scale.

[27] ABBOTT 98P obtain this from a study of 5982 $W \to e \nu_e$ events. The systematic error includes an uncertainty of ±0.00175 due to the electron energy scale.

[28] Scale error cancels in this ratio.

$m_Z - m_W$

The fit uses the W and Z mass, mass difference, and mass ratio measurements.

VALUE (GeV)	*DOCUMENT ID*	*TECN*	*COMMENT*
10.763±0.038 OUR FIT			
10.4 ±1.4 ±0.8	ALBAJAR 89	UA1	$E^{p\overline{p}}_{cm}$= 546,630 GeV
• • • We do not use the following data for averages, fits, limits, etc. • • •			
11.3 ±1.3 ±0.9	ANSARI 87	UA2	$E^{p\overline{p}}_{cm}$= 546,630 GeV

$m_{W^+} - m_{W^-}$

Test of CPT invariance.

VALUE (GeV)	EVTS	DOCUMENT ID		TECN	COMMENT
−0.19±0.58	1722	ABE	90G	CDF	$E^{p\overline{p}}_{\rm cm}$= 1.8 TeV

W WIDTH

The CDF and DØ widths labelled "extracted value" are obtained by measuring $R = [\sigma(W)/\sigma(Z)]\ [\Gamma(W \to \ell\nu_\ell)]/(\mathrm{B}(Z \to \ell\ell)\Gamma(W))$ where the bracketed quantities can be calculated with plausible reliability. $\Gamma(W)$ is then extracted by using a value of $\mathrm{B}(Z \to \ell\ell)$ measured at LEP. The UA1 and UA2 widths used $R = [\sigma(W)/\sigma(Z)]\ [\Gamma(W \to \ell\nu_\ell)/\Gamma(Z \to \ell\ell)]\ \Gamma(Z)/\Gamma(W)$ and the measured value of $\Gamma(Z)$. The Standard Model prediction is 2.0921 ± 0.0025 GeV (see Review on "Electroweak model and constraints on new physics" in this Edition).

To obtain OUR FIT,the correlation between systematics for the Direct Measurements is properly taken into account. The following notes may be consulted for details as well as the respective average values: for the LEP experiments the note LEPEWWG/MASS/2002-01 (http://lepewwg.web.cern.ch/LEPEWWG/lepww/mw/pdg_2002/) of 11 March 2002 and for the Tevatron experiments the note FERMILAB-FN-716 of 1 July 2002 (KOTWAL 02). The respective average values (2.17 ± 0.12 GeV from LEP and 2.115 ± 0.105 GeV from Tevatron) yield an average W width of 2.139 ± 0.079 GeV coming from direct measurements. Combined with the Extracted Values one obtains the quoted value.

VALUE (GeV)	CL%	EVTS	DOCUMENT ID		TECN	COMMENT
2.124±0.041 OUR FIT						
$2.23\ ^{+0.15}_{-0.14}\ \pm0.10$		294	[29] ABAZOV	02E	D0	Direct meas.
2.04 ±0.16 ±0.09		2756	[30] ABBIENDI	01F	OPAL	$E^{ee}_{\rm cm}$= 172+183+189 GeV
2.266±0.176±0.076		3005	[31] ABREU	01K	DLPH	$E^{ee}_{\rm cm}$= 183+189 GeV
2.152±0.066		79176	[32] ABBOTT	00B	D0	Extracted value
2.05 ±0.10 ±0.08		662	[33] AFFOLDER	00M	CDF	Direct meas.
2.24 ±0.20 ±0.13		1711	[34] BARATE	00T	ALEP	$E^{ee}_{\rm cm}$= 189 GeV
1.97 ±0.34 ±0.17		687	[35] ACCIARRI	99	L3	$E^{ee}_{\rm cm}$= 172+183 GeV
2.064±0.060±0.059			[36] ABE	95W	CDF	Extracted value
$2.10\ ^{+0.14}_{-0.13}\ \pm0.09$		3559	[37] ALITTI	92	UA2	Extracted value
$2.18\ ^{+0.26}_{-0.24}\ \pm0.04$			[38] ALBAJAR	91	UA1	Extracted value
• • • We do not use the following data for averages, fits, limits, etc. • • •						
1.84 ±0.32 ±0.20		674	[39] ABBIENDI	99C	OPAL	Repl. by ABBIENDI 01F
2.044±0.097		11858	[40] ABBOTT	99H	D0	Repl. by ABBOTT 00B
2.48 ±0.40 ±0.10		737	[41] ABREU	99T	DLPH	Repl. by ABREU 01K
$2.126\ ^{+0.052}_{-0.048}\pm0.035$			[42] BARATE	99I	ALEP	$E^{ee}_{\rm cm}$= 161+172+183 GeV
$1.74\ ^{+0.88}_{-0.78}\ \pm0.25$		101	[43] ACCIARRI	97S	L3	Repl. by ACCIARRI 99
2.11 ±0.28 ±0.16		58	[44] ABE	95C	CDF	Repl. by AFFOLDER 00M
2.30 ±0.19 ±0.06			[45] ALITTI	90C	UA2	Extracted value
$2.8\ ^{+1.4}_{-1.5}\ \pm1.3$		149	[46] ALBAJAR	89	UA1	$E^{p\overline{p}}_{\rm cm}$= 546,630 GeV
<7	90	119	APPEL	86	UA2	$E^{p\overline{p}}_{\rm cm}$= 546,630 GeV
<6.5	90	86	[47] ARNISON	86	UA1	$E^{p\overline{p}}_{\rm cm}$= 546,630 GeV

[29] ABAZOV 02E obtain this result fitting the high-end tail (90–200 GeV) of the transverse-mass spectrum in semileptonic $W \to e\nu_e$ decays.

[30] ABBIENDI 01F obtain this value from a fit to the reconstructed W mass distribution using data at 172, 183, and 189 GeV. The systematic error includes ±0.010 GeV due to LEP energy uncertainty and ±0.078 GeV due to possible color reconnection and Bose-Einstein effects in the purely hadronic final state.

[31] ABREU 01K obtain this value properly combining results obtained at 183 and 189 GeV using $WW \to \ell\overline{\nu}_\ell q\overline{q}$ and $WW \to q\overline{q}q\overline{q}$ decays. The systematic error includes an uncertainty of ±0.052 GeV due to possible color reconnection and Bose-Einstein effects in the purely hadronic final state.

[32] ABBOTT 00B measure R = 10.43 ± 0.27 for the $W \to e\nu_e$ decay channel. They use the SM theoretical predictions for $\sigma(W)/\sigma(Z)$ and $\Gamma(W \to e\nu_e)$ and the world average for $\mathrm{B}(Z \to ee)$. The value quoted here is obtained combining this result (2.169 ± 0.070 GeV) with that of ABBOTT 99H.

[33] AFFOLDER 00M fit the high transverse mass (100–200 GeV) $W \to e\nu_e$ and $W \to \mu\nu_\mu$ events to obtain $\Gamma(W)$= 2.04 ± 0.11(stat)±0.09(syst) GeV. This is combined with the earlier CDF measurement (ABE 95C) to obtain the quoted result.

[34] BARATE 00T obtain this value using $WW \to q\overline{q}q\overline{q}$, $WW \to e\nu_e q\overline{q}$, and $WW \to \mu\nu_\mu q\overline{q}$ decays. The systematic error includes ±0.015 GeV due to LEP energy uncertainty and ±0.080 GeV due to possible color reconnection and Bose-Einstein effects in the purely hadronic final state.

[35] ACCIARRI 99 obtain this value from a fit to the reconstructed W mass distribution using data at 172 and 183 GeV.

[36] ABE 95W measured R = 10.90 ± 0.32 ± 0.29. They use m_W=80.23 ± 0.18 GeV, $\sigma(W)/\sigma(Z)$ = 3.35 ± 0.03, $\Gamma(W \to e\nu)$ = 225.9 ± 0.9 MeV, $\Gamma(Z \to e^+e^-)$ = 83.98 ± 0.18 MeV, and $\Gamma(Z)$ = 2.4969 ± 0.0038 GeV.

[37] ALITTI 92 measured $R = 10.4^{+0.7}_{-0.6} \pm 0.3$. The values of $\sigma(Z)$ and $\sigma(W)$ come from $O(\alpha_s^2)$ calculations using m_W = 80.14 ± 0.27 GeV, and m_Z = 91.175 ± 0.021 GeV along with the corresponding value of $\sin^2\theta_W$ = 0.2274. They use $\sigma(W)/\sigma(Z)$ = 3.26 ± 0.07 ± 0.05 and $\Gamma(Z)$ = 2.487 ± 0.010 GeV.

[38] ALBAJAR 91 measured $R = 9.5^{+1.1}_{-1.0}$ (stat. + syst.). $\sigma(W)/\sigma(Z)$ is calculated in QCD at the parton level using m_W = 80.18 ± 0.28 GeV and m_Z = 91.172 ± 0.031 GeV along with $\sin^2\theta_W$ = 0.2322 ± 0.0014. They use $\sigma(W)/\sigma(Z)$ = 3.23 ± 0.05 and $\Gamma(Z)$ = 2.498 ± 0.020 GeV. This measurement is obtained combining both the electron and muon channels.

[39] ABBIENDI 99C obtain this value from a fit to the reconstructed Wmass distribution using data at 172 and 183 GeV. The systematic error includes an uncertainty of ±0.12 GeV due to the possible color-reconnection and Bose-Einstein effects in the purely hadronic final states and an uncertainty of ±0.01 GeV due to the beam energy.

[40] ABBOTT 99H measure R= 10.90 ± 0.52 combining electron and muon channels. They use M_W = 80.39 ± 0.06 GeV and the SM theoretical predictions for $\sigma(W)/\sigma(Z)$, $\mathrm{B}(Z \to \ell\ell)$, and $\Gamma(W \to \ell\nu_\ell)$.

[41] ABREU 99T obtain this value using $WW \to \ell\overline{\nu}_\ell q\overline{q}$ and $WW \to q\overline{q}q\overline{q}$ events. The systematic error includes an uncertainty of ±0.080 GeV due to possible color reconnection and Bose-Einstein effects in the purely hadronic final state.

[42] BARATE 99I obtain this result with a fit to the WW measured cross sections at 161, 172, and 183 GeV. The theoretical prediction takes into account the sensitivity to the W total width.

[43] ACCIARRI 97S obtain this value from a fit to the reconstructed W mass distribution.

[44] ABE 95C use the tail of the transverse mass distribution of $W \to e\nu_e$ decays.

[45] ALITTI 90C used the same technique as described for ABE 90. They measured $R = 9.38^{+0.82}_{-0.72} \pm 0.25$, obtained $\Gamma(W)/\Gamma(Z)$ = 0.902 ± 0.074 ± 0.024. Using $\Gamma(Z)$ = 2.546 ± 0.032 GeV, they obtained the $\Gamma(W)$ value quoted above and the limits $\Gamma(W)$ < 2.56 (2.64) GeV at the 90% (95%) CL. $E^{p\overline{p}}_{\rm cm}$ = 546,630 GeV.

[46] ALBAJAR 89 result is from a total sample of 299 $W \to e\nu$ events.

[47] If systematic error is neglected, result is $2.7^{+1.4}_{-1.5}$ GeV. This is enhanced subsample of 172 total events.

W^+ DECAY MODES

W^- modes are charge conjugates of the modes below.

	Mode		Fraction (Γ_i/Γ)	Confidence level
Γ_1	$\ell^+\nu$	[a]	(10.68± 0.12) %	
Γ_2	$e^+\nu$		(10.72± 0.16) %	
Γ_3	$\mu^+\nu$		(10.57± 0.22) %	
Γ_4	$\tau^+\nu$		(10.74± 0.27) %	
Γ_5	hadrons		(67.96± 0.35) %	
Γ_6	$\pi^+\gamma$		< 8 $\times10^{-5}$	95%
Γ_7	$D_s^+\gamma$		< 1.3 $\times10^{-3}$	95%
Γ_8	cX		(33.6 ± 2.7) %	
Γ_9	$c\overline{s}$		$(31\ ^{+13}_{-11}\ )$ %	
Γ_{10}	invisible	[b]	(1.4 ± 2.8) %	

[a] ℓ indicates each type of lepton (e, μ, and τ), not sum over them.

[b] This represents the width for the decay of the W boson into a charged particle with momentum below detectability, p< 200 MeV.

W PARTIAL WIDTHS

Γ(invisible) Γ_{10}

This represents the width for the decay of the W boson into a charged particle with momentum below detectability, p< 200 MeV.

VALUE (MeV)	DOCUMENT ID		TECN	COMMENT
$\mathbf{30^{+52}_{-48}\pm33}$	[48] BARATE	99I	ALEP	$E^{ee}_{\rm cm}$= 161+172+183 GeV
• • • We do not use the following data for averages, fits, limits, etc. • • •				
	[49] BARATE	99L	ALEP	$E^{ee}_{\rm cm}$= 161+172+183 GeV

[48] BARATE 99I measure this quantity using the dependence of the total cross section σ_{WW} upon a change in the total width. The fit is performed to the WW measured cross sections at 161, 172, and 183 GeV. This partial width is < 139 MeV at 95%CL.

[49] BARATE 99L use W-pair production to search for effectively invisible W decays, tagging with the decay of the other W boson to Standard Model particles. The partial width for effectively invisible decay is < 27 MeV at 95%CL.

W BRANCHING RATIOS

Overall fits are performed to determine the branching ratios of the W. For each LEP experiment the correlation matrix of the leptonic branching ratios is used and the common systematic errors among LEP experiments are properly taken into account (see LEP Electroweak Working Group note LEPEWWG/XSEC/2001-02, 30 March 2001, accessible at http://lepewwg.web.cern.ch/LEPEWWG/lepww/4f/PDG01). A first fit determines three individual leptonic branching ratios, $\mathrm{B}(W \to e\nu_e)$, $\mathrm{B}(W \to \mu\nu_\mu)$, and $\mathrm{B}(W \to \tau\nu_\tau)$. This fit has a χ^2 = 11.0 for 22 degrees of freedom. A second fit assumes lepton universality and determines the leptonic branching ratio $\mathrm{B}(W \to \ell\nu_\ell)$ and the hadronic branching ratio is derived as $\mathrm{B}(W \to \text{hadrons})$ = 1–3 $\mathrm{B}(W \to \ell\nu)$. This fit has a χ^2=11.4 for 24 degrees of freedom.

The LEP $W \to \ell\nu$ data are obtained by the Collaborations using individual leptonic channels and are, therefore, not included in the overall fits to avoid double counting.

$\Gamma(\ell^+\nu)/\Gamma_{total}$ — Γ_1/Γ

ℓ indicates average over e, μ, and τ modes, not sum over modes.

VALUE	EVTS	DOCUMENT ID	TECN	COMMENT
0.1068±0.0012 OUR FIT				
0.1056±0.0020±0.0009	5778	ABBIENDI,G 00	OPAL	E^{ee}_{cm}= 161+172+183+189 GeV
0.1071±0.0024±0.0014	4843	ABREU 00K	DLPH	E^{ee}_{cm}= 161+172+183+189 GeV
0.1060±0.0023±0.0011	5328	ACCIARRI 00V	L3	E^{ee}_{cm}= 161+172+183+189 GeV
0.1101±0.0022±0.0011	5258	BARATE 00J	ALEP	E^{ee}_{cm}= 161+172+183+189 GeV
0.1102±0.0052	11858	[50] ABBOTT 99H	D0	$E^{p\overline{p}}_{cm}$= 1.8 TeV
0.104 ±0.008	3642	[51] ABE 92I	CDF	$E^{p\overline{p}}_{cm}$= 1.8 TeV
• • • We do not use the following data for averages, fits, limits, etc. • • •				
0.107 ±0.004 ±0.002	1440	ABBIENDI 99D	OPAL	Repl. by ABBIENDI,G 00
0.1085±0.0048±0.0017	1336	ABREU 99K	DLPH	Repl. by ABREU 00K
0.1036±0.0040±0.0017	1322	BARATE 99I	ALEP	Repl. by BARATE 00J
0.100 ±0.004 ±0.001	1434	ACCIARRI 98P	L3	Repl. by ACCIARRI 00V

[50] ABBOTT 99H measure $R \equiv [\sigma_W \, B(W \to \ell\nu_\ell)]/[\sigma_Z \, B(Z \to \ell\ell)] = 10.90 \pm 0.52$ combining electron and muon channels. They use $M_W = 80.39 \pm 0.06$ GeV and the SM theoretical predictions for $\sigma(W)/\sigma(Z)$ and $B(Z \to \ell\ell)$.

[51] $1216 \pm 38^{+27}_{-31}$ $W \to \mu\nu$ events from ABE 92I and 2426 $W \to e\nu$ events of ABE 91C. ABE 92I give the inverse quantity as 9.6 ± 0.7 and we have inverted.

$\Gamma(e^+\nu)/\Gamma_{total}$ — Γ_2/Γ

VALUE	EVTS	DOCUMENT ID	TECN	COMMENT
0.1072±0.0016 OUR FIT				
0.1046±0.0042±0.0014	801	ABBIENDI,G 00	OPAL	E^{ee}_{cm}= 161+172+183+189 GeV
0.1044±0.0015±0.0028	67318	[52] ABBOTT 00B	D0	$E^{p\overline{p}}_{cm}$= 1.8 TeV
0.1018±0.0054±0.0026	527	ABREU 00K	DLPH	E^{ee}_{cm}= 161+172+183+189 GeV
0.1077±0.0045±0.0016	715	ACCIARRI 00V	L3	E^{ee}_{cm}= 161+172+183+189 GeV
0.1135±0.0046±0.0017	720	BARATE 00J	ALEP	E^{ee}_{cm}= 161+172+183+189 GeV
0.1094±0.0033±0.0031		[53] ABE 95W	CDF	$E^{p\overline{p}}_{cm}$= 1.8 TeV
0.10 ±0.014 $^{+0.02}_{-0.03}$	248	[54] ANSARI 87C	UA2	$E^{p\overline{p}}_{cm}$= 546,630 GeV
• • • We do not use the following data for averages, fits, limits, etc. • • •				
0.117 ±0.009 ±0.002	224	ABBIENDI 99D	OPAL	Repl. by ABBIENDI,G 00
0.1012±0.0107±0.0028	150	ABREU 99K	DLPH	Repl. by ABREU 00K
0.1115±0.0085±0.0024	192	BARATE 99I	ALEP	Repl. by BARATE 00J
0.105 ±0.009 ±0.002	173	ACCIARRI 98P	L3	Repl. by ACCIARRI 00V
seen	119	APPEL 86	UA2	$E^{p\overline{p}}_{cm}$= 546,630 GeV
seen	172	ARNISON 86	UA1	$E^{p\overline{p}}_{cm}$= 546,630 GeV

[52] ABBOTT 00B measure $R \equiv [\sigma_W B(W \to e\nu_e)]/[\sigma_Z B(Z \to ee)] = 10.43 \pm 0.27$ for the $W \to e\nu_e$ decay channel. They use the SM theoretical prediction for $\sigma(W)/\sigma(Z)$ and the world average for $B(Z \to ee)$.

[53] ABE 95W result is from a measurement of $\sigma B(W \to e\nu)/\sigma B(Z \to e^+e^-) = 10.90 \pm 0.32 \pm 0.29$, the theoretical prediction for the cross section ratio, the experimental knowledge of $\Gamma(Z \to e^+e^-) = 83.98 \pm 0.18$ MeV, and $\Gamma(Z) = 2.4969 \pm 0.0038$ GeV.

[54] The first error was obtained by adding the statistical and systematic experimental uncertainties in quadrature. The second error reflects the dependence on theoretical prediction of total W cross section: $\sigma(546 \text{ GeV}) = 4.7^{+1.4}_{-0.7}$ nb and $\sigma(630 \text{ GeV}) = 5.8^{+1.8}_{-1.0}$ nb. See ALTARELLI 85B.

$\Gamma(\mu^+\nu)/\Gamma_{total}$ — Γ_3/Γ

VALUE	EVTS	DOCUMENT ID	TECN	COMMENT
0.1057±0.0022 OUR FIT				
0.1050±0.0041±0.0012	803	ABBIENDI,G 00	OPAL	E^{ee}_{cm}= 161+172+183+189 GeV
0.1092±0.0048±0.0012	649	ABREU 00K	DLPH	E^{ee}_{cm}= 161+172+183+189 GeV
0.0990±0.0046±0.0015	617	ACCIARRI 00V	L3	E^{ee}_{cm}= 161+172+183+189 GeV
0.1110±0.0044±0.0016	710	BARATE 00J	ALEP	E^{ee}_{cm}= 161+172+183+189 GeV
0.10 ±0.01	1216	[55] ABE 92I	CDF	$E^{p\overline{p}}_{cm}$= 1.8 TeV
• • • We do not use the following data for averages, fits, limits, etc. • • •				
0.102 ±0.008 ±0.002	193	ABBIENDI 99D	OPAL	Repl. by ABBIENDI,G 00
0.1139±0.0096±0.0023	186	ABREU 99K	DLPH	Repl. by ABREU 00K
0.1006±0.0078±0.0021	179	BARATE 99I	ALEP	Repl. by BARATE 00J
0.102 ±0.009 ±0.002	160	ACCIARRI 98P	L3	Repl. by ACCIARRI 00V

[55] ABE 92I quote the inverse quantity as 9.9 ± 1.2 which we have inverted.

$\Gamma(\tau^+\nu)/\Gamma_{total}$ — Γ_4/Γ

VALUE	EVTS	DOCUMENT ID	TECN	COMMENT
0.1074±0.0027 OUR FIT				
0.1075±0.0052±0.0021	794	ABBIENDI,G 00	OPAL	E^{ee}_{cm}= 161+172+183+189 GeV
0.1105±0.0075±0.0032	579	ABREU 00K	DLPH	E^{ee}_{cm}= 161+172+183+189 GeV
0.1124±0.0062±0.0022	536	ACCIARRI 00V	L3	E^{ee}_{cm}= 161+172+183+189 GeV
0.1051±0.0055±0.0022	607	BARATE 00J	ALEP	E^{ee}_{cm}= 161+172+183+189 GeV
• • • We do not use the following data for averages, fits, limits, etc. • • •				
0.101 ±0.010 ±0.003	183	ABBIENDI 99D	OPAL	Repl. by ABBIENDI,G 00
0.1095±0.0149±0.0041	142	ABREU 99K	DLPH	Repl. by ABREU 00K
0.0976±0.0101±0.0033	160	BARATE 99I	ALEP	Repl. by BARATE 00J
0.090 ±0.012 ±0.003	123	ACCIARRI 98P	L3	Repl. by ACCIARRI 00V

$\Gamma(\text{hadrons})/\Gamma_{total}$ — Γ_5/Γ

OUR FIT value is obtained by a fit to the lepton branching ratio data assuming lepton universality.

VALUE	EVTS	DOCUMENT ID	TECN	COMMENT
0.6796±0.0035 OUR FIT				
0.679 ±0.004 OUR AVERAGE				
0.6832±0.0061±0.0028	5778	ABBIENDI,G 00	OPAL	E^{ee}_{cm}= 161+172+183+189 GeV
0.6789±0.0073±0.0043	4843	ABREU 00K	DLPH	E^{ee}_{cm}= 161+172+183+189 GeV
0.6820±0.0068±0.0033	5328	ACCIARRI 00V	L3	E^{ee}_{cm}= 161+172+183+189 GeV
0.6697±0.0065±0.0032	5258	BARATE 00J	ALEP	E^{ee}_{cm}= 161+172+183+189 GeV
• • • We do not use the following data for averages, fits, limits, etc. • • •				
0.679 ±0.012 ±0.005	1440	ABBIENDI 99D	OPAL	Repl. by ABBIENDI,G 00
0.6746±0.0143±0.0052	1336	ABREU 99K	DLPH	Repl. by ABREU 00K
0.6893±0.0121±0.0051	1322	BARATE 99I	ALEP	Repl. by BARATE 00J
0.701 ±0.013 ±0.004	1434	ACCIARRI 98P	L3	Repl. by ACCIARRI 00V

$\Gamma(\mu^+\nu)/\Gamma(e^+\nu)$ — Γ_3/Γ_2

VALUE	EVTS	DOCUMENT ID	TECN	COMMENT
0.986±0.024 OUR FIT				
0.89 ±0.10	13k	[56] ABACHI 95D	D0	$E^{p\overline{p}}_{cm}$= 1.8 TeV
1.02 ±0.08	1216	[57] ABE 92I	CDF	$E^{p\overline{p}}_{cm}$= 1.8 TeV
1.00 ±0.14 ±0.08	67	ALBAJAR 89	UA1	$E^{p\overline{p}}_{cm}$= 546,630 GeV
• • • We do not use the following data for averages, fits, limits, etc. • • •				
1.24 $^{+0.6}_{-0.4}$	14	ARNISON 84D	UA1	Repl. by ALBAJAR 89

[56] ABACHI 95D obtain this result from the measured $\sigma_W B(W \to \mu\nu) = 2.09 \pm 0.23 \pm 0.11$ nb and $\sigma_W B(W \to e\nu) = 2.36 \pm 0.07 \pm 0.13$ nb in which the first error is the combined statistical and systematic uncertainty, the second reflects the uncertainty in the luminosity.

[57] ABE 92I obtain $\sigma_W B(W \to \mu\nu) = 2.21 \pm 0.07 \pm 0.21$ and combine with ABE 91C σ_W $B((W \to e\nu))$ to give a ratio of the couplings from which we derive this measurement.

$\Gamma(\tau^+\nu)/\Gamma(e^+\nu)$ — Γ_4/Γ_2

VALUE	EVTS	DOCUMENT ID	TECN	COMMENT
1.002±0.029 OUR FIT				
0.961±0.061	980	[58] ABBOTT 00D	D0	$E^{p\overline{p}}_{cm}$= 1.8 TeV
0.94 ±0.14	179	[59] ABE 92E	CDF	$E^{p\overline{p}}_{cm}$= 1.8 TeV
1.04 ±0.08 ±0.08	754	[60] ALITTI 92F	UA2	$E^{p\overline{p}}_{cm}$= 630 GeV
1.02 ±0.20 ±0.12	32	ALBAJAR 89	UA1	$E^{p\overline{p}}_{cm}$= 546,630 GeV
• • • We do not use the following data for averages, fits, limits, etc. • • •				
0.995±0.112±0.083	198	ALITTI 91C	UA2	Repl. by ALITTI 92F
1.02 ±0.20 ±0.10	32	ALBAJAR 87	UA1	Repl. by ALBAJAR 89

[58] ABBOTT 00D measure $\sigma_W \times B(W \to \tau\nu_\tau) = 2.22 \pm 0.09 \pm 0.10 \pm 0.10$ nb. Using the ABBOTT 00B result $\sigma_W \times B(W \to e\nu_e) = 2.31 \pm 0.01 \pm 0.05 \pm 0.10$ nb, they quote the ratio of the couplings from which we derive this measurement.

[59] ABE 92E use two procedures for selecting $W \to \tau\nu_\tau$ events. The missing E_T trigger leads to $132 \pm 14 \pm 8$ events and the τ trigger to $47 \pm 9 \pm 4$ events. Proper statistical and systematic correlations are taken into account to arrive at $\sigma B(W \to \tau\nu) = 2.05 \pm 0.27$ nb. Combined with ABE 91C result on $\sigma B(W \to e\nu)$, ABE 92E quote a ratio of the couplings from which we derive this measurement.

[60] This measurement is derived by us from the ratio of the couplings of ALITTI 92F.

$\Gamma(\pi^+\gamma)/\Gamma(e^+\nu)$ — Γ_6/Γ_2

VALUE	CL%	DOCUMENT ID	TECN	COMMENT
$< 7 \times 10^{-4}$	95	ABE 98H	CDF	$E^{p\overline{p}}_{cm}$= 1.8 TeV
$< 4.9 \times 10^{-3}$	95	[61] ALITTI 92D	UA2	$E^{p\overline{p}}_{cm}$= 630 GeV
$< 58 \times 10^{-3}$	95	[62] ALBAJAR 90	UA1	$E^{p\overline{p}}_{cm}$= 546, 630 GeV

[61] ALITTI 92D limit is 3.8×10^{-3} at 90%CL.

[62] ALBAJAR 90 obtain < 0.048 at 90%CL.

$\Gamma(D_s^+\gamma)/\Gamma(e^+\nu)$ — Γ_7/Γ_2

VALUE	CL%	DOCUMENT ID		TECN	COMMENT
<1.2 × 10^{-2}	95	ABE	98P	CDF	$E^{p\overline{p}}_{\rm cm}$= 1.8 TeV

$\Gamma(cX)/\Gamma(\text{hadrons})$ — Γ_8/Γ_5

VALUE	EVTS	DOCUMENT ID		TECN	COMMENT
0.49 ±0.04 OUR AVERAGE					
0.481±0.042±0.032	3005	[63] ABBIENDI	00V	OPAL	$E^{ee}_{\rm cm}$= 183 + 189 GeV
0.51 ±0.05 ±0.03	746	[64] BARATE	99M	ALEP	$E^{ee}_{\rm cm}$= 172 + 183 GeV

[63] ABBIENDI 00V tag $W \rightarrow$ cX decays using measured jet properties, lifetime information, and leptons produced in charm decays. From this result, and using the additional measurements of $\Gamma(W)$ and B($W \rightarrow$ hadrons), $|V_{cs}|$ is determined to be $0.969 \pm 0.045 \pm 0.036$.

[64] BARATE 99M tag c jets using a neural network algorithm. From this measurement $|V_{cs}|$ is determined to be $1.00 \pm 0.11 \pm 0.07$.

$R_{cs} = \Gamma(c\overline{s})/\Gamma(\text{hadrons})$ — Γ_9/Γ_5

VALUE	DOCUMENT ID		TECN	COMMENT
$0.46^{+0.18}_{-0.14}\pm0.07$	[65] ABREU	98N	DLPH	$E^{ee}_{\rm cm}$= 161+172 GeV

[65] ABREU 98N tag c and s jets by identifying a charged kaon as the highest momentum particle in a hadronic jet. They also use a lifetime tag to independently identify a c jet, based on the impact parameter distribution of charged particles in a jet. From this measurement $|V_{cs}|$ is determined to be $0.94^{+0.32}_{-0.26} \pm 0.13$.

AVERAGE PARTICLE MULTIPLICITIES IN HADRONIC W DECAY

Summed over particle and antiparticle, when appropriate.

$\langle N_{\pi^\pm}\rangle$

VALUE	DOCUMENT ID		TECN	COMMENT
15.70±0.35	[66] ABREU,P	00F	DLPH	$E^{ee}_{\rm cm}$= 189 GeV

[66] ABREU,P 00F measure $\langle N_{\pi^\pm}\rangle = 31.65 \pm 0.48 \pm 0.76$ and $15.51 \pm 0.38 \pm 0.40$ in the fully hadronic and semileptonic final states respectively. The value quoted is a weighted average without assuming any correlations.

$\langle N_{K^\pm}\rangle$

VALUE	DOCUMENT ID		TECN	COMMENT
2.20±0.19	[67] ABREU,P	00F	DLPH	$E^{ee}_{\rm cm}$= 189 GeV

[67] ABREU,P 00F measure $\langle N_{K^\pm}\rangle = 4.38 \pm 0.42 \pm 0.12$ and $2.23 \pm 0.32 \pm 0.17$ in the fully hadronic and semileptonic final states respectively. The value quoted is a weighted average without assuming any correlations.

$\langle N_p\rangle$

VALUE	DOCUMENT ID		TECN	COMMENT
0.92±0.14	[68] ABREU,P	00F	DLPH	$E^{ee}_{\rm cm}$= 189 GeV

[68] ABREU,P 00F measure $\langle N_p\rangle = 1.82 \pm 0.29 \pm 0.16$ and $0.94 \pm 0.23 \pm 0.06$ in the fully hadronic and semileptonic final states respectively. The value quoted is a weighted average without assuming any correlations.

$\langle N_{\rm charged}\rangle$

VALUE	DOCUMENT ID		TECN	COMMENT
19.41±0.15 OUR AVERAGE				
19.44±0.17	[69] ABREU,P	00F	DLPH	$E^{ee}_{\rm cm}$= 183+189 GeV
19.3 ±0.3 ±0.3	[70] ABBIENDI	99N	OPAL	$E^{ee}_{\rm cm}$= 183 GeV
19.23±0.74	[71] ABREU	98C	DLPH	$E^{ee}_{\rm cm}$= 172 GeV

[69] ABREU,P 00F measure $\langle N_{\rm charged}\rangle = 39.12 \pm 0.33 \pm 0.36$ and $38.11 \pm 0.57 \pm 0.44$ in the fully hadronic final states at 189 and 183 GeV respectively, and $\langle N_{\rm charged}\rangle = 19.49 \pm 0.31 \pm 0.27$ and $19.78 \pm 0.49 \pm 0.43$ in the semileptonic final states. The value quoted is a weighted average without assuming any correlations.

[70] ABBIENDI 99N use the final states $W^+W^- \rightarrow q\overline{q}\ell\overline{\nu}_\ell$ to derive this value.

[71] ABREU 98C combine results from both the fully hadronic as well semileptonic WW final states after demonstrating that the W decay charged multiplicity is independent of the topology within errors.

TRIPLE GAUGE COUPLINGS (TGC'S)

Revised February 2002 by C. Caso (University of Genova) and A. Gurtu (Tata Institute).

Fourteen independent couplings, 7 each for ZWW and γWW, completely describe the VWW vertices within the most general framework of the electroweak Standard Model (SM) consistent with Lorentz invariance and U(1) gauge invariance. Of each of the 7 TGC's, 3 conserve C and P individually, 3 violate CP, and one TGC violates C and P individually while conserving CP. Assumption of C and P conservation and electromagnetic gauge invariance reduces the independent VWW couplings to five: one common set [1,2] is $(\Delta\kappa_\gamma, \Delta\kappa_Z, \lambda_\gamma, \lambda_Z, \Delta g_1^Z)$, where $\Delta\kappa_\gamma = \Delta\kappa_Z = \Delta g_1^Z = 0$ and $\lambda_\gamma = \lambda_Z = 0$ in the Standard Model at the tree level. The W magnetic dipole moment, μ_W, and the W electric quadrupole moment, q_W, are expressed as $\mu_W = e\,(1+\kappa_\gamma+\lambda_\gamma)/2M_W$ and $q_W = -e\,(\kappa_\gamma - \lambda_\gamma)/M_W^2$.

Precision measurements of suitable observables at LEP1 has already led to an exploration of much of the TGC parameter space. For LEP2 data, the LEP Collaborations have agreed to express their results in terms of the parameters Δg_1^Z, $\Delta\kappa_\gamma$ and λ_γ (λ_Z and $\Delta\kappa_Z$ are related to these by gauge invariance).

At LEP2 the VWW coupling arises in W-pair production via s-channel exchange or in single W production via the radiation of a virtual photon off the incident e^+ or e^-. At the TEVATRON hard photon bremstrahlung off a produced W or Z signals the presence of a triple gauge vertex. In order to extract the value of one TGC the others are generally kept fixed to their SM values.

References

1. K. Hagiwara *et al.*, Nucl. Phys. **B282**, 253 (1987).
2. G. Gounaris *et al.*, CERN 96-01 525.

Δg_1^Z

Combining published and unpublished LEP results (as of Summer 2003), a single-parameter fit yields $\Delta g_1^Z = -0.009^{+0.022}_{-0.021}$, where the other two parameters, $\Delta\kappa_\gamma$ and λ_γ, were kept fixed to their Standard Model values.

(See EP Preprint Summer 2003: CERN-EP/2003-091 and hep-ex/0312023, December 2003, on http://lepewwg.web.cern.ch/LEPEWWG/stanmod/)

VALUE	EVTS	DOCUMENT ID		TECN	COMMENT
$-0.013^{+0.034}_{-0.033}$	9800	[72] ABBIENDI	04D	OPAL	$E^{ee}_{\rm cm}$= 183–209 GeV
• • • We do not use the following data for averages, fits, limits, etc. • • •					
$-0.02 \pm0.07 \pm0.01$	2114	[73] ABREU	01I	DLPH	$E^{ee}_{\rm cm}$= 183+189 GeV
$0.023^{+0.059}_{-0.055}$	3586	[74] HEISTER	01C	ALEP	$E^{ee}_{\rm cm}$= 161–189 GeV
	331	[75] ABBOTT	99I	D0	$E^{p\overline{p}}_{\rm cm}$= 1.8 TeV
$0.11\ ^{+0.19}_{-0.18}\ \pm0.10$	1154	[76] ACCIARRI	99Q	L3	$E^{ee}_{\rm cm}$= 161+172+ 183 GeV

[72] ABBIENDI 04D combine results from W^+W^- in all decay channels. Only CP-conserving couplings are considered and each parameter is determined from a single-parameter fit in which the other parameters assume their Standard Model values. The 95% confidence interval is $-0.077 < \Delta g_1^Z < 0.054$.

[73] ABREU 01I combine results from e^+e^- interactions at 189 GeV leading to W^+W^- and $We\nu_e$ final states with results from ABREU 99L at 183 GeV. The 95% confidence interval is $-0.16 < \Delta g_1^Z < 0.13$.

[74] HEISTER 01C study W-pair, single-W, and single photon events and combine with earlier results from BARATE,R 98, BARATE 98Y, and BARATE 99L to obtain the quoted value, fixing $\Delta\kappa_\gamma$ and λ_γ to their Standard Model values. The 95% confidence interval is $-0.087 < \Delta g_1^Z < 0.141$. When all three couplings Δg_1^Z, $\Delta\kappa_\gamma$, and λ_γ are floated freely in the fit, one obtains $\Delta g_1^Z = 0.013^{+0.066}_{-0.068}$.

[75] ABBOTT 99I perform a simultaneous fit to the $W\gamma$, $WW \rightarrow$ dilepton, $WW/WZ \rightarrow e\nu jj$, $WW/WZ \rightarrow \mu\nu jj$, and $WZ \rightarrow$ trilepton data samples. For $\Lambda = 2.0$ TeV, the 95%CL limits are $-0.37 < \Delta g_1^Z < 0.57$, fixing λ_Z=$\Delta\kappa_Z$ =0 and assuming Standard Model values for the $WW\gamma$ couplings.

[76] ACCIARRI 99Q study W-pair, single-W, and single photon events.

$\Delta\kappa_\gamma$

Combining published and unpublished LEP results (as of Summer 2003), a single-parameter fit yields $\Delta\kappa_\gamma = -0.016^{+0.042}_{-0.047}$, where the other two parameters, Δg_1^Z and λ_γ, were kept fixed to their Standard Model values.

(See EP Preprint Summer 2003: CERN-EP/2003-091 and hep-ex/0312023, December 2003, on http://lepewwg.web.cern.ch/LEPEWWG/stanmod/)

VALUE	EVTS	DOCUMENT ID		TECN	COMMENT
$-0.12\ ^{+0.09}_{-0.08}$	9800	[77] ABBIENDI	04D	OPAL	$E^{ee}_{\rm cm}$= 183–209 GeV

• • • We do not use the following data for averages, fits, limits, etc. • • •

$0.116^{+0.082}_{-0.086}\pm0.068$	315	[78] ACHARD	02I L3	E^{ee}_{cm}= 161–209 GeV
$0.25\ ^{+0.21}_{-0.20}\ \pm0.06$	2298	[79] ABREU	01I DLPH	E^{ee}_{cm}= 183+189 GeV
$0.022^{+0.119}_{-0.115}$	3586	[80] HEISTER	01C ALEP	E^{ee}_{cm}= 161–189 GeV
		[81] BREITWEG	00 ZEUS	$e^+p \rightarrow e^+W^{\pm}X$, $\sqrt{s}\approx$ 300 GeV
$-0.08\ \pm0.34$	331	[82] ABBOTT	99I D0	$E^{p\overline{p}}_{cm}$= 1.8 TeV
$0.11\ \pm0.25\ \pm0.17$	1154	[83] ACCIARRI	99Q L3	E^{ee}_{cm}= 161+172+ 183 GeV

[77] ABBIENDI 04D combine results from W^+W^- in all decay channels. Only CP-conserving couplings are considered and each parameter is determined from a single-parameter fit in which the other parameters assume their Standard Model values. The 95% confidence interval is $-0.27 < \Delta\kappa_\gamma < 0.07$.

[78] ACHARD 02I study single W production in e^+e^- interactions from 192 to 209 GeV. The result quoted here is obtained including data from 161 to 189 GeV, ACCIARRI 00N. The 95% C.L. limits are $-0.10 < \Delta\kappa_\gamma < 0.32$ (for λ_γ=0). When both couplings λ_γ and κ_γ are floated freely in the fit one obtains $\Delta\kappa_\gamma$= 0.07 ± 0.10 ± 0.07.

[79] ABREU 01I combine results from e^+e^- interactions at 189 GeV leading to W^+W^-, $We\nu_e$, and $\nu\overline{\nu}\gamma$ final states with results from ABREU 99L at 183 GeV. The 95% confidence interval is $-0.13 < \Delta\kappa_\gamma < 0.68$.

[80] HEISTER 01C study W-pair, single-W, and single photon events and combine with earlier results from BARATE,R 98, BARATE 98Y, and BARATE 99L to obtain the quoted value, fixing Δg^Z_1 and λ_γ to their Standard Model values. The 95% confidence interval is $-0.200 < \Delta\kappa_\gamma < 0.258$. When all three couplings Δg^Z_1, $\Delta\kappa_\gamma$, and λ_γ are floated freely in the fit, one obtains $\Delta\kappa_\gamma$= 0.043 ± 0.110.

[81] BREITWEG 00 search for W production in events with large hadronic p_T. For p_T >20 GeV, the upper limit on the cross section gives the 95%CL limit $-4.7 < \Delta\kappa_\gamma < 1.5$ (for λ_γ=0).

[82] ABBOTT 99I perform a simultaneous fit to the $W\gamma$, $WW \rightarrow$ dilepton, $WW/WZ \rightarrow e\nu jj$, $WW/WZ \rightarrow \mu\nu jj$, and $WZ \rightarrow$ trilepton data samples. For Λ = 2.0 TeV, the 95%CL limits are $-0.25 < \Delta\kappa_\gamma < 0.39$.

[83] ACCIARRI 99Q study W-pair, single-W, and single photon events.

λ_γ

Combining published and unpublished LEP results (as of Summer 2003), a single-parameter fit yields $\lambda_\gamma = -0.016^{+0.021}_{-0.023}$, where the other two parameters, Δg^Z_1 and $\Delta\kappa_\gamma$, were kept fixed to their Standard Model values.

(See EP Preprint Summer 2003: CERN-EP/2003-091 and hep-ex/0312023, December 2003, on http://lepewwg.web.cern.ch/LEPEWWG/stanmod/)

VALUE	*EVTS*	*DOCUMENT ID*	*TECN*	*COMMENT*
$\mathbf{-0.060^{+0.034}_{-0.033}}$	9800	[84] ABBIENDI	04D OPAL	E^{ee}_{cm}= 183–209 GeV
• • • We do not use the following data for averages, fits, limits, etc. • • •				
$0.35\ ^{+0.10}_{-0.13}\ \pm0.08$	315	[85] ACHARD	02I L3	E^{ee}_{cm}= 161–209 GeV
$0.05\ \pm0.09\ \pm0.01$	2298	[86] ABREU	01I DLPH	E^{ee}_{cm}= 183+189 GeV
$0.040^{+0.054}_{-0.052}$	3586	[87] HEISTER	01C ALEP	E^{ee}_{cm}= 161–189 GeV
		[88] BREITWEG	00 ZEUS	$e^+p \rightarrow e^+W^{\pm}X$, $\sqrt{s}\approx$ 300 GeV
$0.00\ ^{+0.10}_{-0.09}$	331	[89] ABBOTT	99I D0	$E^{p\overline{p}}_{cm}$= 1.8 TeV
$0.10\ ^{+0.22}_{-0.20}\ \pm0.10$	1154	[90] ACCIARRI	99Q L3	E^{ee}_{cm}= 161+172+ 183 GeV

[84] ABBIENDI 04D combine results from W^+W^- in all decay channels. Only CP-conserving couplings are considered and each parameter is determined from a single-parameter fit in which the other parameters assume their Standard Model values. The 95% confidence interval is $-0.13 < \lambda_\gamma < 0.01$.

[85] ACHARD 02I study single W production in e^+e^- interactions from 192 to 209 GeV. The result quoted here is obtained including data from 161 to 189 GeV, ACCIARRI 00N. The 95% C.L. limits are $-0.37 < \lambda_\gamma < 0.61$ (for κ_γ=1). When both couplings λ_γ and κ_γ are floated freely in the fit one obtains λ_γ= $0.31^{+0.12}_{-0.20}$ ± 0.07.

[86] ABREU 01I combine results from e^+e^- interactions at 189 GeV leading to W^+W^-, $We\nu_e$, and $\nu\overline{\nu}\gamma$ final states with results from ABREU 99L at 183 GeV. The 95% confidence interval is $-0.11 < \lambda_\gamma < 0.23$.

[87] HEISTER 01C study W-pair, single-W, and single photon events and combine with earlier results from BARATE,R 98, BARATE 98Y, and BARATE 99L to obtain the quoted value, fixing Δg^Z_1 and $\Delta\kappa_\gamma$ to their Standard Model values. The 95% confidence interval is $-0.062 < \lambda_\gamma < 0.147$. When all three couplings Δg^Z_1, $\Delta\kappa_\gamma$, and λ_γ are floated freely in the fit, one obtains λ_γ= $0.023^{+0.074}_{-0.077}$.

[88] BREITWEG 00 search for W production in events with large hadronic p_T. For p_T >20 GeV, the upper limit on the cross section gives the 95%CL limit $-3.2 < \lambda_\gamma < 3.2$ (for $\Delta\kappa_\gamma$=0).

[89] ABBOTT 99I perform a simultaneous fit to the $W\gamma$, $WW \rightarrow$ dilepton, $WW/WZ \rightarrow e\nu jj$, $WW/WZ \rightarrow \mu\nu jj$, and $WZ \rightarrow$ trilepton data samples. For Λ = 2.0 TeV, the 95%CL limits are $-0.18 < \lambda_\gamma < 0.19$.

[90] ACCIARRI 99Q study W-pair, single-W, and single photon events.

Δg^Z_5

This coupling is CP-conserving but C- and P-violating.

VALUE	*EVTS*	*DOCUMENT ID*	*TECN*	*COMMENT*
−0.11±0.16 OUR AVERAGE		Error includes scale factor of 1.4.		
$-0.04^{+0.13}_{-0.12}$	9800	[91] ABBIENDI	04D OPAL	E^{ee}_{cm}= 183–209 GeV
$-0.44^{+0.23}_{-0.22}\pm0.12$	1154	[92] ACCIARRI	99Q L3	E^{ee}_{cm}= 161+172+ 183 GeV
• • • We do not use the following data for averages, fits, limits, etc. • • •				
-0.16 ± 0.23		[93] EBOLI	00 THEO	LEP1, SLC+ Tevatron

[91] ABBIENDI 04D combine results from W^+W^- in all decay channels. Only CP-conserving couplings are considered and each parameter is determined from a single-parameter fit in which the other parameters assume their Standard Model values. The 95% confidence interval is $-0.28 < \Delta g^Z_5 < 0.21$.

[92] ACCIARRI 99Q study W-pair, single-W, and single photon events.

[93] EBOLI 00 extract this indirect value of the coupling studying the non-universal one-loop contributions to the experimental value of the $Z \rightarrow b\overline{b}$ width (Λ=1 TeV is assumed).

g^Z_4

This coupling is CP-violating (C-violating and P-conserving).

VALUE	*EVTS*	*DOCUMENT ID*	*TECN*	*COMMENT*
$\mathbf{-0.02^{+0.32}_{-0.33}}$	1065	[94] ABBIENDI	01H OPAL	E^{ee}_{cm}= 189 GeV

[94] ABBIENDI 01H study W-pair events, with one leptonically and one hadronically decaying W. The coupling is extracted using information from the W production angle together with decay angles from the leptonically decaying W.

$\widetilde{\kappa}_Z$

This coupling is CP-violating (C-conserving and P-violating).

VALUE	*EVTS*	*DOCUMENT ID*	*TECN*	*COMMENT*
$\mathbf{-0.20^{+0.10}_{-0.07}}$	1065	[95] ABBIENDI	01H OPAL	E^{ee}_{cm}= 189 GeV

[95] ABBIENDI 01H study W-pair events, with one leptonically and one hadronically decaying W. The coupling is extracted using information from the W production angle together with decay angles from the leptonically decaying W.

$\widetilde{\lambda}_Z$

This coupling is CP-violating (C-conserving and P-violating).

VALUE	*EVTS*	*DOCUMENT ID*	*TECN*	*COMMENT*
$\mathbf{-0.18^{+0.24}_{-0.16}}$	1065	[96] ABBIENDI	01H OPAL	E^{ee}_{cm}= 189 GeV

[96] ABBIENDI 01H study W-pair events, with one leptonically and one hadronically decaying W. The coupling is extracted using information from the W production angle together with decay angles from the leptonically decaying W.

W ANOMALOUS MAGNETIC MOMENT

The full magnetic moment is given by $\mu_W = e(1+\kappa+\lambda)/2m_W$. In the Standard Model, at tree level, $\kappa = 1$ and $\lambda = 0$. Some papers have defined $\Delta\kappa = 1-\kappa$ and assume that $\lambda = 0$. Note that the electric quadrupole moment is given by $-e(\kappa-\lambda)/m^2_W$. A description of the parameterization of these moments and additional references can be found in HAGIWARA 87 and BAUR 88. The parameter Λ appearing in the theoretical limits below is a regularization cutoff which roughly corresponds to the energy scale where the structure of the W boson becomes manifest.

VALUE ($e/2m_W$)	*EVTS*	*DOCUMENT ID*	*TECN*	*COMMENT*
$\mathbf{2.22^{+0.20}_{-0.19}}$	2298	[97] ABREU	01I DLPH	E^{ee}_{cm}= 183+189 GeV
• • • We do not use the following data for averages, fits, limits, etc. • • •				
		[98] ABE	95G CDF	
		[99] ALITTI	92C UA2	
		[100] SAMUEL	92 THEO	
		[101] SAMUEL	91 THEO	
		[102] GRIFOLS	88 THEO	
		[103] GROTCH	87 THEO	
		[104] VANDERBIJ	87 THEO	
		[105] GRAU	85 THEO	
		[106] SUZUKI	85 THEO	
		[107] HERZOG	84 THEO	

[97] ABREU 01I combine results from e^+e^- interactions at 189 GeV leading to W^+W^-, $We\nu_e$, and $\nu\overline{\nu}\gamma$ final states with results from ABREU 99L at 183 GeV to determine Δg^Z_1, $\Delta\kappa_\gamma$, and λ_γ. $\Delta\kappa_\gamma$ and λ_γ are simultaneously floated in the fit to determine μ_W.

[98] ABE 95G report $-1.3 < \kappa < 3.2$ for λ=0 and $-0.7 < \lambda < 0.7$ for κ=1 in $p\overline{p} \rightarrow e\nu_e\gamma X$ and $\mu\nu_\mu\gamma X$ at $\sqrt{s}$ = 1.8 TeV.

[99] ALITTI 92C measure $\kappa = 1^{+2.6}_{-2.2}$ and $\lambda = 0^{+1.7}_{-1.8}$ in $p\overline{p} \rightarrow e\nu\gamma + X$ at $\sqrt{s}$ = 630 GeV. At 95%CL they report $-3.5 < \kappa < 5.9$ and $-3.6 < \lambda < 3.5$.

[100] SAMUEL 92 use preliminary CDF and UA2 data and find $-2.4 < \kappa < 3.7$ at 96%CL and $-3.1 < \kappa < 4.2$ at 95%CL respectively. They use data for $W\gamma$ production and radiative W decay.

[101] SAMUEL 91 use preliminary CDF data for $p\overline{p} \rightarrow W\gamma X$ to obtain $-11.3 \leq \Delta\kappa \leq 10.9$. Note that their $\kappa = 1-\Delta\kappa$.

[102] GRIFOLS 88 uses deviation from ρ parameter to set limit $\Delta\kappa \lesssim 65\ (M^2_W/\Lambda^2)$.

[103] GROTCH 87 finds the limit $-37 < \Delta\kappa < 73.5$ (90% CL) from the experimental limits on $e^+e^- \rightarrow \nu\overline{\nu}\gamma$ assuming three neutrino generations and $-19.5 < \Delta\kappa < 56$ for four generations. Note their $\Delta\kappa$ has the opposite sign as our definition.

[104] VANDERBIJ 87 uses existing limits to the photon structure to obtain $|\Delta\kappa| < 33$ (m_W/Λ). In addition VANDERBIJ 87 discusses problems with using the ρ parameter of the Standard Model to determine $\Delta\kappa$.
[105] GRAU 85 uses the muon anomaly to derive a coupled limit on the anomalous magnetic dipole and electric quadrupole (λ) moments $1.05 > \Delta\kappa \ln(\Lambda/m_W) + \lambda/2 > -2.77$. In the Standard Model $\lambda = 0$.
[106] SUZUKI 85 uses partial-wave unitarity at high energies to obtain $|\Delta\kappa| \lesssim 190$ $(m_W/\Lambda)^2$. From the anomalous magnetic moment of the muon, SUZUKI 85 obtains $|\Delta\kappa| \lesssim 2.2/\ln(\Lambda/m_W)$. Finally SUZUKI 85 uses deviations from the ρ parameter and obtains a very qualitative, order-of-magnitude limit $|\Delta\kappa| \lesssim 150$ $(m_W/\Lambda)^4$ if $|\Delta\kappa| \ll 1$.
[107] HERZOG 84 consider the contribution of W-boson to muon magnetic moment including anomalous coupling of $WW\gamma$. Obtain a limit $-1 < \Delta\kappa < 3$ for $\Lambda \gtrsim 1$ TeV.

ANOMALOUS W/Z QUARTIC COUPLINGS

Revised November 2003 by C. Caso (University of Genova) and A. Gurtu (Tata Institute).

The Standard Model predictions for $WWWW$, $WWZZ$, $WWZ\gamma$, $WW\gamma\gamma$, and $ZZ\gamma\gamma$ couplings are small at LEP, but expected to become important at a TeV Linear Collider. Outside the Standard Model framework such possible couplings, a_0, a_c, a_n, are expressed in terms of the following dimension-6 operators [1,2];

$$L_6^0 = -\frac{e^2}{16\Lambda^2}\, a_0\, F^{\mu\nu}\, F_{\mu\nu} \vec{W}^\alpha \cdot \vec{W}_\alpha$$
$$L_6^c = -\frac{e^2}{16\Lambda^2}\, a_c\, F^{\mu\alpha}\, F_{\mu\beta} \vec{W}^\beta \cdot \vec{W}_\alpha$$
$$L_6^n = -i\frac{e^2}{16\Lambda^2}\, a_n \epsilon_{ijk}\, W_{\mu\alpha}^{(i)}\, W_\nu^{(j)}\, W^{(k)\alpha} F^{\mu\nu}$$
$$\widetilde{L}_6^0 = -\frac{e^2}{16\Lambda^2}\, \widetilde{a}_0\, F^{\mu\nu}\, \widetilde{F}_{\mu\nu} \vec{W}^\alpha \cdot \vec{W}_\alpha$$
$$\widetilde{L}_6^n = -i\frac{e^2}{16\Lambda^2}\, \widetilde{a}_n \epsilon_{ijk}\, W_{\mu\alpha}^{(i)}\, W_\nu^{(j)}\, W^{(k)\alpha} \widetilde{F}^{\mu\nu}$$

where F, W are photon and W fields, L_6^0 and L_6^c conserve C, P separately ($\widetilde{L}_6^0$ conserves only C) and generate anomalous $W^+W^-\gamma\gamma$ and $ZZ\gamma\gamma$ couplings, L_6^n violates CP ($\widetilde{L}_6^n$ violates both C and P) and generates an anomalous $W^+W^-Z\gamma$ coupling, and Λ is a scale for new physics. For the $ZZ\gamma\gamma$ coupling the CP-violating term represented by L_6^n does not contribute. These couplings are assumed to be real and to vanish at tree level in the Standard Model.

Within the same framework as above, a more recent description of the quartic couplings [3] treats the anomalous parts of the $WW\gamma\gamma$ and $ZZ\gamma\gamma$ couplings separately leading to two sets parameterized as a_0^V/Λ^2 and a_c^V/Λ^2, where $V = W$ or Z.

At LEP the processes studied in search of these quartic couplings are $e^+e^- \to WW\gamma$, $e^+e^- \to \gamma\gamma\nu\overline{\nu}$, and $e^+e^- \to Z\gamma\gamma$ and limits are set on the quantities $a_0^W/\Lambda^2, a_c^W/\Lambda^2, a_n/\Lambda^2$. The characteristics of the first process depend on all the three couplings whereas those of the latter two depend only on the two CP-conserving couplings. The sensitive measured variables are the cross sections for these processes as well as the energy and angular distributions of the photon and recoil mass to the photon pair.

References

1. G. Belanger and F. Boudjema, Phys. Lett. **B288**, 201 (1992).
2. J.W. Stirling and A. Werthenbach, Eur. Phys. J. **C14**, 103 (2000);
J.W. Stirling and A. Werthenbach, Phys. Lett. **B466**, 369 (1999);
A. Denner *et al.*, Eur. Phys. J. **C20**, 201 (2001);
G. Montagna *et al.*, Phys. Lett. **B515**, 197 (2001).
3. G. Belanger *et al.*, Eur. Phys. J. **C13**, 103 (2000).

a_0/Λ^2, a_c/Λ^2, a_n/Λ^2

Using the $WW\gamma$ final state, the LEP combined 95% CL limits on the anomalous contributions to the $WW\gamma\gamma$ and $WWZ\gamma$ vertices (as of summer 2003) are given below:

(See P. Wells, "Experimental Tests of the Standard Model," Int. Europhysics Conference on High-Energy Physics, Aachen, Germany, 17–23 July 2003)

$$-0.02 < a_0^W/\Lambda^2 < 0.02 \text{ GeV}^{-2},$$
$$-0.05 < a_c^W/\Lambda^2 < 0.03 \text{ GeV}^{-2},$$
$$-0.15 < a_n/\Lambda^2 < 0.15 \text{ GeV}^{-2}.$$

VALUE	DOCUMENT ID		TECN
• • • We do not use the following data for averages, fits, limits, etc. • • •			
	[108] ABBIENDI	04B	OPAL
	[109] ABDALLAH	03I	DLPH
	[110] ACHARD	02F	L3

[108] ABBIENDI 04B select 187 $e^+e^- \to W^+W^-\gamma$ events in the C.M. energy range 180–209 GeV, where $E_\gamma >$2.5 GeV, the photon has a polar angle $|\cos\theta_\gamma| < 0.975$ and is well isolated from the nearest jet and charged lepton, and the effective masses of both fermion-antifermion systems agree with the W mass within 3 Γ_W. The measured differential cross section as a function of the photon energy and photon polar angle is used to extract the 95% CL limits: -0.020 GeV^{-2} $< a_0/\Lambda^2 < 0.020$ GeV^{-2}, -0.053 GeV^{-2} $< a_c/\Lambda^2 < 0.037$ GeV^{-2} and -0.16 GeV^{-2} $< a_n/\Lambda^2 < 0.15$ GeV^{-2}.
[109] ABDALLAH 03I select 122 $e^+e^- \to W^+W^-\gamma$ events in the C.M. energy range 189–209 GeV, where $E_\gamma >$5 GeV, the photon has a polar angle $|\cos\theta_\gamma| < 0.95$ and is well isolated from the nearest charged fermion. A fit to the photon energy spectra yields $a_c/\Lambda^2 = 0.000^{+0.019}_{-0.040}$ GeV^{-2}, $a_0/\Lambda^2 = -0.004^{+0.018}_{-0.010}$ GeV^{-2}, $\tilde{a}_0/\Lambda^2 = -0.007^{+0.019}_{-0.008}$ GeV^{-2}, $a_n/\Lambda^2 = -0.09^{+0.16}_{-0.05}$ GeV^{-2}, and $\tilde{a}_n/\Lambda^2 = +0.05^{+0.07}_{-0.15}$ GeV^{-2}, keeping the other parameters fixed to their Standard Model values (0). The 95% CL limits are: -0.063 GeV^{-2} $< a_c/\Lambda^2 < +0.032$ GeV^{-2}, -0.020 GeV^{-2} $< a_0/\Lambda^2 < +0.020$ GeV^{-2}, -0.020 GeV^{-2} $< \tilde{a}_0/\Lambda^2 < +0.020$ GeV^{-2}, -0.18 GeV^{-2} $< a_n/\Lambda^2 < +0.14$ GeV^{-2}, -0.16 GeV^{-2} $< \tilde{a}_n/\Lambda^2 < +0.17$ GeV^{-2}.
[110] ACHARD 02F select 86 $e^+e^- \to W^+W^-\gamma$ events at 192–207 GeV, where $E_\gamma >$5 GeV and the photon is well isolated. They also select 43 acoplanar $e^+e^- \to \nu\overline{\nu}\gamma\gamma$ events in this energy range, where the photon energies are $>$5 GeV and $>$1 GeV and the photon polar angles are between 14° and 166°. All these 43 events are in the recoil mass region corresponding to the Z (75–110 GeV). Using the shape and normalization of the photon spectra in the $W^+W^-\gamma$ events, and combining with the 42 event sample from 189 GeV data (ACCIARRI 00T), they obtain: $a_0/\Lambda^2 = 0.000 \pm 0.010$ GeV^{-2}, $a_c/\Lambda^2 = -0.013 \pm 0.023$ GeV^{-2}, and $a_n/\Lambda^2 = -0.002 \pm 0.076$ GeV^{-2}. Further combining the analyses of $W^+W^-\gamma$ events with the low recoil mass region of $\nu\overline{\nu}\gamma\gamma$ events (including samples collected at 183 + 189 GeV), they obtain the following one-parameter 95% CL limits: -0.015 GeV^{-2} $< a_0/\Lambda^2 < 0.015$ GeV^{-2}, -0.048 GeV^{-2} $< a_c/\Lambda^2 < 0.026$ GeV^{-2}, and -0.14 GeV^{-2} $< a_n/\Lambda^2 < 0.13$ GeV^{-2}.

W REFERENCES

ABBIENDI	04B	PL B580 17	G. Abbiendi *et al.*	(OPAL Collab.)
ABBIENDI	04D	EPJ C33 463	G. Abbiendi *et al.*	(OPAL Collab.)
ABBIENDI	03C	EPJ C26 321	G. Abbiendi *et al.*	(OPAL Collab.)
ABDALLAH	03I	EPJ C31 139	J. Abdallah *et al.*	(DELPHI Collab.)
ABAZOV	02D	PR D66 012001	V.M. Abazov *et al.*	(D0 Collab.)
ABAZOV	02E	PR D66 032008	V.M. Abazov *et al.*	(D0 Collab.)
ACHARD	02F	PL B527 29	P. Achard *et al.*	(L3 Collab.)
ACHARD	02I	PL B547 151	P. Achard *et al.*	(L3 Collab.)
CHEKANOV	02C	PL B539 197	S. Chekanov *et al.*	(ZEUS Collab.)
KOTWAL	02	FERMILAB-FN-0716	A. Kotwal *et al.*	
ABBIENDI	01F	PL B507 29	G. Abbiendi *et al.*	(OPAL Collab.)
ABBIENDI	01H	EPJ C19 229	G. Abbiendi *et al.*	(OPAL Collab.)
ABREU	01I	PL B502 9	P. Abreu *et al.*	(DELPHI Collab.)
ABREU	01K	PL B511 159	P. Abreu *et al.*	(DELPHI Collab.)
ADLOFF	01A	EPJ C19 269	C. Adloff *et al.*	(H1 Collab.)
AFFOLDER	01E	PR D64 052001	T. Affolder *et al.*	(CDF Collab.)
HEISTER	01C	EPJ C21 423	A. Heister *et al.*	(ALEPH Collab.)
ABBIENDI	00V	PL B490 71	G. Abbiendi *et al.*	(OPAL Collab.)
ABBIENDI,G	00	PL B493 249	G. Abbiendi *et al.*	(OPAL Collab.)
ABBOTT	00	PRL 84 222	B. Abbott *et al.*	(D0 Collab.)
ABBOTT	00B	PR D61 072001	B. Abbott *et al.*	(D0 Collab.)
ABBOTT	00D	PRL 84 5710	B. Abbott *et al.*	(D0 Collab.)
ABREU	00K	PL B479 89	P. Abreu *et al.*	(DELPHI Collab.)
ABREU,P	00F	EPJ C18 203	P. Abreu *et al.*	(DELPHI Collab.)
Also	02	EPJ C25 493 (erratum)	P. Abreu *et al.*	(DELPHI Collab.)
ACCIARRI	00N	PL B487 229	M. Acciarri *et al.*	(L3 Collab.)
ACCIARRI	00T	PL B490 187	M. Acciarri *et al.*	(L3 Collab.)
ACCIARRI	00V	PL B496 19	M. Acciarri *et al.*	(L3 Collab.)
ADLOFF	00B	EPJ C13 609	C. Adloff *et al.*	(H1 Collab.)
AFFOLDER	00M	PRL 85 3347	T. Affolder *et al.*	(CDF Collab.)
BARATE	00J	PL B484 205	R. Barate *et al.*	(ALEPH Collab.)
BARATE	00T	EPJ C17 241	R. Barate *et al.*	(ALEPH Collab.)
BREITWEG	00	PL B471 411	J. Breitweg *et al.*	(ZEUS Collab.)
BREITWEG	00D	EPJ C12 411	J. Breitweg *et al.*	(ZEUS Collab.)
EBOLI	00	MPL A15 1	O. Eboli, M. Gonzalez-Garcia, S. Novaes	
ABBIENDI	99C	PL B453 138	G. Abbiendi *et al.*	(OPAL Collab.)
ABBIENDI	99D	EPJ C8 191	G. Abbiendi *et al.*	(OPAL Collab.)
ABBIENDI	99N	PL B453 153	G. Abbiendi *et al.*	(OPAL Collab.)
ABBOTT	99H	PR D60 052003	B. Abbott *et al.*	(D0 Collab.)
ABBOTT	99I	PR D60 072002	B. Abbott *et al.*	(D0 Collab.)
ABREU	99K	PL B456 310	P. Abreu *et al.*	(DELPHI Collab.)
ABREU	99L	PL B459 382	P. Abreu *et al.*	(DELPHI Collab.)
ABREU	99T	PL B462 410	P. Abreu *et al.*	(DELPHI Collab.)
ACCIARRI	99	PL B454 386	M. Acciarri *et al.*	(L3 Collab.)
ACCIARRI	99Q	PL B467 171	M. Acciarri *et al.*	(L3 Collab.)
BARATE	99	PL B453 121	R. Barate *et al.*	(ALEPH Collab.)
BARATE	99I	PL B453 107	R. Barate *et al.*	(ALEPH Collab.)
BARATE	99L	PL B462 389	R. Barate *et al.*	(ALEPH Collab.)
BARATE	99M	PL B465 349	R. Barate *et al.*	(ALEPH Collab.)
ABBOTT	98N	PR D58 092003	B. Abbott *et al.*	(D0 Collab.)
ABBOTT	98P	PR D58 012002	B. Abbott *et al.*	(D0 Collab.)
ABE	98H	PR D58 031101	F. Abe *et al.*	(CDF Collab.)

ABE	98P	PR D58 091101	F. Abe *et al.*	(CDF Collab.)
ABREU	98C	PL B416 233	P. Abreu *et al.*	(DELPHI Collab.)
ABREU	98N	PL B439 209	P. Abreu *et al.*	(DELPHI Collab.)
ACCIARRI	98P	PL B436 437	M. Acciarri *et al.*	(L3 Collab.)
BARATE	98Y	PL B422 369	R. Barate *et al.*	(ALEPH Collab.)
BARATE,R	98	PL B445 239	R. Barate *et al.*	(ALEPH Collab.)
ACCIARRI	97	PL B398 223	M. Acciarri *et al.*	(L3 Collab.)
ACCIARRI	97M	PL B407 419	M. Acciarri *et al.*	(L3 Collab.)
ACCIARRI	97S	PL B413 176	M. Acciarri *et al.*	(L3 Collab.)
ABACHI	95D	PRL 75 1456	S. Abachi *et al.*	(D0 Collab.)
ABE	95C	PRL 74 341	F. Abe *et al.*	(CDF Collab.)
ABE	95G	PRL 74 1936	F. Abe *et al.*	(CDF Collab.)
ABE	95P	PRL 75 11	F. Abe *et al.*	(CDF Collab.)
Also	95Q	PR D52 4784	F. Abe *et al.*	(CDF Collab.)
ABE	95W	PR D52 2624	F. Abe *et al.*	(CDF Collab.)
Also	94B	PRL 73 220	F. Abe *et al.*	(CDF Collab.)
ABE	92E	PRL 68 3398	F. Abe *et al.*	(CDF Collab.)
ABE	92I	PRL 69 28	F. Abe *et al.*	(CDF Collab.)
ALITTI	92	PL B276 365	J. Alitti *et al.*	(UA2 Collab.)
ALITTI	92B	PL B276 354	J. Alitti *et al.*	(UA2 Collab.)
ALITTI	92C	PL B277 194	J. Alitti *et al.*	(UA2 Collab.)
ALITTI	92D	PL B277 203	J. Alitti *et al.*	(UA2 Collab.)
ALITTI	92F	PL B280 137	J. Alitti *et al.*	(UA2 Collab.)
SAMUEL	92	PL B280 124	M.A. Samuel *et al.*	(OKSU, CARL)
ABE	91C	PR D44 29	F. Abe *et al.*	(CDF Collab.)
ALBAJAR	91	PL B253 503	C. Albajar *et al.*	(UA1 Collab.)
ALITTI	91C	ZPHY C52 209	J. Alitti *et al.*	(UA2 Collab.)
SAMUEL	91	PRL 67 9	M.A. Samuel *et al.*	(OKSU, CARL)
Also	91C	PRL 67 2920 erratum	M.A. Samuel *et al.*	
ABE	90	PRL 64 152	F. Abe *et al.*	(CDF Collab.)
Also	91C	PR D44 29	F. Abe *et al.*	(CDF Collab.)
ABE	90G	PRL 65 2243	F. Abe *et al.*	(CDF Collab.)
Also	91B	PR D43 2070	F. Abe *et al.*	(CDF Collab.)
ALBAJAR	90	PL B241 283	C. Albajar *et al.*	(UA1 Collab.)
ALITTI	90B	PL B241 150	J. Alitti *et al.*	(UA2 Collab.)
ALITTI	90C	ZPHY C47 11	J. Alitti *et al.*	(UA2 Collab.)
ABE	89I	PRL 62 1005	F. Abe *et al.*	(CDF Collab.)
ALBAJAR	89	ZPHY C44 15	C. Albajar *et al.*	(UA1 Collab.)
BAUR	88	NP B308 127	U. Baur, D. Zeppenfeld	(FSU, WISC)
GRIFOLS	88	IJMP A3 225	J.A. Grifols, S. Peris, J. Sola	(BARC, DESY)
Also	87	PL B197 437	J.A. Grifols, S. Peris, J. Sola	(BARC, DESY)
ALBAJAR	87	PL B185 233	C. Albajar *et al.*	(UA1 Collab.)
ANSARI	87	PL B186 440	R. Ansari *et al.*	(UA2 Collab.)
ANSARI	87C	PL B194 158	R. Ansari *et al.*	(UA2 Collab.)
GROTCH	87	PR D36 2153	H. Grotch, R.W. Robinett	(PSU)
HAGIWARA	87	NP B282 253	K. Hagiwara *et al.*	(KEK, UCLA, FSU)
VANDERBIJ	87	PR D35 1088	J.J. van der Bij	(FNAL)
APPEL	86	ZPHY C30 1	J.A. Appel *et al.*	(UA2 Collab.)
ARNISON	86	PL 166B 484	G.T.J. Arnison *et al.*	(UA1 Collab.) J
ALTARELLI	85B	ZPHY C27 617	G. Altarelli, R.K. Ellis, G. Martinelli	(CERN+)
GRAU	85	PL 154B 283	A. Grau, J.A. Grifols	(BARC)
SUZUKI	85	PL 153B 289	M. Suzuki	(LBL)
ARNISON	84D	PL 134B 469	G.T.J. Arnison *et al.*	(UA1 Collab.)
HERZOG	84	PL 148B 355	F. Herzog	(WISC)
Also	84B	PL 155B 468 erratum	F. Herzog	(WISC)
ARNISON	83	PL 122B 103	G.T.J. Arnison *et al.*	(UA1 Collab.)
BANNER	83B	PL 122B 476	M. Banner *et al.*	(UA2 Collab.)

Z

$J = 1$

THE Z BOSON

Revised November 2003 by C. Caso (University of Genova) and A. Gurtu (Tata Institute).

Precision measurements at the Z-boson resonance using electron–positron colliding beams began in 1989 at the SLC and at LEP. During 1989–95, the four CERN experiments made high-statistics studies of the Z. The availability of longitudinally polarized electron beams at the SLC since 1993 enabled a precision determination of the effective electroweak mixing angle $\sin^2\overline{\theta}_W$ that is competitive with the CERN results on this parameter.

The Z-boson properties reported in this section may broadly be categorized as:

- The standard 'lineshape' parameters of the Z consisting of its mass, M_Z, its total width, Γ_Z, and its partial decay widths, Γ(hadrons), and $\Gamma(\ell\overline{\ell})$ where $\ell = e, \mu, \tau, \nu$;
- Z asymmetries in leptonic decays and extraction of Z couplings to charged and neutral leptons;
- The b- and c-quark-related partial widths and charge asymmetries which require special techniques;
- Determination of Z decay modes and the search for modes that violate known conservation laws;
- Average particle multiplicities in hadronic Z decay;
- Z anomalous couplings.

Details on Z-parameter determination and the study of $Z \to b\overline{b}, c\overline{c}$ at LEP and SLC are given in this note.

The standard 'lineshape' parameters of the Z are determined from an analysis of the production cross sections of these final states in e^+e^- collisions. The $Z \to \nu\overline{\nu}(\gamma)$ state is identified directly by detecting single photon production and indirectly by subtracting the visible partial widths from the total width. Inclusion in this analysis of the forward-backward asymmetry of charged leptons, $A_{FB}^{(0,\ell)}$, of the τ polarization, $P(\tau)$, and its forward-backward asymmetry, $P(\tau)^{fb}$, enables the separate determination of the effective vector ($\overline{g}_V$) and axial vector ($\overline{g}_A$) couplings of the Z to these leptons and the ratio ($\overline{g}_V/\overline{g}_A$) which is related to the effective electroweak mixing angle $\sin^2\overline{\theta}_W$ (see the "Electroweak Model and Constraints on New Physics" Review).

Determination of the b- and c-quark-related partial widths and charge asymmetries involves tagging the b and c quarks. Traditionally this was done by requiring the presence of a prompt lepton in the event with high momentum and high transverse momentum (with respect to the accompanying jet). Precision vertex measurement with high-resolution detectors enabled one to do impact parameter and lifetime tagging. Neural-network techniques have also been used to classify events as b or non-b on a statistical basis using event–shape variables. Finally, the presence of a charmed meson (D/D^*) has been used to tag heavy quarks.

Z-parameter determination

LEP was run at energy points on and around the Z mass (88–94 GeV) constituting an energy 'scan.' The shape of the cross-section variation around the Z peak can be described by a Breit-Wigner *ansatz* with an energy-dependent total width [1–3]. The **three** main properties of this distribution, viz., the **position** of the peak, the **width** of the distribution, and the **height** of the peak, determine respectively the values of M_Z, Γ_Z, and $\Gamma(e^+e^-) \times \Gamma(f\overline{f})$, where $\Gamma(e^+e^-)$ and $\Gamma(f\overline{f})$ are the electron and fermion partial widths of the Z. The quantitative determination of these parameters is done by writing analytic expressions for these cross sections in terms of the parameters and fitting the calculated cross sections to the measured ones by varying these parameters, taking properly into account all the errors. Single-photon exchange (σ_γ^0) and γ-Z interference ($\sigma_{\gamma Z}^0$) are included, and the large ($\sim$25 %) initial-state radiation (ISR) effects are taken into account by convoluting the analytic expressions over a 'Radiator Function' [1–5] $H(s, s')$. Thus for the process $e^+e^- \to f\overline{f}$:

$$\sigma_f(s) = \int H(s, s')\ \sigma_f^0(s')\ ds' \tag{1}$$

$$\sigma_f^0(s) = \sigma_Z^0 + \sigma_\gamma^0 + \sigma_{\gamma Z}^0 \tag{2}$$

$$\sigma_Z^0 = \frac{12\pi}{M_Z^2}\ \frac{\Gamma(e^+e^-)\Gamma(f\overline{f})}{\Gamma_Z^2}\ \frac{s\ \Gamma_Z^2}{(s - M_Z^2)^2\ +\ s^2\Gamma_Z^2/M_Z^2} \tag{3}$$

$$\sigma_\gamma^0 = \frac{4\pi\alpha^2(s)}{3s}\ Q_f^2 N_c^f \tag{4}$$

$$\sigma^0_{\gamma Z} = -\frac{2\sqrt{2}\alpha(s)}{3}\ (Q_f G_F N_c^f \mathcal{G}_V^e \mathcal{G}_V^f) \times \frac{(s-M_Z^2)M_Z^2}{(s-M_Z^2)^2 + s^2\Gamma_Z^2/M_Z^2} \qquad (5)$$

where Q_f is the charge of the fermion, $N_c^f = 3(1)$ for quark (lepton) and $\mathcal{G}_V^f$ is the neutral vector coupling of the Z to the fermion-antifermion pair $f\overline{f}$.

Since $\sigma^0_{\gamma Z}$ is expected to be much less than σ^0_Z, the LEP Collaborations have generally calculated the interference term in the framework of the Standard Model. This fixing of $\sigma^0_{\gamma Z}$ leads to a tighter constraint on M_Z and consequently a smaller error on its fitted value.

In the above framework, the QED radiative corrections have been explicitly taken into account by convoluting over the ISR and allowing the electromagnetic coupling constant to run [9]: $\alpha(s) = \alpha/(1-\Delta\alpha)$. On the other hand, weak radiative corrections that depend upon the assumptions of the electroweak theory and on the values of $M_{\rm top}$ and $M_{\rm Higgs}$ are accounted for by **absorbing them into the couplings**, which are then called the *effective* couplings $\mathcal{G}_V$ and $\mathcal{G}_A$ (or alternatively the effective parameters of the $\star$ scheme of Kennedy and Lynn [10]).

$\mathcal{G}_V^f$ and $\mathcal{G}_A^f$ are complex numbers with a small imaginary part. As experimental data does not allow simultaneous extraction of both real and imaginary parts of the effective couplings, the convention $g_A^f = {\rm Re}(\mathcal{G}_A^f)$ and $g_V^f = {\rm Re}(\mathcal{G}_V^f)$ is used and the imaginary parts are added in the fitting code [4].

Defining

$$A_f = 2\frac{g_V^f \cdot g_A^f}{(g_V^f)^2 + (g_A^f)^2} \qquad (6)$$

the lowest-order expressions for the various lepton-related asymmetries on the Z pole are [6–8] $A_{FB}^{(0,\ell)} = (3/4)A_e A_f$, $P(\tau) = -A_\tau$, $P(\tau)^{fb} = -(3/4)A_e$, $A_{LR} = A_e$. The full analysis takes into account the energy dependence of the asymmetries. Experimentally A_{LR} is defined as $(\sigma_L - \sigma_R)/(\sigma_L + \sigma_R)$ where $\sigma_{L(R)}$ are the $e^+e^- \rightarrow Z$ production cross sections with left-(right)-handed electrons.

The definition of the partial decay width of the Z to $f\overline{f}$ includes the effects of QED and QCD final state corrections as well as the contribution due to the imaginary parts of the couplings:

$$\Gamma(f\overline{f}) = \frac{G_F M_Z^3}{6\sqrt{2}\pi}\ N_c^f\left(\left|\mathcal{G}_A^f\right|^2 R_A^f + \left|\mathcal{G}_V^f\right|^2 R_V^f\right) + \Delta_{ew/{\rm QCD}} \qquad (7)$$

where R_V^f and R_A^f are radiator factors to account for final state QED and QCD corrections as well as effects due to nonzero fermion masses, and $\Delta_{ew/{\rm QCD}}$ represents the non-factorizable electroweak/QCD corrections.

S-matrix approach to the Z

While practically all experimental analyses of LEP/SLC data have followed the 'Breit-Wigner' approach described above, an alternative S-matrix-based analysis is also possible. The Z, like all unstable particles, is associated with a complex pole in the S matrix. The pole position is process independent and gauge invariant. The mass, $\overline{M}_Z$, and width, $\overline{\Gamma}_Z$, can be defined in terms of the pole in the energy plane via [11–14]

$$\overline{s} = \overline{M}_Z^2 - i\overline{M}_Z\overline{\Gamma}_Z \qquad (8)$$

leading to the relations

$$\overline{M}_Z = M_Z/\sqrt{1+\Gamma_Z^2/M_Z^2} \approx M_Z\ - 34.1\ {\rm MeV} \qquad (9)$$

$$\overline{\Gamma}_Z = \Gamma_Z/\sqrt{1+\Gamma_Z^2/M_Z^2} \approx \Gamma_Z\ - 0.9\ {\rm MeV}\ . \qquad (10)$$

Some authors [15] choose to define the Z mass and width via

$$\overline{s} = (\overline{M}_Z - \frac{i}{2}\overline{\Gamma}_Z)^2 \qquad (11)$$

which yields $\overline{M}_Z \approx M_Z - 26$ MeV, $\overline{\Gamma}_Z \approx \Gamma_Z - 1.2$ MeV.

The L3 and OPAL Collaborations at LEP (ACCIARRI 00Q and ACKERSTAFF 97C) have analyzed their data using the S–matrix approach as defined in Eq. (8), in addition to the conventional one. They observe a downward shift in the Z mass as expected.

Handling the large-angle e^+e^- final state

Unlike other $f\overline{f}$ decay final states of the Z, the e^+e^- final state has a contribution not only from the s-channel but also from the t-channel and s-t interference. The full amplitude is not amenable to fast calculation, which is essential if one has to carry out minimization fits within reasonable computer time. The usual procedure is to calculate the non-s channel part of the cross section separately using the Standard Model programs ALIBABA [16] or TOPAZ0 [17] with the measured value of $M_{\rm top}$, and $M_{\rm Higgs} = 150$ GeV and add it to the s-channel cross section calculated as for other channels. This leads to two additional sources of error in the analysis: firstly, the theoretical calculation in ALIBABA itself is known to be accurate to $\sim 0.5\%$, and secondly, there is uncertainty due to the error on $M_{\rm top}$ and the unknown value of $M_{\rm Higgs}$ (100–1000 GeV). These errors are propagated into the analysis by including them in the systematic error on the e^+e^- final state. As these errors are common to the four LEP experiments, this is taken into account when performing the LEP average.

Errors due to uncertainty in LEP energy determination [18–23]

The systematic errors related to the LEP energy measurement can be classified as:

- The absolute energy scale error;
- Energy-point-to-energy-point errors due to the non-linear response of the magnets to the exciting currents;
- Energy-point-to-energy-point errors due to possible higher-order effects in the relationship between the dipole field and beam energy;
- Energy reproducibility errors due to various unknown uncertainties in temperatures, tidal effects, corrector settings, RF status, *etc.*

Precise energy calibration was done outside normal data taking using the resonant depolarization technique. Run-time energies were determined every 10 minutes by measuring the relevant machine parameters and using a model which takes into account all the known effects, including leakage currents produced by trains in the Geneva area and the tidal effects due to gravitational forces of the Sun and the Moon. The LEP Energy Working Group has provided a covariance matrix from the determination of LEP energies for the different running periods during 1993–1995 [18].

Choice of fit parameters

The LEP Collaborations have chosen the following primary set of parameters for fitting: M_Z, Γ_Z, $\sigma^0_{\rm hadron}$, R(lepton), $A^{(0,\ell)}_{FB}$, where R(lepton) = Γ(hadrons)/Γ(lepton), $\sigma^0_{\rm hadron} = 12\pi\Gamma(e^+e^-)\Gamma({\rm hadrons})/M^2_Z\Gamma^2_Z$. With a knowledge of these fitted parameters and their covariance matrix, any other parameter can be derived. The main advantage of these parameters is that they form the **least correlated** set of parameters, so that it becomes easy to combine results from the different LEP experiments.

Thus, the most general fit carried out to cross section and asymmetry data determines the **nine parameters**: M_Z, Γ_Z, $\sigma^0_{\rm hadron}$, $R(e)$, $R(\mu)$, $R(\tau)$, $A^{(0,e)}_{FB}$, $A^{(0,\mu)}_{FB}$, $A^{(0,\tau)}_{FB}$. Assumption of lepton universality leads to a **five-parameter fit** determining M_Z, Γ_Z, $\sigma^0_{\rm hadron}$, R(lepton), $A^{(0,\ell)}_{FB}$.

Combining results from LEP and SLC experiments

With steady increase in statistics over the years and improved understanding of the common systematic errors between LEP experiments, the procedures for combining results have evolved continuously [24]. The Line Shape Sub-group of the LEP Electroweak Working Group investigated the effects of these common errors and devised a combination procedure for the precise determination of the Z parameters from LEP experiments [25]. Using these procedures this note also gives the results after combining the final parameter sets from the four experiments and these are the results quoted as the fit results in the Z listings below. Transformation of variables leads to values of derived parameters like partial decay widths and branching ratios to hadrons and leptons. Finally, transforming the LEP combined nine parameter set to (M_Z, Γ_Z, $\sigma^\circ_{\rm hadron}$, g^f_A, g^f_V, $f = e, \mu, \tau$) using the average values of lepton asymmetry parameters (A_e, A_μ, A_τ) as constraints, leads to the best fitted values of the vector and axial-vector couplings (g_V, g_A) of the charged leptons to the Z.

Brief remarks on the handling of common errors and their magnitudes are given below. The identified common errors are those coming from

(a) LEP energy calibration uncertainties, and

(b) the theoretical uncertainties in (i) the luminosity determination using small angle Bhabha scattering, (ii) estimating the non-s channel contribution to large angle Bhabha scattering, (iii) the calculation of QED radiative effects, and (iv) the parametrization of the cross section in terms of the parameter set used.

Common LEP energy errors

All the collaborations incorporate in their fit the full LEP energy error matrix as provided by the LEP energy group for their intersection region [18]. The effect of these errors is separated out from that of other errors by carrying out fits with energy errors scaled up and down by $\sim$ 10% and redoing the fits. From the observed changes in the overall error matrix the covariance matrix of the common energy errors is determined. Common LEP energy errors lead to uncertainties on M_Z, Γ_Z, and $\sigma^\circ_{\rm hadron}$ of 1.7, 1.2 MeV, and 0.011 nb respectively.

Common luminosity errors

BHLUMI 4.04 [26] is used by all LEP collaborations for small angle Bhabha scattering leading to a common uncertainty in their measured cross sections of 0.061% [27]. BHLUMI does not include a correction for production of light fermion pairs. OPAL explicitly correct for this effect and reduce their luminosity uncertainty to 0.054% which is taken fully correlated with the other experiments. The other three experiments among themselves have a common uncertainty of 0.061%.

Common non-s channel uncertainties

The same standard model programs ALIBABA [16] and TOPAZ0 [17] are used to calculate the non-s channel contribution to the large angle Bhabha scattering [28]. As this contribution is a function of the Z mass, which itself is a variable in the fit, it is parametrized as a function of M_Z by each collaboration to properly track this contribution as M_Z varies in the fit. The common errors on R_e and $A^{0,e}_{FB}$ are 0.024 and 0.0014 respectively and are correlated between them.

Common theoretical uncertainties: QED

There are large initial state photon and fermion pair radiation effects near the Z resonance for which the best currently available evaluations include contributions up to $\mathcal{O}(\alpha^3)$. To estimate the remaining uncertainties different schemes are incorporated in the standard model programs ZFITTER [5], TOPAZ0 [17] and MIZA [29]. Comparing the different options leads to error estimates of 0.3 and 0.2 MeV on M_Z and Γ_Z respectively and of 0.02% on $\sigma^\circ_{\rm hadron}$.

Common theoretical uncertainties: parametrization of lineshape and asymmetries

To estimate uncertainties arising from ambiguities in the model-independent parametrization of the differential cross-section near the Z resonance, results from TOPAZ0 and ZFITTER were compared by using ZFITTER to fit the cross sections and asymmetries calculated using TOPAZ0. The resulting uncertainties on M_Z, Γ_Z, $\sigma^\circ_{\rm hadron}$, R(lepton) and $A^{0,\ell}_{FB}$ are 0.1 MeV, 0.1 MeV, 0.001 nb, 0.004, and 0.0001 respectively.

Thus the overall theoretical errors on M_Z, Γ_Z, $\sigma^\circ_{\rm hadron}$ are 0.3 MeV, 0.2 MeV, and 0.008 nb respectively; on each R(lepton) is 0.004 and on each $A^{0,\ell}_{FB}$ is 0.0001. Within the set of three

R(lepton)'s and the set of three $A_{FB}^{0,\ell}$'s the respective errors are fully correlated.

All the theory related errors mentioned above utilize standard model programs which need the Higgs mass and running electromagnetic coupling constant as inputs; uncertainties on these inputs will also lead to common errors. All LEP collaborations used the same set of inputs for standard model calculations: $M_Z = 91.187$ GeV, the Fermi constant $G_F = (1.16637 \pm 0.00001) \times 10^{-5}$ GeV^{-2} [30], $\alpha^{(5)}(M_Z) = 1/128.877 \pm 0.090$ [31], $\alpha_s(M_Z) = 0.119$ [32], $M_{\text{top}} = 174.3 \pm 5.1$ GeV [32] and $M_{\text{Higgs}} = 150$ GeV. The only observable effect, on M_Z, is due to the variation of M_{Higgs} between 100–1000 GeV (due to the variation of the γ/Z interference term which is taken from the standard model): M_Z changes by $+0.23$ MeV per unit change in $\log_{10} M_{\text{Higgs}}/\text{GeV}$, which is not an error but a correction to be applied once M_{Higgs} is determined. The effect is much smaller than the error on M_Z (± 2.1 MeV).

Methodology of combining the LEP experimental results

The LEP experimental results actually used for combination are slightly modified from those published by the experiments (which are given in the Listings below). This has been done in order to facilitate the procedure by making the inputs more consistent. These modified results are given explicitly in [25]. The main differences compared to the published results are

(a) consistent use of ZFITTER 6.23 and TOPAZ0. The published ALEPH results used ZFITTER 6.10. (b) use of the combined energy error matrix which makes a difference of 0.1 MeV on the M_Z and Γ_Z for L3 only as at that intersection the RF modeling uncertainties are the largest.

Thus, nine-parameter sets from all four experiments with their covariance matrices are used together with all the common errors correlations. A grand covariance matrix, V, is constructed and a combined nine-parameter set is obtained by minimizing $\chi^2 = \Delta^T V^{-1} \Delta$, where Δ is the vector of residuals of the combined parameter set to the results of individual experiments.

Study of $Z \to b\overline{b}$ and $Z \to c\overline{c}$

In the sector of c- and b-physics the LEP experiments have measured the ratios of partial widths $R_b = \Gamma(Z \to b\overline{b})/\Gamma(Z \to \text{hadrons})$ and $R_c = \Gamma(Z \to c\overline{c})/\Gamma(Z \to \text{hadrons})$ and the forward-backward (charge) asymmetries $A_{FB}^{b\overline{b}}$ and $A_{FB}^{c\overline{c}}$. The final state coupling parameters A_b and A_c have been obtained from the left-right forward-backward asymmetry at SLD. Several of the analyses have also determined other quantities, in particular the semileptonic branching ratios, $\text{B}(b \to \ell^-)$, $\text{B}(b \to c \to \ell^+)$, and $\text{B}(c \to \ell^+)$, the average $B^0\overline{B}^0$ mixing parameter $\overline{\chi}$ and the probabilities for a c–quark to fragment into a D^+, a D_s, a D^{*+} , or a charmed baryon. The latter measurements do not concern properties of the Z boson and hence they do not appear in the listing below. However, for completeness, we will report at the end of this minireview their values as obtained fitting the data contained in the Z section. All these quantities are correlated with the electroweak parameters, and since the mixture of b hadrons is different from the one at the $\Upsilon(4S)$, their values might differ from those measured at the $\Upsilon(4S)$.

All the above quantities are correlated to each other since:

- Several analyses (for example the lepton fits) determine more than one parameter simultaneously;
- Some of the electroweak parameters depend explicitly on the values of other parameters (for example R_b depends on R_c);
- Common tagging and analysis techniques produce common systematic uncertainties.

The LEP Electroweak Heavy Flavour Working Group has developed [33] a procedure for combining the measurements taking into account known sources of correlation. The combining procedure determines twelve parameters: the four parameters of interest in the electroweak sector, R_b, R_c, $A_{FB}^{b\overline{b}}$, and $A_{FB}^{c\overline{c}}$ and, in addition, $\text{B}(b \to \ell^-)$, $\text{B}(b \to c \to \ell^+)$, $\text{B}(c \to \ell^+)$, $\overline{\chi}$, $f(D^+)$, $f(D_s)$, $f(c_{\text{baryon}})$ and $P(c \to D^{*+}) \times \text{B}(D^{*+} \to \pi^+ D^0)$, to take into account their correlations with the electroweak parameters. Before the fit both the peak and off-peak asymmetries are translated to the common energy $\sqrt{s} = 91.26$ GeV using the predicted energy dependence from ZFITTER [5].

Summary of the measurements and of the various kinds of analysis

The measurements of R_b and R_c fall into two classes. In the first, named single-tag measurement, a method for selecting b and c events is applied and the number of tagged events is counted. The second technique, named double-tag measurement, is based on the following principle: if the number of events with a single hemisphere tagged is N_t and with both hemispheres tagged is N_{tt}, then given a total number of N_{had} hadronic Z decays one has:

$$\frac{N_t}{2N_{\text{had}}} = \varepsilon_b R_b + \varepsilon_c R_c + \varepsilon_{uds}(1 - R_b - R_c) \tag{12}$$

$$\frac{N_{tt}}{N_{\text{had}}} = \mathcal{C}_b \varepsilon_b^2 R_b + \mathcal{C}_c \varepsilon_c^2 R_c + \mathcal{C}_{uds} \varepsilon_{uds}^2 (1 - R_b - R_c) \tag{13}$$

where ε_b, ε_c, and ε_{uds} are the tagging efficiencies per hemisphere for b, c, and light quark events, and $\mathcal{C}_q \neq 1$ accounts for the fact that the tagging efficiencies between the hemispheres may be correlated. In tagging the b one has $\varepsilon_b \gg \varepsilon_c \gg \varepsilon_{uds}$, $C_b \approx 1$. Neglecting the c and uds background and the hemisphere correlations, these equations give:

$$\varepsilon_b = 2N_{tt}/N_t \tag{14}$$

$$R_b = N_t^2/(4 N_{tt} N_{\text{had}}) \, . \tag{15}$$

The double-tagging method has thus the great advantage that the tagging efficiency is directly derived from the data, reducing the systematic error of the measurement. The backgrounds, dominated by $c\overline{c}$ events, obviously complicate this simple picture, and their level must still be inferred by other means. The rate of charm background in these analyses depends explicitly on the value of R_c. The correlations in the tagging efficiencies between the hemispheres (due for instance to correlations in momentum between the b hadrons in the two hemispheres) are small but nevertheless lead to further systematic uncertainties.

The measurements in the b- and c-sector can be essentially grouped in the following categories:

- Lifetime (and lepton) double-tagging measurements of R_b. These are the most precise measurements of R_b and obviously dominate the combined result. The main sources of systematics come from the charm contamination and from estimating the hemisphere b-tagging efficiency correlation. The charm rejection has been improved (and hence the systematic errors reduced) by using either the information of the secondary vertex invariant mass or the information from the energy of all particles at the secondary vertex and their rapidity;
- Analyses with $D/D^{*\pm}$ to measure R_c. These measurements make use of several different tagging techniques (inclusive/exclusive double tag, exclusive double tag, reconstruction of all weakly decaying charmed states) and no assumptions are made on the energy dependence of charm fragmentation;
- Lepton fits which use hadronic events with one or more leptons in the final state to measure $A_{FB}^{b\bar{b}}$ and $A_{FB}^{c\bar{c}}$. Each analysis usually gives several other electroweak parameters. The dominant sources of systematics are due to lepton identification, to other semileptonic branching ratios and to the modeling of the semileptonic decay;
- Measurements of $A_{FB}^{b\bar{b}}$ using lifetime tagged events with a hemisphere charge measurement. Their contribution to the combined result has roughly the same weight as the lepton fits;
- Analyses with $D/D^{*\pm}$ to measure $A_{FB}^{c\bar{c}}$ or simultaneously $A_{FB}^{b\bar{b}}$ and $A_{FB}^{c\bar{c}}$;
- Measurements of A_b and A_c from SLD, using several tagging methods (lepton, kaon, D/D^*, and vertex mass). These quantities are directly extracted from a measurement of the left–right forward–backward asymmetry in $c\bar{c}$ and $b\bar{b}$ production using a polarized electron beam.

Averaging procedure

All the measurements are provided by the LEP Collaborations in the form of tables with a detailed breakdown of the systematic errors of each measurement and its dependence on other electroweak parameters.

The averaging proceeds via the following steps:

- Define and propagate a consistent set of external inputs such as branching ratios, hadron lifetimes, fragmentation models *etc*. All the measurements are also consistently checked to ensure that all use a common set of assumptions (for instance since the QCD corrections for the forward–backward asymmetries are strongly dependent on the experimental conditions, the data are corrected before combining);
- Form the full (statistical and systematic) covariance matrix of the measurements. The systematic correlations between different analyses are calculated from the detailed error breakdown in the measurement tables. The correlations relating several measurements made by the same analysis are also used;
- Take into account any explicit dependence of a measurement on the other electroweak parameters. As an example of this dependence we illustrate the case of the double-tag measurement of R_b, where c-quarks constitute the main background. The normalization of the charm contribution is not usually fixed by the data and the measurement of R_b depends on the assumed value of R_c, which can be written as:

$$R_b = R_b^{\rm meas} + a(R_c)\frac{(R_c - R_c^{\rm used})}{R_c} , \qquad (16)$$

  where $R_b^{\rm meas}$ is the result of the analysis which assumed a value of $R_c = R_c^{\rm used}$ and $a(R_c)$ is the constant which gives the dependence on R_c;
- Perform a χ^2 minimization with respect to the combined electroweak parameters.

After the fit the average peak asymmetries $A_{FB}^{c\bar{c}}$ and $A_{FB}^{b\bar{b}}$ are corrected for the energy shift from 91.26 GeV to M_Z and for QED (initial state radiation), γ exchange, and γZ interference effects to obtain the corresponding pole asymmetries $A_{FB}^{0,c}$ and $A_{FB}^{0,b}$.

This averaging procedure, using the fourteen parameters described above and applied to the data contained in the Z particle listing below, gives the following results:

$$\begin{aligned}
R_b^0 &= 0.21643 \pm 0.00072 \\
R_c^0 &= 0.1689 \pm 0.0047 \\
A_{FB}^{0,b} &= 0.1001 \pm 0.0017 \\
A_{FB}^{0,c} &= 0.0704 \pm 0.0036 \\
A_b &= 0.926 \pm 0.024 \\
A_c &= 0.666 \pm 0.036 \\
B(b \to \ell^-) &= 0.1069 \pm 0.0021 \\
\mathrm{B}(b \to c \to \ell^+) &= 0.0801 \pm 0.0018
\end{aligned}$$

$$B(c \to \ell^+) = 0.0980 \pm 0.0033$$

$$\overline{\chi} = 0.1251 \pm 0.0040$$

$$f(D^+) = 0.237 \pm 0.016$$

$$f(D_s) = 0.119 \pm 0.025$$

$$f(c_{\text{baryon}}) = 0.090 \pm 0.022$$

$$P(c \to D^{*+}) \times \mathrm{B}(D^{*+} \to \pi^+ D^0) = 0.1648 \pm 0.0056$$

References

1. R.N. Cahn, Phys. Rev. **D36**, 2666 (1987).
2. F.A. Berends *et al.*, "*Z* Physics at LEP 1", CERN Report 89-08 (1989), Vol. 1, eds. G. Altarelli, R. Kleiss, and C. Verzegnassi, p. 89.
3. A. Borrelli *et al.*, Nucl. Phys. **B333**, 357 (1990).
4. D. Bardin and G. Passarino, "Upgrading of Precision Calculations for Electroweak Observables," hep-ph/9803425; D. Bardin, G. Passarino, and M. Grünewald, "Precision Calculation Project Report," hep-ph/9902452.
5. D. Bardin *et al.*, Z. Phys. **C44**, 493 (1989); Comp. Phys. Comm. **59**, 303 (1990); D. Bardin *et al.*, Nucl. Phys. **B351**, 1 (1991); Phys. Lett. **B255**, 290 (1991) and CERN-TH/6443/92 (1992); Comp. Phys. Comm. **133**, 229 (2001).
6. M. Consoli *et al.*, "*Z* Physics at LEP 1", CERN Report 89-08 (1989), Vol. 1, eds. G. Altarelli, R. Kleiss, and C. Verzegnassi, p. 7.
7. M. Bohm *et al.*, *ibid*, p. 203.
8. S. Jadach *et al.*, *ibid*, p. 235.
9. G. Burgers *et al.*, *ibid*, p. 55.
10. D.C. Kennedy and B.W. Lynn, SLAC-PUB 4039 (1986, revised 1988).
11. R. Stuart, Phys. Lett. **B262**, 113 (1991).
12. A. Sirlin, Phys. Rev. Lett. **67**, 2127 (1991).
13. A. Leike, T. Riemann, and J. Rose, Phys. Lett. **B273**, 513 (1991).
14. See also D. Bardin *et al.*, Phys. Lett. **B206**, 539 (1988).
15. S. Willenbrock and G. Valencia, Phys. Lett. **B259**, 373 (1991).
16. W. Beenakker, F.A. Berends, and S.C. van der Marck, Nucl. Phys. **B349**, 323 (1991).
17. G. Montagna *et al.*, Nucl. Phys. **B401**, 3 (1993); Comp. Phys. Comm. **76**, 328 (1993); Comp. Phys. Comm. **93**, 120 (1996); G. Montagna *et al.*, Comp. Phys. Comm. **117**, 278 (1999).
18. R. Assmann *et al.* (Working Group on LEP Energy), Eur. Phys. J. **C6**, 187 (1999).
19. R. Assmann *et al.* (Working Group on LEP Energy), Z. Phys. **C66**, 567 (1995).
20. L. Arnaudon *et al.* (Working Group on LEP Energy and LEP Collaborations), Phys. Lett. **B307**, 187 (1993).
21. L. Arnaudon *et al.* (Working Group on LEP Energy), CERN-PPE/92-125 (1992).
22. L. Arnaudon *et al.*, Phys. Lett. **B284**, 431 (1992).
23. R. Bailey *et al.*, 'LEP Energy Calibration' CERN-SL-90-95-AP, Proceedings of the "2^{nd} European Particle Accelerator Conference," Nice, France, 12–16 June 1990, pp. 1765-1767.
24. The LEP Collaborations: ALEPH, DELPHI, L3, OPAL, the LEP Electroweak Working Group, and the SLD Heavy Flavour Group: CERN-EP/2002-091 (2002); CERN-EP/2001-098 (2001); CERN-EP/2001-021 (2001); CERN-EP/2000-016 (1999); CERN-EP/99-15 (1998); CERN-PPE/97-154 (1997); CERN-PPE/96-183 (1996); CERN-PPE/95-172 (1995); CERN-PPE/94-187 (1994); CERN-PPE/93-157 (1993).
25. The LEP Collaborations ALEPH, DELPHI, L3, OPAL, and the Line Shape Sub-group of the LEP Electroweak Working Group: CERN-EP/2000-153, hep-ex/0101027 (to be published as part of a review in Physics Reports).
26. S. Jadach *et al.*, BHLUMI 4.04, Comp. Phys. Comm. **102**, 229 (1997); S. Jadach and O. Nicrosini, Event generators for Bhabha scattering, in Physics at LEP2, CERN-96-01 Vol. 2, February 1996.
27. B.F.L. Ward *et al.*, Phys. Lett. **B450**, 262 (1999).
28. W. Beenakker and G. Passarino, Phys. Lett. **B425**, 199 (1998).
29. L. Garrido *et al.*, Z. Phys. **C49**, 645 (1991); M. Martinez and F. Teubert, Z. Phys. **C65**, 267 (1995), updated with results summarized in S. Jadach, B. Pietrzyk and M. Skrzypek, Phys. Lett. **B456**, 77 (1999) and Reports of the working group on precision calculations for the *Z* resonance, CERN 95-03, ed. D. Bardin, W. Hollik, and G. Passarino, and references therein.
30. T. van Ritbergen, R. Stuart, Phys. Lett. **B437**, 201 (1998); Phys. Rev. Lett. **81**, 488 (1999).
31. S. Eidelman and F. Jegerlehner, Z. Phys. **C67**, 585 (1995); M. Steinhauser, Phys. Lett. **B249**, 158 (1998).
32. Particle Data Group (D.E. Groom *et al.*), Eur. Phys. J. **C15**, 1 (2000).
33. The LEP Experiments: ALEPH, DELPHI, L3, and OPAL Nucl. Instrum. Methods **A378**, 101 (1996).

Z MASS

OUR FIT is obtained using the fit procedure and correlations as determined by the LEP Electroweak Working Group (see the "Note on the *Z* boson"). The fit is performed using the *Z* mass and width, the *Z* hadronic pole cross section, the ratios of hadronic to leptonic partial widths, and the *Z* pole forward-backward lepton asymmetries. This set is believed to be most free of correlations.

The *Z*-boson mass listed here corresponds to a Breit-Wigner resonance parameter. The value is 34 MeV greater than the real part of the position of the pole (in the energy-squared plane) in the *Z*-boson propagator. Also the LEP experiments have generally assumed a fixed value of the $\gamma - Z$ interferences term based on the standard model. Keeping this term as free parameter leads to a somewhat larger error on the fitted *Z* mass. See ACCIARRI 00Q and ACKERSTAFF 97C for a detailed investigation of both these issues.

VALUE (GeV)	*EVTS*	*DOCUMENT ID*		*TECN*	*COMMENT*
91.1876±0.0021 OUR FIT					
91.1852±0.0030	4.57M	[1] ABBIENDI	01A	OPAL	E^{ee}_{cm} = 88–94 GeV
91.1863±0.0028	4.08M	[2] ABREU	00F	DLPH	E^{ee}_{cm} = 88–94 GeV
91.1898±0.0031	3.96M	[3] ACCIARRI	00C	L3	E^{ee}_{cm} = 88–94 GeV
91.1885±0.0031	4.57M	[4] BARATE	00C	ALEP	E^{ee}_{cm} = 88–94 GeV
• • • We do not use the following data for averages, fits, limits, etc. • • •					
91.1875±0.0039	3.97M	[5] ACCIARRI	00Q	L3	E^{ee}_{cm} = LEP1 + 130–189 GeV
91.185 ±0.010		[6] ACKERSTAFF	97C	OPAL	E^{ee}_{cm} = LEP1 + 130–136 GeV + 161 GeV
91.151 ±0.008		[7] MIYABAYASHI	95	TOPZ	E^{ee}_{cm} = 57.8 GeV
91.187 ±0.007 ±0.006	1.16M	[8] ABREU	94	DLPH	Repl. by ABREU 00F
91.195 ±0.006 ±0.007	1.19M	[8] ACCIARRI	94	L3	Repl. by ACCIARRI 00C
91.182 ±0.007 ±0.006	1.33M	[8] AKERS	94	OPAL	Repl. by ABBIENDI 01A
91.187 ±0.007 ±0.006	1.27M	[8] BUSKULIC	94	ALEP	Repl. by BARATE 00C
91.74 ±0.28 ±0.93	156	[9] ALITTI	92B	UA2	$E^{p\overline{p}}_{cm}$ = 630 GeV
90.9 ±0.3 ±0.2	188	[10] ABE	89C	CDF	$E^{p\overline{p}}_{cm}$ = 1.8 TeV
91.14 ±0.12	480	[11] ABRAMS	89B	MRK2	E^{ee}_{cm} = 89–93 GeV
93.1 ±1.0 ±3.0	24	[12] ALBAJAR	89	UA1	$E^{p\overline{p}}_{cm}$ = 546,630 GeV

[1] ABBIENDI 01A error includes approximately 2.3 MeV due to statistics and 1.8 MeV due to LEP energy uncertainty.
[2] The error includes 1.6 MeV due to LEP energy uncertainty.
[3] The error includes 1.8 MeV due to LEP energy uncertainty.
[4] BARATE 00C error includes approximately 2.4 MeV due to statistics, 0.2 MeV due to experimental systematics, and 1.7 MeV due to LEP energy uncertainty.
[5] ACCIARRI 00Q interpret the s-dependence of the cross sections and lepton forward-backward asymmetries in the framework of the S-matrix formalism. They fit to their cross section and asymmetry data at high energies, using the results of S-matrix fits to Z-peak data (ACCIARRI 00C) as constraints. The 130–189 GeV data constrains the γ/Z interference term. The authors have corrected the measurement for the 34.1 MeV shift with respect to the Breit-Wigner fits. The error contains a contribution of ± 2.3 MeV due to the uncertainty on the γZ interference.
[6] ACKERSTAFF 97C obtain this using the S-matrix formalism for a combined fit to their cross-section and asymmetry data at the Z peak (AKERS 94) and their data at 130, 136, and 161 GeV. The authors have corrected the measurement for the 34 MeV shift with respect to the Breit-Wigner fits.
[7] MIYABAYASHI 95 combine their low energy total hadronic cross-section measurement with the ACTON 93D data and perform a fit using an S-matrix formalism. As expected, this result is below the mass values obtained with the standard Breit-Wigner parametrization.
[8] The second error of 6.3 MeV is due to a common LEP energy uncertainty.
[9] Enters fit through W/Z mass ratio given in the W Particle Listings. The ALITTI 92B systematic error (± 0.93) has two contributions: one (± 0.92) cancels in m_W/m_Z and one (± 0.12) is noncancelling. These were added in quadrature.
[10] First error of ABE 89 is combination of statistical and systematic contributions; second is mass scale uncertainty.
[11] ABRAMS 89B uncertainty includes 35 MeV due to the absolute energy measurement.
[12] ALBAJAR 89 result is from a total sample of 33 $Z \to e^+e^-$ events.

Z WIDTH

OUR FIT is obtained using the fit procedure and correlations as determined by the LEP Electroweak Working Group (see the "Note on the Z boson").

VALUE (GeV)			*EVTS*	*DOCUMENT ID*		*TECN*	*COMMENT*
2.4952±0.0023 OUR FIT							
2.4948±0.0041			4.57M	[13] ABBIENDI	01A	OPAL	E^{ee}_{cm}= 88–94 GeV
2.4876±0.0041			4.08M	[14] ABREU	00F	DLPH	E^{ee}_{cm}= 88–94 GeV
2.5024±0.0042			3.96M	[15] ACCIARRI	00C	L3	E^{ee}_{cm}= 88–94 GeV
2.4951±0.0043			4.57M	[16] BARATE	00C	ALEP	E^{ee}_{cm}= 88–94 GeV
• • • We do not use the following data for averages, fits, limits, etc. • • •							
2.5025±0.0041			3.97M	[17] ACCIARRI	00Q	L3	E^{ee}_{cm}= LEP1 + 130–189 GeV
2.50	±0.21	±0.06		[18] ABREU	96R	DLPH	E^{ee}_{cm}= 91.2 GeV
2.483	±0.011	±0.0045	1.16M	[19] ABREU	94	DLPH	Repl. by ABREU 00F
2.494	±0.009	±0.0045	1.19M	[19] ACCIARRI	94	L3	Repl. by ACCIARRI 00C
2.483	±0.011	±0.0045	1.33M	[19] AKERS	94	OPAL	Repl. by ABBIENDI 01A
2.501	±0.011	±0.0045	1.27M	[19] BUSKULIC	94	ALEP	Repl. by BARATE 00C
3.8	±0.8	±1.0	188	ABE	89C	CDF	$E^{p\overline{p}}_{cm}$= 1.8 TeV
2.42	$^{+0.45}_{-0.35}$		480	[20] ABRAMS	89B	MRK2	E^{ee}_{cm}= 89–93 GeV
2.7	$^{+1.2}_{-1.0}$	±1.3	24	[21] ALBAJAR	89	UA1	$E^{p\overline{p}}_{cm}$= 546,630 GeV
2.7	±2.0	±1.0	25	[22] ANSARI	87	UA2	$E^{p\overline{p}}_{cm}$= 546,630 GeV

[13] ABBIENDI 01A error includes approximately 3.6 MeV due to statistics, 1 MeV due to event selection systematics, and 1.3 MeV due to LEP energy uncertainty.
[14] The error includes 1.2 MeV due to LEP energy uncertainty.
[15] The error includes 1.3 MeV due to LEP energy uncertainty.
[16] BARATE 00C error includes approximately 3.8 MeV due to statistics, 0.9 MeV due to experimental systematics, and 1.3 MeV due to LEP energy uncertainty.
[17] ACCIARRI 00Q interpret the s-dependence of the cross sections and lepton forward-backward asymmetries in the framework of the S-matrix formalism. They fit to their cross section and asymmetry data at high energies, using the results of S-matrix fits to Z-peak data (ACCIARRI 00C) as constraints. The 130–189 GeV data constrains the γ/Z interference term. The authors have corrected the measurement for the 0.9 MeV shift with respect to the Breit-Wigner fits.
[18] ABREU 96R obtain this value from a study of the interference between initial and final state radiation in the process $e^+e^- \to Z \to \mu^+\mu^-$.
[19] The second error of 4.5 MeV is due to a common LEP energy uncertainty.
[20] ABRAMS 89B uncertainty includes 50 MeV due to the miniSAM background subtraction error.
[21] ALBAJAR 89 result is from a total sample of 33 $Z \to e^+e^-$ events.
[22] Quoted values of ANSARI 87 are from direct fit. Ratio of Z and W production gives either $\Gamma(Z) < (1.09\pm0.07)\times\Gamma(W)$, CL = 90% or $\Gamma(Z) = (0.82^{+0.19}_{-0.14}\pm0.06)\times\Gamma(W)$. Assuming Standard-Model value $\Gamma(W) = 2.65$ GeV then gives $\Gamma(Z) < 2.89 \pm 0.19$ or $= 2.17^{+0.50}_{-0.37} \pm 0.16$.

Z DECAY MODES

	Mode			Fraction (Γ_i/Γ)	Scale factor/ Confidence level
Γ_1	e^+e^-			(3.363 ±0.004) %	
Γ_2	$\mu^+\mu^-$			(3.366 ±0.007) %	
Γ_3	$\tau^+\tau^-$			(3.370 ±0.008) %	
Γ_4	$\ell^+\ell^-$		[a]	(3.3658±0.0023) %	
Γ_5	invisible			(20.00 ±0.06) %	
Γ_6	hadrons			(69.91 ±0.06) %	
Γ_7	$(u\overline{u}+c\overline{c})/2$			(10.1 ±1.1) %	
Γ_8	$(d\overline{d}+s\overline{s}+b\overline{b})/3$			(16.6 ±0.6) %	
Γ_9	$c\overline{c}$			(11.81 ±0.33) %	
Γ_{10}	$b\overline{b}$			(15.13 ±0.05) %	
Γ_{11}	$b\overline{b}b\overline{b}$			(3.6 ±1.3) $\times 10^{-4}$	
Γ_{12}	ggg			< 1.1 %	CL=95%
Γ_{13}	$\pi^0\gamma$			< 5.2 $\times 10^{-5}$	CL=95%
Γ_{14}	$\eta\gamma$			< 5.1 $\times 10^{-5}$	CL=95%
Γ_{15}	$\omega\gamma$			< 6.5 $\times 10^{-4}$	CL=95%
Γ_{16}	$\eta'(958)\gamma$			< 4.2 $\times 10^{-5}$	CL=95%
Γ_{17}	$\gamma\gamma$			< 5.2 $\times 10^{-5}$	CL=95%
Γ_{18}	$\gamma\gamma\gamma$			< 1.0 $\times 10^{-5}$	CL=95%
Γ_{19}	$\pi^\pm W^\mp$		[b]	< 7 $\times 10^{-5}$	CL=95%
Γ_{20}	$\rho^\pm W^\mp$		[b]	< 8.3 $\times 10^{-5}$	CL=95%
Γ_{21}	$J/\psi(1S)$X			(3.51 $^{+0.23}_{-0.25}$) $\times 10^{-3}$	S=1.1
Γ_{22}	$\psi(2S)$X			(1.60 ±0.29) $\times 10^{-3}$	
Γ_{23}	$\chi_{c1}(1P)$X			(2.9 ±0.7) $\times 10^{-3}$	
Γ_{24}	$\chi_{c2}(1P)$X			< 3.2 $\times 10^{-3}$	CL=90%
Γ_{25}	$\Upsilon(1S)$ X + $\Upsilon(2S)$ X + $\Upsilon(3S)$ X			(1.0 ±0.5) $\times 10^{-4}$	
Γ_{26}	$\Upsilon(1S)$X			< 4.4 $\times 10^{-5}$	CL=95%
Γ_{27}	$\Upsilon(2S)$X			< 1.39 $\times 10^{-4}$	CL=95%
Γ_{28}	$\Upsilon(3S)$X			< 9.4 $\times 10^{-5}$	CL=95%
Γ_{29}	$(D^0/\overline{D}^0)$ X			(20.7 ±2.0) %	
Γ_{30}	$D^\pm$X			(12.2 ±1.7) %	
Γ_{31}	$D^*(2010)^\pm$X		[b]	(11.4 ±1.3) %	
Γ_{32}	$D_{s1}(2536)^\pm$X			(3.6 ±0.8) $\times 10^{-3}$	
Γ_{33}	$D_{sJ}(2573)^\pm$X			(5.8 ±2.2) $\times 10^{-3}$	
Γ_{34}	$D^{*\prime}(2629)^\pm$X			searched for	
Γ_{35}	BX				
Γ_{36}	B^*X				
Γ_{37}	B^0_sX			seen	
Γ_{38}	B^+_cX			searched for	
Γ_{39}	anomalous $\gamma+$ hadrons		[c]	< 3.2 $\times 10^{-3}$	CL=95%
Γ_{40}	$e^+e^-\gamma$		[c]	< 5.2 $\times 10^{-4}$	CL=95%
Γ_{41}	$\mu^+\mu^-\gamma$		[c]	< 5.6 $\times 10^{-4}$	CL=95%
Γ_{42}	$\tau^+\tau^-\gamma$		[c]	< 7.3 $\times 10^{-4}$	CL=95%
Γ_{43}	$\ell^+\ell^-\gamma\gamma$		[d]	< 6.8 $\times 10^{-6}$	CL=95%
Γ_{44}	$q\overline{q}\gamma\gamma$		[d]	< 5.5 $\times 10^{-6}$	CL=95%
Γ_{45}	$\nu\overline{\nu}\gamma\gamma$		[d]	< 3.1 $\times 10^{-6}$	CL=95%
Γ_{46}	$e^\pm\mu^\mp$	*LF*	[b]	< 1.7 $\times 10^{-6}$	CL=95%
Γ_{47}	$e^\pm\tau^\mp$	*LF*	[b]	< 9.8 $\times 10^{-6}$	CL=95%
Γ_{48}	$\mu^\pm\tau^\mp$	*LF*	[b]	< 1.2 $\times 10^{-5}$	CL=95%
Γ_{49}	pe	*L,B*		< 1.8 $\times 10^{-6}$	CL=95%
Γ_{50}	$p\mu$	*L,B*		< 1.8 $\times 10^{-6}$	CL=95%

[a] ℓ indicates each type of lepton (e, μ, and τ), not sum over them.

[b] The value is for the sum of the charge states or particle/antiparticle states indicated.

[c] See the Particle Listings below for the γ energy range used in this measurement.

[d] For $m_{\gamma\gamma} = (60 \pm 5)$ GeV.

Z PARTIAL WIDTHS

$\Gamma(e^+e^-)$ **Γ_1**

For the LEP experiments, this parameter is not directly used in the overall fit but is derived using the fit results; see the 'Note on the Z Boson.'

VALUE (MeV)	*EVTS*	*DOCUMENT ID*		*TECN*	*COMMENT*
83.91±0.12 OUR FIT					
83.66±0.20	137.0K	ABBIENDI	01A	OPAL	E^{ee}_{cm}= 88–94 GeV
83.54±0.27	117.8k	ABREU	00F	DLPH	E^{ee}_{cm}= 88–94 GeV
84.16±0.22	124.4k	ACCIARRI	00C	L3	E^{ee}_{cm}= 88–94 GeV
83.88±0.19		BARATE	00C	ALEP	E^{ee}_{cm}= 88–94 GeV
82.89±1.20±0.89		[23] ABE	95J	SLD	E^{ee}_{cm}= 91.31 GeV

[23] ABE 95J obtain this measurement from Bhabha events in a restricted fiducial region to improve systematics. They use the values 91.187 and 2.489 GeV for the Z mass and total decay width to extract this partial width.

$\Gamma(\mu^+\mu^-)$ Γ_2

This parameter is not directly used in the overall fit but is derived using the fit results; see the 'Note on the Z Boson.'

VALUE (MeV)	EVTS	DOCUMENT ID	TECN	COMMENT
83.99±0.18 OUR FIT				
84.03±0.30	182.8K	ABBIENDI	01A OPAL	$E^{ee}_{\rm cm}$= 88–94 GeV
84.48±0.40	157.6k	ABREU	00F DLPH	$E^{ee}_{\rm cm}$= 88–94 GeV
83.95±0.44	113.4k	ACCIARRI	00C L3	$E^{ee}_{\rm cm}$= 88–94 GeV
84.02±0.28		BARATE	00C ALEP	$E^{ee}_{\rm cm}$= 88–94 GeV

$\Gamma(\tau^+\tau^-)$ Γ_3

This parameter is not directly used in the overall fit but is derived using the fit results; see the 'Note on the Z Boson.'

VALUE (MeV)	EVTS	DOCUMENT ID	TECN	COMMENT
84.08±0.22 OUR FIT				
83.94±0.41	151.5K	ABBIENDI	01A OPAL	$E^{ee}_{\rm cm}$= 88–94 GeV
83.71±0.58	104.0k	ABREU	00F DLPH	$E^{ee}_{\rm cm}$= 88–94 GeV
84.23±0.58	103.0k	ACCIARRI	00C L3	$E^{ee}_{\rm cm}$= 88–94 GeV
84.38±0.31		BARATE	00C ALEP	$E^{ee}_{\rm cm}$= 88–94 GeV

$\Gamma(\ell^+\ell^-)$ Γ_4

In our fit $\Gamma(\ell^+\ell^-)$ is defined as the partial Z width for the decay into a pair of massless charged leptons. This parameter is not directly used in the 5-parameter fit assuming lepton universality but is derived using the fit results. See the 'Note on the Z Boson.'

VALUE (MeV)	EVTS	DOCUMENT ID	TECN	COMMENT
83.984±0.086 OUR FIT				
83.82 ±0.15	471.3K	ABBIENDI	01A OPAL	$E^{ee}_{\rm cm}$= 88–94 GeV
83.85 ±0.17	379.4k	ABREU	00F DLPH	$E^{ee}_{\rm cm}$= 88–94 GeV
84.14 ±0.17	340.8k	ACCIARRI	00C L3	$E^{ee}_{\rm cm}$= 88–94 GeV
84.02 ±0.15	500k	BARATE	00C ALEP	$E^{ee}_{\rm cm}$= 88–94 GeV

Γ(invisible) Γ_5

We use only direct measurements of the invisible partial width using the single photon channel to obtain the average value quoted below. OUR FIT value is obtained as a difference between the total and the observed partial widths assuming lepton universality.

VALUE (MeV)	EVTS	DOCUMENT ID	TECN	COMMENT
499.0± 1.5 OUR FIT				
503 ±16 OUR AVERAGE Error includes scale factor of 1.2.				
498 ±12 ±12	1791	ACCIARRI	98G L3	$E^{ee}_{\rm cm}$= 88–94 GeV
539 ±26 ±17	410	AKERS	95C OPAL	$E^{ee}_{\rm cm}$= 88–94 GeV
450 ±34 ±34	258	BUSKULIC	93L ALEP	$E^{ee}_{\rm cm}$= 88–94 GeV
540 ±80 ±40	52	ADEVA	92 L3	$E^{ee}_{\rm cm}$= 88–94 GeV
• • • We do not use the following data for averages, fits, limits, etc. • • •				
498.1± 2.6		[24] ABBIENDI	01A OPAL	$E^{ee}_{\rm cm}$= 88–94 GeV
498.1± 3.2		[24] ABREU	00F DLPH	$E^{ee}_{\rm cm}$= 88–94 GeV
499.1± 2.9		[24] ACCIARRI	00C L3	$E^{ee}_{\rm cm}$= 88–94 GeV
499.1± 2.5		[24] BARATE	00C ALEP	$E^{ee}_{\rm cm}$= 88–94 GeV

[24] This is an indirect determination of Γ(invisible) from a fit to the visible Z decay modes.

Γ(hadrons) Γ_6

This parameter is not directly used in the 5-parameter fit assuming lepton universality, but is derived using the fit results. See the 'Note on the Z Boson.'

VALUE (MeV)	EVTS	DOCUMENT ID	TECN	COMMENT
1744.4±2.0 OUR FIT				
1745.4±3.5	4.10M	ABBIENDI	01A OPAL	$E^{ee}_{\rm cm}$= 88–94 GeV
1738.1±4.0	3.70M	ABREU	00F DLPH	$E^{ee}_{\rm cm}$= 88–94 GeV
1751.1±3.8	3.54M	ACCIARRI	00C L3	$E^{ee}_{\rm cm}$= 88–94 GeV
1744.0±3.4	4.07M	BARATE	00C ALEP	$E^{ee}_{\rm cm}$= 88–94 GeV

Z BRANCHING RATIOS

OUR FIT is obtained using the fit procedure and correlations as determined by the LEP Electroweak Working Group (see the "Note on the Z boson").

$\Gamma(\text{hadrons})/\Gamma(e^+e^-)$ Γ_6/Γ_1

VALUE	EVTS	DOCUMENT ID	TECN	COMMENT
20.804± 0.050 OUR FIT				
20.902± 0.084	137.0K	[25] ABBIENDI	01A OPAL	$E^{ee}_{\rm cm}$= 88–94 GeV
20.88 ± 0.12	117.8k	ABREU	00F DLPH	$E^{ee}_{\rm cm}$= 88–94 GeV
20.816± 0.089	124.4k	ACCIARRI	00C L3	$E^{ee}_{\rm cm}$= 88–94 GeV
20.677± 0.075		[26] BARATE	00C ALEP	$E^{ee}_{\rm cm}$= 88–94 GeV
• • • We do not use the following data for averages, fits, limits, etc. • • •				
20.74 ± 0.18	31.4k	ABREU	94 DLPH	Repl. by ABREU 00F
20.96 ± 0.15	38k	ACCIARRI	94 L3	Repl. by ACCIARRI 00C
20.83 ± 0.16	42k	AKERS	94 OPAL	Repl. by ABBIENDI 01A
20.59 ± 0.15	45.8k	BUSKULIC	94 ALEP	Repl. by BARATE 00C
27.0 $^{+11.7}_{-8.8}$	12	[27] ABRAMS	89D MRK2	$E^{ee}_{\rm cm}$= 89–93 GeV

[25] ABBIENDI 01A error includes approximately 0.067 due to statistics, 0.040 due to event selection systematics, 0.027 due to the theoretical uncertainty in t-channel prediction, and 0.014 due to LEP energy uncertainty.
[26] BARATE 00C error includes approximately 0.062 due to statistics, 0.033 due to experimental systematics, and 0.026 due to the theoretical uncertainty in t-channel prediction.
[27] ABRAMS 89D have included both statistical and systematic uncertainties in their quoted errors.

$\Gamma(\text{hadrons})/\Gamma(\mu^+\mu^-)$ Γ_6/Γ_2

OUR FIT is obtained using the fit procedure and correlations as determined by the LEP Electroweak Working Group (see the "Note on the Z boson").

VALUE	EVTS	DOCUMENT ID	TECN	COMMENT
20.785±0.033 OUR FIT				
20.811±0.058	182.8K	[28] ABBIENDI	01A OPAL	$E^{ee}_{\rm cm}$= 88–94 GeV
20.65 ±0.08	157.6k	ABREU	00F DLPH	$E^{ee}_{\rm cm}$= 88–94 GeV
20.861±0.097	113.4k	ACCIARRI	00C L3	$E^{ee}_{\rm cm}$= 88–94 GeV
20.799±0.056		[29] BARATE	00C ALEP	$E^{ee}_{\rm cm}$= 88–94 GeV
• • • We do not use the following data for averages, fits, limits, etc. • • •				
20.54 ±0.14	45.6k	ABREU	94 DLPH	Repl. by ABREU 00F
21.02 ±0.16	34k	ACCIARRI	94 L3	Repl. by ACCIARRI 00C
20.78 ±0.11	57k	AKERS	94 OPAL	Repl. by ABBIENDI 01A
20.83 ±0.15	46.4k	BUSKULIC	94 ALEP	Repl. by BARATE 00C
18.9 $^{+7.1}_{-5.3}$	13	[30] ABRAMS	89D MRK2	$E^{ee}_{\rm cm}$= 89–93 GeV

[28] ABBIENDI 01A error includes approximately 0.050 due to statistics and 0.027 due to event selection systematics.
[29] BARATE 00C error includes approximately 0.053 due to statistics and 0.021 due to experimental systematics.
[30] ABRAMS 89D have included both statistical and systematic uncertainties in their quoted errors.

$\Gamma(\text{hadrons})/\Gamma(\tau^+\tau^-)$ Γ_6/Γ_3

OUR FIT is obtained using the fit procedure and correlations as determined by the LEP Electroweak Working Group (see the "Note on the Z boson").

VALUE	EVTS	DOCUMENT ID	TECN	COMMENT
20.764±0.045 OUR FIT				
20.832±0.091	151.5K	[31] ABBIENDI	01A OPAL	$E^{ee}_{\rm cm}$= 88–94 GeV
20.84 ±0.13	104.0k	ABREU	00F DLPH	$E^{ee}_{\rm cm}$= 88–94 GeV
20.792±0.133	103.0k	ACCIARRI	00C L3	$E^{ee}_{\rm cm}$= 88–94 GeV
20.707±0.062		[32] BARATE	00C ALEP	$E^{ee}_{\rm cm}$= 88–94 GeV
• • • We do not use the following data for averages, fits, limits, etc. • • •				
20.68 ±0.18	25k	ABREU	94 DLPH	Repl. by ABREU 00F
20.80 ±0.20	25k	ACCIARRI	94 L3	Repl. by ACCIARRI 00C
21.01 ±0.15	47k	AKERS	94 OPAL	Repl. by ABBIENDI 01A
20.70 ±0.16	45.1k	BUSKULIC	94 ALEP	Repl. by BARATE 00C
15.2 $^{+4.8}_{-3.9}$	21	[33] ABRAMS	89D MRK2	$E^{ee}_{\rm cm}$= 89–93 GeV

[31] ABBIENDI 01A error includes approximately 0.055 due to statistics and 0.071 due to event selection systematics.
[32] BARATE 00C error includes approximately 0.054 due to statistics and 0.033 due to experimental systematics.
[33] ABRAMS 89D have included both statistical and systematic uncertainties in their quoted errors.

$\Gamma(\text{hadrons})/\Gamma(\ell^+\ell^-)$ Γ_6/Γ_4

ℓ indicates each type of lepton (e, μ, and τ), not sum over them.

Our fit result is obtained requiring lepton universality.

VALUE	EVTS	DOCUMENT ID	TECN	COMMENT
20.767±0.025 OUR FIT				
20.823±0.044	471.3K	[34] ABBIENDI	01A OPAL	$E^{ee}_{\rm cm}$= 88–94 GeV
20.730±0.060	379.4k	ABREU	00F DLPH	$E^{ee}_{\rm cm}$= 88–94 GeV
20.810±0.060	340.8k	ACCIARRI	00C L3	$E^{ee}_{\rm cm}$= 88–94 GeV
20.725±0.039	500k	[35] BARATE	00C ALEP	$E^{ee}_{\rm cm}$= 88–94 GeV
• • • We do not use the following data for averages, fits, limits, etc. • • •				
20.62 ±0.10	102k	ABREU	94 DLPH	Repl. by ABREU 00F
20.93 ±0.10	97k	ACCIARRI	94 L3	Repl. by ACCIARRI 00C
20.835±0.086	146k	AKERS	94 OPAL	Repl. by ABBIENDI 01A
20.69 ±0.09	137.3k	BUSKULIC	94 ALEP	Repl. by BARATE 00C
18.9 $^{+3.6}_{-3.2}$	46	ABRAMS	89B MRK2	$E^{ee}_{\rm cm}$= 89–93 GeV

[34] ABBIENDI 01A error includes approximately 0.034 due to statistics and 0.027 due to event selection systematics.
[35] BARATE 00C error includes approximately 0.033 due to statistics, 0.020 due to experimental systematics, and 0.005 due to the theoretical uncertainty in t-channel prediction.

$\Gamma(\text{hadrons})/\Gamma_{\text{total}}$ — Γ_6/Γ

This parameter is not directly used in the overall fit but is derived using the fit results; see the 'Note on the Z Boson.'

VALUE (%)	DOCUMENT ID
69.911±0.056 OUR FIT	

$\Gamma(e^+e^-)/\Gamma_{\text{total}}$ — Γ_1/Γ

This parameter is not directly used in the overall fit but is derived using the fit results; see the 'Note on the Z Boson.'

VALUE (%)	DOCUMENT ID
3.3632±0.0042 OUR FIT	

$\Gamma(\mu^+\mu^-)/\Gamma_{\text{total}}$ — Γ_2/Γ

This parameter is not directly used in the overall fit but is derived using the fit results; see the 'Note on the Z Boson.'

VALUE (%)	DOCUMENT ID
3.3662±0.0066 OUR FIT	

$\Gamma(\tau^+\tau^-)/\Gamma_{\text{total}}$ — Γ_3/Γ

This parameter is not directly used in the overall fit but is derived using the fit results; see the 'Note on the Z Boson.'

VALUE (%)	DOCUMENT ID
3.3696±0.0083 OUR FIT	

$\Gamma(\ell^+\ell^-)/\Gamma_{\text{total}}$ — Γ_4/Γ

ℓ indicates each type of lepton (e, μ, and τ), not sum over them.

Our fit result assumes lepton universality.

This parameter is not directly used in the overall fit but is derived using the fit results; see the 'Note on the Z Boson.'

VALUE (%)	DOCUMENT ID
3.3658±0.0023 OUR FIT	

$\Gamma(\text{invisible})/\Gamma_{\text{total}}$ — Γ_5/Γ

See the data, the note, and the fit result for the partial width, Γ_5, above.

VALUE (%)	DOCUMENT ID
20.000±0.055 OUR FIT	

$\Gamma(\mu^+\mu^-)/\Gamma(e^+e^-)$ — Γ_2/Γ_1

This parameter is not directly used in the overall fit but is derived using the fit results; see the 'Note on the Z Boson.'

VALUE	DOCUMENT ID
1.0009±0.0028 OUR FIT	

$\Gamma(\tau^+\tau^-)/\Gamma(e^+e^-)$ — Γ_3/Γ_1

This parameter is not directly used in the overall fit but is derived using the fit results; see the 'Note on the Z Boson.'

VALUE	DOCUMENT ID
1.0019±0.0032 OUR FIT	

$\Gamma((u\overline{u}+c\overline{c})/2)/\Gamma(\text{hadrons})$ — Γ_7/Γ_6

This quantity is the branching ratio of $Z \to$ "up-type" quarks to $Z \to$ hadrons. Except ACKERSTAFF 97T the values of $Z \to$ "up-type" and $Z \to$ "down-type" branchings are extracted from measurements of Γ(hadrons), and $\Gamma(Z \to \gamma+\text{ jets})$ where γ is a high-energy (>5 GeV) isolated photon. As the experiments use different procedures and slightly different values of M_Z, Γ(hadrons) and α_s in their extraction procedures, our average has to be taken with caution.

VALUE	DOCUMENT ID	TECN	COMMENT
0.145±0.015 OUR AVERAGE			
0.160±0.019±0.019	[36] ACKERSTAFF 97T	OPAL	E^{ee}_{cm}= 88–94 GeV
$0.137^{+0.038}_{-0.054}$	[37] ABREU 95X	DLPH	E^{ee}_{cm}= 88–94 GeV
0.139±0.026	[38] ACTON 93F	OPAL	E^{ee}_{cm}= 88–94 GeV
0.137±0.033	[39] ADRIANI 93	L3	E^{ee}_{cm}= 91.2 GeV

[36] ACKERSTAFF 97T measure $\Gamma_{u\overline{u}}/(\Gamma_{d\overline{d}}+\Gamma_{u\overline{u}}+\Gamma_{s\overline{s}})$ = 0.258 ± 0.031 ± 0.032. To obtain this branching ratio authors use R_c+R_b = 0.380 ± 0.010. This measurement is fully negatively correlated with the measurement of $\Gamma_{d\overline{d},s\overline{s}}/(\Gamma_{d\overline{d}}+\Gamma_{u\overline{u}}+\Gamma_{s\overline{s}})$ given in the next data block.

[37] ABREU 95X use M_Z = 91.187 ± 0.009 GeV, Γ(hadrons) = 1725 ± 12 MeV and α_s = 0.123 ± 0.005. To obtain this branching ratio we divide their value of $C_{2/3} = 0.91^{+0.25}_{-0.36}$ by their value of $(3C_{1/3} + 2C_{2/3})$ = 6.66 ± 0.05.

[38] ACTON 93F use the LEP 92 value of Γ(hadrons) = 1740 ± 12 MeV and $\alpha_s = 0.122^{+0.006}_{-0.005}$.

[39] ADRIANI 93 use M_Z = 91.181 ± 0.022 GeV, Γ(hadrons) = 1742 ± 19 MeV and α_s = 0.125 ± 0.009. To obtain this branching ratio we divide their value of $C_{2/3}$ = 0.92 ± 0.22 by their value of $(3C_{1/3} + 2C_{2/3})$ = 6.720 ± 0.076.

$\Gamma((d\overline{d}+s\overline{s}+b\overline{b})/3)/\Gamma(\text{hadrons})$ — Γ_8/Γ_6

This quantity is the branching ratio of $Z \to$ "down-type" quarks to $Z \to$ hadrons. Except ACKERSTAFF 97T the values of $Z \to$ "up-type" and $Z \to$ "down-type" branchings are extracted from measurements of Γ(hadrons), and $\Gamma(Z \to \gamma+\text{ jets})$ where γ is a high-energy (>5 GeV) isolated photon. As the experiments use different procedures and slightly different values of M_Z, Γ(hadrons) and α_s in their extraction procedures, our average has to be taken with caution.

VALUE	DOCUMENT ID	TECN	COMMENT
0.237±0.009 OUR AVERAGE			
0.230±0.010±0.010	[40] ACKERSTAFF 97T	OPAL	E^{ee}_{cm}= 88–94 GeV
$0.243^{+0.036}_{-0.026}$	[41] ABREU 95X	DLPH	E^{ee}_{cm}= 88–94 GeV
0.241±0.017	[42] ACTON 93F	OPAL	E^{ee}_{cm}= 88–94 GeV
0.243±0.022	[43] ADRIANI 93	L3	E^{ee}_{cm}= 91.2 GeV

[40] ACKERSTAFF 97T measure $\Gamma_{d\overline{d},s\overline{s}}/(\Gamma_{d\overline{d}}+\Gamma_{u\overline{u}}+\Gamma_{s\overline{s}})$ = 0.371 ± 0.016 ± 0.016. To obtain this branching ratio authors use R_c+R_b = 0.380 ± 0.010. This measurement is fully negatively correlated with the measurement of $\Gamma_{u\overline{u}}/(\Gamma_{d\overline{d}}+\Gamma_{u\overline{u}}+\Gamma_{s\overline{s}})$ presented in the previous data block.

[41] ABREU 95X use M_Z = 91.187 ± 0.009 GeV, Γ(hadrons) = 1725 ± 12 MeV and α_s = 0.123 ± 0.005. To obtain this branching ratio we divide their value of $C_{1/3} = 1.62^{+0.24}_{-0.17}$ by their value of $(3C_{1/3} + 2C_{2/3})$ = 6.66 ± 0.05.

[42] ACTON 93F use the LEP 92 value of Γ(hadrons) = 1740 ± 12 MeV and $\alpha_s = 0.122^{+0.006}_{-0.005}$.

[43] ADRIANI 93 use M_Z = 91.181 ± 0.022 GeV, Γ(hadrons) = 1742 ± 19 MeV and α_s = 0.125 ± 0.009. To obtain this branching ratio we divide their value of $C_{1/3}$ = 1.63 ± 0.15 by their value of $(3C_{1/3} + 2C_{2/3})$ = 6.720 ± 0.076.

$R_c = \Gamma(c\overline{c})/\Gamma(\text{hadrons})$ — Γ_9/Γ_6

OUR FIT is obtained by a simultaneous fit to several c- and b-quark measurements as explained in the "Note on the Z boson." As a cross check we have also performed a weighted average of the R_c measurements. Taking into account the various common systematic errors, we obtain R_c = 0.1679 ± 0.0059.

The Standard Model predicts R_c = 0.1723 for m_t = 174.3 GeV and M_H = 150 GeV.

VALUE	DOCUMENT ID	TECN	COMMENT
0.1689±0.0047 OUR FIT			
0.1665±0.0051±0.0081	[44] ABREU 00	DLPH	E^{ee}_{cm}= 88–94 GeV
0.1698±0.0069	[45] BARATE 00B	ALEP	E^{ee}_{cm}= 88–94 GeV
0.180 ±0.011 ±0.013	[46] ACKERSTAFF 98E	OPAL	E^{ee}_{cm}= 88–94 GeV
0.167 ±0.011 ±0.012	[47] ALEXANDER 96R	OPAL	E^{ee}_{cm}= 88–94 GeV
• • • We do not use the following data for averages, fits, limits, etc. • • •			
0.1675±0.0062±0.0103	[48] BARATE 98T	ALEP	Repl. by BARATE 00B
0.1689±0.0095±0.0068	[49] BARATE 98T	ALEP	Repl. by BARATE 00B
0.1623±0.0085±0.0209	[50] ABREU 95D	DLPH	E^{ee}_{cm}= 88–94 GeV
0.142 ±0.008 ±0.014	[51] AKERS 95O	OPAL	Repl. by ACKERSTAFF 98E
0.165 ±0.005 ±0.020	[52] BUSKULIC 94G	ALEP	Repl. by BARATE 00B

[44] ABREU 00 obtain this result properly combining the measurement from the D^{*+} production rate (R_c= 0.1610 ± 0.0104 ± 0.0077 ± 0.0043 (BR)) with that from the overall charm counting (R_c= 0.1692 ± 0.0047 ± 0.0063 ± 0.0074 (BR)) in $c\overline{c}$ events. The systematic error includes an uncertainty of ±0.0054 due to the uncertainty on the charmed hadron branching fractions.

[45] BARATE 00B use exclusive decay modes to independently determine the quantities $R_c\times$f($c \to$ X), X=D^0, D^+, D^+_s, and Λ_c. Estimating $R_c\times$f($c \to \Xi_c/\Omega_c$)= 0.0034, they simply sum over all the charm decays to obtain R_c= 0.1738 ± 0.0047 ± 0.0088 ± 0.0075(BR). This is combined with all previous ALEPH measurements (BARATE 98T and BUSKULIC 94G, R_c= 0.1681 ± 0.0054 ± 0.0062) to obtain the quoted value.

[46] ACKERSTAFF 98E use an inclusive/exclusive double tag. In one jet $D^{*\pm}$ mesons are exclusively reconstructed in several decay channels and in the opposite jet a slow pion (opposite charge inclusive $D^{*\pm}$) tag is used. The b content of this sample is measured by the simultaneous detection of a lepton in one jet and an inclusively reconstructed $D^{*\pm}$ meson in the opposite jet. The systematic error includes an uncertainty of ±0.006 due to the external branching ratios.

[47] ALEXANDER 96R obtain this value via direct charm counting, summing the partial contributions from D^0, D^+, D^+_s, and Λ^+_c, and assuming that strange-charmed baryons account for the 15% of the Λ^+_c production. An uncertainty of ±0.005 due to the uncertainties in the charm hadron branching ratios is included in the overall systematics.

[48] BARATE 98T perform a simultaneous fit to the p and p_T spectra of electrons from hadronic Z decays. The semileptonic branching ratio B($c \to e$) is taken as 0.098 ± 0.005 and the systematic error includes an uncertainty of ±0.0084 due to this.

[49] BARATE 98T obtain this result combining two double-tagging techniques. Searching for a D meson in each hemisphere by full reconstruction in an exclusive decay mode gives R_c= 0.173 ± 0.014 ± 0.0009. The same tag in combination with inclusive identification using the slow pion from the $D^{*+} \to D^0\pi^+$ decay in the opposite hemisphere yields R_c= 0.166 ± 0.012 ± 0.009. The R_b dependence is given by R_c= 0.1689–0.023×(R_b–0.2159). The three measurements of BARATE 98T are combined with BUSKULIC 94G to give the average R_c= 0.1681 ± 0.0054 ± 0.0062.

[50] ABREU 95D perform a maximum likelihood fit to the combined p and p_T distributions of single and dilepton samples. The second error includes an uncertainty of ±0.0124 due to models and branching ratios.

[51] AKERS 95O use the presence of a $D^{*\pm}$ to tag $Z \to c\overline{c}$ with $D^* \to D^0\pi$ and $D^0 \to K\pi$. They measure $P_c*\Gamma(c\overline{c})/\Gamma$(hadrons) to be (1.006 ± 0.055 ± 0.061)×10^{-3}, where P_c is the product branching ratio B($c \to D^*$)B($D^* \to D^0\pi$)B($D^0 \to K\pi$). Assuming that P_c remains unchanged with energy, they use its value (7.1 ± 0.5)×10^{-3} determined at CESR/PETRA to obtain $\Gamma(c\overline{c})/\Gamma$(hadrons). The second error of AKERS 95O includes an uncertainty of ±0.011 from the uncertainty on P_c.

[52] BUSKULIC 94G perform a simultaneous fit to the p and p_T spectra of both single and dilepton events.

$R_b = \Gamma(b\overline{b})/\Gamma(\text{hadrons})$ — Γ_{10}/Γ_6

OUR FIT is obtained by a simultaneous fit to several c- and b-quark measurements as explained in the "Note on the Z boson." As a cross check we have also performed a weighted average of the R_b measurements taking into account the various common systematic errors. For R_c = 0.1689 (as given by OUR FIT above), we obtain R_b = 0.21622 ± 0.00076. For an expected Standard Model value of R_c = 0.1723, our weighted average gives R_b = 0.21614 ± 0.00076.

The Standard Model predicts R_b = 0.21581 for m_t = 174.3 GeV and M_H = 150 GeV.

VALUE			DOCUMENT ID		TECN	COMMENT
0.21643±0.00072 OUR FIT						
0.2174	±0.0015	±0.0028	[53] ACCIARRI	00	L3	$E^{ee}_{\rm cm}$= 89–93 GeV
0.2178	±0.0011	±0.0013	[54] ABBIENDI	99B	OPAL	$E^{ee}_{\rm cm}$= 88–94 GeV
0.21634	±0.00067	±0.00060	[55] ABREU	99B	DLPH	$E^{ee}_{\rm cm}$= 88–94 GeV
0.2142	±0.0034	±0.0015	[56] ABE	98D	SLD	$E^{ee}_{\rm cm}$= 91.2 GeV
0.2159	±0.0009	±0.0011	[57] BARATE	97F	ALEP	$E^{ee}_{\rm cm}$= 88–94 GeV
• • • We do not use the following data for averages, fits, limits, etc. • • •						
0.2175	±0.0014	±0.0017	[58] ACKERSTAFF	97K	OPAL	Repl. by ABBIENDI 99B
0.2167	±0.0011	±0.0013	[59] BARATE	97E	ALEP	$E^{ee}_{\rm cm}$= 88–94 GeV
0.229	±0.011		[60] ABE	96E	SLD	Repl. by ABE 98D
0.2216	±0.0016	±0.0021	[61] ABREU	96	DLPH	Repl. by ABREU 99B
0.2145	±0.0089	±0.0067	[62] ABREU	95D	DLPH	$E^{ee}_{\rm cm}$= 88–94 GeV
0.219	±0.006	±0.005	[63] BUSKULIC	94G	ALEP	$E^{ee}_{\rm cm}$= 88–94 GeV
0.251	±0.049	±0.030	[64] JACOBSEN	91	MRK2	$E^{ee}_{\rm cm}$= 91 GeV

[53] ACCIARRI 00 obtain this result using a double-tagging technique, with a high p_T lepton tag and an impact parameter tag in opposite hemispheres.

[54] ABBIENDI 99B tag $Z \to b\overline{b}$ decays using leptons and/or separated decay vertices. The b-tagging efficiency is measured directly from the data using a double-tagging technique.

[55] ABREU 99B obtain this result combining in a multivariate analysis several tagging methods (impact parameter and secondary vertex reconstruction, complemented by event shape variables). For R_c different from its Standard Model value of 0.172, R_b varies as $-0.024\times(R_c-0.172)$.

[56] ABE 98D use a double tag based on 3D impact parameter with reconstruction of secondary vertices. The charm background is reduced by requiring the invariant mass at the secondary vertex to be above 2 GeV. The systematic error includes an uncertainty of ±0.0002 due to the uncertainty on R_c.

[57] BARATE 97F combine the lifetime-mass hemisphere tag (BARATE 97E) with event shape information and lepton tag to identify $Z \to b\overline{b}$ candidates. They further use c- and uds-selection tags to identify the background. For R_c different from its Standard Model value of 0.172, R_b varies as $-0.019\times(R_c - 0.172)$.

[58] ACKERSTAFF 97K use lepton and/or separated decay vertex to tag independently each hemisphere. Comparing the numbers of single- and double-tagged events, they determine the b-tagging efficiency directly from the data.

[59] BARATE 97E combine a lifetime tag with a mass cut based on the mass difference between c hadrons and b hadrons. Included in BARATE 97F.

[60] ABE 96E obtain this value by combining results from three different b-tagging methods (2D impact parameter, 3D impact parameter, and 3D displaced vertex).

[61] ABREU 96 obtain this result combining several analyses (double lifetime tag, mixed tag and multivariate analysis). This value is obtained assuming R_c=Γ($c\overline{c}$)/Γ(hadrons) = 0.172. For a value of R_c different from this by an amount ΔR_c the change in the value is given by $-0.087 \cdot \Delta R_c$.

[62] ABREU 95D perform a maximum likelihood fit to the combined p and p_T distributions of single and dilepton samples. The second error includes an uncertainty of ±0.0023 due to models and branching ratios.

[63] BUSKULIC 94G perform a simultaneous fit to the p and p_T spectra of both single and dilepton events.

[64] JACOBSEN 91 tagged $b\overline{b}$ events by requiring coincidence of ≥ 3 tracks with significant impact parameters using vertex detector. Systematic error includes lifetime and decay uncertainties (±0.014).

$\Gamma(b\overline{b}b\overline{b})/\Gamma(\text{hadrons})$ $\qquad\Gamma_{11}/\Gamma_6$

VALUE (units 10^{-4})	DOCUMENT ID		TECN	COMMENT
5.2±1.9 OUR AVERAGE				
3.6±1.7±2.7	[65] ABBIENDI	01G	OPAL	$E^{ee}_{\rm cm}$= 88–94 GeV
6.0±1.9±1.4	[66] ABREU	99U	DLPH	$E^{ee}_{\rm cm}$= 88–94 GeV

[65] ABBIENDI 01G use a sample of four-jet events from hadronic Z decays. To enhance the $b\overline{b}b\overline{b}$ signal, at least three of the four jets are required to have a significantly detached secondary vertex.

[66] ABREU 99U force hadronic Z decays into 3 jets to use all the available phase space and require a b tag for every jet. This decay mode includes primary and secondary $4b$ production, *e.g*, from gluon splitting to $b\overline{b}$.

$\Gamma(ggg)/\Gamma(\text{hadrons})$ $\qquad\Gamma_{12}/\Gamma_6$

VALUE	CL%	DOCUMENT ID		TECN	COMMENT
<1.6 × 10^{-2}	95	[67] ABREU	96S	DLPH	$E^{ee}_{\rm cm}$= 88–94 GeV

[67] This branching ratio is slightly dependent on the jet-finder algorithm. The value we quote is obtained using the JADE algorithm, while using the DURHAM algorithm ABREU 96S obtain an upper limit of 1.5×10^{-2}.

$\Gamma(\pi^0\gamma)/\Gamma_{\rm total}$ $\qquad\Gamma_{13}/\Gamma$

VALUE	CL%	DOCUMENT ID		TECN	COMMENT
<5.2 × 10^{-5}	95	[68] ACCIARRI	95G	L3	$E^{ee}_{\rm cm}$= 88–94 GeV
$<5.5 \times 10^{-5}$	95	ABREU	94B	DLPH	$E^{ee}_{\rm cm}$= 88–94 GeV
$<2.1 \times 10^{-4}$	95	DECAMP	92	ALEP	$E^{ee}_{\rm cm}$= 88–94 GeV
$<1.4 \times 10^{-4}$	95	AKRAWY	91F	OPAL	$E^{ee}_{\rm cm}$= 88–94 GeV

[68] This limit is for both decay modes $Z \to \pi^0\gamma/\gamma\gamma$ which are indistinguishable in ACCIARRI 95G.

$\Gamma(\eta\gamma)/\Gamma_{\rm total}$ $\qquad\Gamma_{14}/\Gamma$

VALUE	CL%	DOCUMENT ID		TECN	COMMENT
$<7.6 \times 10^{-5}$	95	ACCIARRI	95G	L3	$E^{ee}_{\rm cm}$= 88–94 GeV
$<8.0 \times 10^{-5}$	95	ABREU	94B	DLPH	$E^{ee}_{\rm cm}$= 88–94 GeV
<5.1 × 10^{-5}	95	DECAMP	92	ALEP	$E^{ee}_{\rm cm}$= 88–94 GeV
$<2.0 \times 10^{-4}$	95	AKRAWY	91F	OPAL	$E^{ee}_{\rm cm}$= 88–94 GeV

$\Gamma(\omega\gamma)/\Gamma_{\rm total}$ $\qquad\Gamma_{15}/\Gamma$

VALUE	CL%	DOCUMENT ID		TECN	COMMENT
<6.5 × 10^{-4}	95	ABREU	94B	DLPH	$E^{ee}_{\rm cm}$= 88–94 GeV

$\Gamma(\eta'(958)\gamma)/\Gamma_{\rm total}$ $\qquad\Gamma_{16}/\Gamma$

VALUE	CL%	DOCUMENT ID		TECN	COMMENT
<4.2 × 10^{-5}	95	DECAMP	92	ALEP	$E^{ee}_{\rm cm}$= 88–94 GeV

$\Gamma(\gamma\gamma)/\Gamma_{\rm total}$ $\qquad\Gamma_{17}/\Gamma$

This decay would violate the Landau-Yang theorem.

VALUE	CL%	DOCUMENT ID		TECN	COMMENT
<5.2 × 10^{-5}	95	[69] ACCIARRI	95G	L3	$E^{ee}_{\rm cm}$= 88–94 GeV
$<5.5 \times 10^{-5}$	95	ABREU	94B	DLPH	$E^{ee}_{\rm cm}$= 88–94 GeV
$<1.4 \times 10^{-4}$	95	AKRAWY	91F	OPAL	$E^{ee}_{\rm cm}$= 88–94 GeV

[69] This limit is for both decay modes $Z \to \pi^0\gamma/\gamma\gamma$ which are indistinguishable in ACCIARRI 95G.

$\Gamma(\gamma\gamma\gamma)/\Gamma_{\rm total}$ $\qquad\Gamma_{18}/\Gamma$

VALUE	CL%	DOCUMENT ID		TECN	COMMENT
<1.0 × 10^{-5}	95	[70] ACCIARRI	95C	L3	$E^{ee}_{\rm cm}$= 88–94 GeV
$<1.7 \times 10^{-5}$	95	[70] ABREU	94B	DLPH	$E^{ee}_{\rm cm}$= 88–94 GeV
$<6.6 \times 10^{-5}$	95	AKRAWY	91F	OPAL	$E^{ee}_{\rm cm}$= 88–94 GeV

[70] Limit derived in the context of composite Z model.

$\Gamma(\pi^\pm W^\mp)/\Gamma_{\rm total}$ $\qquad\Gamma_{19}/\Gamma$

The value is for the sum of the charge states indicated.

VALUE	CL%	DOCUMENT ID		TECN	COMMENT
<7 × 10^{-5}	95	DECAMP	92	ALEP	$E^{ee}_{\rm cm}$= 88–94 GeV

$\Gamma(\rho^\pm W^\mp)/\Gamma_{\rm total}$ $\qquad\Gamma_{20}/\Gamma$

The value is for the sum of the charge states indicated.

VALUE	CL%	DOCUMENT ID		TECN	COMMENT
<8.3 × 10^{-5}	95	DECAMP	92	ALEP	$E^{ee}_{\rm cm}$= 88–94 GeV

$\Gamma(J/\psi(1S)X)/\Gamma_{\rm total}$ $\qquad\Gamma_{21}/\Gamma$

VALUE (units 10^{-3})	EVTS	DOCUMENT ID		TECN	COMMENT
$3.51^{+0.23}_{-0.25}$ OUR AVERAGE Error includes scale factor of 1.1.					
$3.21\pm0.21^{+0.19}_{-0.28}$	553	[71] ACCIARRI	99F	L3	$E^{ee}_{\rm cm}$= 88–94 GeV
3.9 ±0.2 ±0.3	511	[72] ALEXANDER	96B	OPAL	$E^{ee}_{\rm cm}$= 88–94 GeV
3.73±0.39±0.36	153	[73] ABREU	94P	DLPH	$E^{ee}_{\rm cm}$= 88–94 GeV
• • • We do not use the following data for averages, fits, limits, etc. • • •					
3.40±0.23±0.27	441	[74] ACCIARRI	97J	L3	Repl. by ACCIARRI 99F

[71] ACCIARRI 99F combine $\mu^+\mu^-$ and e^+e^- $J/\psi(1S)$ decay channels. The branching ratio for prompt $J/\psi(1S)$ production is measured to be $(2.1 \pm 0.6 \pm 0.4^{+0.4}_{-0.2}(\text{theor.}))\times10^{-4}$.

[72] ALEXANDER 96B identify $J/\psi(1S)$ from the decays into lepton pairs. (4.8 ± 2.4)% of this branching ratio is due to prompt $J/\psi(1S)$ production (ALEXANDER 96N).

[73] Combining $\mu^+\mu^-$ and e^+e^- channels and taking into account the common systematic errors. $(7.7^{+6.3}_{-5.4})$% of this branching ratio is due to prompt $J/\psi(1S)$ production.

[74] ACCIARRI 97J combine $\mu^+\mu^-$ and e^+e^- $J/\psi(1S)$ decay channels and take into account the common systematic error.

$\Gamma(\psi(2S)X)/\Gamma_{\rm total}$ $\qquad\Gamma_{22}/\Gamma$

VALUE (units 10^{-3})	EVTS	DOCUMENT ID		TECN	COMMENT
1.60±0.29 OUR AVERAGE					
1.6 ±0.5 ±0.3	39	[75] ACCIARRI	97J	L3	$E^{ee}_{\rm cm}$= 88–94 GeV
1.6 ±0.3 ±0.2	46.9	[76] ALEXANDER	96B	OPAL	$E^{ee}_{\rm cm}$= 88–94 GeV
1.60±0.73±0.33	5.4	[77] ABREU	94P	DLPH	$E^{ee}_{\rm cm}$= 88–94 GeV

[75] ACCIARRI 97J measure this branching ratio via the decay channel $\psi(2S) \to \ell^+\ell^-$ ($\ell = \mu$, e).

[76] ALEXANDER 96B measure this branching ratio via the decay channel $\psi(2S) \to J/\psi\pi^+\pi^-$, with $J/\psi \to \ell^+\ell^-$.

[77] ABREU 94P measure this branching ratio via decay channel $\psi(2S) \to J/\psi\pi^+\pi^-$, with $J/\psi \to \mu^+\mu^-$.

$\Gamma(\chi_{c1}(1P)X)/\Gamma_{\rm total}$ $\qquad\Gamma_{23}/\Gamma$

VALUE (units 10^{-3})	EVTS	DOCUMENT ID		TECN	COMMENT
2.9±0.7 OUR AVERAGE					
2.7±0.6±0.5	33	[78] ACCIARRI	97J	L3	$E^{ee}_{\rm cm}$= 88–94 GeV
$5.0\pm2.1^{+1.5}_{-0.9}$	6.4	[79] ABREU	94P	DLPH	$E^{ee}_{\rm cm}$= 88–94 GeV

[78] ACCIARRI 97J measure this branching ratio via the decay channel $\chi_{c1} \to J/\psi + \gamma$, with $J/\psi \to \ell^+\ell^-$ ($\ell = \mu$, e). The $M(\ell^+\ell^-\gamma)$–$M(\ell^+\ell^-)$ mass difference spectrum is fitted with two gaussian shapes for χ_{c1} and χ_{c2}.

[79] This branching ratio is measured via the decay channel $\chi_{c1} \to J/\psi + \gamma$, with $J/\psi \to \mu^+\mu^-$.

$\Gamma(\chi_{c2}(1P)X)/\Gamma_{\rm total}$ — Γ_{24}/Γ

VALUE	CL%	DOCUMENT ID		TECN	COMMENT
<3.2 × 10⁻³	90	[80] ACCIARRI	97J	L3	$E^{ee}_{\rm cm}$= 88–94 GeV

[80] ACCIARRI 97J derive this limit via the decay channel $\chi_{c2} \to J/\psi + \gamma$, with $J/\psi \to \ell^+\ell^-$ ($\ell = \mu$, e). The $M(\ell^+\ell^-\gamma)$–$M(\ell^+\ell^-)$ mass difference spectrum is fitted with two gaussian shapes for χ_{c1} and χ_{c2}.

$\Gamma(\Upsilon(1S)X+\Upsilon(2S)X+\Upsilon(3S)X)/\Gamma_{\rm total}$ — $\Gamma_{25}/\Gamma = (\Gamma_{26}+\Gamma_{27}+\Gamma_{28})/\Gamma$

VALUE (units 10^{-4})	EVTS	DOCUMENT ID		TECN	COMMENT
1.0±0.4±0.22	6.4	[81] ALEXANDER	96F	OPAL	$E^{ee}_{\rm cm}$= 88–94 GeV

[81] ALEXANDER 96F identify the Υ (which refers to any of the three lowest bound states) through its decay into e^+e^- and $\mu^+\mu^-$. The systematic error includes an uncertainty of ±0.2 due to the production mechanism.

$\Gamma(\Upsilon(1S)X)/\Gamma_{\rm total}$ — Γ_{26}/Γ

VALUE	CL%	DOCUMENT ID		TECN	COMMENT
<4.4 × 10⁻⁵	95	[82] ACCIARRI	99F	L3	$E^{ee}_{\rm cm}$= 88–94 GeV

[82] ACCIARRI 99F search for $\Upsilon(1S)$ through its decay into $\ell^+\ell^-$ ($\ell = e$ or μ).

$\Gamma(\Upsilon(2S)X)/\Gamma_{\rm total}$ — Γ_{27}/Γ

VALUE	CL%	DOCUMENT ID		TECN	COMMENT
<13.9 × 10⁻⁵	95	[83] ACCIARRI	97R	L3	$E^{ee}_{\rm cm}$= 88–94 GeV

[83] ACCIARRI 97R search for $\Upsilon(2S)$ through its decay into $\ell^+\ell^-$ ($\ell = e$ or μ).

$\Gamma(\Upsilon(3S)X)/\Gamma_{\rm total}$ — Γ_{28}/Γ

VALUE	CL%	DOCUMENT ID		TECN	COMMENT
<9.4 × 10⁻⁵	95	[84] ACCIARRI	97R	L3	$E^{ee}_{\rm cm}$= 88–94 GeV

[84] ACCIARRI 97R search for $\Upsilon(3S)$ through its decay into $\ell^+\ell^-$ ($\ell = e$ or μ).

$\Gamma((D^0/\overline{D}^0)X)/\Gamma(\text{hadrons})$ — Γ_{29}/Γ_6

VALUE	EVTS	DOCUMENT ID		TECN	COMMENT
0.296±0.019±0.021	369	[85] ABREU	93I	DLPH	$E^{ee}_{\rm cm}$= 88–94 GeV

[85] The $(D^0/\overline{D}^0)$ states in ABREU 93I are detected by the $K\pi$ decay mode. This is a corrected result (see the erratum of ABREU 93I).

$\Gamma(D^\pm X)/\Gamma(\text{hadrons})$ — Γ_{30}/Γ_6

VALUE	EVTS	DOCUMENT ID		TECN	COMMENT
0.174±0.016±0.018	539	[86] ABREU	93I	DLPH	$E^{ee}_{\rm cm}$= 88–94 GeV

[86] The $D^\pm$ states in ABREU 93I are detected by the $K\pi\pi$ decay mode. This is a corrected result (see the erratum of ABREU 93I).

$\Gamma(D^*(2010)^\pm X)/\Gamma(\text{hadrons})$ — Γ_{31}/Γ_6

The value is for the sum of the charge states indicated.

VALUE	EVTS	DOCUMENT ID		TECN	COMMENT
0.163±0.019 OUR AVERAGE	Error includes scale factor of 1.3.				
0.155±0.010±0.013	358	[87] ABREU	93I	DLPH	$E^{ee}_{\rm cm}$= 88–94 GeV
0.21 ±0.04	362	[88] DECAMP	91J	ALEP	$E^{ee}_{\rm cm}$= 88–94 GeV

[87] $D^*(2010)^\pm$ in ABREU 93I are reconstructed from $D^0\pi^\pm$, with $D^0 \to K^-\pi^+$. The new CLEO II measurement of B($D^{*\pm} \to D^0\pi^\pm$) = (68.1 ± 1.6) % is used. This is a corrected result (see the erratum of ABREU 93I).

[88] DECAMP 91J report B($D^*(2010)^+ \to D^0\pi^+$) B($D^0 \to K^-\pi^+$) $\Gamma(D^*(2010)^\pm X)$ / Γ(hadrons) = (5.11 ± 0.34) × 10^{-3}. They obtained the above number assuming B($D^0 \to K^-\pi^+$) = (3.62 ± 0.34 ± 0.44)% and B($D^*(2010)^+ \to D^0\pi^+$) = (55 ± 4)%. We have rescaled their original result of 0.26 ± 0.05 taking into account the new CLEO II branching ratio B($D^*(2010)^+ \to D^0\pi^+$) = (68.1 ± 1.6)%.

$\Gamma(D_{s1}(2536)^\pm X)/\Gamma(\text{hadrons})$ — Γ_{32}/Γ_6

$D_{s1}(2536)^\pm$ is an expected orbitally-excited state of the D_s meson.

VALUE (%)	EVTS	DOCUMENT ID		TECN	COMMENT
0.52±0.09±0.06	92	[89] HEISTER	02B	ALEP	$E^{ee}_{\rm cm}$= 88–94 GeV

[89] HEISTER 02B reconstruct this meson in the decay modes $D_{s1}(2536)^\pm \to D^{*\pm}K^0$ and $D_{s1}(2536)^\pm \to D^{*0}K^\pm$. The quoted branching ratio assumes that the decay width of the $D_{s1}(2536)$ is saturated by the two measured decay modes.

$\Gamma(D_{sJ}(2573)^\pm X)/\Gamma(\text{hadrons})$ — Γ_{33}/Γ_6

$D_{sJ}(2573)^\pm$ is an expected orbitally-excited state of the D_s meson.

VALUE (%)	EVTS	DOCUMENT ID		TECN	COMMENT
$0.83\pm0.29^{+0.07}_{-0.13}$	64	[90] HEISTER	02B	ALEP	$E^{ee}_{\rm cm}$= 88–94 GeV

[90] HEISTER 02B reconstruct this meson in the decay mode $D_{s2}(2573)^\pm \to D^0K^\pm$. The quoted branching ratio assumes that the detected decay mode represents 45% of the full decay width.

$\Gamma(D^{*\prime}(2629)^\pm X)/\Gamma(\text{hadrons})$ — Γ_{34}/Γ_6

$D^{*\prime}(2629)^\pm$ is a predicted radial excitation of the $D^*(2010)^\pm$ meson.

VALUE	DOCUMENT ID		TECN	COMMENT
searched for	[91] ABBIENDI	01N	OPAL	$E^{ee}_{\rm cm}$= 88–94 GeV

[91] ABBIENDI 01N searched for the decay mode $D^{*\prime}(2629)^\pm \to D^{*\pm}\pi^+\pi^-$ with $D^{*+} \to D^0\pi^+$, and $D^0 \to K^-\pi^+$. They quote a 95% CL limit for $Z \to D^{*\prime}(2629)^\pm \times$B($D^{*\prime}(2629)^+ \to D^{*+}\pi^+\pi^-$) < 3.1 × 10^{-3}.

$\Gamma(B^0_s X)/\Gamma(\text{hadrons})$ — Γ_{37}/Γ_6

VALUE	DOCUMENT ID		TECN	COMMENT
seen	[92] ABREU	92M	DLPH	$E^{ee}_{\rm cm}$= 88–94 GeV
seen	[93] ACTON	92N	OPAL	$E^{ee}_{\rm cm}$= 88–94 GeV
seen	[94] BUSKULIC	92E	ALEP	$E^{ee}_{\rm cm}$= 88–94 GeV

[92] ABREU 92M reported value is $\Gamma(B^0_s X)*$B($B^0_s \to D_s\mu\nu_\mu X$) $*$B($D_s \to \phi\pi$)/Γ(hadrons) = (18 ± 8) × 10^{-5}.

[93] ACTON 92N find evidence for B^0_s production using D_s-ℓ correlations, with $D^+_s \to \phi\pi^+$ and $K^*(892)K^+$. Assuming R_b from the Standard Model and averaging over the e and μ channels, authors measure the product branching fraction to be $f(\overline{b} \to B^0_s)\times$B($B^0_s \to D^-_s\ell^+\nu_\ell X$)×B($D^-_s \to \phi\pi^-$) = (3.9 ± 1.1 ± 0.8) × 10^{-4}.

[94] BUSKULIC 92E find evidence for B^0_s production using D_s-ℓ correlations, with $D^+_s \to \phi\pi^+$ and $K^*(892)K^+$. Using B($D^+_s \to \phi\pi^+$) = (2.7 ± 0.7)% and summing up the e and μ channels, the weighted average product branching fraction is measured to be B($\overline{b} \to B^0_s$)×B($B^0_s \to D^-_s\ell^+\nu_\ell X$) = $0.040 \pm 0.011^{+0.010}_{-0.012}$.

$\Gamma(B^+_c X)/\Gamma(\text{hadrons})$ — Γ_{38}/Γ_6

VALUE	DOCUMENT ID		TECN	COMMENT
searched for	[95] ACKERSTAFF	98O	OPAL	$E^{ee}_{\rm cm}$= 88–94 GeV
searched for	[96] ABREU	97E	DLPH	$E^{ee}_{\rm cm}$= 88–94 GeV
searched for	[97] BARATE	97H	ALEP	$E^{ee}_{\rm cm}$= 88–94 GeV

[95] ACKERSTAFF 98O searched for the decay modes $B_c \to J/\psi\pi^+$, $J/\psi a^+_1$, and $J/\psi\ell^+\nu_\ell$, with $J/\psi \to \ell^+\ell^-$, $\ell = e,\mu$. The number of candidates (background) for the three decay modes is 2 (0.63 ± 0.2), 0 (1.10 ± 0.22), and 1 (0.82 ± 0.19) respectively. Interpreting the 2 $B_c \to J/\psi\pi^+$ candidates as signal, they report $\Gamma(B^+_c X)\times$B($B_c \to J/\psi\pi^+$)/Γ(hadrons) = $(3.8^{+5.0}_{-2.4}\pm0.5)\times10^{-5}$. Interpreted as background, the 90% CL bounds are $\Gamma(B^+_c X)*$B($B_c \to J/\psi\pi^+$)/Γ(hadrons) < 1.06 × 10^{-4}, $\Gamma(B^+_c X)*$B($B_c \to J/\psi a^+_1$)/Γ(hadrons) < 5.29 × 10^{-4}, $\Gamma(B^+_c X)*$B($B_c \to J/\psi\ell^+\nu_\ell$)/$\Gamma$(hadrons) < 6.96 × 10^{-5}.

[96] ABREU 97E searched for the decay modes $B_c \to J/\psi\pi^+$, $J/\psi\ell^+\nu_\ell$, and $J/\psi(3\pi)^+$, with $J/\psi \to \ell^+\ell^-$, $\ell = e,\mu$. The number of candidates (background) for the three decay modes is 1 (1.7), 0 (0.3), and 1 (2.3) respectively. They report the following 90% CL limits: $\Gamma(B^+_c X)*$B($B_c \to J/\psi\pi^+$)/Γ(hadrons) <(1.05–0.84) × 10^{-4}, $\Gamma(B^+_c X)*$B($B_c \to J/\psi\ell\nu_\ell$)/$\Gamma$(hadrons) <(5.8–5.0) × 10^{-5}, $\Gamma(B^+_c X)*$B($B_c \to J/\psi(3\pi)^+$)/Γ(hadrons) < 1.75 × 10^{-4}, where the ranges are due to the predicted B_c lifetime (0.4–1.4) ps.

[97] BARATE 97H searched for the decay modes $B_c \to J/\psi\pi^+$ and $J/\psi\ell^+\nu_\ell$ with $J/\psi \to \ell^+\ell^-$, $\ell = e,\mu$. The number of candidates (background) for the two decay modes is 0 (0.44) and 2 (0.81) respectively. They report the following 90% CL limits: $\Gamma(B^+_c X)*$B($B_c \to J/\psi\pi^+$)/Γ(hadrons) < 3.6 × 10^{-5} and $\Gamma(B^+_c X)*$B($B_c \to J/\psi\ell^+\nu_\ell$)/$\Gamma$(hadrons) < 5.2 × 10^{-5}.

$\Gamma(B^*X)/[\Gamma(BX)+\Gamma(B^*X)]$ — $\Gamma_{36}/(\Gamma_{35}+\Gamma_{36})$

As the experiments assume different values of the b-baryon contribution, our average should be taken with caution. If we assume a common baryon production fraction of (11.8 ± 2.0)% as given in the 2002 edition of this *Review* OUR AVERAGE becomes 0.75 ± 0.04.

VALUE	EVTS	DOCUMENT ID		TECN	COMMENT
0.75 ±0.04 OUR AVERAGE					
0.760±0.036±0.083		[98] ACKERSTAFF	97M	OPAL	$E^{ee}_{\rm cm}$= 88–94 GeV
0.771±0.026±0.070		[99] BUSKULIC	96D	ALEP	$E^{ee}_{\rm cm}$= 88–94 GeV
0.72 ±0.03 ±0.06		[100] ABREU	95R	DLPH	$E^{ee}_{\rm cm}$= 88–94 GeV
0.76 ±0.08 ±0.06	1378	[101] ACCIARRI	95B	L3	$E^{ee}_{\rm cm}$= 88–94 GeV

[98] ACKERSTAFF 97M use an inclusive B reconstruction method and assume a (13.2 ± 4.1)% b-baryon contribution. The value refers to a b-flavored meson mixture of B_u, B_d, and B_s.

[99] BUSKULIC 96D use an inclusive reconstruction of B hadrons and assume a (12.2 ± 4.3)% b-baryon contribution. The value refers to a b-flavored mixture of B_u, B_d, and B_s.

[100] ABREU 95R use an inclusive B-reconstruction method and assume a (10 ± 4)% b-baryon contribution. The value refers to a b-flavored meson mixture of B_u, B_d, and B_s.

[101] ACCIARRI 95B assume a 9.4% b-baryon contribution. The value refers to a b-flavored mixture of B_u, B_d, and B_s.

$\Gamma(\text{anomalous }\gamma+\text{hadrons})/\Gamma_{\rm total}$ — Γ_{39}/Γ

Limits on additional sources of prompt photons beyond expectations for final-state bremsstrahlung.

VALUE	CL%	DOCUMENT ID		TECN	COMMENT
<3.2 × 10⁻³	95	[102] AKRAWY	90J	OPAL	$E^{ee}_{\rm cm}$= 88–94 GeV

[102] AKRAWY 90J report $\Gamma(\gamma X)$ < 8.2 MeV at 95%CL. They assume a three-body $\gamma q\overline{q}$ distribution and use E(γ) > 10 GeV.

$\Gamma(e^+e^-\gamma)/\Gamma_{\rm total}$ — Γ_{40}/Γ

VALUE	CL%	DOCUMENT ID		TECN	COMMENT
<5.2 × 10⁻⁴	95	[103] ACTON	91B	OPAL	$E^{ee}_{\rm cm}$= 91.2 GeV

[103] ACTON 91B looked for isolated photons with E>2% of beam energy (> 0.9 GeV).

$\Gamma(\mu^+\mu^-\gamma)/\Gamma_{total}$ — Γ_{41}/Γ

VALUE	CL%	DOCUMENT ID		TECN	COMMENT
<5.6 × 10^{-4}	95	[104] ACTON	91B	OPAL	E^{ee}_{cm}= 91.2 GeV

[104] ACTON 91B looked for isolated photons with E>2% of beam energy (> 0.9 GeV).

$\Gamma(\tau^+\tau^-\gamma)/\Gamma_{total}$ — Γ_{42}/Γ

VALUE	CL%	DOCUMENT ID		TECN	COMMENT
<7.3 × 10^{-4}	95	[105] ACTON	91B	OPAL	E^{ee}_{cm}= 91.2 GeV

[105] ACTON 91B looked for isolated photons with E>2% of beam energy (> 0.9 GeV).

$\Gamma(\ell^+\ell^-\gamma\gamma)/\Gamma_{total}$ — Γ_{43}/Γ

The value is the sum over $\ell = e, \mu, \tau$.

VALUE	CL%	DOCUMENT ID		TECN	COMMENT
<6.8 × 10^{-6}	95	[106] ACTON	93E	OPAL	E^{ee}_{cm}= 88–94 GeV

[106] For $m_{\gamma\gamma} = 60 \pm 5$ GeV.

$\Gamma(q\overline{q}\gamma\gamma)/\Gamma_{total}$ — Γ_{44}/Γ

VALUE	CL%	DOCUMENT ID		TECN	COMMENT
<5.5 × 10^{-6}	95	[107] ACTON	93E	OPAL	E^{ee}_{cm}= 88–94 GeV

[107] For $m_{\gamma\gamma} = 60 \pm 5$ GeV.

$\Gamma(\nu\overline{\nu}\gamma\gamma)/\Gamma_{total}$ — Γ_{45}/Γ

VALUE	CL%	DOCUMENT ID		TECN	COMMENT
<3.1 × 10^{-6}	95	[108] ACTON	93E	OPAL	E^{ee}_{cm}= 88–94 GeV

[108] For $m_{\gamma\gamma} = 60 \pm 5$ GeV.

$\Gamma(e^\pm\mu^\mp)/\Gamma(e^+e^-)$ — Γ_{46}/Γ_1

Test of lepton family number conservation. The value is for the sum of the charge states indicated.

VALUE	CL%	DOCUMENT ID		TECN	COMMENT
<0.07	90	ALBAJAR	89	UA1	$E^{p\overline{p}}_{cm}$= 546,630 GeV

$\Gamma(e^\pm\mu^\mp)/\Gamma_{total}$ — Γ_{46}/Γ

Test of lepton family number conservation. The value is for the sum of the charge states indicated.

VALUE	CL%	DOCUMENT ID		TECN	COMMENT
<2.5 × 10^{-6}	95	ABREU	97C	DLPH	E^{ee}_{cm}= 88–94 GeV
<1.7 × 10^{-6}	95	AKERS	95W	OPAL	E^{ee}_{cm}= 88–94 GeV
<0.6 × 10^{-5}	95	ADRIANI	93I	L3	E^{ee}_{cm}= 88–94 GeV
<2.6 × 10^{-5}	95	DECAMP	92	ALEP	E^{ee}_{cm}= 88–94 GeV

$\Gamma(e^\pm\tau^\mp)/\Gamma_{total}$ — Γ_{47}/Γ

Test of lepton family number conservation. The value is for the sum of the charge states indicated.

VALUE	CL%	DOCUMENT ID		TECN	COMMENT
<2.2 × 10^{-5}	95	ABREU	97C	DLPH	E^{ee}_{cm}= 88–94 GeV
<9.8 × 10^{-6}	95	AKERS	95W	OPAL	E^{ee}_{cm}= 88–94 GeV
<1.3 × 10^{-5}	95	ADRIANI	93I	L3	E^{ee}_{cm}= 88–94 GeV
<1.2 × 10^{-4}	95	DECAMP	92	ALEP	E^{ee}_{cm}= 88–94 GeV

$\Gamma(\mu^\pm\tau^\mp)/\Gamma_{total}$ — Γ_{48}/Γ

Test of lepton family number conservation. The value is for the sum of the charge states indicated.

VALUE	CL%	DOCUMENT ID		TECN	COMMENT
<1.2 × 10^{-5}	95	ABREU	97C	DLPH	E^{ee}_{cm}= 88–94 GeV
<1.7 × 10^{-5}	95	AKERS	95W	OPAL	E^{ee}_{cm}= 88–94 GeV
<1.9 × 10^{-5}	95	ADRIANI	93I	L3	E^{ee}_{cm}= 88–94 GeV
<1.0 × 10^{-4}	95	DECAMP	92	ALEP	E^{ee}_{cm}= 88–94 GeV

$\Gamma(pe)/\Gamma_{total}$ — Γ_{49}/Γ

Test of baryon number and lepton number conservations. Charge conjugate states are implied.

VALUE	CL%	DOCUMENT ID		TECN	COMMENT
<1.8 × 10^{-6}	95	[109] ABBIENDI	99I	OPAL	E^{ee}_{cm}= 88–94 GeV

[109] ABBIENDI 99I give the 95%CL limit on the partial width $\Gamma(Z^0 \rightarrow pe)$< 4.6 KeV and we have transformed it into a branching ratio.

$\Gamma(p\mu)/\Gamma_{total}$ — Γ_{50}/Γ

Test of baryon number and lepton number conservations. Charge conjugate states are implied.

VALUE	CL%	DOCUMENT ID		TECN	COMMENT
<1.8 × 10^{-6}	95	[110] ABBIENDI	99I	OPAL	E^{ee}_{cm}= 88–94 GeV

[110] ABBIENDI 99I give the 95%CL limit on the partial width $\Gamma(Z^0 \rightarrow p\mu)$< 4.4 KeV and we have transformed it into a branching ratio.

AVERAGE PARTICLE MULTIPLICITIES IN HADRONIC Z DECAY

Summed over particle and antiparticle, when appropriate.

$\langle N_\gamma \rangle$

VALUE	DOCUMENT ID		TECN	COMMENT
20.97±0.02±1.15	ACKERSTAFF	98A	OPAL	E^{ee}_{cm}= 91.2 GeV

$\langle N_{\pi^\pm} \rangle$

VALUE	DOCUMENT ID		TECN	COMMENT
16.99±0.20 OUR AVERAGE				
16.84±0.37	ABE	99E	SLD	E^{ee}_{cm}= 91.2 GeV
17.26±0.10±0.88	ABREU	98L	DLPH	E^{ee}_{cm}= 91.2 GeV
17.04±0.31	BARATE	98V	ALEP	E^{ee}_{cm}= 91.2 GeV
17.05±0.43	AKERS	94P	OPAL	E^{ee}_{cm}= 91.2 GeV

$\langle N_{\pi^0} \rangle$

VALUE	DOCUMENT ID		TECN	COMMENT
9.76±0.26 OUR AVERAGE				
9.55±0.06±0.75	ACKERSTAFF	98A	OPAL	E^{ee}_{cm}= 91.2 GeV
9.63±0.13±0.63	BARATE	97J	ALEP	E^{ee}_{cm}= 91.2 GeV
9.90±0.02±0.33	ACCIARRI	96	L3	E^{ee}_{cm}= 91.2 GeV
9.2 ±0.2 ±1.0	ADAM	96	DLPH	E^{ee}_{cm}= 91.2 GeV

$\langle N_\eta \rangle$

VALUE	DOCUMENT ID		TECN	COMMENT
1.01±0.08 OUR AVERAGE Error includes scale factor of 1.3. See the ideogram below.				
1.20±0.04±0.11	HEISTER	02C	ALEP	E^{ee}_{cm}= 91.2 GeV
0.97±0.03±0.11	ACKERSTAFF	98A	OPAL	E^{ee}_{cm}= 91.2 GeV
0.93±0.01±0.09	ACCIARRI	96	L3	E^{ee}_{cm}= 91.2 GeV

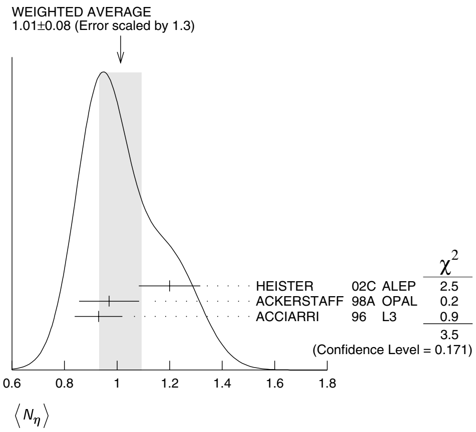

$\langle N_{\rho^\pm} \rangle$

VALUE	DOCUMENT ID		TECN	COMMENT
2.40±0.06±0.43	ACKERSTAFF	98A	OPAL	E^{ee}_{cm}= 91.2 GeV

$\langle N_{\rho^0} \rangle$

VALUE	DOCUMENT ID		TECN	COMMENT
1.24±0.10 OUR AVERAGE Error includes scale factor of 1.1.				
1.19±0.10	ABREU	99J	DLPH	E^{ee}_{cm}= 91.2 GeV
1.45±0.06±0.20	BUSKULIC	96H	ALEP	E^{ee}_{cm}= 91.2 GeV

$\langle N_\omega \rangle$

VALUE	DOCUMENT ID		TECN	COMMENT
1.02±0.06 OUR AVERAGE				
1.00±0.03±0.06	HEISTER	02C	ALEP	E^{ee}_{cm}= 91.2 GeV
1.04±0.04±0.14	ACKERSTAFF	98A	OPAL	E^{ee}_{cm}= 91.2 GeV
1.17±0.09±0.15	ACCIARRI	97D	L3	E^{ee}_{cm}= 91.2 GeV

$\langle N_{\eta'} \rangle$

VALUE	DOCUMENT ID		TECN	COMMENT
0.17 ±0.05 OUR AVERAGE Error includes scale factor of 2.4.				
0.14 ±0.01 ±0.02	ACKERSTAFF	98A	OPAL	E^{ee}_{cm}= 91.2 GeV
0.25 ±0.04	[111] ACCIARRI	97D	L3	E^{ee}_{cm}= 91.2 GeV
• • • We do not use the following data for averages, fits, limits, etc. • • •				
0.068±0.018±0.016	[112] BUSKULIC	92D	ALEP	E^{ee}_{cm}= 91.2 GeV

[111] ACCIARRI 97D obtain this value averaging over the two decay channels $\eta' \rightarrow \pi^+\pi^-\eta$ and $\eta' \rightarrow \rho^0\gamma$.

[112] BUSKULIC 92D obtain this value for x> 0.1.

$\langle N_{f_0(980)} \rangle$

VALUE	DOCUMENT ID		TECN	COMMENT
0.147±0.011 OUR AVERAGE				
0.164±0.021	ABREU	99J	DLPH	E^{ee}_{cm}= 91.2 GeV
0.141±0.007±0.011	ACKERSTAFF	98Q	OPAL	E^{ee}_{cm}= 91.2 GeV

$\langle N_{a_0(980)^\pm} \rangle$

VALUE	DOCUMENT ID		TECN	COMMENT
0.27±0.04±0.10	ACKERSTAFF	98A	OPAL	E^{ee}_{cm}= 91.2 GeV

$\langle N_{\phi} \rangle$

VALUE	DOCUMENT ID		TECN	COMMENT
0.098±0.006 OUR AVERAGE	Error includes scale factor of 2.0. See the ideogram below.			
0.105±0.008	ABE	99E	SLD	E^{ee}_{cm}= 91.2 GeV
0.091±0.002±0.003	ACKERSTAFF	98Q	OPAL	E^{ee}_{cm}= 91.2 GeV
0.104±0.003±0.007	ABREU	96U	DLPH	E^{ee}_{cm}= 91.2 GeV
0.122±0.004±0.008	BUSKULIC	96H	ALEP	E^{ee}_{cm}= 91.2 GeV

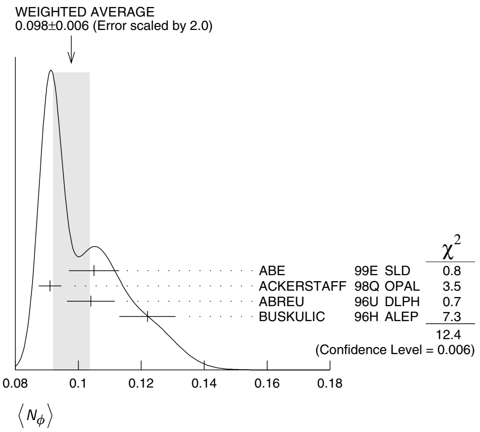

$\langle N_{f_2(1270)} \rangle$

VALUE	DOCUMENT ID		TECN	COMMENT
0.169±0.025 OUR AVERAGE	Error includes scale factor of 1.4.			
0.214±0.038	ABREU	99J	DLPH	E^{ee}_{cm}= 91.2 GeV
0.155±0.011±0.018	ACKERSTAFF	98Q	OPAL	E^{ee}_{cm}= 91.2 GeV

$\langle N_{f_1(1285)} \rangle$

VALUE	DOCUMENT ID		TECN	COMMENT
0.165±0.051	[113] ABDALLAH	03H	DLPH	E^{ee}_{cm}= 91.2 GeV

[113] ABDALLAH 03H assume a $K\overline{K}\pi$ branching ratio of (9.0 ± 0.4)%.

$\langle N_{f_1(1420)} \rangle$

VALUE	DOCUMENT ID		TECN	COMMENT
0.056±0.012	[114] ABDALLAH	03H	DLPH	E^{ee}_{cm}= 91.2 GeV

[114] ABDALLAH 03H assume a $K\overline{K}\pi$ branching ratio of 100%.

$\langle N_{f'_2(1525)} \rangle$

VALUE	DOCUMENT ID		TECN	COMMENT
0.012±0.006	ABREU	99J	DLPH	E^{ee}_{cm}= 91.2 GeV

$\langle N_{K^\pm} \rangle$

VALUE	DOCUMENT ID		TECN	COMMENT
2.25±0.05 OUR AVERAGE				
2.22±0.16	ABE	99E	SLD	E^{ee}_{cm}= 91.2 GeV
2.21±0.05±0.05	ABREU	98L	DLPH	E^{ee}_{cm}= 91.2 GeV
2.26±0.12	BARATE	98V	ALEP	E^{ee}_{cm}= 91.2 GeV
2.42±0.13	AKERS	94P	OPAL	E^{ee}_{cm}= 91.2 GeV

$\langle N_{K^0} \rangle$

VALUE	DOCUMENT ID		TECN	COMMENT
2.039±0.025 OUR AVERAGE	Error includes scale factor of 1.3. See the ideogram below.			
2.093±0.004±0.029	BARATE	00O	ALEP	E^{ee}_{cm}= 91.2 GeV
2.01 ±0.08	ABE	99E	SLD	E^{ee}_{cm}= 91.2 GeV
2.024±0.006±0.042	ACCIARRI	97L	L3	E^{ee}_{cm}= 91.2 GeV
1.962±0.022±0.056	ABREU	95L	DLPH	E^{ee}_{cm}= 91.2 GeV
1.99 ±0.01 ±0.04	AKERS	95U	OPAL	E^{ee}_{cm}= 91.2 GeV

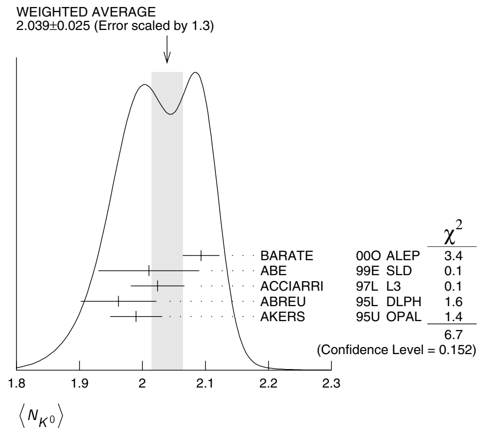

$\langle N_{K^*(892)^\pm} \rangle$

VALUE	DOCUMENT ID		TECN	COMMENT
0.72 ±0.05 OUR AVERAGE				
0.712±0.031±0.059	ABREU	95L	DLPH	E^{ee}_{cm}= 91.2 GeV
0.72 ±0.02 ±0.08	ACTON	93	OPAL	E^{ee}_{cm}= 91.2 GeV

$\langle N_{K^*(892)^0} \rangle$

VALUE	DOCUMENT ID		TECN	COMMENT
0.739±0.022 OUR AVERAGE				
0.707±0.041	ABE	99E	SLD	E^{ee}_{cm}= 91.2 GeV
0.74 ±0.02 ±0.02	ACKERSTAFF	97S	OPAL	E^{ee}_{cm}= 91.2 GeV
0.77 ±0.02 ±0.07	ABREU	96U	DLPH	E^{ee}_{cm}= 91.2 GeV
0.83 ±0.01 ±0.09	BUSKULIC	96H	ALEP	E^{ee}_{cm}= 91.2 GeV
0.97 ±0.18 ±0.31	ABREU	93	DLPH	E^{ee}_{cm}= 91.2 GeV

$\langle N_{K^*_2(1430)} \rangle$

VALUE	DOCUMENT ID		TECN	COMMENT
0.073±0.023	ABREU	99J	DLPH	E^{ee}_{cm}= 91.2 GeV
• • • We do not use the following data for averages, fits, limits, etc. • • •				
0.19 ±0.04 ±0.06	[115] AKERS	95X	OPAL	E^{ee}_{cm}= 91.2 GeV

[115] AKERS 95X obtain this value for $x<$ 0.3.

$\langle N_{D^\pm} \rangle$

VALUE	DOCUMENT ID		TECN	COMMENT
0.187±0.020 OUR AVERAGE	Error includes scale factor of 1.5. See the ideogram below.			
0.170±0.009±0.014	ALEXANDER	96R	OPAL	E^{ee}_{cm}= 91.2 GeV
0.251±0.026±0.025	BUSKULIC	94J	ALEP	E^{ee}_{cm}= 91.2 GeV
0.199±0.019±0.024	[116] ABREU	93I	DLPH	E^{ee}_{cm}= 91.2 GeV

[116] See ABREU 95 (erratum).

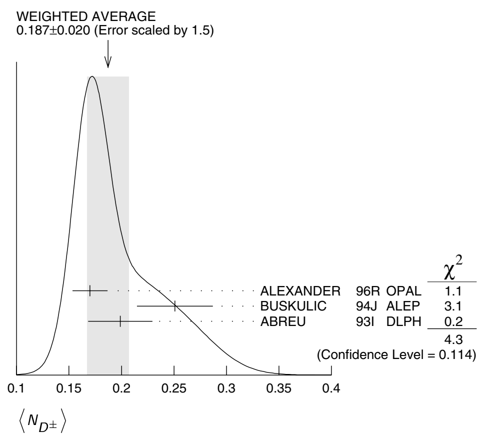

$\langle N_{D^0} \rangle$

VALUE	DOCUMENT ID		TECN	COMMENT
0.462±0.026 OUR AVERAGE				
0.465±0.017±0.027	ALEXANDER	96R	OPAL	$E^{ee}_{\rm cm}$= 91.2 GeV
0.518±0.052±0.035	BUSKULIC	94J	ALEP	$E^{ee}_{\rm cm}$= 91.2 GeV
0.403±0.038±0.044	[117] ABREU	93I	DLPH	$E^{ee}_{\rm cm}$= 91.2 GeV

[117] See ABREU 95 (erratum).

$\langle N_{D_s^\pm} \rangle$

VALUE	DOCUMENT ID		TECN	COMMENT
0.131±0.010±0.018	ALEXANDER	96R	OPAL	$E^{ee}_{\rm cm}$= 91.2 GeV

$\langle N_{D^*(2010)^\pm} \rangle$

VALUE	DOCUMENT ID		TECN	COMMENT
0.183 ±0.008 OUR AVERAGE				
0.1854±0.0041±0.0091	[118] ACKERSTAFF	98E	OPAL	$E^{ee}_{\rm cm}$= 91.2 GeV
0.187 ±0.015 ±0.013	BUSKULIC	94J	ALEP	$E^{ee}_{\rm cm}$= 91.2 GeV
0.171 ±0.012 ±0.016	[119] ABREU	93I	DLPH	$E^{ee}_{\rm cm}$= 91.2 GeV

[118] ACKERSTAFF 98E systematic error includes an uncertainty of ±0.0069 due to the branching ratios B($D^{*+} \to D^0 \pi^+$) = 0.683 ± 0.014 and B($D^0 \to K^- \pi^+$) = 0.0383 ± 0.0012.

[119] See ABREU 95 (erratum).

$\langle N_{D_{s1}(2536)^+} \rangle$

VALUE (units 10^{-3})	DOCUMENT ID		TECN	COMMENT
• • • We do not use the following data for averages, fits, limits, etc. • • •				
$2.9^{+0.7}_{-0.6}$±0.2	[120] ACKERSTAFF	97W	OPAL	$E^{ee}_{\rm cm}$= 91.2 GeV

[120] ACKERSTAFF 97W obtain this value for x> 0.6 and with the assumption that its decay width is saturated by the $D^* K$ final states.

$\langle N_{B^*} \rangle$

VALUE	DOCUMENT ID		TECN	COMMENT
0.28 ±0.01 ±0.03	[121] ABREU	95R	DLPH	$E^{ee}_{\rm cm}$= 91.2 GeV

[121] ABREU 95R quote this value for a flavor-averaged excited state.

$\langle N_{J/\psi(1S)} \rangle$

VALUE	DOCUMENT ID		TECN	COMMENT
0.0056±0.0003±0.0004	[122] ALEXANDER	96B	OPAL	$E^{ee}_{\rm cm}$= 91.2 GeV

[122] ALEXANDER 96B identify $J/\psi(1S)$ from the decays into lepton pairs.

$\langle N_{\psi(2S)} \rangle$

VALUE	DOCUMENT ID		TECN	COMMENT
0.0023±0.0004±0.0003	ALEXANDER	96B	OPAL	$E^{ee}_{\rm cm}$= 91.2 GeV

$\langle N_p \rangle$

VALUE	DOCUMENT ID		TECN	COMMENT
1.04±0.04 OUR AVERAGE				
1.03±0.13	ABE	99E	SLD	$E^{ee}_{\rm cm}$= 91.2 GeV
1.08±0.04±0.03	ABREU	98L	DLPH	$E^{ee}_{\rm cm}$= 91.2 GeV
1.00±0.07	BARATE	98V	ALEP	$E^{ee}_{\rm cm}$= 91.2 GeV
0.92±0.11	AKERS	94P	OPAL	$E^{ee}_{\rm cm}$= 91.2 GeV

$\langle N_{\Delta(1232)^{++}} \rangle$

VALUE	DOCUMENT ID		TECN	COMMENT
0.087±0.033 OUR AVERAGE	Error includes scale factor of 2.4.			
0.079±0.009±0.011	ABREU	95W	DLPH	$E^{ee}_{\rm cm}$= 91.2 GeV
0.22 ±0.04 ±0.04	ALEXANDER	95D	OPAL	$E^{ee}_{\rm cm}$= 91.2 GeV

$\langle N_\Lambda \rangle$

VALUE	DOCUMENT ID		TECN	COMMENT
0.388±0.009 OUR AVERAGE	Error includes scale factor of 1.7. See the ideogram below.			
0.404±0.002±0.007	BARATE	00O	ALEP	$E^{ee}_{\rm cm}$= 91.2 GeV
0.395±0.022	ABE	99E	SLD	$E^{ee}_{\rm cm}$= 91.2 GeV
0.364±0.004±0.017	ACCIARRI	97L	L3	$E^{ee}_{\rm cm}$= 91.2 GeV
0.374±0.002±0.010	ALEXANDER	97D	OPAL	$E^{ee}_{\rm cm}$= 91.2 GeV
0.357±0.003±0.017	ABREU	93L	DLPH	$E^{ee}_{\rm cm}$= 91.2 GeV

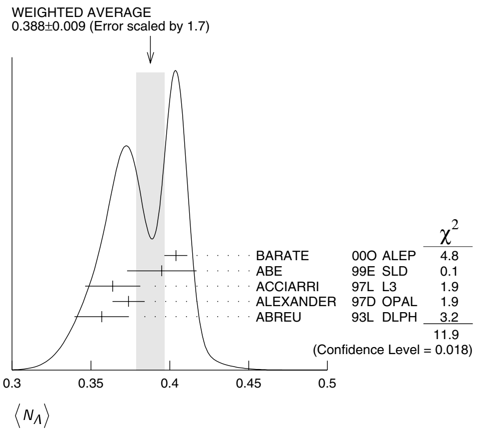

$\langle N_{\Lambda(1520)} \rangle$

VALUE	DOCUMENT ID		TECN	COMMENT
0.0224±0.0027 OUR AVERAGE				
0.029 ±0.005 ±0.005	ABREU	00P	DLPH	$E^{ee}_{\rm cm}$= 91.2 GeV
0.0213±0.0021±0.0019	ALEXANDER	97D	OPAL	$E^{ee}_{\rm cm}$= 91.2 GeV

$\langle N_{\Sigma^+} \rangle$

VALUE	DOCUMENT ID		TECN	COMMENT
0.107±0.010 OUR AVERAGE				
0.114±0.011±0.009	ACCIARRI	00J	L3	$E^{ee}_{\rm cm}$= 91.2 GeV
0.099±0.008±0.013	ALEXANDER	97E	OPAL	$E^{ee}_{\rm cm}$= 91.2 GeV

$\langle N_{\Sigma^-} \rangle$

VALUE	DOCUMENT ID		TECN	COMMENT
0.082±0.007 OUR AVERAGE				
0.081±0.002±0.010	ABREU	00P	DLPH	$E^{ee}_{\rm cm}$= 91.2 GeV
0.083±0.006±0.009	ALEXANDER	97E	OPAL	$E^{ee}_{\rm cm}$= 91.2 GeV

$\langle N_{\Sigma^+ + \Sigma^-} \rangle$

VALUE	DOCUMENT ID		TECN	COMMENT
0.181±0.018 OUR AVERAGE				
0.182±0.010±0.016	[123] ALEXANDER	97E	OPAL	$E^{ee}_{\rm cm}$= 91.2 GeV
0.170±0.014±0.061	ABREU	95O	DLPH	$E^{ee}_{\rm cm}$= 91.2 GeV

[123] We have combined the values of $\langle N_{\Sigma^+} \rangle$ and $\langle N_{\Sigma^-} \rangle$ from ALEXANDER 97E adding the statistical and systematic errors of the two final states separately in quadrature. If isospin symmetry is assumed this value becomes 0.174 ± 0.010 ± 0.015.

$\langle N_{\Sigma^0} \rangle$

VALUE	DOCUMENT ID		TECN	COMMENT
0.076±0.010 OUR AVERAGE				
0.095±0.015±0.013	ACCIARRI	00J	L3	$E^{ee}_{\rm cm}$= 91.2 GeV
0.071±0.012±0.013	ALEXANDER	97E	OPAL	$E^{ee}_{\rm cm}$= 91.2 GeV
0.070±0.010±0.010	ADAM	96B	DLPH	$E^{ee}_{\rm cm}$= 91.2 GeV

$\langle N_{(\Sigma^+ + \Sigma^- + \Sigma^0)/3} \rangle$

VALUE	DOCUMENT ID		TECN	COMMENT
0.084±0.005±0.008	ALEXANDER	97E	OPAL	$E^{ee}_{\rm cm}$= 91.2 GeV

$\langle N_{\Sigma(1385)^+} \rangle$

VALUE	DOCUMENT ID		TECN	COMMENT
0.0239±0.0009±0.0012	ALEXANDER	97D	OPAL	$E^{ee}_{\rm cm}$= 91.2 GeV

$\langle N_{\Sigma(1385)^-} \rangle$

VALUE	DOCUMENT ID		TECN	COMMENT
0.0240±0.0010±0.0014	ALEXANDER	97D	OPAL	$E^{ee}_{\rm cm}$= 91.2 GeV

$\langle N_{\Sigma(1385)^+ + \Sigma(1385)^-} \rangle$

VALUE	DOCUMENT ID		TECN	COMMENT
0.046 ±0.004 OUR AVERAGE	Error includes scale factor of 1.6.			
0.0479±0.0013±0.0026	ALEXANDER	97D	OPAL	$E^{ee}_{\rm cm}$= 91.2 GeV
0.0382±0.0028±0.0045	ABREU	95O	DLPH	$E^{ee}_{\rm cm}$= 91.2 GeV

$\langle N_{\Xi^-} \rangle$

VALUE	DOCUMENT ID		TECN	COMMENT
0.0258±0.0009 OUR AVERAGE				
0.0259±0.0004±0.0009	ALEXANDER	97D	OPAL	$E^{ee}_{\rm cm}$= 91.2 GeV
0.0250±0.0009±0.0021	ABREU	95O	DLPH	$E^{ee}_{\rm cm}$= 91.2 GeV

$\langle N_{\Xi(1530)^0} \rangle$

VALUE	DOCUMENT ID		TECN	COMMENT
0.0053±0.0013 OUR AVERAGE	Error includes scale factor of 3.2.			
0.0068±0.0005±0.0004	ALEXANDER	97D	OPAL	E^{ee}_{cm}= 91.2 GeV
0.0041±0.0004±0.0004	ABREU	95O	DLPH	E^{ee}_{cm}= 91.2 GeV

$\langle N_{\Omega^-} \rangle$

VALUE	DOCUMENT ID		TECN	COMMENT
0.00164±0.00028 OUR AVERAGE				
0.0018 ±0.0003 ±0.0002	ALEXANDER	97D	OPAL	E^{ee}_{cm}= 91.2 GeV
0.0014 ±0.0002 ±0.0004	ADAM	96B	DLPH	E^{ee}_{cm}= 91.2 GeV

$\langle N_{\Lambda_c^+} \rangle$

VALUE	DOCUMENT ID		TECN	COMMENT
0.078±0.012±0.012	ALEXANDER	96R	OPAL	E^{ee}_{cm}= 91.2 GeV

$\langle N_{charged} \rangle$

VALUE	DOCUMENT ID		TECN	COMMENT
21.07±0.11 OUR AVERAGE				
21.21±0.01±0.20	ABREU	99	DLPH	E^{ee}_{cm}= 91.2 GeV
21.05±0.20	AKERS	95Z	OPAL	E^{ee}_{cm}= 91.2 GeV
20.91±0.03±0.22	BUSKULIC	95R	ALEP	E^{ee}_{cm}= 91.2 GeV
21.40±0.43	ACTON	92B	OPAL	E^{ee}_{cm}= 91.2 GeV
20.71±0.04±0.77	ABREU	91H	DLPH	E^{ee}_{cm}= 91.2 GeV
20.7 ±0.7	ADEVA	91I	L3	E^{ee}_{cm}= 91.2 GeV
20.1 ±1.0 ±0.9	ABRAMS	90	MRK2	E^{ee}_{cm}= 91.1 GeV

Z HADRONIC POLE CROSS SECTION

OUR FIT is obtained using the fit procedure and correlations as determined by the LEP Electroweak Working Group (see the "Note on the Z boson"). This quantity is defined as

$$\sigma^0_h = \frac{12\pi}{M_Z^2}\,\frac{\Gamma(e^+e^-)\,\Gamma(\text{hadrons})}{\Gamma_Z^2}$$

It is one of the parameters used in the Z lineshape fit.

VALUE (nb)	EVTS	DOCUMENT ID		TECN	COMMENT
41.541±0.037 OUR FIT					
41.501±0.055	4.10M	[124] ABBIENDI	01A	OPAL	E^{ee}_{cm}= 88–94 GeV
41.578±0.069	3.70M	ABREU	00F	DLPH	E^{ee}_{cm}= 88–94 GeV
41.535±0.055	3.54M	ACCIARRI	00C	L3	E^{ee}_{cm}= 88–94 GeV
41.559±0.058	4.07M	[125] BARATE	00C	ALEP	E^{ee}_{cm}= 88–94 GeV
• • • We do not use the following data for averages, fits, limits, etc. • • •					
41.23 ±0.20	1.05M	ABREU	94	DLPH	Repl. by ABREU 00F
41.39 ±0.26	1.09M	ACCIARRI	94	L3	Repl. by ACCIARRI 00C
41.70 ±0.23	1.19M	AKERS	94	OPAL	Repl. by ABBIENDI 01A
41.60 ±0.16	1.27M	BUSKULIC	94	ALEP	Repl. by BARATE 00C
42 ±4	450	ABRAMS	89B	MRK2	E^{ee}_{cm}= 89.2–93.0 GeV

[124] ABBIENDI 01A error includes approximately 0.031 due to statistics, 0.033 due to event selection systematics, 0.029 due to uncertainty in luminosity measurement, and 0.011 due to LEP energy uncertainty.

[125] BARATE 00C error includes approximately 0.030 due to statistics, 0.026 due to experimental systematics, and 0.025 due to uncertainty in luminosity measurement.

Z VECTOR COUPLINGS TO CHARGED LEPTONS

These quantities are the effective vector couplings of the Z to charged leptons. Their magnitude is derived from a measurement of the Z lineshape and the forward-backward lepton asymmetries as a function of energy around the Z mass. The relative sign among the vector to axial-vector couplings is obtained from a measurement of the Z asymmetry parameters, A_e, A_μ, and A_τ. By convention the sign of g^e_A is fixed to be negative (and opposite to that of g^{ν_e} obtained using ν_e scattering measurements). The fit values quoted below correspond to global nine- or five-parameter fits to lineshape, lepton forward-backward asymmetry, and A_e, A_μ, and A_τ measurements. See "Note on the Z boson" for details.

g^e_V

VALUE	EVTS	DOCUMENT ID		TECN	COMMENT
−0.03816±0.00047 OUR FIT					
−0.0346 ±0.0023	137.0K	[126] ABBIENDI	01O	OPAL	E^{ee}_{cm}= 88–94 GeV
−0.0412 ±0.0027	124.4k	[127] ACCIARRI	00C	L3	E^{ee}_{cm}= 88–94 GeV
−0.0400 ±0.0037		BARATE	00C	ALEP	E^{ee}_{cm}= 88–94 GeV
−0.0414 ±0.0020		[128] ABE	95J	SLD	E^{ee}_{cm}= 91.31 GeV

[126] ABBIENDI 01O use their measurement of the τ polarization in addition to the lineshape and forward-backward lepton asymmetries.

[127] ACCIARRI 00C use their measurement of the τ polarization in addition to forward-backward lepton asymmetries.

[128] ABE 95J obtain this result combining polarized Bhabha results with the A_{LR} measurement of ABE 94C. The Bhabha results alone give −0.0507 ± 0.0096 ± 0.0020.

g^μ_V

VALUE	EVTS	DOCUMENT ID		TECN	COMMENT
−0.0367±0.0023 OUR FIT					
$-0.0388^{+0.0060}_{-0.0064}$	182.8K	[129] ABBIENDI	01O	OPAL	E^{ee}_{cm}= 88–94 GeV
−0.0386±0.0073	113.4k	[130] ACCIARRI	00C	L3	E^{ee}_{cm}= 88–94 GeV
−0.0362±0.0061		BARATE	00C	ALEP	E^{ee}_{cm}= 88–94 GeV
• • • We do not use the following data for averages, fits, limits, etc. • • •					
−0.0413±0.0060	66143	[131] ABBIENDI	01K	OPAL	E^{ee}_{cm}= 89–93 GeV

[129] ABBIENDI 01O use their measurement of the τ polarization in addition to the lineshape and forward-backward lepton asymmetries.

[130] ACCIARRI 00C use their measurement of the τ polarization in addition to forward-backward lepton asymmetries.

[131] ABBIENDI 01K obtain this from an angular analysis of the muon pair asymmetry which takes into account effects of initial state radiation on an event by event basis and of initial-final state interference.

g^τ_V

VALUE	EVTS	DOCUMENT ID		TECN	COMMENT
−0.0366±0.0010 OUR FIT					
−0.0365±0.0023	151.5K	[132] ABBIENDI	01O	OPAL	E^{ee}_{cm}= 88–94 GeV
−0.0384±0.0026	103.0k	[133] ACCIARRI	00C	L3	E^{ee}_{cm}= 88–94 GeV
−0.0361±0.0068		BARATE	00C	ALEP	E^{ee}_{cm}= 88–94 GeV

[132] ABBIENDI 01O use their measurement of the τ polarization in addition to the lineshape and forward-backward lepton asymmetries.

[133] ACCIARRI 00C use their measurement of the τ polarization in addition to forward-backward lepton asymmetries.

g^ℓ_V

VALUE	EVTS	DOCUMENT ID		TECN	COMMENT
−0.03783±0.00041 OUR FIT					
−0.0358 ±0.0014	471.3K	[134] ABBIENDI	01O	OPAL	E^{ee}_{cm}= 88–94 GeV
−0.0397 ±0.0020	379.4k	[135] ABREU	00F	DLPH	E^{ee}_{cm}= 88–94 GeV
−0.0397 ±0.0017	340.8k	[136] ACCIARRI	00C	L3	E^{ee}_{cm}= 88–94 GeV
−0.0383 ±0.0018	500k	BARATE	00C	ALEP	E^{ee}_{cm}= 88–94 GeV

[134] ABBIENDI 01O use their measurement of the τ polarization in addition to the lineshape and forward-backward lepton asymmetries.

[135] Using forward-backward lepton asymmetries.

[136] ACCIARRI 00C use their measurement of the τ polarization in addition to forward-backward lepton asymmetries.

Z AXIAL-VECTOR COUPLINGS TO CHARGED LEPTONS

These quantities are the effective axial-vector couplings of the Z to charged leptons. Their magnitude is derived from a measurement of the Z lineshape and the forward-backward lepton asymmetries as a function of energy around the Z mass. The relative sign among the vector to axial-vector couplings is obtained from a measurement of the Z asymmetry parameters, A_e, A_μ, and A_τ. By convention the sign of g^e_A is fixed to be negative (and opposite to that of g^{ν_e} obtained using ν_e scattering measurements). The fit values quoted below correspond to global nine- or five-parameter fits to lineshape, lepton forward-backward asymmetry, and A_e, A_μ, and A_τ measurements. See "Note on the Z boson" for details.

g^e_A

VALUE	EVTS	DOCUMENT ID		TECN	COMMENT
−0.50111±0.00035 OUR FIT					
−0.50062±0.00062	137.0K	[137] ABBIENDI	01O	OPAL	E^{ee}_{cm}= 88–94 GeV
−0.5015 ±0.0007	124.4k	[138] ACCIARRI	00C	L3	E^{ee}_{cm}= 88–94 GeV
−0.50166±0.00057		BARATE	00C	ALEP	E^{ee}_{cm}= 88–94 GeV
−0.4977 ±0.0045		[139] ABE	95J	SLD	E^{ee}_{cm}= 91.31 GeV

[137] ABBIENDI 01O use their measurement of the τ polarization in addition to the lineshape and forward-backward lepton asymmetries.

[138] ACCIARRI 00C use their measurement of the τ polarization in addition to forward-backward lepton asymmetries.

[139] ABE 95J obtain this result combining polarized Bhabha results with the A_{LR} measurement of ABE 94C. The Bhabha results alone give −0.4968 ± 0.0039 ± 0.0027.

g_A^{μ}

VALUE	EVTS	DOCUMENT ID	TECN	COMMENT
−0.50120±0.00054 OUR FIT				
−0.50117±0.00099	182.8K	[140] ABBIENDI	01O OPAL	$E_{\rm cm}^{ee}$= 88–94 GeV
−0.5009 ±0.0014	113.4k	[141] ACCIARRI	00C L3	$E_{\rm cm}^{ee}$= 88–94 GeV
−0.50046±0.00093		BARATE	00C ALEP	$E_{\rm cm}^{ee}$= 88–94 GeV
• • • We do not use the following data for averages, fits, limits, etc. • • •				
−0.520 ±0.015	66143	[142] ABBIENDI	01K OPAL	$E_{\rm cm}^{ee}$= 89–93 GeV

[140] ABBIENDI 01O use their measurement of the τ polarization in addition to the lineshape and forward-backward lepton asymmetries.

[141] ACCIARRI 00C use their measurement of the τ polarization in addition to forward-backward lepton asymmetries.

[142] ABBIENDI 01K obtain this from an angular analysis of the muon pair asymmetry which takes into account effects of initial state radiation on an event by event basis and of initial-final state interference.

g_A^{τ}

VALUE	EVTS	DOCUMENT ID	TECN	COMMENT
−0.50204±0.00064 OUR FIT				
−0.50165±0.00124	151.5K	[143] ABBIENDI	01O OPAL	$E_{\rm cm}^{ee}$= 88–94 GeV
−0.5023 ±0.0017	103.0k	[144] ACCIARRI	00C L3	$E_{\rm cm}^{ee}$= 88–94 GeV
−0.50216±0.00100		BARATE	00C ALEP	$E_{\rm cm}^{ee}$= 88–94 GeV

[143] ABBIENDI 01O use their measurement of the τ polarization in addition to the lineshape and forward-backward lepton asymmetries.

[144] ACCIARRI 00C use their measurement of the τ polarization in addition to forward-backward lepton asymmetries.

g_A^{ℓ}

VALUE	EVTS	DOCUMENT ID	TECN	COMMENT
−0.50123±0.00026 OUR FIT				
−0.50089±0.00045	471.3K	[145] ABBIENDI	01O OPAL	$E_{\rm cm}^{ee}$= 88–94 GeV
−0.5007 ±0.0005	379.4k	ABREU	00F DLPH	$E_{\rm cm}^{ee}$= 88–94 GeV
−0.50153±0.00053	340.8k	[146] ACCIARRI	00C L3	$E_{\rm cm}^{ee}$= 88–94 GeV
−0.50150±0.00046	500k	BARATE	00C ALEP	$E_{\rm cm}^{ee}$= 88–94 GeV

[145] ABBIENDI 01O use their measurement of the τ polarization in addition to the lineshape and forward-backward lepton asymmetries.

[146] ACCIARRI 00C use their measurement of the τ polarization in addition to forward-backward lepton asymmetries.

Z COUPLINGS TO NEUTRAL LEPTONS

These quantities are the effective couplings of the Z to neutral leptons. $\nu_e e$ and $\nu_\mu e$ scattering results are combined with g_A^e and g_V^e measurements at the Z mass to obtain g^{ν_e} and g^{ν_μ} following NOVIKOV 93C.

g^{ν_e}

VALUE	DOCUMENT ID	TECN	COMMENT
0.528±0.085	[147] VILAIN 94	CHM2	From $\nu_\mu e$ and $\nu_e e$ scattering

[147] VILAIN 94 derive this value from their value of g^{ν_μ} and their ratio $g^{\nu_e}/g^{\nu_\mu} = 1.05^{+0.15}_{-0.18}$.

g^{ν_μ}

VALUE	DOCUMENT ID	TECN	COMMENT
0.502±0.017	[148] VILAIN 94	CHM2	From $\nu_\mu e$ scattering

[148] VILAIN 94 derive this value from their measurement of the couplings $g_A^{e\nu_\mu} = -0.503 \pm 0.017$ and $g_V^{e\nu_\mu} = -0.035 \pm 0.017$ obtained from $\nu_\mu e$ scattering. We have re-evaluated this value using the current PDG values for g_A^e and g_V^e.

Z ASYMMETRY PARAMETERS

For each fermion-antifermion pair coupling to the Z these quantities are defined as

$$A_f = \frac{2 g_V^f g_A^f}{(g_V^f)^2 + (g_A^f)^2}$$

where g_V^f and g_A^f are the effective vector and axial-vector couplings. For their relation to the various lepton asymmetries see the 'Note on the Z Boson.'

A_e

Using polarized beams, this quantity can also be measured as $(\sigma_L - \sigma_R)/(\sigma_L + \sigma_R)$, where σ_L and σ_R are the $e^+ e^-$ production cross sections for Z bosons produced with left-handed and right-handed electrons respectively.

VALUE	EVTS	DOCUMENT ID	TECN	COMMENT
0.1515 ±0.0019 OUR AVERAGE				
0.1454 ±0.0108 ±0.0036	144810	[149] ABBIENDI	01O OPAL	$E_{\rm cm}^{ee}$= 88–94 GeV
0.1516 ±0.0021	559000	[150] ABE	01B SLD	$E_{\rm cm}^{ee}$= 91.24 GeV
0.1504 ±0.0068 ±0.0008		[151] HEISTER	01 ALEP	$E_{\rm cm}^{ee}$= 88–94 GeV
0.1382 ±0.0116 ±0.0005	105000	[152] ABREU	00E DLPH	$E_{\rm cm}^{ee}$= 88–94 GeV
0.1678 ±0.0127 ±0.0030	137092	[153] ACCIARRI	98H L3	$E_{\rm cm}^{ee}$= 88–94 GeV
0.162 ±0.041 ±0.014	89838	[154] ABE	97 SLD	$E_{\rm cm}^{ee}$= 91.27 GeV
0.202 ±0.038 ±0.008		[155] ABE	95J SLD	$E_{\rm cm}^{ee}$= 91.31 GeV
• • • We do not use the following data for averages, fits, limits, etc. • • •				
0.15138±0.00216	537000	[156] ABE	00B SLD	Repl. by ABE 01B
0.152 ±0.012	4527	[157] ABE	97N SLD	Repl. by ABE 01B
0.129 ±0.014 ±0.005	89075	[158] ALEXANDER	96U OPAL	Repl. by ABBIENDI 01O
0.136 ±0.027 ±0.003		[153] ABREU	95I DLPH	Repl. by ABREU 00E
0.129 ±0.016 ±0.005	33000	[159] BUSKULIC	95Q ALEP	Repl. by HEISTER 01
0.157 ±0.020 ±0.005	86000	[153] ACCIARRI	94E L3	Repl. by ACCIARRI 98H

[149] ABBIENDI 01O fit for A_e and A_τ from measurements of the τ polarization at varying τ production angles. The correlation between A_e and A_τ is less than 0.03.

[150] ABE 01B use the left-right production and left-right forward-backward decay asymmetries in leptonic Z decays to obtain a value of 0.1544 ± 0.0060. This is combined with left-right production asymmetry measurement using hadronic Z decays (ABE 00B) to obtain the quoted value.

[151] HEISTER 01 obtain this result fitting the τ polarization as a function of the polar production angle of the τ.

[152] ABREU 00E obtain this result fitting the τ polarization as a function of the polar τ production angle. This measurement is a combination of different analyses (exclusive τ decay modes, inclusive hadronic 1-prong reconstruction, and a neural network analysis).

[153] Derived from the measurement of forward-backward τ polarization asymmetry.

[154] ABE 97 obtain this result from a measurement of the observed left-right charge asymmetry, $A_Q^{\rm obs} = 0.225 \pm 0.056 \pm 0.019$, in hadronic Z decays. If they combine this value of $A_Q^{\rm obs}$ with their earlier measurement of $A_{LR}^{\rm obs}$ they determine A_e to be $0.1574 \pm 0.0197 \pm 0.0067$ independent of the beam polarization.

[155] ABE 95J obtain this result from polarized Bhabha scattering.

[156] ABE 00B obtain this value measuring the left-right Z boson cross-section asymmetry. This is equivalent to an effective weak mixing angle of $\sin^2\theta_W^{\rm eff} = 0.23097 \pm 0.00027$.

[157] ABE 97N obtain this direct measurement using the left-right cross section asymmetry and the left-right forward-backward asymmetry in leptonic decays of the Z boson obtained with a polarized electron beam.

[158] ALEXANDER 96U measure the τ-lepton polarization and the forward-backward polarization asymmetry.

[159] BUSKULIC 95Q obtain this result fitting the τ polarization as a function of the polar τ production angle.

A_μ

This quantity is directly extracted from a measurement of the left-right forward-backward asymmetry in $\mu^+\mu^-$ production at SLC using a polarized electron beam. This double asymmetry eliminates the dependence on the Z-e-e coupling parameter A_e.

VALUE	EVTS	DOCUMENT ID	TECN	COMMENT
0.142±0.015	16844	[160] ABE	01B SLD	$E_{\rm cm}^{ee}$= 91.24 GeV
• • • We do not use the following data for averages, fits, limits, etc. • • •				
0.102±0.034	3788	[161] ABE	97N SLD	Repl. by ABE 01B

[160] ABE 01B obtain this direct measurement using the left-right production and left-right forward-backward polar angle asymmetries in $\mu^+\mu^-$ decays of the Z boson obtained with a polarized electron beam.

[161] ABE 97N obtain this direct measurement using the left-right cross section asymmetry and the left-right forward-backward asymmetry in $\mu^+\mu^-$ decays of the Z boson obtained with a polarized electron beam.

A_τ

The LEP Collaborations derive this quantity from the measurement of the τ polarization in $Z \to \tau^+\tau^-$. The SLD Collaboration directly extracts this quantity from its measured left-right forward-backward asymmetry in $Z \to \tau^+\tau^-$ produced using a polarized e^- beam. This double asymmetry eliminates the dependence on the Z-e-e coupling parameter A_e.

VALUE	EVTS	DOCUMENT ID	TECN	COMMENT
0.143 ±0.004 OUR AVERAGE				
0.1456±0.0076±0.0057	144810	[162] ABBIENDI	01O OPAL	$E_{\rm cm}^{ee}$= 88–94 GeV
0.136 ±0.015	16083	[163] ABE	01B SLD	$E_{\rm cm}^{ee}$= 91.24 GeV
0.1451±0.0052±0.0029		[164] HEISTER	01 ALEP	$E_{\rm cm}^{ee}$= 88–94 GeV
0.1359±0.0079±0.0055	105000	[165] ABREU	00E DLPH	$E_{\rm cm}^{ee}$= 88–94 GeV
0.1476±0.0088±0.0062	137092	ACCIARRI	98H L3	$E_{\rm cm}^{ee}$= 88–94 GeV
• • • We do not use the following data for averages, fits, limits, etc. • • •				
0.195 ±0.034	3748	[166] ABE	97N SLD	Repl. by ABE 01B
0.134 ±0.009 ±0.010	89075	[167] ALEXANDER	96U OPAL	Repl. by ABBIENDI 01O
0.148 ±0.017 ±0.014		ABREU	95I DLPH	Repl. by ABREU 00E
0.136 ±0.012 ±0.009	33000	[168] BUSKULIC	95Q ALEP	Repl. by HEISTER 01
0.150 ±0.013 ±0.009	86000	ACCIARRI	94E L3	Repl. by ACCIARRI 98H

[162] ABBIENDI 01O fit for A_e and A_τ from measurements of the τ polarization at varying τ production angles. The correlation between A_e and A_τ is less than 0.03.

[163] ABE 01B obtain this direct measurement using the left-right production and left-right forward-backward polar angle asymmetries in $\tau^+\tau^-$ decays of the Z boson obtained with a polarized electron beam.

[164] HEISTER 01 obtain this result fitting the τ polarization as a function of the polar production angle of the τ.

[165] ABREU 00E obtain this result fitting the τ polarization as a function of the polar τ production angle. This measurement is a combination of different analyses (exclusive τ decay modes, inclusive hadronic 1-prong reconstruction, and a neural network analysis).

[166] ABE 97N obtain this direct measurement using the left-right cross section asymmetry and the left-right forward-backward asymmetry in $\tau^+\tau^-$ decays of the Z boson obtained with a polarized electron beam.

[167] ALEXANDER 96U measure the τ-lepton polarization and the forward-backward polarization asymmetry.

[168] BUSKULIC 95Q obtain this result fitting the τ polarization as a function of the polar τ production angle.

A_s

The SLD Collaboration directly extracts this quantity by a simultaneous fit to four measured s-quark polar angle distributions corresponding to two states of e^- polarization (positive and negative) and to the K^+K^- and $K^\pm K^0_S$ strange particle tagging modes in the hadronic final states.

VALUE	EVTS	DOCUMENT ID		TECN	COMMENT
0.895±0.066±0.062	2870	[169] ABE	00D	SLD	$E^{ee}_{\rm cm}$= 91.2 GeV

[169] ABE 00D tag $Z \to s\overline{s}$ events by an absence of B or D hadrons and the presence in each hemisphere of a high momentum $K^\pm$ or K^0_S.

A_c

This quantity is directly extracted from a measurement of the left-right forward-backward asymmetry in $c\overline{c}$ production at SLC using polarized electron beam. This double asymmetry eliminates the dependence on the Z-e-e coupling parameter A_e. OUR FIT is obtained by a simultaneous fit to several c- and b-quark measurements as explained in the note "The Z Boson."

VALUE	DOCUMENT ID		TECN	COMMENT
0.666±0.036 OUR FIT				
0.583±0.055±0.055	[170] ABE	02G	SLD	$E^{ee}_{\rm cm}$= 91.24 GeV
0.688±0.041	[171] ABE	01C	SLD	$E^{ee}_{\rm cm}$= 91.25 GeV
• • • We do not use the following data for averages, fits, limits, etc. • • •				
0.642±0.110±0.063	[172] ABE	99O	SLD	Repl. by ABE 02G
0.73 ±0.22 ±0.10	[173] ABE,K	95	SLD	Repl. by ABE 01C

[170] ABE 02G tag b and c quarks through their semileptonic decays into electrons and muons. A maximum likelihood fit is performed to extract simultaneously A_b and A_c.

[171] ABE 01C tag $Z \to c\overline{c}$ events using two techniques: exclusive reconstruction of D^{*+}, D^+ and D^0 mesons and the soft pion tag for $D^{*+} \to D^0\pi^+$. The large background from D mesons produced in $b\overline{b}$ events is separated efficiently from the signal using precision vertex information. When combining the A_c values from these two samples, care is taken to avoid double counting of events common to the two samples, and common systematic errors are properly taken into account.

[172] ABE 99O tag b and c quarks through their semileptonic decays into electrons and muons. A maximum likelihood fit is performed to extract simultaneously A_b and A_c.

[173] ABE,K 95 tag $Z \to c\overline{c}$ events using D^{*+} and D^+ meson production. To take care of the $b\overline{b}$ contamination in their analysis they use A^D_b= 0.64 ± 0.11 (which is A_b from D^*/D tagging). This is obtained by starting with a Standard Model value of 0.935, assigning it an estimated error of ±0.105 to cover LEP and SLD measurements, and finally taking into account B-$\overline{B}$ mixing $(1-2\chi_{\rm mix} = 0.72 \pm 0.09)$.

A_b

This quantity is directly extracted from a measurement of the left-right forward-backward asymmetry in $b\overline{b}$ production at SLC using polarized electron beam. This double asymmetry eliminates the dependence on the Z-e-e coupling parameter A_e. OUR FIT is obtained by a simultaneous fit to several c- and b-quark measurements as explained in the note "The Z Boson."

VALUE	EVTS	DOCUMENT ID		TECN	COMMENT
0.926±0.024 OUR FIT					
0.907±0.020±0.024	48028	[174] ABE	03F	SLD	$E^{ee}_{\rm cm}$= 91.24 GeV
0.919±0.030±0.024		[175] ABE	02G	SLD	$E^{ee}_{\rm cm}$= 91.24 GeV
0.855±0.088±0.102	7473	[176] ABE	99L	SLD	$E^{ee}_{\rm cm}$= 91.27 GeV
• • • We do not use the following data for averages, fits, limits, etc. • • •					
0.910±0.068±0.037		[177] ABE	99O	SLD	Repl. by ABE 02G
0.911±0.045±0.045	11092	[178] ABE	98I	SLD	Repl. by ABE 03F

[174] ABE 03F obtain an enriched sample of $b\overline{b}$ events tagging on the invariant mass of a 3-dimensional topologically reconstructed secondary decay. The charge of the underlying b quark is obtained using a self-calibrating track-charge method. For the 1996–1998 data sample they measure A_b = 0.906 ± 0.022 ± 0.023. The value quoted here is obtained combining the above with the result of ABE 98I (1993–1995 data sample).

[175] ABE 02G tag b and c quarks through their semileptonic decays into electrons and muons. A maximum likelihood fit is performed to extract simultaneously A_b and A_c.

[176] ABE 99L obtain an enriched sample of $b\overline{b}$ events tagging with an inclusive vertex mass cut. For distinguishing b and $\overline{b}$ quarks they use the charge of identified $K^\pm$.

[177] ABE 99O tag b and c quarks through their semileptonic decays into electrons and muons. A maximum likelihood fit is performed to extract simultaneously A_b and A_c.

[178] ABE 98I obtain an enriched sample of $b\overline{b}$ events tagging with an inclusive vertex mass cut. A momentum-weighted track charge is used to identify the sign of the charge of the underlying b quark.

TRANSVERSE SPIN CORRELATIONS IN $Z \to \tau^+\tau^-$

The correlations between the transverse spin components of $\tau^+\tau^-$ produced in Z decays may be expressed in terms of the vector and axial-vector couplings:

$$C_{TT} = \frac{|g^\tau_A|^2 - |g^\tau_V|^2}{|g^\tau_A|^2 + |g^\tau_V|^2}$$

$$C_{TN} = -2\frac{|g^\tau_A||g^\tau_V|}{|g^\tau_A|^2 + |g^\tau_V|^2}\sin(\Phi_{g^\tau_V} - \Phi_{g^\tau_A})$$

C_{TT} refers to the transverse-transverse (within the collision plane) spin correlation and C_{TN} refers to the transverse-normal (to the collision plane) spin correlation.

The longitudinal τ polarization P_τ $(= -A_\tau)$ is given by:

$$P_\tau = -2\frac{|g^\tau_A||g^\tau_V|}{|g^\tau_A|^2 + |g^\tau_V|^2}\cos(\Phi_{g^\tau_V} - \Phi_{g^\tau_A})$$

Here Φ is the phase and the phase difference $\Phi_{g^\tau_V} - \Phi_{g^\tau_A}$ can be obtained using both the measurements of C_{TN} and P_τ.

C_{TT}

VALUE	EVTS	DOCUMENT ID		TECN	COMMENT
1.01±0.12 OUR AVERAGE					
$0.87 \pm 0.20 ^{+0.10}_{-0.12}$	9.1k	ABREU	97G	DLPH	$E^{ee}_{\rm cm}$= 91.2 GeV
1.06±0.13±0.05	120k	BARATE	97D	ALEP	$E^{ee}_{\rm cm}$= 91.2 GeV

C_{TN}

VALUE	EVTS	DOCUMENT ID		TECN	COMMENT
0.08±0.13±0.04	120k	[179] BARATE	97D	ALEP	$E^{ee}_{\rm cm}$= 91.2 GeV

[179] BARATE 97D combine their value of C_{TN} with the world average $P_\tau = -0.140 \pm 0.007$ to obtain $\tan(\Phi_{g^\tau_V} - \Phi_{g^\tau_A}) = -0.57 \pm 0.97$.

FORWARD-BACKWARD $e^+e^- \to f\overline{f}$ CHARGE ASYMMETRIES

These asymmetries are experimentally determined by tagging the respective lepton or quark flavor in e^+e^- interactions. Details of heavy flavor (c- or b-quark) tagging at LEP are described in the note on "The Z Boson." The Standard Model predictions for LEP data have been (re)computed using the ZFITTER package (version 6.36) with input parameters M_Z=91.187 GeV, $M_{\rm top}$=174.3 GeV, $M_{\rm Higgs}$=150 GeV, α_s=0.119, $\alpha^{(5)}$ (M_Z)= 1/128.877 and the Fermi constant G_F= 1.16637×10^{-5} GeV^{-2} (see the note on "The Z Boson" for references). For non-LEP data the Standard Model predictions are as given by the authors of the respective publications.

$A^{(0,e)}_{FB}$ CHARGE ASYMMETRY IN $e^+e^- \to e^+e^-$

OUR FIT is obtained using the fit procedure and correlations as determined by the LEP Electroweak Working Group (see the "Note on the Z boson"). For the Z peak, we report the pole asymmetry defined by $(3/4)A^2_e$ as determined by the nine-parameter fit to cross-section and lepton forward-backward asymmetry data.

ASYMMETRY (%)	STD. MODEL	$\sqrt{s}$ (GeV)	DOCUMENT ID		TECN
1.45±0.25 OUR FIT					
0.89±0.44	1.57	91.2	[180] ABBIENDI	01A	OPAL
1.71±0.49	1.57	91.2	ABREU	00F	DLPH
1.06±0.58	1.57	91.2	ACCIARRI	00C	L3
1.88±0.34	1.57	91.2	[181] BARATE	00C	ALEP
• • • We do not use the following data for averages, fits, limits, etc. • • •					
2.5 ±0.9	1.57	91.2	ABREU	94	DLPH
1.04±0.92	1.57	91.2	ACCIARRI	94	L3
0.62±0.80	1.57	91.2	AKERS	94	OPAL
1.85±0.66	1.57	91.2	BUSKULIC	94	ALEP

[180] ABBIENDI 01A error includes approximately 0.38 due to statistics, 0.16 due to event selection systematics, and 0.18 due to the theoretical uncertainty in t-channel prediction.

[181] BARATE 00C error includes approximately 0.31 due to statistics, 0.06 due to experimental systematics, and 0.13 due to the theoretical uncertainty in t-channel prediction.

$A^{(0,\mu)}_{FB}$ CHARGE ASYMMETRY IN $e^+e^- \to \mu^+\mu^-$

OUR FIT is obtained using the fit procedure and correlations as determined by the LEP Electroweak Working Group (see the "Note on the Z boson"). For the Z peak, we report the pole asymmetry defined by $(3/4)A_eA_\mu$ as determined by the nine-parameter fit to cross-section and lepton forward-backward asymmetry data.

ASYMMETRY (%)	STD. MODEL	$\sqrt{s}$ (GeV)	DOCUMENT ID		TECN
1.69± 0.13 OUR FIT					
1.59± 0.23	1.57	91.2	[182] ABBIENDI	01A	OPAL
1.65± 0.25	1.57	91.2	ABREU	00F	DLPH
1.88± 0.33	1.57	91.2	ACCIARRI	00C	L3
1.71± 0.24	1.57	91.2	[183] BARATE	00C	ALEP
• • • We do not use the following data for averages, fits, limits, etc. • • •					
9 ±30	−1.3	20	[184] ABREU	95M	DLPH
7 ±26	−8.3	40	[184] ABREU	95M	DLPH
−11 ±33	−24.1	57	[184] ABREU	95M	DLPH
−62 ±17	−44.6	69	[184] ABREU	95M	DLPH
−56 ±10	−63.5	79	[184] ABREU	95M	DLPH
−13 ± 5	−34.4	87.5	[184] ABREU	95M	DLPH
1.4 ± 0.5	1.57	91.2	ABREU	94	DLPH
1.79± 0.61	1.57	91.2	ACCIARRI	94	L3
0.99± 0.42	1.57	91.2	AKERS	94	OPAL
1.46± 0.48	1.57	91.2	BUSKULIC	94	ALEP
$-29.0 \ ^{+5.0}_{-4.8} \pm 0.5$	−32.1	56.9	[185] ABE	90I	VNS
− 9.9 ± 1.5 ±0.5	−9.2	35	HEGNER	90	JADE
0.05± 0.22	0.026	91.14	[186] ABRAMS	89D	MRK2
−43.4 ±17.0	−24.9	52.0	[187] BACALA	89	AMY

−11.0 ±16.5	−29.4	55.0	[187] BACALA 89	AMY
−30.0 ±12.4	−31.2	56.0	[187] BACALA 89	AMY
−46.2 ±14.9	−33.0	57.0	[187] BACALA 89	AMY
−29 ±13	−25.9	53.3	ADACHI 88C	TOPZ
+ 5.3 ± 5.0 ±0.5	−1.2	14.0	ADEVA 88	MRKJ
−10.4 ± 1.3 ±0.5	−8.6	34.8	ADEVA 88	MRKJ
−12.3 ± 5.3 ±0.5	−10.7	38.3	ADEVA 88	MRKJ
−15.6 ± 3.0 ±0.5	−14.9	43.8	ADEVA 88	MRKJ
− 1.0 ± 6.0	−1.2	13.9	BRAUNSCH... 88D	TASS
− 9.1 ± 2.3 ±0.5	−8.6	34.5	BRAUNSCH... 88D	TASS
$-10.6\ {}^{+2.2}_{-2.3}\ \pm 0.5$	−8.9	35.0	BRAUNSCH... 88D	TASS
$-17.6\ {}^{+4.4}_{-4.3}\ \pm 0.5$	−15.2	43.6	BRAUNSCH... 88D	TASS
− 4.8 ± 6.5 ±1.0	−11.5	39	BEHREND 87C	CELL
−18.8 ± 4.5 ±1.0	−15.5	44	BEHREND 87C	CELL
+ 2.7 ± 4.9	−1.2	13.9	BARTEL 86C	JADE
−11.1 ± 1.8 ±1.0	−8.6	34.4	BARTEL 86C	JADE
−17.3 ± 4.8 ±1.0	−13.7	41.5	BARTEL 86C	JADE
−22.8 ± 5.1 ±1.0	−16.6	44.8	BARTEL 86C	JADE
− 6.3 ± 0.8 ±0.2	−6.3	29	ASH 85	MAC
− 4.9 ± 1.5 ±0.5	−5.9	29	DERRICK 85	HRS
− 7.1 ± 1.7	−5.7	29	LEVI 83	MRK2
−16.1 ± 3.2	−9.2	34.2	BRANDELIK 82C	TASS

[182] ABBIENDI 01A error is almost entirely on account of statistics.
[183] BARATE 00C error is almost entirely on account of statistics.
[184] ABREU 95M perform this measurement using radiative muon-pair events associated with high-energy isolated photons.
[185] ABE 90I measurements in the range $50 \leq \sqrt{s} \leq 60.8$ GeV.
[186] ABRAMS 89D asymmetry includes both 9 $\mu^+\mu^-$ and 15 $\tau^+\tau^-$ events.
[187] BACALA 89 systematic error is about 5%.

$A_{FB}^{(0,\tau)}$ CHARGE ASYMMETRY IN $e^+e^- \rightarrow \tau^+\tau^-$

OUR FIT is obtained using the fit procedure and correlations as determined by the LEP Electroweak Working Group (see the "Note on the *Z* boson"). For the *Z* peak, we report the pole asymmetry defined by $(3/4)A_e A_\tau$ as determined by the nine-parameter fit to cross-section and lepton forward-backward asymmetry data.

ASYMMETRY (%)	*STD. MODEL*	*$\sqrt{s}$ (GeV)*	*DOCUMENT ID*	*TECN*
1.88± 0.17 OUR FIT				
1.45± 0.30	1.57	91.2	[188] ABBIENDI 01A	OPAL
2.41± 0.37	1.57	91.2	ABREU 00F	DLPH
2.60± 0.47	1.57	91.2	ACCIARRI 00C	L3
1.70± 0.28	1.57	91.2	[189] BARATE 00C	ALEP
• • • We do not use the following data for averages, fits, limits, etc. • • •				
2.2 ± 0.7	1.57	91.2	ABREU 94	DLPH
2.65± 0.88	1.57	91.2	ACCIARRI 94	L3
2.05± 0.52	1.57	91.2	AKERS 94	OPAL
1.97± 0.56	1.57	91.2	BUSKULIC 94	ALEP
$-32.8\ {}^{+6.4}_{-6.2}\ \pm 1.5$	−32.1	56.9	[190] ABE 90I	VNS
− 8.1 ± 2.0 ±0.6	−9.2	35	HEGNER 90	JADE
−18.4 ±19.2	−24.9	52.0	[191] BACALA 89	AMY
−17.7 ±26.1	−29.4	55.0	[191] BACALA 89	AMY
−45.9 ±16.6	−31.2	56.0	[191] BACALA 89	AMY
−49.5 ±18.0	−33.0	57.0	[191] BACALA 89	AMY
−20 ±14	−25.9	53.3	ADACHI 88C	TOPZ
−10.6 ± 3.1 ±1.5	−8.5	34.7	ADEVA 88	MRKJ
− 8.5 ± 6.6 ±1.5	−15.4	43.8	ADEVA 88	MRKJ
− 6.0 ± 2.5 ±1.0	8.8	34.6	BARTEL 85F	JADE
−11.8 ± 4.6 ±1.0	14.8	43.0	BARTEL 85F	JADE
− 5.5 ± 1.2 ±0.5	−0.063	29.0	FERNANDEZ 85	MAC
− 4.2 ± 2.0	0.057	29	LEVI 83	MRK2
−10.3 ± 5.2	−9.2	34.2	BEHREND 82	CELL
− 0.4 ± 6.6	−9.1	34.2	BRANDELIK 82C	TASS

[188] ABBIENDI 01A error includes approximately 0.26 due to statistics and 0.14 due to event selection systematics.
[189] BARATE 00C error includes approximately 0.26 due to statistics and 0.11 due to experimental systematics.
[190] ABE 90I measurements in the range $50 \leq \sqrt{s} \leq 60.8$ GeV.
[191] BACALA 89 systematic error is about 5%.

$A_{FB}^{(0,\ell)}$ CHARGE ASYMMETRY IN $e^+e^- \rightarrow \ell^+\ell^-$

For the *Z* peak, we report the pole asymmetry defined by $(3/4)A_\ell^2$ as determined by the five-parameter fit to cross-section and lepton forward-backward asymmetry data assuming lepton universality. For details see the "Note on the *Z* boson."

ASYMMETRY (%)	*STD. MODEL*	*$\sqrt{s}$ (GeV)*	*DOCUMENT ID*	*TECN*
1.71±0.10 OUR FIT				
1.45±0.17	1.57	91.2	[192] ABBIENDI 01A	OPAL
1.87±0.19	1.57	91.2	ABREU 00F	DLPH
1.92±0.24	1.57	91.2	ACCIARRI 00C	L3
1.73±0.16	1.57	91.2	[193] BARATE 00C	ALEP
• • • We do not use the following data for averages, fits, limits, etc. • • •				
1.77±0.37	1.57	91.2	ABREU 94	DLPH
1.84±0.45	1.57	91.2	ACCIARRI 94	L3
1.28±0.30	1.57	91.2	AKERS 94	OPAL
1.71±0.33	1.57	91.2	BUSKULIC 94	ALEP

[192] ABBIENDI 01A error includes approximately 0.15 due to statistics, 0.06 due to event selection systematics, and 0.03 due to the theoretical uncertainty in *t*-channel prediction.
[193] BARATE 00C error includes approximately 0.15 due to statistics, 0.04 due to experimental systematics, and 0.02 due to the theoretical uncertainty in *t*-channel prediction.

$A_{FB}^{(0,u)}$ CHARGE ASYMMETRY IN $e^+e^- \rightarrow u\overline{u}$

ASYMMETRY (%)	*STD. MODEL*	*$\sqrt{s}$ (GeV)*	*DOCUMENT ID*	*TECN*
4.0±6.7±2.8	**7.2**	**91.2**	[194] ACKERSTAFF 97T	OPAL

[194] ACKERSTAFF 97T measure the forward-backward asymmetry of various fast hadrons made of light quarks. Then using SU(2) isospin symmetry and flavor independence for down and strange quarks authors solve for the different quark types.

$A_{FB}^{(0,s)}$ CHARGE ASYMMETRY IN $e^+e^- \rightarrow s\overline{s}$

The *s*-quark asymmetry is derived from measurements of the forward-backward asymmetry of fast hadrons containing an *s* quark.

ASYMMETRY (%)	*STD. MODEL*	*$\sqrt{s}$ (GeV)*	*DOCUMENT ID*	*TECN*
9.8 ±1.1 OUR AVERAGE				
10.08±1.13±0.40	10.1	91.2	[195] ABREU 00B	DLPH
6.8 ±3.5 ±1.1	10.1	91.2	[196] ACKERSTAFF 97T	OPAL
• • • We do not use the following data for averages, fits, limits, etc. • • •				
13.1 ±3.5 ±1.3	10.1	91.2	[197] ABREU 95G	DLPH

[195] ABREU 00B tag the presence of an *s* quark requiring a high-momentum-identified charged kaon. The *s*-quark pole asymmetry is extracted from the charged-kaon asymmetry taking the expected *d*- and *u*-quark asymmetries from the Standard Model and using the measured values for the *c*- and *b*-quark asymmetries.
[196] ACKERSTAFF 97T measure the forward-backward asymmetry of various fast hadrons made of light quarks. Then using SU(2) isospin symmetry and flavor independence for down and strange quarks authors solve for the different quark types. The value reported here corresponds then to the forward-backward asymmetry for "down-type" quarks.
[197] ABREU 95G require the presence of a high-momentum charged kaon or Λ^0 to tag the *s* quark. An unresolved *s*- and *d*-quark asymmetry of $(11.2 \pm 3.1 \pm 5.4)$% is obtained by tagging the presence of a high-energy neutron or neutral kaon in the hadron calorimeter. Superseded by ABREU 00B.

$A_{FB}^{(0,c)}$ CHARGE ASYMMETRY IN $e^+e^- \rightarrow c\overline{c}$

OUR FIT, which is obtained by a simultaneous fit to several *c*- and *b*-quark measurements as explained in the "Note on the *Z* boson," refers to the ***Z* pole** asymmetry. The experimental values, on the other hand, correspond to the measurements carried out at the respective energies. As a cross check we have also performed a weighted average of the "near peak" measurements taking into account the various common systematic errors. Applying to this combined "peak" measurement QED and energy-dependence corrections, our weighted average gives a pole asymmetry of (6.98 ± 0.42)%, the Standard Model prediction being 7.25%.

ASYMMETRY (%)	*STD. MODEL*	*$\sqrt{s}$ (GeV)*	*DOCUMENT ID*	*TECN*
7.04± 0.36 OUR FIT				
5.68± 0.54±0.39	6.3	91.25	[198] ABBIENDI 03P	OPAL
6.45± 0.57±0.37	6.10	91.21	[199] HEISTER 02H	ALEP
6.59± 0.94±0.35	6.2	91.235	[200] ABREU 99Y	DLPH
6.3 ± 0.9 ±0.3	6.1	91.22	[201] BARATE 98O	ALEP
6.3 ± 1.2 ±0.6	6.1	91.22	[202] ALEXANDER 97C	OPAL
8.3 ± 2.2 ±1.6	6.4	91.27	[203] ABREU 95K	DLPH
8.3 ± 3.8 ±2.7	6.2	91.24	[204] ADRIANI 92D	L3
• • • We do not use the following data for averages, fits, limits, etc. • • •				
− 6.8 ± 2.5 ±0.9	−3.0	89.51	[198] ABBIENDI 03P	OPAL
14.6 ± 2.0 ±0.8	12.2	92.95	[198] ABBIENDI 03P	OPAL
−12.4 ±15.9 ±2.0	−9.6	88.38	[199] HEISTER 02H	ALEP
− 2.3 ± 2.6 ±0.2	−3.8	89.38	[199] HEISTER 02H	ALEP
− 0.3 ± 8.3 ±0.6	0.9	90.21	[199] HEISTER 02H	ALEP
10.6 ± 7.7 ±0.7	9.6	92.05	[199] HEISTER 02H	ALEP
11.9 ± 2.1 ±0.6	12.2	92.94	[199] HEISTER 02H	ALEP
12.1 ±11.0 ±1.0	14.2	93.90	[199] HEISTER 02H	ALEP
− 4.96± 3.68±0.53	−3.5	89.434	[200] ABREU 99Y	DLPH
11.80± 3.18±0.62	12.3	92.990	[200] ABREU 99Y	DLPH
− 1.0 ± 4.3 ±1.0	−3.9	89.37	[201] BARATE 98O	ALEP
11.0 ± 3.3 ±0.8	12.3	92.96	[201] BARATE 98O	ALEP
3.9 ± 5.1 ±0.9	−3.4	89.45	[202] ALEXANDER 97C	OPAL
15.8 ± 4.1 ±1.1	12.4	93.00	[202] ALEXANDER 97C	OPAL
−12.9 ± 7.8 ±5.5	−13.6	35	BEHREND 90D	CELL
7.7 ±13.4 ±5.0	−22.1	43	BEHREND 90D	CELL
−12.8 ± 4.4 ±4.1	−13.6	35	ELSEN 90	JADE
−10.9 ±12.9 ±4.6	−23.2	44	ELSEN 90	JADE
−14.9 ± 6.7	−13.3	35	OULD-SAADA 89	JADE

[198] ABBIENDI 03P tag heavy flavors using events with one or two identified leptons. This allows the simultaneous fitting of the b and c quark forward-backward asymmetries as well as the average B^0-$\overline{B}^0$ mixing.
[199] HEISTER 02H measure simultaneously b and c quark forward-backward asymmetries using their semileptonic decays to tag the quark charge. The flavor separation is obtained with a discriminating multivariate analysis.
[200] ABREU 99Y tag $Z \to b\overline{b}$ and $Z \to c\overline{c}$ events by an exclusive reconstruction of several D meson decay modes (D^{*+}, D^0, and D^+ with their charge-conjugate states).
[201] BARATE 98O tag $Z \to c\overline{c}$ events requiring the presence of high-momentum reconstructed D^{*+}, D^+, or D^0 mesons.
[202] ALEXANDER 97C identify the b and c events using a D/D^* tag.
[203] ABREU 95K identify c and b quarks using both electron and muon semileptonic decays.
[204] ADRIANI 92D use both electron and muon semileptonic decays.

$A_{FB}^{(0,b)}$ CHARGE ASYMMETRY IN $e^+e^- \to b\overline{b}$

OUR FIT, which is obtained by a simultaneous fit to several c- and b-quark measurements as explained in the "Note on the Z boson," refers to the **Z pole** asymmetry. The experimental values, on the other hand, correspond to the measurements carried out at the respective energies. As a cross check we have also performed a weighted average of the "near peak" measurements taking into account the various common systematic errors. Applying to this combined "peak" measurement QED and energy-dependence corrections, our weighted average gives a pole asymmetry of (10.14 ± 0.18)%, the Standard Model prediction being 10.15%. For the jet-charge measurements (where the QCD effects are included since they represent an inherent part of the analysis), we use the corrections given by the authors.

ASYMMETRY (%)	STD. MODEL	$\sqrt{s}$ (GeV)	DOCUMENT ID		TECN
10.01± 0.17 OUR FIT					
9.72± 0.42± 0.15	9.67	91.25	[205] ABBIENDI	03P	OPAL
9.77± 0.36± 0.18	9.69	91.26	[206] ABBIENDI	02I	OPAL
9.52± 0.41± 0.17	9.59	91.21	[207] HEISTER	02H	ALEP
10.00± 0.27± 0.11	9.63	91.232	[208] HEISTER	01D	ALEP
9.82± 0.47± 0.16	9.69	91.26	[209] ABREU	99M	DLPH
7.62± 1.94± 0.85	9.64	91.235	[210] ABREU	99Y	DLPH
9.60± 0.66± 0.33	9.69	91.26	[211] ACCIARRI	99D	L3
9.31± 1.01± 0.55	9.65	91.24	[212] ACCIARRI	98U	L3
9.4 ± 2.7 ± 2.2	9.61	91.22	[213] ALEXANDER	97C	OPAL
10.4 ± 1.3 ± 0.5	9.70	91.27	[214] ABREU	95K	DLPH
• • • We do not use the following data for averages, fits, limits, etc. • • •					
4.7 ± 1.8 ± 0.1	5.9	89.51	[205] ABBIENDI	03P	OPAL
10.3 ± 1.5 ± 0.2	12.0	92.95	[205] ABBIENDI	03P	OPAL
5.82± 1.53± 0.12	5.9	89.50	[206] ABBIENDI	02I	OPAL
12.21± 1.23± 0.25	12.0	92.91	[206] ABBIENDI	02I	OPAL
−13.1 ±13.5 ± 1.0	3.2	88.38	[207] HEISTER	02H	ALEP
5.5 ± 1.9 ± 0.1	5.6	89.38	[207] HEISTER	02H	ALEP
− 0.4 ± 6.7 ± 0.8	7.5	90.21	[207] HEISTER	02H	ALEP
11.1 ± 6.4 ± 0.5	11.0	92.05	[207] HEISTER	02H	ALEP
10.4 ± 1.5 ± 0.3	12.0	92.94	[207] HEISTER	02H	ALEP
13.8 ± 9.3 ± 1.1	12.9	93.90	[207] HEISTER	02H	ALEP
4.36± 1.19± 0.11	5.8	89.472	[208] HEISTER	01D	ALEP
11.72± 0.97± 0.11	12.0	92.950	[208] HEISTER	01D	ALEP
6.8 ± 1.8 ± 0.13	6.0	89.55	[209] ABREU	99M	DLPH
12.3 ± 1.6 ± 0.27	12.0	92.94	[209] ABREU	99M	DLPH
5.67± 7.56± 1.17	5.7	89.434	[210] ABREU	99Y	DLPH
8.82± 6.33± 1.22	12.1	92.990	[210] ABREU	99Y	DLPH
6.11± 2.93± 0.43	5.9	89.50	[211] ACCIARRI	99D	L3
13.71± 2.40± 0.44	12.2	93.10	[211] ACCIARRI	99D	L3
4.95± 5.23± 0.40	5.8	89.45	[212] ACCIARRI	98U	L3
11.37± 3.99± 0.65	12.1	92.99	[212] ACCIARRI	98U	L3
− 8.6 ±10.8 ± 2.9	5.8	89.45	[213] ALEXANDER	97C	OPAL
− 2.1 ± 9.0 ± 2.6	12.1	93.00	[213] ALEXANDER	97C	OPAL
$-71 \pm 34 {}^{+7}_{-8}$	−58	58.3	SHIMONAKA	91	TOPZ
−22.2 ± 7.7 ± 3.5	−26.0	35	BEHREND	90D	CELL
−49.1 ±16.0 ± 5.0	−39.7	43	BEHREND	90D	CELL
−28 ±11	−23	35	BRAUNSCH...	90	TASS
−16.6 ± 7.7 ± 4.8	−24.3	35	ELSEN	90	JADE
−33.6 ±22.2 ± 5.2	−39.9	44	ELSEN	90	JADE
3.4 ± 7.0 ± 3.5	−16.0	29.0	BAND	89	MAC
−72 ±28 ±13	−56	55.2	SAGAWA	89	AMY

[205] ABBIENDI 03P tag heavy flavors using events with one or two identified leptons. This allows the simultaneous fitting of the b and c quark forward-backward asymmetries as well as the average B^0-$\overline{B}^0$ mixing.
[206] ABBIENDI 02I tag $Z^0 \to b\overline{b}$ decays using a combination of secondary vertex and lepton tags. The sign of the b-quark charge is determined using an inclusive tag based on jet, vertex, and kaon charges.
[207] HEISTER 02H measure simultaneously b and c quark forward-backward asymmetries using their semileptonic decays to tag the quark charge. The flavor separation is obtained with a discriminating multivariate analysis.
[208] HEISTER 01D tag $Z \to b\overline{b}$ events using the impact parameters of charged tracks complemented with information from displaced vertices, event shape variables, and lepton identification. The b-quark direction and charge is determined using the hemisphere charge method along with information from fast kaon tagging and charge estimators of primary and secondary vertices. The change in the quoted value due to variation of A^c_{FB} and R_b is given as $+0.103$ ($A^c_{FB} - 0.0651$) -0.440 ($R_b - 0.21585$).
[209] ABREU 99M tag $Z \to b\overline{b}$ events using lifetime and vertex charge. The original quark charge is obtained from the charge flow, the difference between the forward and backward hemisphere charges.
[210] ABREU 99Y tag $Z \to b\overline{b}$ and $Z \to c\overline{c}$ events by an exclusive reconstruction of several D meson decay modes (D^{*+}, D^0, and D^+ with their charge-conjugate states).
[211] ACCIARRI 99D tag $Z \to b\overline{b}$ events using high p and p_T leptons. The analysis determines simultaneously a mixing parameter $\chi_b = 0.1192 \pm 0.0068 \pm 0.0051$ which is used to correct the observed asymmetry.
[212] ACCIARRI 98U tag $Z \to b\overline{b}$ events using lifetime and measure the jet charge using the hemisphere charge.
[213] ALEXANDER 97C identify the b and c events using a D/D^* tag.
[214] ABREU 95K identify c and b quarks using both electron and muon semileptonic decays. The systematic error includes an uncertainty of ±0.3 due to the mixing correction ($\chi = 0.115 \pm 0.011$).

CHARGE ASYMMETRY IN $e^+e^- \to q\overline{q}$

Summed over five lighter flavors.

Experimental and Standard Model values are somewhat event-selection dependent. Standard Model expectations contain some assumptions on B^0-$\overline{B}^0$ mixing and on other electroweak parameters.

ASYMMETRY (%)	STD. MODEL	$\sqrt{s}$ (GeV)	DOCUMENT ID		TECN
• • • We do not use the following data for averages, fits, limits, etc. • • •					
− 0.76±0.12±0.15		91.2	[215] ABREU	92I	DLPH
4.0 ±0.4 ±0.63	4.0	91.3	[216] ACTON	92L	OPAL
9.1 ±1.4 ±1.6	9.0	57.9	ADACHI	91	TOPZ
− 0.84±0.15±0.04		91	DECAMP	91B	ALEP
8.3 ±2.9 ±1.9	8.7	56.6	STUART	90	AMY
11.4 ±2.2 ±2.1	8.7	57.6	ABE	89L	VNS
6.0 ±1.3	5.0	34.8	GREENSHAW	89	JADE
8.2 ±2.9	8.5	43.6	GREENSHAW	89	JADE

[215] ABREU 92I has 0.14 systematic error due to uncertainty of quark fragmentation.
[216] ACTON 92L use the weight function method on 259k selected $Z \to$ hadrons events. The systematic error includes a contribution of 0.2 due to B^0-$\overline{B}^0$ mixing effect, 0.4 due to Monte Carlo (MC) fragmentation uncertainties and 0.3 due to MC statistics. ACTON 92L derive a value of $\sin^2\theta_W^{\text{eff}}$ to be $0.2321 \pm 0.0017 \pm 0.0028$.

CHARGE ASYMMETRY IN $p\overline{p} \to Z \to e^+e^-$

ASYMMETRY (%)	STD. MODEL	$\sqrt{s}$ (GeV)	DOCUMENT ID		TECN
• • • We do not use the following data for averages, fits, limits, etc. • • •					
5.2±5.9±0.4		91	ABE	91E	CDF

ANOMALOUS $ZZ\gamma$, $Z\gamma\gamma$, AND ZZV COUPLINGS

Revised February 2002 by C. Caso (University of Genova) and A. Gurtu (Tata Institute).

In the reaction $e^+e^- \to Z\gamma$, deviations from the Standard Model for the $Z\gamma\gamma^*$ and $Z\gamma Z^*$ couplings may be described in terms of 8 parameters, h_i^V ($i = 1, 4$; $V = \gamma, Z$) [1]. The parameters h_i^γ describe the $Z\gamma\gamma^*$ couplings and the parameters h_i^Z the $Z\gamma Z^*$ couplings. In this formalism h_1^V and h_2^V lead to CP-violating and h_3^V and h_4^V to CP-conserving effects. All these anomalous contributions to the cross section increase rapidly with center-of-mass energy. In order to ensure unitarity, these parameters are usually described by a form-factor representation, $h_i^V(s) = h_{i0}^V/(1 + s/\Lambda^2)^n$, where Λ is the energy scale for the manifestation of a new phenomenon and n is a sufficiently large power. By convention one uses $n = 3$ for $h_{1,3}^V$ and $n = 4$ for $h_{2,4}^V$. Usually limits on h_i^V's are put assuming some value of Λ (sometimes ∞).

Above the $e^+e^- \to ZZ$ threshold, deviations from the Standard Model for the $ZZ\gamma^*$ and ZZZ^* couplings may be described by means of four anomalous couplings f_i^V ($i = 4, 5; V = \gamma, Z$) [2]. As above, the parameters f_i^γ describe the $Z\gamma\gamma^*$ couplings and the parameters f_i^Z the ZZZ^* couplings. The anomalous couplings f_5^V lead to violation of C and P symmetries while f_4^V introduces CP violation.

All these couplings h_i^V and f_i^V are zero at tree level in the Standard Model.

References

1. U. Baur and E.L. Berger Phys. Rev. **D47**, 4889 (1993).
2. K. Hagiwara *et al.*, Nucl. Phys. **B282**, 253 (1987).

h_i^V

Combining the LEP results properly taking into account the correlations the following 95% CL limits are derived:

(See EP Preprint Summer 2003: CERN-EP/2003-091 and hep-ex/0312023, December 2003, on http://lepewwg.web.cern.ch/LEPEWWG/stanmod/)

$-0.13 < h_1^Z < +0.13$, $-0.078 < h_2^Z < +0.071$,
$-0.20 < h_3^Z < +0.07$, $-0.05 < h_4^Z < +0.12$,
$-0.056 < h_1^\gamma < +0.055$, $-0.045 < h_2^\gamma < +0.025$,
$-0.049 < h_3^\gamma < -0.008$, $-0.002 < h_4^\gamma < +0.034$.

VALUE	DOCUMENT ID	TECN
• • • We do not use the following data for averages, fits, limits, etc. • • •		
	[217] ABBIENDI,G 00C	OPAL
	[218] ACCIARRI 00O	L3
	[219] ABBOTT 98M	D0
	[220] ABREU 98K	DLPH

[217] ABBIENDI,G 00C study $e^+e^- \to Z\gamma$ events (with $Z \to q\overline{q}$ and $Z \to \nu\overline{\nu}$) at 189 GeV to obtain the central values (and 95% CL limits) of these couplings: $h_1^Z = 0.000 \pm 0.100$ $(-0.190, 0.190)$, $h_2^Z = 0.000 \pm 0.068$ $(-0.128, 0.128)$, $h_3^Z = -0.074^{+0.102}_{-0.103}$ $(-0.269, 0.119)$, $h_4^Z = 0.046 \pm 0.068$ $(-0.084, 0.175)$, $h_1^\gamma = 0.000 \pm 0.061$ $(-0.115, 0.115)$, $h_2^\gamma = 0.000 \pm 0.041$ $(-0.077, 0.077)$, $h_3^\gamma = -0.080^{+0.039}_{-0.041}$ $(-0.164, -0.006)$, $h_4^\gamma = 0.064^{+0.033}_{-0.030}$ $(+0.007, +0.134)$. The results are derived assuming that only one coupling at a time is different from zero.

[218] ACCIARRI 00O study 189 GeV $e^+e^- \to q\overline{q}\gamma$ and $e^+e^- \to \nu\overline{\nu}\gamma$ events to derive 95% CL limits on h_i^V. For deriving each limit the others are fixed at zero. They report: $-0.26 < h_1^Z < 0.09$, $-0.10 < h_2^Z < 0.16$, $-0.26 < h_3^Z < 0.21$, $-0.11 < h_4^Z < 0.19$, $-0.20 < h_1^\gamma < 0.08$, $-0.11 < h_2^\gamma < 0.11$, $-0.11 < h_3^\gamma < 0.03$, $-0.02 < h_4^\gamma < 0.10$.

[219] ABBOTT 98M study $p\overline{p} \to Z\gamma$ +X, with $Z \to e^+e^-$, $\mu^+\mu^-$, $\overline{\nu}\nu$ at 1.8 TeV, to obtain 95% CL limits at Λ= 750 GeV: $|h_{30}^Z| < 0.36$, $|h_{40}^Z| < 0.05$ (keeping $|h_{30}^\gamma| < 0.37$, $|h_{40}^\gamma| < 0.05$ (keeping h_i^Z=0). Limits on the *CP*-violating couplings are $|h_{10}^Z| < 0.36$, $|h_{20}^Z| < 0.05$ (keeping h_i^γ=0), and $|h_{10}^\gamma| < 0.37$, $|h_{20}^\gamma| < 0.05$ (keeping h_i^Z=0).

[220] ABREU 98K determine a 95% CL upper limit on $\sigma(e^+e^- \to \gamma +$ invisible particles) < 2.5 pb using 161 and 172 GeV data. This is used to set 95% CL limits on $|h_{30}^\gamma| < 0.8$ and $|h_{30}^Z| < 1.3$, derived at a scale Λ=1 TeV and with n=3 in the form factor representation.

f_i^V

Combining the LEP results properly taking into account the correlations the following 95% CL limits are derived:

(See EP Preprint Summer 2003: CERN-EP/2003-091 and hep-ex/0312023, December 2003, on http://lepewwg.web.cern.ch/LEPEWWG/stanmod/)

$-0.30 < f_4^Z < +0.30$, $-0.34 < f_5^Z < +0.38$,
$-0.17 < f_4^\gamma < +0.19$, $-0.32 < f_5^\gamma < +0.36$.

VALUE	DOCUMENT ID	TECN
• • • We do not use the following data for averages, fits, limits, etc. • • •		
	[221] ABBIENDI 04C	OPAL
	[222] ACHARD 03D	L3

[221] ABBIENDI 04C study ZZ production in e^+e^- collisions in the C.M. energy range 190–209 GeV. They select 340 events with an expected background of 180 events. Including the ABBIENDI 00N data at 183 and 189 GeV (118 events with an expected background of 65 events) they report the following 95% CL limits: $-0.45 < f_4^Z < 0.58$, $-0.94 < f_5^Z < 0.25$, $-0.32 < f_4^\gamma < 0.33$, and $-0.71 < f_5^\gamma < 0.59$.

[222] ACHARD 03D study Z-boson pair production in e^+e^- collisions in the C.M. energy range 200–209 GeV. They select 549 events with an expected background of 432 events. Including the ACCIARRI 99G and ACCIARRI 99O data (183 and 189 GeV respectively, 286 events with an expected background of 241 events) and the 192–202 GeV ACCIARRI 01I results (656 events, expected background of 512 events), they report the following 95% CL limits: $-0.48 \leq f_4^Z \leq 0.46$, $-0.36 \leq f_5^Z \leq 1.03$, $-0.28 \leq f_4^\gamma \leq 0.28$, and $-0.40 \leq f_5^\gamma \leq 0.47$.

ANOMALOUS W/Z QUARTIC COUPLINGS

Revised November 2003 by C. Caso (University of Genova) and A. Gurtu (Tata Institute).

The Standard Model predictions for $WWWW$, $WWZZ$, $WWZ\gamma$, $WW\gamma\gamma$, and $ZZ\gamma\gamma$ couplings are small at LEP, but expected to become important at a TeV Linear Collider. Outside the Standard Model framework such possible couplings, a_0, a_c, a_n, are expressed in terms of the following dimension-6 operators [1,2];

$$L_6^0 = -\frac{e^2}{16\Lambda^2}\, a_0\, F^{\mu\nu}\, F_{\mu\nu}\vec{W}^\alpha \cdot \vec{W}_\alpha$$
$$L_6^c = -\frac{e^2}{16\Lambda^2}\, a_c\, F^{\mu\alpha}\, F_{\mu\beta}\vec{W}^\beta \cdot \vec{W}_\alpha$$
$$L_6^n = -i\frac{e^2}{16\Lambda^2}\, a_n\epsilon_{ijk}\, W_{\mu\alpha}^{(i)}\, W_\nu^{(j)}\, W^{(k)\alpha}F^{\mu\nu}$$
$$\widetilde{L}_6^0 = -\frac{e^2}{16\Lambda^2}\, \widetilde{a}_0\, F^{\mu\nu}\, \widetilde{F}_{\mu\nu}\vec{W}^\alpha \cdot \vec{W}_\alpha$$
$$\widetilde{L}_6^n = -i\frac{e^2}{16\Lambda^2}\, \widetilde{a}_n\epsilon_{ijk}\, W_{\mu\alpha}^{(i)}\, W_\nu^{(j)}\, W^{(k)\alpha}\widetilde{F}^{\mu\nu}$$

where F, W are photon and W fields, L_6^0 and L_6^c conserve C, P separately ($\widetilde{L}_6^0$ conserves only C) and generate anomalous $W^+W^-\gamma\gamma$ and $ZZ\gamma\gamma$ couplings, L_6^n violates CP ($\widetilde{L}_6^n$ violates both C and P) and generates an anomalous $W^+W^-Z\gamma$ coupling, and Λ is a scale for new physics. For the $ZZ\gamma\gamma$ coupling the CP-violating term represented by L_6^n does not contribute. These couplings are assumed to be real and to vanish at tree level in the Standard Model.

Within the same framework as above, a more recent description of the quartic couplings [3] treats the anomalous parts of the $WW\gamma\gamma$ and $ZZ\gamma\gamma$ couplings separately leading to two sets parameterized as a_0^V/Λ^2 and a_c^V/Λ^2, where $V = W$ or Z.

At LEP the processes studied in search of these quartic couplings are $e^+e^- \to WW\gamma$, $e^+e^- \to \gamma\gamma\nu\overline{\nu}$, and $e^+e^- \to Z\gamma\gamma$ and limits are set on the quantities a_0^W/Λ^2, a_c^W/Λ^2, a_n/Λ^2. The characteristics of the first process depend on all the three couplings whereas those of the latter two depend only on the two CP-conserving couplings. The sensitive measured variables are the cross sections for these processes as well as the energy and angular distributions of the photon and recoil mass to the photon pair.

References

1. G. Belanger and F. Boudjema, Phys. Lett. **B288**, 201 (1992).
2. J.W. Stirling and A. Werthenbach, Eur. Phys. J. **C14**, 103 (2000);
   J.W. Stirling and A. Werthenbach, Phys. Lett. **B466**, 369 (1999);
   A. Denner *et al.*, Eur. Phys. J. **C20**, 201 (2001);
   G. Montagna *et al.*, Phys. Lett. **B515**, 197 (2001).
3. G. Belanger *et al.*, Eur. Phys. J. **C13**, 103 (2000).

a_0/Λ^2, a_c/Λ^2

Combining published and unpublished preliminary LEP results the following 95% CL intervals for the QGCs associated with the $ZZ\gamma\gamma$ vertex are derived:

(See EP Preprint Summer 2003: CERN-EP/2003-091 and hep-ex/0312023, December 2003, on http://lepewwg.web.cern.ch/LEPEWWG/stanmod/)

$-0.008 < a_0^Z/\Lambda^2 < +0.021$
$-0.029 < a_c^Z/\Lambda^2 < +0.039$

VALUE	DOCUMENT ID	TECN

• • • We do not use the following data for averages, fits, limits, etc. • • •

[223] ACHARD 02G L3

[223] ACHARD 02G study $e^+e^- \to Z\gamma\gamma \to q\overline{q}\gamma\gamma$ events using data at center-of-mass energies from 200 to 209 GeV. The photons are required to be isolated, each with energy >5 GeV and $|\cos\theta| < 0.97$, and the di-jet invariant mass to be compatible with that of the Z boson (74–111 GeV). Cuts on Z velocity ($\beta < 0.73$) and on the energy of the most energetic photon reduce the backgrounds due to non-resonant production of the $q\overline{q}\gamma\gamma$ state and due to ISR respectively, yielding a total of 40 candidate events of which 8.6 are expected to be due to background. The energy spectra of the least energetic photon are fitted for all ten center-of-mass energy values from 130 GeV to 209 GeV (as obtained adding to the present analysis 130–202 GeV data of ACCIARRI 01E, for a total of 137 events with an expected background of 34.1 events) to obtain the fitted values $a_0/\Lambda^2 = 0.00^{+0.02}_{-0.01}$ GeV^{-2} and $a_c/\Lambda^2 = 0.03^{+0.01}_{-0.02}$ GeV^{-2}, where the other parameter is kept fixed to its Standard Model value (0). A simultaneous fit to both parameters yields the 95% CL limits -0.02 GeV^{-2} $< a_0/\Lambda^2 < 0.03$ GeV^{-2} and -0.07 GeV^{-2} $< a_c/\Lambda^2 < 0.05$ GeV^{-2}.

Z REFERENCES

ABBIENDI 04C EPJ C32 303 G. Abbiendi *et al.* (OPAL Collab.)
ABBIENDI 03P PL B577 18 G. Abbiendi *et al.* (OPAL Collab.)
ABDALLAH 03H PL B569 129 J. Abdallah *et al.* (DELPHI Collab.)
ABE 03F PRL 90 141804 K. Abe *et al.* (SLD Collab.)
ACHARD 03D PL B572 133 P. Achard *et al.* (L3 Collab.)
ABBIENDI 02I PL B546 29 G. Abbiendi *et al.* (OPAL Collab.)
ABE 02G PRL 88 151801 K. Abe *et al.* (SLD Collab.)
ACHARD 02G PL B540 43 P. Achard *et al.* (L3 Collab.)
HEISTER 02B PL B526 34 A. Heister *et al.* (ALEPH Collab.)
HEISTER 02C PL B528 19 A. Heister *et al.* (ALEPH Collab.)
HEISTER 02H EPJ C24 177 A. Heister *et al.* (ALEPH Collab.)
ABBIENDI 01A EPJ C19 587 G. Abbiendi *et al.* (OPAL Collab.)
ABBIENDI 01G EPJ C18 447 G. Abbiendi *et al.* (OPAL Collab.)
ABBIENDI 01K PL B516 1 G. Abbiendi *et al.* (OPAL Collab.)
ABBIENDI 01N EPJ C20 445 G. Abbiendi *et al.* (OPAL Collab.)
ABBIENDI 01O EPJ C21 1 G. Abbiendi *et al.* (OPAL Collab.)
ABE 01B PRL 86 1162 K. Abe *et al.* (SLD Collab.)
ABE 01C PR D63 032005 K. Abe *et al.* (SLD Collab.)
ACCIARRI 01E PL B505 47 M. Acciarri *et al.* (L3 Collab.)
ACCIARRI 01I PL B497 23 M. Acciarri *et al.* (L3 Collab.)
HEISTER 01 EPJ C20 401 A. Heister *et al.* (ALEPH Collab.)
HEISTER 01D EPJ C22 201 A. Heister *et al.* (ALEPH Collab.)
ABBIENDI 00N PL B476 256 G. Abbiendi *et al.* (OPAL Collab.)
ABBIENDI,G 00C EPJ C17 553 G. Abbiendi *et al.* (OPAL Collab.)
ABE 00B PRL 84 5945 K. Abe *et al.* (SLD Collab.)
ABE 00D PRL 85 5059 K. Abe *et al.* (SLD Collab.)
ABREU 00 EPJ C12 225 P. Abreu *et al.* (DELPHI Collab.)
ABREU 00B EPJ C14 613 P. Abreu *et al.* (DELPHI Collab.)
ABREU 00E EPJ C14 585 P. Abreu *et al.* (DELPHI Collab.)
ABREU 00F EPJ C16 371 P. Abreu *et al.* (DELPHI Collab.)
ABREU 00P PL B475 429 P. Abreu *et al.* (DELPHI Collab.)
ACCIARRI 00 EPJ C13 47 M. Acciarri *et al.* (L3 Collab.)
ACCIARRI 00C EPJ C16 1 M. Acciarri *et al.* (L3 Collab.)
ACCIARRI 00J PL B479 79 M. Acciarri *et al.* (L3 Collab.)
ACCIARRI 00O PL B489 55 M. Acciarri *et al.* (L3 Collab.)
ACCIARRI 00Q PL B489 93 M. Acciarri *et al.* (L3 Collab.)
BARATE 00B EPJ C16 597 R. Barate *et al.* (ALEPH Collab.)
BARATE 00C EPJ C14 1 R. Barate *et al.* (ALEPH Collab.)
BARATE 00O EPJ C16 613 R. Barate *et al.* (ALEPH Collab.)
ABBIENDI 99B EPJ C8 217 G. Abbiendi *et al.* (OPAL Collab.)
ABBIENDI 99I PL B447 157 G. Abbiendi *et al.* (OPAL Collab.)
ABE 99E PR D59 052001 K. Abe *et al.* (SLD Collab.)
ABE 99L PRL 83 1902 K. Abe *et al.* (SLD Collab.)
ABE 99O PRL 83 3384 K. Abe *et al.* (SLD Collab.)
ABREU 99 EPJ C6 19 P. Abreu *et al.* (DELPHI Collab.)
ABREU 99B EPJ C10 415 P. Abreu *et al.* (DELPHI Collab.)
ABREU 99J PL B449 364 P. Abreu *et al.* (DELPHI Collab.)
ABREU 99M EPJ C9 367 P. Abreu *et al.* (DELPHI Collab.)
ABREU 99U PL B462 425 P. Abreu *et al.* (DELPHI Collab.)
ABREU 99Y EPJ C10 219 P. Abreu *et al.* (DELPHI Collab.)
ACCIARRI 99D PL B448 152 M. Acciarri *et al.* (L3 Collab.)
ACCIARRI 99F PL B453 94 M. Acciarri *et al.* (L3 Collab.)
ACCIARRI 99G PL B450 281 M. Acciarri *et al.* (L3 Collab.)
ACCIARRI 99O PL B465 363 M. Acciarri *et al.* (L3 Collab.)
ABBOTT 98M PR D57 R3817 B. Abbott *et al.* (D0 Collab.)
ABE 98D PRL 80 660 K. Abe *et al.* (SLD Collab.)
ABE 98I PRL 81 942 K. Abe *et al.* (SLD Collab.)
ABREU 98K PL B423 194 P. Abreu *et al.* (DELPHI Collab.)
ABREU 98L EPJ C5 585 P. Abreu *et al.* (DELPHI Collab.)
ACCIARRI 98G PL B431 199 M. Acciarri *et al.* (L3 Collab.)
ACCIARRI 98H PL B429 387 M. Acciarri *et al.* (L3 Collab.)
ACCIARRI 98U PL B439 225 M. Acciarri *et al.* (L3 Collab.)
ACKERSTAFF 98A EPJ C5 411 K. Ackerstaff *et al.* (OPAL Collab.)
ACKERSTAFF 98E EPJ C1 439 K. Ackerstaff *et al.* (OPAL Collab.)
ACKERSTAFF 98O PL B420 157 K. Ackerstaff *et al.* (OPAL Collab.)
ACKERSTAFF 98Q EPJ C4 19 K. Ackerstaff *et al.* (OPAL Collab.)
BARATE 98O PL B434 415 R. Barate *et al.* (ALEPH Collab.)
BARATE 98T EPJ C4 557 R. Barate *et al.* (ALEPH Collab.)
BARATE 98V EPJ C5 205 R. Barate *et al.* (ALEPH Collab.)
ABE 97 PRL 78 17 K. Abe *et al.* (SLD Collab.)
ABE 97N PRL 79 804 K. Abe *et al.* (SLD Collab.)
ABREU 97C ZPHY C73 243 P. Abreu *et al.* (DELPHI Collab.)
ABREU 97E PL B398 207 P. Abreu *et al.* (DELPHI Collab.)
ABREU 97G PL B404 194 P. Abreu *et al.* (DELPHI Collab.)
ACCIARRI 97D PL B393 465 M. Acciarri *et al.* (L3 Collab.)
ACCIARRI 97J PL B407 351 M. Acciarri *et al.* (L3 Collab.)
ACCIARRI 97L PL B407 389 M. Acciarri *et al.* (L3 Collab.)
ACCIARRI 97R PL B413 167 M. Acciarri *et al.* (L3 Collab.)
ACKERSTAFF 97C PL B391 221 K. Ackerstaff *et al.* (OPAL Collab.)
ACKERSTAFF 97K ZPHY C74 1 K. Ackerstaff *et al.* (OPAL Collab.)
ACKERSTAFF 97M ZPHY C74 413 K. Ackerstaff *et al.* (OPAL Collab.)
ACKERSTAFF 97S PL B412 210 K. Ackerstaff *et al.* (OPAL Collab.)
ACKERSTAFF 97T ZPHY C76 387 K. Ackerstaff *et al.* (OPAL Collab.)
ACKERSTAFF 97W ZPHY C76 425 K. Ackerstaff *et al.* (OPAL Collab.)
ALEXANDER 97C ZPHY C73 379 G. Alexander *et al.* (OPAL Collab.)
ALEXANDER 97D ZPHY C73 569 G. Alexander *et al.* (OPAL Collab.)
ALEXANDER 97E ZPHY C73 587 G. Alexander *et al.* (OPAL Collab.)
BARATE 97D PL B405 191 R. Barate *et al.* (ALEPH Collab.)
BARATE 97E PL B401 150 R. Barate *et al.* (ALEPH Collab.)
BARATE 97F PL B401 163 R. Barate *et al.* (ALEPH Collab.)
BARATE 97H PL B402 213 R. Barate *et al.* (ALEPH Collab.)
BARATE 97J ZPHY C74 451 R. Barate *et al.* (ALEPH Collab.)
ABE 96E PR D53 1023 K. Abe *et al.* (SLD Collab.)
ABREU 96 ZPHY C70 531 P. Abreu *et al.* (DELPHI Collab.)
ABREU 96R ZPHY C72 31 P. Abreu *et al.* (DELPHI Collab.)
ABREU 96S PL B389 405 P. Abreu *et al.* (DELPHI Collab.)
ABREU 96U ZPHY C73 61 P. Abreu *et al.* (DELPHI Collab.)
ACCIARRI 96 PL B371 126 M. Acciarri *et al.* (L3 Collab.)
ADAM 96 ZPHY C69 561 W. Adam *et al.* (DELPHI Collab.)
ADAM 96B ZPHY C70 371 W. Adam *et al.* (DELPHI Collab.)
ALEXANDER 96B ZPHY C70 197 G. Alexander *et al.* (OPAL Collab.)
ALEXANDER 96F PL B370 185 G. Alexander *et al.* (OPAL Collab.)
ALEXANDER 96N PL B384 343 G. Alexander *et al.* (OPAL Collab.)
ALEXANDER 96R ZPHY C72 1 G. Alexander *et al.* (OPAL Collab.)
ALEXANDER 96U ZPHY C72 365 G. Alexander *et al.* (OPAL Collab.)
BUSKULIC 96D ZPHY C69 393 D. Buskulic *et al.* (ALEPH Collab.)
BUSKULIC 96H ZPHY C69 379 D. Buskulic *et al.* (ALEPH Collab.)
ABE 95J PRL 74 2880 K. Abe *et al.* (SLD Collab.)
ABE,K 95 PRL 75 3609 K. Abe *et al.* (SLD Collab.)
ABREU 95 ZPHY C65 709 erratum P. Abreu *et al.* (DELPHI Collab.)
ABREU 95D ZPHY C66 323 P. Abreu *et al.* (DELPHI Collab.)
ABREU 95G ZPHY C67 1 P. Abreu *et al.* (DELPHI Collab.)
ABREU 95I ZPHY C67 183 P. Abreu *et al.* (DELPHI Collab.)
ABREU 95K ZPHY C65 569 P. Abreu *et al.* (DELPHI Collab.)
ABREU 95L ZPHY C65 587 P. Abreu *et al.* (DELPHI Collab.)
ABREU 95M ZPHY C65 603 P. Abreu *et al.* (DELPHI Collab.)
ABREU 95O ZPHY C67 543 P. Abreu *et al.* (DELPHI Collab.)
ABREU 95R ZPHY C68 353 P. Abreu *et al.* (DELPHI Collab.)
ABREU 95W PL B361 207 P. Abreu *et al.* (DELPHI Collab.)
ABREU 95X ZPHY C69 1 P. Abreu *et al.* (DELPHI Collab.)
ACCIARRI 95B PL B345 589 M. Acciarri *et al.* (L3 Collab.)
ACCIARRI 95C PL B345 609 M. Acciarri *et al.* (L3 Collab.)
ACCIARRI 95G PL B353 136 M. Acciarri *et al.* (L3 Collab.)
AKERS 95C ZPHY C65 47 R. Akers *et al.* (OPAL Collab.)
AKERS 95O ZPHY C67 27 R. Akers *et al.* (OPAL Collab.)
AKERS 95U ZPHY C67 389 R. Akers *et al.* (OPAL Collab.)
AKERS 95W ZPHY C67 555 R. Akers *et al.* (OPAL Collab.)
AKERS 95X ZPHY C68 1 R. Akers *et al.* (OPAL Collab.)
AKERS 95Z ZPHY C68 203 R. Akers *et al.* (OPAL Collab.)
ALEXANDER 95D PL B358 162 G. Alexander *et al.* (OPAL Collab.)
BUSKULIC 95Q ZPHY C69 183 D. Buskulic *et al.* (ALEPH Collab.)
BUSKULIC 95R ZPHY C69 15 D. Buskulic *et al.* (ALEPH Collab.)
MIYABAYASHI 95 PL B347 171 K. Miyabayashi *et al.* (TOPAZ Collab.)
ABE 94C PRL 73 25 K. Abe *et al.* (SLD Collab.)
ABREU 94 NP B418 403 P. Abreu *et al.* (DELPHI Collab.)
ABREU 94B PL B327 386 P. Abreu *et al.* (DELPHI Collab.)
ABREU 94P PL B341 109 P. Abreu *et al.* (DELPHI Collab.)
ACCIARRI 94 ZPHY C62 551 M. Acciarri *et al.* (L3 Collab.)
ACCIARRI 94E PL B341 245 M. Acciarri *et al.* (L3 Collab.)
AKERS 94 ZPHY C61 19 R. Akers *et al.* (OPAL Collab.)
AKERS 94P ZPHY C63 181 R. Akers *et al.* (OPAL Collab.)
BUSKULIC 94 ZPHY C62 539 D. Buskulic *et al.* (ALEPH Collab.)
BUSKULIC 94G ZPHY C62 179 D. Buskulic *et al.* (ALEPH Collab.)
BUSKULIC 94J ZPHY C62 1 D. Buskulic *et al.* (ALEPH Collab.)
VILAIN 94 PL B320 203 P. Vilain *et al.* (CHARM II Collab.)
ABREU 93 PL B298 236 P. Abreu *et al.* (DELPHI Collab.)
ABREU 93I ZPHY C59 533 P. Abreu *et al.* (DELPHI Collab.)
Also 95 ZPHY C65 709 erratum P. Abreu *et al.* (DELPHI Collab.)
ABREU 93L PL B318 249 P. Abreu *et al.* (DELPHI Collab.)
ACTON 93 PL B305 407 P.D. Acton *et al.* (OPAL Collab.)
ACTON 93D ZPHY C58 219 P.D. Acton *et al.* (OPAL Collab.)
ACTON 93E PL B311 391 P.D. Acton *et al.* (OPAL Collab.)
ACTON 93F ZPHY C58 405 P.D. Acton *et al.* (OPAL Collab.)
ADRIANI 93 PL B301 136 O. Adriani *et al.* (L3 Collab.)
ADRIANI 93I PL B316 427 O. Adriani *et al.* (L3 Collab.)
BUSKULIC 93L PL B313 520 D. Buskulic *et al.* (ALEPH Collab.)
NOVIKOV 93C PL B298 453 V.A. Novikov, L.B. Okun, M.I. Vysotsky (ITEP)
ABREU 92I PL B277 371 P. Abreu *et al.* (DELPHI Collab.)
ABREU 92M PL B289 199 P. Abreu *et al.* (DELPHI Collab.)
ACTON 92B ZPHY C53 539 D.P. Acton *et al.* (OPAL Collab.)
ACTON 92L PL B294 436 P.D. Acton *et al.* (OPAL Collab.)
ACTON 92N PL B295 357 P.D. Acton *et al.* (OPAL Collab.)
ADEVA 92 PL B275 209 B. Adeva *et al.* (L3 Collab.)
ADRIANI 92D PL B292 454 O. Adriani *et al.* (L3 Collab.)
ALITTI 92B PL B276 354 J. Alitti *et al.* (UA2 Collab.)
BUSKULIC 92D PL B292 210 D. Buskulic *et al.* (ALEPH Collab.)
BUSKULIC 92E PL B294 145 D. Buskulic *et al.* (ALEPH Collab.)
DECAMP 92 PRPL 216 253 D. Decamp *et al.* (ALEPH Collab.)
LEP 92 PL B276 247 LEP Collabs. (LEP, ALEPH, DELPHI, L3, OPAL)
ABE 91E PRL 67 1502 F. Abe *et al.* (CDF Collab.)
ABREU 91H ZPHY C50 185 P. Abreu *et al.* (DELPHI Collab.)
ACTON 91B PL B273 338 D.P. Acton *et al.* (OPAL Collab.)
ADACHI 91 PL B255 613 I. Adachi *et al.* (TOPAZ Collab.)
ADEVA 91I PL B259 199 B. Adeva *et al.* (L3 Collab.)
AKRAWY 91F PL B257 531 M.Z. Akrawy *et al.* (OPAL Collab.)
DECAMP 91B PL B259 377 D. Decamp *et al.* (ALEPH Collab.)
DECAMP 91J PL B266 218 D. Decamp *et al.* (ALEPH Collab.)
JACOBSEN 91 PRL 67 3347 R.G. Jacobsen *et al.* (Mark II Collab.)
SHIMONAKA 91 PL B268 457 A. Shimonaka *et al.* (TOPAZ Collab.)
ABE 90I ZPHY C48 13 K. Abe *et al.* (VENUS Collab.)
ABRAMS 90 PRL 64 1334 G.S. Abrams *et al.* (Mark II Collab.)
AKRAWY 90J PL B246 285 M.Z. Akrawy *et al.* (OPAL Collab.)
BEHREND 90D ZPHY C47 333 H.J. Behrend *et al.* (CELLO Collab.)
BRAUNSCH... 90 ZPHY C48 433 W. Braunschweig *et al.* (TASSO Collab.)
ELSEN 90 ZPHY C46 349 E. Elsen *et al.* (JADE Collab.)
HEGNER 90 ZPHY C46 547 S. Hegner *et al.* (JADE Collab.)
STUART 90 PRL 64 983 D. Stuart *et al.* (AMY Collab.)
ABE 89 PRL 62 613 F. Abe *et al.* (CDF Collab.)
ABE 89C PRL 63 720 F. Abe *et al.* (CDF Collab.)
ABE 89L PL B232 425 K. Abe *et al.* (VENUS Collab.)
ABRAMS 89B PRL 63 2173 G.S. Abrams *et al.* (Mark II Collab.)
ABRAMS 89D PRL 63 2780 G.S. Abrams *et al.* (Mark II Collab.)
ALBAJAR 89 ZPHY C44 15 C. Albajar *et al.* (UA1 Collab.)
BACALA 89 PL B218 112 A. Bacala *et al.* (AMY Collab.)
BAND 89 PL B218 369 H.R. Band *et al.* (MAC Collab.)
GREENSHAW 89 ZPHY C42 1 T. Greenshaw *et al.* (JADE Collab.)
OULD-SAADA 89 ZPHY C44 567 F. Ould-Saada *et al.* (JADE Collab.)
SAGAWA 89 PRL 63 2341 H. Sagawa *et al.* (AMY Collab.)
ADACHI 88C PL B208 319 I. Adachi *et al.* (TOPAZ Collab.)
ADEVA 88 PR D38 2665 B. Adeva *et al.* (Mark-J Collab.)
BRAUNSCH... 88D ZPHY C40 163 W. Braunschweig *et al.* (TASSO Collab.)
ANSARI 87 PL B186 440 R. Ansari *et al.* (UA2 Collab.)
BEHREND 87C PL B191 209 H.J. Behrend *et al.* (CELLO Collab.)
BARTEL 86C ZPHY C30 371 W. Bartel *et al.* (JADE Collab.)
Also 85B ZPHY C26 507 W. Bartel *et al.* (JADE Collab.)
Also 82 PL 108B 140 W. Bartel *et al.* (JADE Collab.)
ASH 85 PRL 55 1831 W.W. Ash *et al.* (MAC Collab.)
BARTEL 85F PL 161B 188 W. Bartel *et al.* (JADE Collab.)
DERRICK 85 PR D31 2352 M. Derrick *et al.* (HRS Collab.)
FERNANDEZ 85 PRL 54 1624 E. Fernandez *et al.* (MAC Collab.)
LEVI 83 PRL 51 1941 M.E. Levi *et al.* (Mark II Collab.)
BEHREND 82 PL 114B 282 H.J. Behrend *et al.* (CELLO Collab.)
BRANDELIK 82C PL 110B 173 R. Brandelik *et al.* (TASSO Collab.)

Higgs Bosons — H^0 and $H^{\pm}$, Searches for

SEARCHES FOR HIGGS BOSONS

Updated October 2003 by P. Igo-Kemenes
(Physikalisches Institut, Heidelberg, Germany).

I. Introduction

One of the main challenges in high-energy physics is to understand electroweak symmetry breaking and the origin of mass. In the Standard Model (SM) [1], the electroweak interaction is described by a gauge field theory based on the $\mathrm{SU}(2)_L\times\mathrm{U}(1)_Y$ symmetry group. Masses can be introduced by the Higgs mechanism [2]. In the simplest form of this mechanism, which is implemented in the SM, fundamental scalar "Higgs" fields interact with each other such that they acquire non-zero vacuum expectation values, and the $\mathrm{SU}(2)_L\times\mathrm{U}(1)_Y$ symmetry is spontaneously broken down to the electromagnetic $\mathrm{U}(1)_{\mathrm{EM}}$ symmetry. Gauge bosons and fermions obtain their masses by interacting with the vacuum Higgs fields. Associated with this description is the existence of massive scalar particles, Higgs bosons.

The minimal SM requires one Higgs field doublet and predicts a single neutral Higgs boson. Beyond the SM, supersymmetric (SUSY) extensions [3] are of interest, since they provide a consistent framework for the unification of the gauge interactions at a high-energy scale, $\Lambda_{\mathrm{GUT}} \approx 10^{16}$ GeV, and an explanation for the stability of the electroweak energy scale in the presence of quantum corrections (the "scale hierarchy problem"). Moreover, their predictions are compatible with existing high-precision data.

The Minimal Supersymmetric Standard Model (MSSM) (reviewed *e.g.*, in Ref. 4) is the SUSY extension of the SM with minimal new particle content. It introduces two Higgs field doublets, which is the minimal Higgs structure required to keep the theory free of anomalies and to provide masses to all charged fermions. The MSSM predicts three neutral and two charged Higgs bosons. The lightest of the neutral Higgs bosons is predicted to have its mass close to the electroweak energy scale ($\approx M_W$) [5,6].

Prior to 1989, when the e^+e^- collider LEP at CERN came into operation, the searches for Higgs bosons were sensitive to masses below a few GeV only (see Ref. 7 for a review). From 1989 to 1994 (the LEP1 phase) the LEP collider was operating at a center-of-mass energy $\sqrt{s} \approx M_Z$. After 1994 (the LEP2 phase), the center-of-mass energy increased each year, reaching 209 GeV in the year 2000 before the final shutdown. The combined data of the four LEP experiments, ALEPH, DELPHI, L3, and OPAL, are sensitive to neutral Higgs boson masses up to about 117 GeV.

Higgs boson searches have also been carried out at the Tevatron $p\overline{p}$ collider. With the currently analyzed data samples, the sensitivity of the two experiments, CDF and DØ, is rather limited, but with increasing energy and sample sizes, the range of sensitivity should eventually exceed the LEP range [8]. The searches will continue later at the LHC pp collider, covering masses up to about 1 TeV [9]. If Higgs bosons are indeed discovered, the Higgs mechanism could be studied in great detail at future e^+e^- [10,11] and $\mu^+\mu^-$ colliders [12].

In order to keep this review up-to-date, some recent but unpublished results are also quoted. These are marked with (*) in the reference list and can be accessed conveniently from the public web page `http://lephiggs.web.cern.ch/LEPHIGGS/pdg2004/index.html`.

II. The Standard Model Higgs boson

The mass of the SM Higgs boson H^0 is given by $m_{H^0} = \sqrt{2\lambda}\ v$. While the vacuum expectation value of the Higgs field, $v = 247$ GeV, is fixed by the Fermi coupling, the quartic Higgs self-coupling λ is a free parameter; thus, the mass m_{H^0} is not predicted. However, arguments of self-consistency of the theory can be used to place approximate upper and lower bounds upon the mass [13]. Since for large Higgs boson masses the running coupling λ rises with energy, the theory would eventually become non-perturbative. The requirement that this does not occur below a given energy scale Λ defines an upper bound for the Higgs mass. A lower bound is obtained from the study of quantum corrections to the SM and requiring the effective potential to be positive definite. These theoretical bounds imply that if the SM is to be self-consistent up to $\Lambda_{\mathrm{GUT}} \approx 10^{16}$ GeV, the Higgs boson mass should be within about 130 and 190 GeV. In other terms, the discovery of a Higgs boson with mass below 130 GeV would suggest the onset of new physics at a scale below Λ_{GUT}.

Indirect experimental bounds for the SM Higgs boson mass are obtained from fits to precision measurements of electroweak observables, and to the measured top and $W^{\pm}$ masses. These measurements are sensitive to $\log(m_{H^0})$ through radiative corrections. The current best fit value is $m_{H^0} = 96^{+60}_{-38}$ GeV, or $m_{H^0} <219$ GeV at the 95% confidence level (CL) [14], which is consistent with the SM being valid up to the GUT scale.

Production processes

The principal mechanism for producing the SM Higgs particle in e^+e^- collisions at LEP energies is Higgs-strahlung in the s-channel [15], $e^+e^- \to H^0Z^0$. The Z^0 boson in the final state is either virtual (LEP1), or on mass shell (LEP2). The cross section [16] $\sigma^{\mathrm{SM}}_{HZ}$ is shown in Fig. 1 (top) for the LEP energy range, together with those of the dominant background processes, $e^+e^- \to$ fermion pairs, W^+W^-, and Z^0Z^0. The SM Higgs boson can also be produced by W^+W^- and Z^0Z^0 fusion in the t-channel [17], but at LEP energies these processes have small cross sections.

At hadron colliders, the most important Higgs production processes are [18]: gluon fusion ($gg \to H^0$), Higgs production in association with a vector boson (WH^0 or ZH^0) or with a top quark pair ($t\bar{t}H^0$), and the WW fusion process giving (ppH^0 or $p\overline{p}H^0$). At the Tevatron and for masses less than

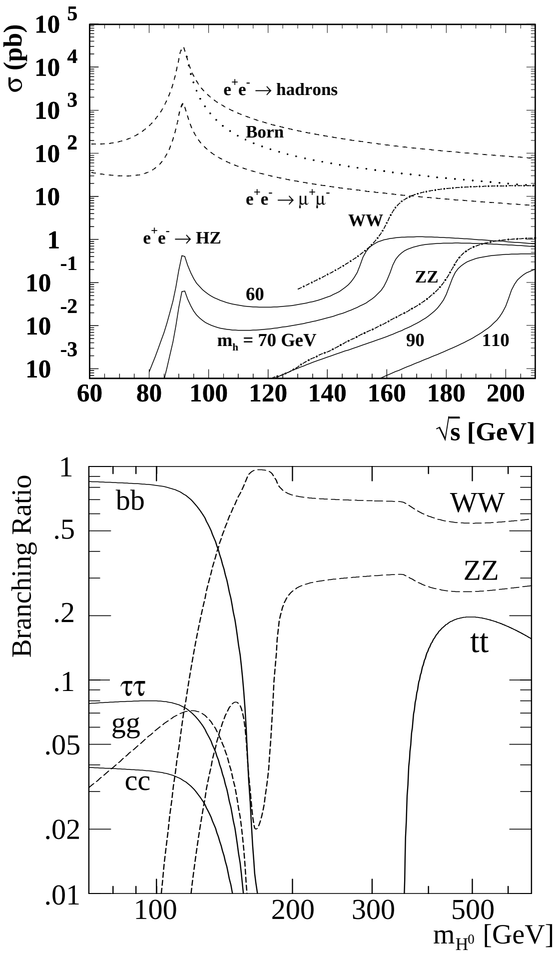

Figure 1: Cross sections, as a function of $\sqrt{s}$, for the Higgs-strahlung process in the SM for fixed values of m_{H^0} (full lines) and for other SM processes which contribute to the background; Bottom: Branching ratios for the main decay modes of the SM Higgs boson (from Ref. 10).

about 140 GeV (where the Higgs boson mainly decays to $b\overline{b}$), the most promising discovery channels are WH^0 and ZH^0 with $H^0 \to b\overline{b}$ ($H^0 \to W^*W$ is also contributing). At the future pp collider LHC, the gluon fusion channels $gg \to H^0 \to \gamma\gamma$, WW, ZZ, the associated production channel $t\overline{t}H^0 \to t\overline{t}b\overline{b}$ and the WW fusion channel $qqH^0 \to qq\tau^+\tau^-$ are all expected to contribute. Their relative sensitivity as well as the relevance of the WH^0 and ZH^0 channels strongly depend upon the precise value of the Higgs boson mass.

Decay of the SM Higgs boson

The most relevant decays of the SM Higgs boson [16,19] are summarized in Fig. 1 (bottom). For masses below about 140 GeV, decays to fermion pairs dominate, of which the decay $H^0 \to b\overline{b}$ has the largest branching ratio. Decays to $\tau^+\tau^-$, $c\overline{c}$, and gluon pairs (via loops) contribute less than 10%. For such low masses, the decay width is less than 10 MeV. For larger masses, the W^+W^- and Z^0Z^0 final states dominate, and the decay width rises rapidly, reaching about 1 GeV at m_{H^0}=200 GeV, and even 100 GeV at m_{H^0}=500 GeV.

Searches for the SM Higgs boson

During the LEP1 phase, the experiments ALEPH, DELPHI, L3, and OPAL analyzed over 17 million Z^0 decays, and have set lower bounds of approximately 65 GeV on the mass of the SM Higgs boson [20]. Substantial data samples have also been collected during the LEP2 phase at energies up to 209 GeV, including more than 40,000 $e^+e^- \to W^+W^-$ events. At LEP2, the composition of the background is more complex than at LEP1, due to the four-fermion processes $e^+e^- \to W^+W^-$ and Z^0Z^0, in addition to the two-fermion processes known from LEP1 (see Fig. 1 (top)). These have kinematic properties similar to the signal process (especially for $m_{H^0} \approx M_W$, M_Z), but since at LEP2 the Z^0 boson is on mass shell, constrained kinematic fits yield additional separation power. Furthermore, jets with b flavor, such as occurring in Higgs boson decays, are identified in high-precision silicon microvertex detectors.

The following final states provide good sensitivity for the SM Higgs boson. (a) The most abundant, four-jet, topology is produced in the $e^+e^- \to (H^0 \to b\overline{b})(Z^0 \to q\overline{q})$ process, and occurs with a branching ratio of about 60% for a Higgs boson with 115 GeV mass. The invariant mass of two jets is close to M_Z, while the other two jets contain b flavor. (b) The missing energy topology is produced mainly in the $e^+e^- \to (H^0 \to b\overline{b})(Z^0 \to \nu\overline{\nu})$ process, and occurs with a branching ratio of about 17%. The signal has two b jets, substantial missing transverse momentum, and missing mass compatible with M_Z. (c) In the leptonic final states, $e^+e^- \to (H^0 \to b\overline{b})(Z^0 \to e^+e^-, \mu^+\mu^-)$, the two leptons reconstruct to M_Z, and the two jets have b flavor. Although the branching ratio is small (only about 6%), this channel adds significantly to the overall search sensitivity, since it has low background. (d) Final states with tau leptons are produced in the processes $e^+e^- \to (H^0 \to \tau^+\tau^-)(Z^0 \to q\overline{q})$ and $(H^0 \to q\overline{q})(Z^0 \to \tau^+\tau^-)$; they occur with a branching ratio of about 10% in total. At LEP1, only the missing energy (b) and leptonic (c) final states could be used in the search for the SM Higgs boson, because of prohibitive backgrounds in the other channels; at LEP2 all four search topologies could be exploited.

The overall sensitivity of the searches is improved by combining statistically the data of the four LEP experiments in different decay channels, and at different LEP energies. After preselection, the combined data configuration (distribution in several discriminating variables) is compared in a frequentist approach to Monte-Carlo simulated configurations for two hypotheses: the background "b" hypothesis, and the signal plus background "$s + b$" hypothesis; in the latter case a SM Higgs boson of hypothetical mass (test-mass), m_H, is assumed in addition to the background.

The ratio $Q = \mathcal{L}_{s+b}/\mathcal{L}_b$ of the corresponding likelihoods is used as test statistic. The predicted, normalized, distributions of Q (probability density functions) are integrated to obtain the p-values $1 - CL_b = 1 - \mathcal{P}_b(Q \leq Q_{\text{observed}})$ and $CL_{s+b} = \mathcal{P}_{s+b}(Q \leq Q_{\text{observed}})$, which measure the compatibility of the observed data configuration with the two hypotheses [21].

The searches carried out at LEP prior to the year 2000, and their combinations [22], did not reveal any evidence for the production of a SM Higgs boson. However, in the data of the year 2000, mostly at energies $\sqrt{s} > 205$ GeV, ALEPH reported an excess of about three standard deviations beyond the background prediction [23], arising mainly from a few four-jet candidates with clean b tags and kinematic properties suggesting a SM Higgs boson with mass in the vicinity of 115 GeV. The data of DELPHI [24], L3 [25], and OPAL [26] do not show evidence for such an excess, but do not, however, exclude a 115 GeV Higgs boson. When the data of the four experiments are combined [27], the overall significance decreases to about 1.7 standard deviations. Figure 2 shows the test statistic $-2\ln Q$ for the ALEPH data and for the LEP data combined. For a test-mass $m_H = 115$ GeV, one calculates the p-values $1 - CL_b = 0.09$ for the background hypothesis and $CL_{s+b} = 0.15$ for the signal-plus-background hypothesis. From the same combination, a 95% CL lower bound of 114.4 GeV is obtained for the mass of the SM Higgs boson.

At the Tevatron, the currently published results of the CDF collaboration [28] are based on the Run I data sample of about 100 pb^{-1}. The searches concentrate on the associated production of a Higgs boson with a vector boson, $p\overline{p} \to VH^0$ ($V \equiv Z^0$, $W^\pm$), where the vector boson decays into the leptonic and hadronic channels and the Higgs boson into a $b\overline{b}$ pair. The main source of background is from QCD processes with genuine $b\overline{b}$ pairs. The Run I data sample is too small for a discovery, but allows model-independent upper bounds to be set on the cross section for such Higgs-like event topologies. These are currently higher by an order of magnitude than the SM predictions. However, Run II started in the year 2001, and with the projected data samples, the search sensitivity will increase considerably [8]. First results from the DØ collaboration, searching for the $H^0 \to W^*W$ channel and using Run II data of about 118 pb^{-1}, have been reported [29].

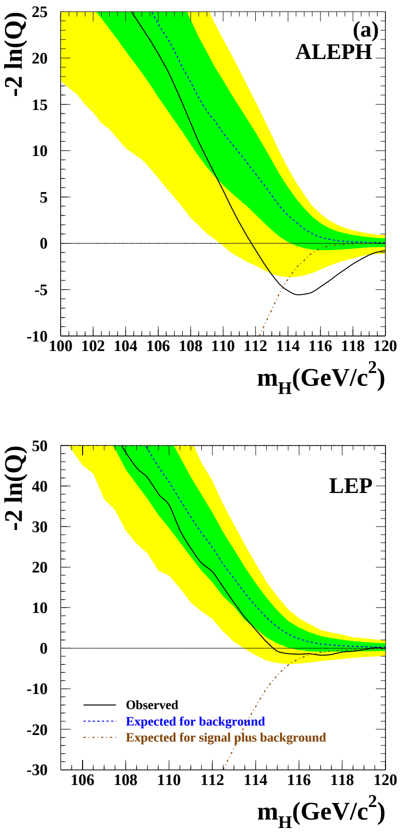

Figure 2: Observed (solid line), and expected behaviors of the test statistic $-2\ln Q$ for the background (dashed line), and the signal + background hypothesis (dash-dotted line) as a function of the test mass m_H. Top: ALEPH data alone; bottom: LEP data combined [27]. The dark and light shaded areas represent the 68% and 95% probability bands about the background expectation. See full-color version on color pages at end of book.

III. Higgs bosons in the MSSM

Most of the experimental investigations carried out so far assume CP invariance in the MSSM Higgs sector, in which case the three neutral Higgs bosons are CP eigenstates [4–6]. However, CP-violating (CPV) phases in the mechanism of soft SUSY breaking can lead to sizeable CP violation in the MSSM Higgs sector [30,31]. Such scenarios are theoretically appealing, since they provide one of the ingredients needed to explain the observed cosmic matter-antimatter asymmetry. In such models, the three neutral Higgs mass eigenstates are mixtures of CP-even and CP-odd fields. Consequently, their production and decay properties are different, and the experimental limits obtained for CP conserving (CPC) scenarios may thus be invalidated by CP-violating effects.

An important prediction of the MSSM, both CPC and CPV, is the relatively small mass of the lightest neutral scalar boson, less than about 130 GeV after radiative corrections. This prediction strongly motivated the investigations at LEP and supports future searches.

1. The CP-conserving MSSM scenario

Assuming CP invariance, the spectrum of MSSM Higgs bosons consists of two CP-even neutral scalars h^0 and H^0 (h^0 is defined to be the lighter of the two), one CP-odd neutral scalar A^0, and one pair of charged Higgs bosons $H^{\pm}$. At tree level, two parameters are required (beyond known parameters of the SM fermion and gauge sectors) to fix all Higgs boson masses and couplings. A convenient choice is the mass m_{A^0} of the CP-odd scalar A^0 and the ratio $\tan\beta = v_2/v_1$ of the vacuum expectation values associated to the neutral components of the two Higgs fields (v_2 and v_1 couple to up and down fermions, respectively). Often the mixing angle α is used, which diagonalizes the CP-even Higgs mass matrix (α can also be expressed in terms of m_{A^0} and $\tan\beta$).

The following ordering of masses is valid at tree level: $m_{h^0} < (M_Z,\ m_{A^0}) < m_{H^0}$ and $M_W < m_{H^{\pm}}$. These relations are modified by radiative corrections [32,33], with the largest contribution arising from the incomplete cancelation between top and scalar-top (stop) loops. The corrections affect mainly the masses in the neutral Higgs sector; they depend strongly on the top quark mass ($\sim m_t^4$), and logarithmically on the scalar-top (stop) masses. Furthermore, they involve a detailed parametrization of soft SUSY breaking and the mixing between the SUSY partners of left- and right-handed top quarks (stop mixing).

Production of neutral MSSM Higgs bosons

In e^+e^- collisions, the main production mechanisms of the neutral MSSM Higgs bosons are the Higgs-strahlung processes $e^+e^- \to h^0Z^0$, H^0Z^0 and the pair production processes $e^+e^- \to h^0A^0$, H^0A^0. Fusion processes play a marginal role at LEP energies. The cross sections for these processes can be expressed in terms of the SM Higgs boson cross section $\sigma_{HZ}^{\rm SM}$ and the parameters α and β introduced before. For the light CP-even Higgs boson h^0 the following expressions hold

$$\sigma_{\mathrm{h}^0 Z^0} = \sin^2(\beta-\alpha)\ \sigma_{HZ}^{\rm SM} \tag{1}$$

$$\sigma_{\mathrm{h}^0 A^0} = \cos^2(\beta-\alpha)\overline{\lambda}\ \sigma_{HZ}^{\rm SM} \tag{2}$$

with the kinematic factor

$$\overline{\lambda} = \lambda_{A^0\mathrm{h}^0}^{3/2} / \left[\lambda_{Z^0\mathrm{h}^0}^{1/2}(12M_Z^2/s + \lambda_{Z^0\mathrm{h}^0})\right] \tag{3}$$

and $\lambda_{ij} = [1-(m_i+m_j)^2/s][1-(m_i-m_j)^2/s]$. These Higgs-strahlung and pair production cross sections are complementary, obeying the sum rule $\sin^2(\beta-\alpha)+\cos^2(\beta-\alpha) = 1$. Typically, the process $e^+e^- \to h^0Z^0$ is more abundant at small $\tan\beta$ and $e^+e^- \to h^0A^0$ at large $\tan\beta$, unless the latter is suppressed by the kinematic factor $\overline{\lambda}$. The cross sections for the heavy scalar boson H^0 are obtained by interchanging $\sin^2(\beta-\alpha)$ by $\cos^2(\beta-\alpha)$ in Eqs. 1 and 2, and replacing the index h^0 by H^0 in Eq. 3.

At the Tevatron, and over most of the MSSM parameter space, one of the CP-even neutral Higgs bosons (h^0 or H^0) couples to the vector bosons with SM-like strength. The associated production $p\overline{p} \to (h^0 \text{ or } H^0)V$ (with $V \equiv W^{\pm}$, Z^0), and the Yukawa process $p\overline{p} \to h^0 b\overline{b}$ are the most promising search mechanisms. The gluon fusion processes $gg \to h^0$, H^0, A^0 have the highest cross section, but in these cases, only the Higgs to $\tau^+\tau^-$ decay mode is promising, since the $b\overline{b}$ decay mode is overwhelmed by QCD background.

Decay properties of neutral MSSM Higgs bosons

In the MSSM, the couplings of the neutral Higgs bosons to quarks, leptons, and gauge bosons are modified with respect to the SM couplings by factors which depend upon the angles α and β. These factors, valid at tree level, are summarized in Table 1.

Table 1: Factors relating the MSSM Higgs couplings to the couplings in the SM.

	“Up” fermions	“Down” fermions	Vector bosons
SM-Higgs:	1	1	1
MSSM h^0:	$\cos\alpha/\sin\beta$	$-\sin\alpha/\cos\beta$	$\sin(\beta-\alpha)$
H^0:	$\sin\alpha/\sin\beta$	$\cos\alpha/\cos\beta$	$\cos(\beta-\alpha)$
A^0:	$1/\tan\beta$	$\tan\beta$	0

The following decay features are relevant to the MSSM. The h^0 boson will decay mainly to fermion pairs, since the mass is smaller than about 130 GeV. The A^0 boson also decays predominantly to fermion pairs, independently of its mass, since its coupling to vector bosons is zero at leading order (see Table 1). For $\tan\beta > 1$, decays of h^0 and A^0 to $b\overline{b}$ and $\tau^+\tau^-$ pairs are preferred, with branching ratios of about 90% and 8%, while the decays to $c\overline{c}$ and gluon pairs are suppressed. Decays to $c\overline{c}$ may become important for $\tan\beta < 1$. The decay $h^0 \to A^0A^0$ may be dominant if it is kinematically allowed. Other decays could imply SUSY particles such as sfermions, charginos, or invisible neutralinos, thus requiring special search strategies.

Searches for neutral Higgs bosons (CPC scenario)

The searches at LEP address the Higgs-strahlung process $e^+e^- \to h^0Z^0$ and the pair production process $e^+e^- \to h^0A^0$, and exploit the complementarity of the two cross sections. The results for h^0Z^0 are obtained by re-interpreting the SM Higgs searches, taking into account the MSSM reduction factor $\sin^2(\beta-\alpha)$. Those for h^0A^0 are obtained from specific searches for $(b\overline{b})(b\overline{b})$ and $(\tau^+\tau^-)(q\overline{q})$ final states.

The search results are interpreted in a constrained MSSM model where universal soft SUSY breaking masses, $M_{\rm SUSY}$ and M_2, are assumed for the electroweak scale for sfermions and SU(2)×U(1) gauginos, respectively. Besides the tree-level parameters m_{A^0} and $\tan\beta$, the Higgs mixing parameter μ and trilinear Higgs-fermion coupling A_t also enter at the loop level. Most results assume a top quark mass of 174.3 GeV [34]. Furthermore, the gluino mass, entering at the two-loop level, is fixed at 800 GeV. The widths of the Higgs bosons are taken to be small compared to the experimental mass resolution, which is a valid assumption for $\tan\beta$ less than about 50.

Most interpretations are limited to specific "benchmark" scenarios [33], where some of the parameters have fixed values: $M_{\rm SUSY} = 1$ TeV, $M_2 = 200$ GeV, and $\mu = -200$ GeV. In the *no-mixing* benchmark scenario, stop mixing is put to zero by choosing $X_t \equiv A_t - \mu\cot\beta = 0$, while in the m_{h^0}-*max* benchmark scenario, $X_t = 2M_{\rm SUSY}$ is chosen. The m_{h^0}-*max* scenario is designed to maximize the allowed parameter space in the (m_{h^0}, $\tan\beta$) projection, and therefore yields the most conservative exclusion limits.

The limits from the four LEP experiments are described in Refs. [23,35,36]. Preliminary combined LEP limits [37] are shown in Fig. 3 for the m_{h^0}-*max* scenario (in the *no mixing* scenario, the unexcluded region is much smaller). The current 95% CL mass bounds are: m_{h^0} >91.0 GeV, m_{A^0} >91.9 GeV. Furthermore, values of $\tan\beta$ from 0.5 to 2.4 are excluded, but this exclusion can be smaller if, for example, the top mass turns out to be higher than assumed, or if $\mathcal{O}(\alpha_t^2 m_t^2)$ corrections to $(m_{h^0})^2$ are included in the model calculation.

The neutral Higgs bosons may also be produced by Yukawa processes $e^+e^- \to f\overline{f}\phi$ with $\phi \equiv h^0$, H^0, A^0, where the Higgs particles are radiated off a massive fermion ($f \equiv b$ or $\tau^\pm$). These processes can be dominant where the "standard" processes, $e^+e^- \to h^0Z^0$ and h^0A^0, are suppressed. The corresponding enhancement factors (ratios of the $f\overline{f}h^0$ and $f\overline{f}A^0$ couplings to the SM $f\overline{f}H^0$ coupling) are $\sin\alpha/\cos\beta$ and $\tan\beta$, respectively. The LEP data have been analyzed searching specifically for $b\overline{b}b\overline{b}$, $b\overline{b}\tau^+\tau^-$, and $\tau^+\tau^-\tau^+\tau^-$ final states [38]. Regions of low mass and high enhancement factors are excluded by these searches. The CDF collaboration has searched for the Yukawa process $p\overline{p} \to b\overline{b}\ \phi \to b\overline{b}b\overline{b}$ [39]; the domains excluded, at large $\tan\beta$, are indicated in Fig. 3 along with the limits from LEP.

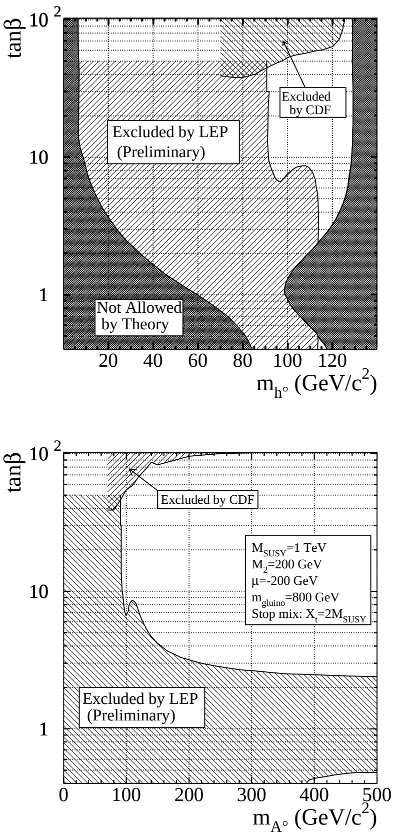

Figure 3: The 95% CL bounds on m_{h^0}, m_{A^0} and $\tan\beta$ for the m_{h^0}-*max* benchmark scenario, from LEP [37]. The exclusions at large $\tan\beta$ from CDF [39] are also indicated.

2. The CP-violating MSSM scenario

Within the SM, the size of CP violation is insufficient to drive the cosmological baryon asymmetry. In the MSSM, however, while the Higgs potential is invariant under the CP transformation at tree level, CP symmetry could be broken substantially by radiative corrections, especially by contributions from third generation scalar-quarks [31]. Such a scenario has recently been investigated by the OPAL Collaboration [36].

In the CPV MSSM scenario, the three neutral Higgs eigenstates H_i $(i = 1,2,3)$ do not have well defined CP quantum numbers; each of them can thus be produced by Higgs-strahlung, $e^+e^- \to H_iZ^0$, and in pairs, $e^+e^- \to H_iH_j$ $(i \neq j)$. For wide ranges of the model parameters, the lightest neutral Higgs boson H_1 has a predicted mass that is accessible at LEP, but it may decouple from the Z^0 boson. On the other hand, the second- and third-lightest Higgs bosons H_2 and H_3 may be either out of reach, or may also have small cross sections. Thus, the searches in the CPV MSSM scenario are experimentally more challenging than in the CPC scenario.

The cross section for the Higgs-strahlung and pair production processes are given by [31]

$$\sigma_{H_iZ^0} = g^2_{H_iZZ}\ \sigma^{\rm SM}_{HZ} \tag{4}$$

$$\sigma_{H_iH_j} = g^2_{H_iH_jZ}\ \overline{\lambda}\ \sigma^{\rm SM}_{HZ} \tag{5}$$

(in the expression of $\overline{\lambda}$, Eq. 3, the indices h^0 and A^0 have to be replaced by H_1 and H_2). The couplings

$$g_{H_iZZ} = \cos\beta\mathcal{O}_{1i} + \sin\beta\mathcal{O}_{2i} \tag{6}$$

$$\begin{aligned} g_{H_iH_jZ} = {} & \mathcal{O}_{3i}(\cos\beta\mathcal{O}_{2j} - \sin\beta\mathcal{O}_{1j}) \\ & - \mathcal{O}_{3j}(\cos\beta\mathcal{O}_{2i} - \sin\beta\mathcal{O}_{1i}) \end{aligned} \tag{7}$$

obey sum rules which, similarly to the CPC case, express the complementarity of the two cross sections. The orthogonal matrix $\mathcal{O}_{ij}$ $(i,j = 1,2,3)$ relating the weak CP eigenstates to the mass eigenstates has non-zero off-diagonal elements,

$$\mathcal{M}^2_{ij} \sim m_t^4 \cdot {\rm Im}(\mu A_t)/M^2_{\rm SUSY}\ ; \tag{8}$$

their size is a measure for CP-violating effects in the production processes.

Regarding the decay properties, the lightest mass eigenstate, H_1, predominantly decays to $b\overline{b}$ if kinematically allowed, with only a small fraction decaying to $\tau^+\tau^-$. The second-lightest Higgs boson, H_2, decays predominantly to H_1H_1 when kinematically allowed, otherwise preferentially to $b\overline{b}$.

The OPAL search [36] is performed for a number of variants of the CPX benchmark scenario [40], where the parameters are chosen in such a way as to maximize the off-diagonal elements $\mathcal{M}^2_{ij}$, and thereby enhance the phenomenological differences with respect to the CPC scenario. This is obtained typically for small $M_{\rm SUSY}$ (*e.g.*, 500 GeV) and large μ (up to 4 TeV), and when the CPV phases related to $A_{t,b}$ and $m_{\widetilde{g}}$ are put to their maximal values. The precise choice of the top quark mass is also an issue. Figure 4 shows the preliminary OPAL exclusions in the $(m_{H_1}, \tan\beta)$ plane [36]. Values of $\tan\beta$ less than about 3 are excluded at the 95% CL, but no absolute limit can be set today for the mass of H_1 .

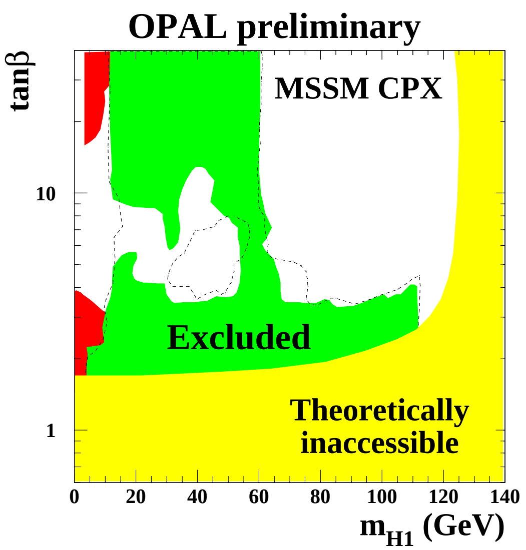

Figure 4: The 95% CL bounds on m_{H_1} and $\tan\beta$ in the CPX MSSM scenario with μ = 2 TeV and $M_{\rm SUSY}$ = 500 GeV, from a preliminary OPAL analysis [36]. The shaded areas are excluded either by the model or by the experiment. The areas delimited by the dashed lines are expected to be excluded on the basis of Monte Carlo simulations. The top mass is fixed to 174.3 GeV. See full-color version on color pages at end of book.

IV. Charged Higgs bosons

Charged Higgs bosons are predicted in models with two Higgs field doublets (2HDM), thus also in the MSSM [4,5]. While in the MSSM, the mass of the charged Higgs boson is restricted essentially to $m_{H^{\pm}} > M_W$, such a restriction does not exist in the general 2HDM case. The searches conducted at LEP and at the Tevatron are, therefore, interpreted primarily in the general 2HDM framework.

Searches for charged Higgs bosons at LEP

In e^+e^- collisions, charged Higgs bosons are expected to be pair-produced via s-channel exchange of a photon or a Z^0 boson [5,19]. In the 2HDM framework, the couplings are specified by the electric charge and the weak mixing angle θ_W, and the cross section only depends on the mass $m_{H^{\pm}}$ at tree level. Charged Higgs bosons decay preferentially to heavy particles, but the precise branching ratios are model dependent. In 2HDM of "type 2,"* and for masses which are accessible at LEP energies, the decays $H^+ \to c\overline{s}$ and $\tau^+\nu$ dominate. The final states $H^+H^- \to (c\overline{s})(\overline{c}s)$, $(\tau^+\nu_\tau)(\tau^-\overline{\nu}_\tau)$, and $(c\overline{s})(\tau^-\overline{\nu}_\tau)$+$(\overline{c}s)(\tau^+\nu_\tau)$ are therefore considered, and the results are presented with the $H^+ \to \tau^+\nu$ decay branching ratio as a free parameter.

At LEP2 energies, the background process $e^+e^- \to W^+W^-$ constrains the search sensitivity essentially to $m_{H^{\pm}}$ less than M_W. The searches of the four LEP experiments are described in Ref. 41. A preliminary combination [42] resulted in a general 2HDM ("type 2") bound of $m_{H^{\pm}}$ >78.6 GeV (95% CL), which is valid for arbitrary $H^+ \to \tau^+\nu$ branching ratio.

In the 2HDM of "type 1" [43], and if the CP-odd neutral Higgs boson A^0 is light (which is not excluded in the general 2HDM case), the decay $H^{\pm} \to W^{(\pm *)}A^0$ may be predominant for masses of interest at LEP. To cover this eventuality, the search of the DELPHI Collaboration is extended to this decay mode [44].

Searches for charged Higgs bosons at the Tevatron

In $p\overline{p}$ collisions at Tevatron energies, charged Higgs bosons with mass less than $m_t - m_b$ can be produced in the decay of the top quark. The decay $t \to bH^+$ would then compete with the SM process $t \to bW^+$, and the relative rate would depend on the value of $\tan\beta$. In the 2HDM of "type 2," the decay to charged Higgs bosons could have a detectable rate for $\tan\beta$ larger than 30, or for $\tan\beta$ less than one.

The DØ Collaboration adopted an indirect "disappearance technique" optimized for the detection of $t \to bW^+$, and a direct search for $t \to bH^+ \to b\tau^+\nu_\tau$ [45]. The CDF Collaboration also reported an indirect approach [46], in which the rate of dileptons and lepton+jets in top quark decays was compared to the SM prediction, and on a direct search for $t \to bH^+$ [47]. The results

* In the 2HDM of "type 2," the two Higgs fields couple separately to "up" and "down" type fermions; in the 2HDM of "type 1," one field couples to all fermions while the other field is decoupled.

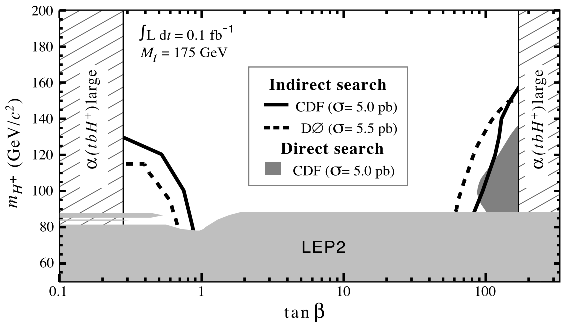

Figure 5: Summary of the 95% CL exclusions in the $(m_{H^+}, \tan\beta)$ plane from DØ [45] and CDF [47], using various indirect and direct observation techniques (the regions below the curves are excluded). The two experiments use slightly different theoretical $t\bar{t}$ cross sections, as indicated. The shaded domains at extreme values of $\tan\beta$ are not considered in these searches, since there the tbH^+ coupling becomes large and perturbative calculations do not apply. The dark region labeled LEP2 is excluded by LEP [42]. See full-color version on color pages at end of book.

from the Tevatron are summarized in Fig. 5, together with the exclusion obtained at LEP. The Tevatron limits are subject to potentially large theoretical uncertainties [48].

Indirect limits in the $(m_{H^\pm}, \tan\beta)$ plane can be derived by comparing the measured rate of the flavor-changing neutral-current process $b \rightarrow s\gamma$ to the SM prediction. In the SM, this process is mediated by virtual W exchange [49], while in the 2HDM of "type 2," the branching ratio is altered by contributions from the exchange of charged Higgs bosons [50]. The current experimental value, obtained from combining the measurements of CLEO, BELLE, and ALEPH [51], is in agreement with the SM prediction. From the comparison, the bound $m_{H^\pm} >$316 GeV (95% CL) is obtained, which is much stronger than the current bounds from direct searches. However, these indirect bounds may be invalidated by anomalous couplings or, in SUSY models, by sparticle loops.

Doubly-charged Higgs bosons

Higgs bosons with double electric charge, $H^{\pm\pm}$, are predicted, for example, by models with additional triplet scalar fields or left-right symmetric models [5,52]. It has been emphasized that the see-saw mechanism could lead to doubly-charged Higgs bosons with masses accessible to current and future colliders [53]. Searches were performed at LEP for the pair-production process $Z^0 \rightarrow H^{++}H^{--}$ with four prompt leptons in the final state [54–56]. Lower mass bounds between 95 GeV and 100 GeV were obtained for left-right symmetric models (the exact limits depend on the lepton flavors). Doubly-charged Higgs bosons were also searched in single production [57]. Furthermore, if such particles existed, they would affect the Bhabha scattering cross-section and forward-backward asymmetry via t-channel exchange. The absence of a significant deviation from the SM prediction puts constraints on the Yukawa coupling of $H^{\pm\pm}$ to electrons for Higgs masses which reach into the TeV range [56,57].

V. Model extensions

The addition of a singlet scalar field to the CP-conserving MSSM [58] gives rise to two additional neutral scalars, one CP-even and one CP-odd. The radiative corrections to the masses are similar to those in the MSSM, and arguments of perturbative continuation to the GUT scale lead to an upper bound of about 135-140 GeV for the mass of the lightest neutral CP-even scalar. DELPHI has reinterpreted their searches for neutral Higgs bosons to constrain such models [59].

Decays into invisible (weakly interacting neutral) particles may occur, for example in the MSSM, if the Higgs bosons decay to pairs of neutralinos. In a different context, Higgs bosons might also decay into pairs of massless Goldstone bosons or Majorons [60]. In the process $e^+e^- \rightarrow h^0Z^0$, the mass of the invisible Higgs boson can be inferred from the reconstructed Z^0 boson using the beam energy constraint. Results from the LEP experiments can be found in Refs. [23,61]. Some LEP results have recently been combined and yield a 95% CL lower bound of 114.4 GeV for the mass of a Higgs boson with SM production rate, and decaying exclusively into invisible final states [62].

Most of the searches for the processes $e^+e^- \rightarrow h^0Z^0$ and h^0A^0, which have been discussed in the context of the CPC MSSM, rely on the experimental signature of Higgs bosons decaying into $b\bar{b}$. However, in the general 2HDM case, decays to non-$b\bar{b}$ final states may be strongly enhanced. Recently flavor-independent searches have been reported at LEP which do not require b tagging [63], and a preliminary combination has been performed [64]. In conjunction with the b-flavor sensitive searches, large domains of the general 2HDM parameter space of "type 2" could be excluded [65].

Photonic final states from the processes $e^+e^- \rightarrow Z^0\,/\gamma^* \rightarrow H^0\gamma$ and $H^0 \rightarrow \gamma\gamma$, do not occur in the SM at tree level, but may have a low rate due to $W^\pm$ and top quark loops [66]. Additional loops, for example, from SUSY particles, would increase the rates only slightly [67], but models with anomalous couplings predict enhancements by orders of magnitude. Searches for the processes $e^+e^- \rightarrow (H^0 \rightarrow b\bar{b})\gamma$, $(H^0 \rightarrow \gamma\gamma)q\bar{q}$, and $(H^0 \rightarrow \gamma\gamma)\gamma$ have been used to set model-independent limits on such anomalous couplings, and to constrain the very specific "fermiophobic" 2HDM of "type 1" [68], which also predicts an enhanced $h^0 \rightarrow \gamma\gamma$ rate. The LEP searches are described in Ref. 69. In a preliminary combination [70], a fermiophobic Higgs boson with mass less than 108.2 GeV (95% CL) has been excluded. Limits of about 80 GeV are obtained at the Tevatron [71]. Along with the photonic decay, the 2HDM of "type 1" also predicts an enhanced rate for the decays $h^0 \rightarrow W^*W$ and $Z^{0*}Z^0$. This possibility has been addressed by the L3 Collaboration [72].

The OPAL Collaboration has performed a decay-mode independent search for the Bjorken process $e^+e^- \rightarrow \ S^0 Z^0$ [73], where S^0 denotes a generic scalar particle. The search is based on studies of the recoil mass spectrum in events with $Z^0 \rightarrow e^+e^-$ and $Z^0 \rightarrow \mu^+\mu^-$ decays, and on the final states $(Z^0 \rightarrow \nu\overline{\nu})(S^0 \rightarrow e^+e^-$ or photons), and produces upper bounds for the cross section for a broad range of S^0 masses between 10^{-6} GeV to 100 GeV.

VI. Prospects

The LEP collider stopped producing data in November 2000. At the Tevatron, Run II started in 2001. Performance studies suggest [8] that collecting data samples in excess of 2 fb^{-1} per experiment would extend the combined sensitivity of CDF and DØ beyond the LEP reach; with 4 fb^{-1} (9 fb^{-1}) per experiment, the Tevatron should be able to exclude (detect at the 3σ level) the Higgs boson up to about 130 GeV mass. Such data samples would also provide sensitivity to MSSM Higgs bosons in large domains of the parameter space.

The Large Hadron Collider (LHC) should deliver proton-proton collisions at 14 TeV in the year 2007. The ATLAS and CMS detectors have been optimized for Higgs boson searches [9]. The discovery of the SM Higgs boson will be possible over the mass range between about 100 GeV and 1 TeV. This broad range is covered by a variety of production and decay processes. The LHC experiments will provide full coverage of the MSSM parameter space by direct searches for the h^0, H^0, A^0, and $H^{\pm}$ bosons, and by detecting the h^0 boson in cascade decays of SUSY particles. The discovery of several of the Higgs bosons is possible over extended domains of the parameter space. Decay branching fractions can be determined and masses measured with statistical accuracies between 10^{-3} (at 400 GeV mass) and 10^{-2} (at 700 GeV mass).

A high-energy e^+e^- linear collider could be realized after the year 2010, running initially at energies up to 500 GeV and at 1 TeV or more at a later stage [11]. One of the prime goals would be to extend the precision measurements, which are typical of e^+e^- colliders, to the Higgs sector. At such a collider the Higgs couplings to fermions and vector bosons can be measured with precisions of a few percent. The MSSM parameters can be studied in great detail. At the highest collider energies and luminosities, the self-coupling of the Higgs fields can be studied directly through final states with two Higgs bosons [74]. At a future $\mu^+\mu^-$ collider, the Higgs bosons can be generated as s-channel resonances [12]. Mass measurements with precisions of a few MeV would be possible and the widths could be obtained directly from Breit-Wigner scans. The heavy CP-even and CP-odd bosons, H^0 and A^0, degenerate over most of the MSSM parameter space, could be disentangled experimentally.

Models are emerging which propose solutions to the electroweak scale hierarchy problem without introducing SUSY. The "little Higgs model" [75] proposes an additional set of heavy gauge bosons with Higgs-gauge couplings tuned in such a way that the quadratic divergences induced by the SM gauge boson loops are cancelled. Among the strong signatures of this model, there are the new gauge bosons, but there is also a doubly charged Higgs boson with mass in the TeV range, decaying to W^+W^+. These predictions can be tested at future colliders. Alternatively, models with extra space dimensions [76] propose a natural way for avoiding the scale hierarchy problem. In this class of models, the Planck scale looses its fundamental character and becomes merely an effective scale in 3-dimensional space. The model predicts a light Higgs-like particle, the radion, which differs from the Higgs boson in that it couples more strongly to gluons. A first search for the radion in LEP data, conducted by OPAL, gave negative results [77].

Finally, if Higgs bosons are not discovered at the TeV scale, both the LHC and the future lepton colliders will be in a position to test alternative theories of electroweak symmetry breaking, such as those with strongly interacting vector bosons [78] expected in theories with dynamical symmetry breaking [79].

References

1. S.L. Glashow, Nucl. Phys. **20**, 579 (1961);
S. Weinberg, Phys. Rev. Lett. **19**, 1264 (1967);
A. Salam, *Elementary Particle Theory*, eds.: N. Svartholm, Almquist, and Wiksells, Stockholm, 1968;
S. Glashow, J. Iliopoulos, and L. Maiani, Phys. Rev. **D2**, 1285 (1970).
2. P.W. Higgs, Phys. Rev. Lett. **12**, 132 (1964);
idem Phys. Rev. **145**, 1156 (1966);
F. Englert and R. Brout, Phys. Rev. Lett. **13**, 321 (1964);
G.S. Guralnik, C.R. Hagen, and T.W. Kibble, Phys. Rev. Lett. **13**, 585 (1964).
3. J. Wess and B. Zumino, Nucl. Phys. **B70**, 39 (1974);
idem, Phys. Lett. **49B**, 52 (1974);
P. Fayet, Phys. Lett. **69B**, 489 (1977);
ibid. **84B**, 421 (1979), *ibid.* **86B**, 272 (1979).
4. H.E. Haber and G.L. Kane, Phys. Rev. **C117**, 75 (1985).
5. J.F. Gunion, H.E. Haber, G.L. Kane, and S. Dawson, *The Higgs Hunter's Guide* (Addison-Wesley) 1990.
6. H.E. Haber and M. Schmitt, *Supersymmetry*, in this volume.
7. P.J. Franzini and P. Taxil, in *Z physics at LEP 1*, CERN 89-08 (1989).
8. *Results of the Tevatron Higgs Sensitivity Study,* `http://www-d0.fnal.gov/Run2Physics/Higgs_sensitivity_study.html`.
9. ATLAS TDR on Physics performance, Vol. II, Chap. 19, *Higgs Bosons* (1999);
CMS TP, CERN/LHC 94-38 (1994).
10. E. Accomando *et al.*, Physics Reports **299**, 1–78 (1998).
11. J.A. Aguilar-Saavedra *et al.*, TESLA Technical Design Report, Part III: *Physics at an e^+e^- Linear Collider*, `hep-ph/0106315`;
T. Abe *et al.*, SLAC-R-570 (2001), `hep-ph/0109166`;
M. Battaglia, `hep-ph/0103338`.
12. B. Autin, A. Blondel, and J. Ellis (eds.), CERN 99-02;
C.M. Ankenbrandt *et al.*, Phys. Rev. ST Acc. Beams **2**, 081001 (1999).
13. N. Cabibbo *et al.*, Nucl. Phys. **B158**, 295 (1979);

T. Hambye and K. Riesselmann, Phys. Rev. **D55**, 7255 (1997);
G. Isidori, G. Ridolfi, and A. Strumia, Nucl. Phys. **B609**, 387 (2001).

14. LEP Electroweak Working Group, status of July 2003, `http://lepewwg.web.cern.ch/LEPEWWG/`.
15. J. Ellis, M.K. Gaillard, and D.V. Nanopoulos, Nucl. Phys. **B106**, 292 (1976);
B.L. Ioffe and V.A. Khoze, Sov. J. Nucl. Phys. **9**, 50 (1978).
16. E. Gross, B.A. Kniehl, and G. Wolf, Z. Phys. **C63**, 417 (1994); Erratum: *ibid.* **C66**, 32 (1995).
17. D.R.T. Jones and S.T. Petcov, Phys. Lett. **84B**, 440 (1979);
R.N. Cahn and S. Dawson, Phys. Lett. **136B**, 96 (1984); *ibid.* **138B**, 464 (1984);
W. Kilian, M. Krämer, and P.M. Zerwas, Phys. Lett. **B373**, 135 (1996).
18. S.L. Glashow, D.V. Nanopoulos, and A. Yildiz, Phys. Rev. **D18**, 1724 (1978);
A. Stange, W. Marciano, and S. Willenbrock, Phys. Rev. **D49**, 1354 (1994); *ibid.* **D50**, 4491 (1994).
19. A. Djouadi, M. Spira, and P.M. Zerwas, Z. Phys. **C70**, 675 (1996).
20. P. Janot, *Searching for Higgs Bosons at LEP 1 and LEP 2*, in Perspectives in Higgs Physics II, World Scientific, ed. G.L. Kane (1998).
21. K. Hagiwara *et al.*, Phys. Rev. **D66**, 010001-1 (2002), Review No. 31 on *Statistics*, p. 229.
22. ALEPH, DELPHI, L3, OPAL, The LEP Working Group for Higgs Boson Searches, CERN-EP/2000-055.
23. ALEPH Collab., Phys. Lett. **B526**, 191 (2002).
24. DELPHI Collab., CERN-EP/2003-008, to be published in Eur. Phys. J. **C**.
25. L3 Collab., Phys. Lett. **B517**, 319 (2001).
26. OPAL Collab., Eur. Phys. J. **C26**, 479 (2003).
27. ALEPH, DELPHI, L3, OPAL, The LEP Working Group for Higgs Boson Searches, Phys. Lett. **B565**, 61 (2003).
28. CDF Collab., Phys. Rev. Lett. **79**, 3819 (1997);
ibid, **81**, 5748 (1998).
29. M. Schmitt, *Higgs and Susy Searches*, Lepton Photon Conference 2003,
`http://conferences.fnal.gov/lp2003/program/index.html`.
30. A. D. Sakharov, JETP Lett. **5**, 24 (1967).
31. M. Carena *et al.*, Nucl. Phys. **B599**, 158 (2001).
32. Y. Okada, M. Yamaguchi, and T. Yanagida, Theor. Phys. **85**, 1 (1991);
H. Haber and R. Hempfling, Phys. Rev. Lett. **66**, 1815 (1991);
J. Ellis, G. Ridolfi, and F. Zwirner, Phys. Lett. **B257**, 83 (1991);
M. Carena, M. Quiros, and C.E.M. Wagner, Nucl. Phys. **B461**, 407 (1996);
S. Heinemeyer, W. Hollik, and G. Weiglein, Phys. Lett. **B455**, 179 (1999);
idem, Eur. Phys. J. **C9**, 343 (1999);
J. R. Espinosa and R.-J. Zhang, Nucl. Phys. **B586**, 3 (2000);
A. Brignole, G. Degrassi, P. Slavich, and F. Zwirner, `hep-ph/0112177`.
33. M. Carena, S. Heinemeyer, C.E.M. Wagner, and G. Weiglein, `hep-ph/9912223`, *idem*, `hep-ph/0202167`.
34. D.E. Groom *et al.*, Eur. Phys. J. **C15**, 1 (2000).
35. DELPHI Collab., CERN-EP/2003-008;
L3 Collab., Phys. Lett. **B545**, 30 (2002).
36. (*)OPAL Physics Note PN524 (2003).
37. (*)LHWG Note 2001-04.
38. (*)DELPHI 1999-76 CONF-263;
(*)DELPHI 2002-037 CONF-571;
OPAL Collab., Eur. Phys. J. **C23**, 397 (2002).
39. CDF Collab., Phys. Rev. Lett. **86**, 4472 (2001).
40. M. Carena *et al.*, Phys. Lett. **B495**, 155 (2000).
41. ALEPH Collab., Phys. Lett. **B543**, 1 (2002);
DELPHI Collab., Phys. Lett. **B525**, 17 (2002);
L3 Collab., CERN-EP/2003-054;
OPAL Collab., Eur. Phys. J. **C7**, 407 (1999).
42. (*)LHWG Note/2001-05.
43. A. G. Akeroyd *et al.*, Eur. Phys. J. **C20**, 51 (2001).
44. DELPHI Collab., CERN-EP/2003-064.
45. DØ Collab., Phys. Rev. Lett. **82**, 4975 (1999);
idem, **88**, 151803 (2002).
46. CDF Collab., Phys. Rev. **D62**, 012004 (2000).
47. CDF Collab., Phys. Rev. Lett. **79**, 357 (1997).
48. J.A. Coarasa, J. Guasch, J. Solá, and W. Hollik, Phys. Lett. **B442**, 326 (1998);
J.A. Coarasa, J. Guasch, and J. Solá, `hep-ph/9903212`;
F.M. Borzumati and A. Djouadi, `hep-ph/9806301`.
49. P. Gambino and M. Misiak, Nucl. Phys. **B611**, 338 (2001).
50. R. Ellis *et al.*, Phys. Lett. **B179**, 119 (1986);
V. Barger, J. Hewett, and R. Phillips, Phys. Rev. **D41**, 3421 (1990).
51. S. Chen *et al.*, CLEO Collab., `hep-ex/0108032`;
G. Taylor, BELLE Collab., XXXVIth Rencontres de Moriond, March 2001;
ALEPH Collab., Phys. Lett. **B429**, 169 (1998).
52. G.B. Gelmini and M. Roncadelli, Phys. Lett. **B99**, 411 (1981);
R.N. Mohapatra and J.D. Vergados, Phys. Rev. Lett. **47**, 1713 (1981);
V. Barger *et al.*, Phys. Rev. **D26**, 218 (1982).
53. B. Dutta and R.N. Mohapatra, Phys. Rev. **D59**, 015018-1 (1999).
54. OPAL Collab., Phys. Lett. **B295**, 347 (1992);
idem, **B526**, 221 (2002).
55. DELPHI Collab., Phys. Lett. **B552**, 127 (2003).
56. L3 Collab., CERN-EP/2003-060.
57. OPAL Collab., CERN-EP/2003-041.
58. P. Fayet, Nucl. Phys. **B90**, 104 (1975);
S.F. King and P.L. White, Phys. Rev. **D53**, 4049 (1996).
59. (*)DELPHI 1999-97 CONF 284.
60. Y. Chikashige, R.N. Mohapatra, and P.D. Peccei, Phys. Lett. **98B**, 265 (1981);
A.S. Joshipura and S.D. Rindani, Phys. Rev. Lett. **69**, 3269 (1992);
F. de Campos *et al.*, Phys. Rev. **D55**, 1316 (1997).
61. ALEPH Collab., Phys. Lett. **B526**, 191 (2002);
DELPHI Collab., CERN-EP/2003-046;
(*)L3 Note 2690 (2001);
OPAL Collab., Phys. Lett. **B377**, 273 (1996).
62. (*)LHWG-Note/2001-06.

63. ALEPH Collab., Phys. Lett. **B544**, 25 (2002);
(*)DELPHI 2001-070 CONF 498;
(*)DELPHI 2003-005 CONF 628;
(*)L3 Note 2806 (2003);
(*)OPAL Physics Note 525 (2003).
64. (*)LHWG Note 2001-07.
65. OPAL Collab., Eur. Phys. J. **C18**, 425 (2001);
(*)OPAL Physics Note 475 (2001);
(*)DELPHI 2001-068 CONF 496.
66. J. Ellis, M.K. Gaillard, and D.V. Nanopoulos, Nucl. Phys. **B106**, 292 (1976);
A. Abbasabadi *et al.*, Phys. Rev. **D52**, 3919 (1995);
R.N. Cahn, M.S. Chanowitz, and N. Fleishon, Phys. Lett. **B82**, 113 (1997).
67. G. Gamberini, G.F. Giudice, and G. Ridolfi, Nucl. Phys. **B292**, 237 (1987);
R. Bates, J.N. Ng, and P. Kalyniak, Phys. Rev. **D34**, 172 (1986);
K. Hagiwara, R. Szalapski, and D. Zeppenfeld, Phys. Lett. **B318**, 155 (1993);
O.J.P. Éboli *et al.*, Phys. Lett. **B434**, 340 (1998).
68. A. G. Akeroyd, Phys. Lett. **B368**, 89 (1996);
H.Haber, G. Kane, and T. Stirling, Nucl. Phys. **B161**, 493 (1979).
69. ALEPH Collab., Phys. Lett. **B544**, 16 (2002);
(*)DELPHI 2003-004 CONF 627;
L3 Collab., Phys. Lett. **B534**, 28 (2002);
OPAL Collab., Phys. Lett. **B544**, 44 (2002).
70. (*)LHWG Note/2002-02.
71. DØ Collab., Phys. Rev. Lett. **82**, 2244 (1999);
CDF Collab., Phys. Rev. **D64**, 092002 (2001).
72. L3 Collab., CERN-EP/2002-080.
73. OPAL Collab., CERN-EP/2002-032.
74. G.J. Gounaris, F. Renard, and D. Schildknecht, Phys. Lett. **B83**, 191 (1979);
V. Barger, T. Han, and R.J.N. Phillips, Phys. Rev. **D38**, 2766 (1988);
F. Boudjema and E. Chopin, Z. Phys. **C37**, 85 (1996);
A. Djouadi *et al.*, Eur. Phys. J. **C10**, 27 (1999).
75. N. Arkani-Hamed *et al.*, Phys. Lett. **B513**, 232 (2001);
I. Low *et al.*, Phys. Rev. **D66**, 072001 (2002);
M. Schmaltz, hep-ph/0210415;
T. Han *et al.*, hep-ph/0301040.
76. L. Randall and R. Sundrum, Phys. Rev. Lett. **83**, 3370 (1999);
idem **84**, 4690 (1999);
G.F. Giudice, R. Rattazzi, and J.D. Wells, Nucl. Phys. **B544**, 3 (1999);
C. Csáki, M.L. Graesser, and G.D. Kribs, Phys. Rev. **D63**, 065002 (2001).
77. (*)OPAL Physics-Note 526 (2003).
78. B.W. Lee, C. Quigg, and H.B. Thacker, Phys. Rev. **D16**, 1519 (1977);
R.S. Chivukula *et al.*, hep-ph/9503202;
C. Yuan, hep-ph/9712513;
M. Chanowitz, hep-ph/9812215.
79. S. Weinberg, Phys. Rev. **D13**, 974 (1976); *ibid.* **D19**, 1277 (1979);
L. Susskind, Phys. Rev. **D20**, 2619 (1979).

STANDARD MODEL H^0 (Higgs Boson) MASS LIMITS

These limits apply to the Higgs boson of the three-generation Standard Model with the minimal Higgs sector. For a review and a bibliography, see the above Note on 'Searches for Higgs Bosons' by P. Igo-Kemenes.

Limits from Coupling to $Z/W^\pm$

Limits on the Standard Model Higgs obtained from the study of Z^0 decays rule out conclusively its existence in the whole mass region $m_{H^0} \lesssim 60$ GeV. These limits, as well as stronger limits obtained from e^+e^- collisions at LEP at energies up to 202 GeV, and weaker limits obtained from other sources, have been superseded by the most recent data of LEP. They have been removed from this comiplation, and are documented in previous editions of this Review of Particle Physics.

In this Section, unless otherwise stated, limits from the four LEP experiments (ALEPH, DELPHI, L3, and OPAL) are obtained from the study of the $e^+e^- \to H^0 Z$ process, at center-of-mass energies reported in the comment lines.

VALUE (GeV)	*CL%*	*DOCUMENT ID*		*TECN*	*COMMENT*
>114.1	95	[1] ABDALLAH	04	DLPH	$E_{cm} \leq 209$ GeV
>112.7	95	[1] ABBIENDI	03B	OPAL	$E_{cm} \leq 209$ GeV
>114.4	95	[1,2] HEISTER	03D	LEP	$E_{cm} \leq 209$ GeV
>111.5	95	[1,3] HEISTER	02	ALEP	$E_{cm} \leq 209$ GeV
>112.0	95	[1] ACHARD	01C	L3	$E_{cm} \leq 209$ GeV
• • • We do not use the following data for averages, fits, limits, etc. • • •					
		[4] ABAZOV	01E	D0	$p\overline{p} \to H^0 WX$, $H^0 ZX$
		[5] ABE	98T	CDF	$p\overline{p} \to H^0 WX$, $H^0 ZX$

[1] Search for $e^+e^- \to H^0 Z$ in the final states $H^0 \to b\overline{b}$ with $Z \to \ell\overline{\ell}$, $\nu\overline{\nu}$, $q\overline{q}$, $\tau^+\tau^-$ and $H^0 \to \tau^+\tau^-$ with $Z \to q\overline{q}$.

[2] Combination of the results of all LEP experiments.

[3] A 3σ excess of candidate events compatible with m_{H^0} near 114 GeV is observed in the combined channels $q\overline{q}q\overline{q}$, $q\overline{q}\ell\overline{\ell}$, $q\overline{q}\tau^+\tau^-$.

[4] ABAZOV 01E search for associated $H^0 W$ and $H^0 Z$ production in $p\overline{p}$ collisions at $E_{cm}=$ 1.8 TeV. The limits of $\sigma(H^0 W)\times B(W \to e\nu)\times B(H^0 \to q\overline{q}) < 2.0$ pb (95%CL) and $\sigma(H^0 Z)\times B(Z \to e^+e^-)\times B(H^0 \to q\overline{q}) < 0.8$ pb (95%CL) are given for m_H=115 GeV.

[5] ABE 98T search for associated $H^0 W$ and $H^0 Z$ production in $p\overline{p}$ collisions at $\sqrt{s}=$ 1.8 TeV with $W(Z) \to q\overline{q}^{(\prime)}$, $H^0 \to b\overline{b}$. The results are combined with the search in ABE 97W, resulting in the cross-section limit $\sigma(H^0 + W/Z)\cdot B(H^0 \to b\overline{b})<$(23–17) pb (95%CL) for $m_H=$ 70–140 GeV. This limit is one to two orders of magnitude larger than the expected cross section in the Standard Model.

H^0 Indirect Mass Limits from Electroweak Analysis

For limits obtained before the direct measurement of the top quark mass, see the 1996 (Physical Review **D54** 1 (1996)) Edition of this Review. Other studies based on data available prior to 1996 can be found in the 1998 Edition (The European Physical Journal **C3** 1 (1998)) of this Review. For indirect limits obtained from other considerations of theoretical nature, see the Note on "Searches for Higgs Bosons."

Because of the high current interest, we mention here the following unpublished result (LEP 02,) although we do not include it in the Listings or Tables: $m_H = 81^{+52}_{-33}$ GeV. This is obtained from a fit to LEP, SLD, W mass, top mass, and neutrino scattering data available in the Summer of 2002, with $\Delta\alpha^{(5)}_{had}(m_Z) = 0.0276 \pm 0.0036$. The 95%CL limit is 193 GeV.

VALUE (GeV)	*CL%*	*DOCUMENT ID*		*TECN*	*COMMENT*
• • • We do not use the following data for averages, fits, limits, etc. • • •					
		[6] CHANOWITZ	02	RVUE	
390^{+750}_{-280}		[7] ABBIENDI	01A	OPAL	
		[8] CHANOWITZ	99	RVUE	
<290	95	[9] D'AGOSTINI	99	RVUE	
<211	95	[10] FIELD	99	RVUE	
		[11] CHANOWITZ	98	RVUE	
170^{+150}_{-90}		[12] HAGIWARA	98B	RVUE	
141^{+140}_{-77}		[13] DEBOER	97B	RVUE	
127^{+143}_{-71}		[14] DEGRASSI	97	RVUE	$\sin^2\theta_W$(eff,lept)
158^{+148}_{-84}		[15] DITTMAIER	97	RVUE	
149^{+148}_{-82}		[16] RENTON	97	RVUE	
145^{+164}_{-77}		[17] ELLIS	96C	RVUE	
185^{+251}_{-134}		[18] GURTU	96	RVUE	

[6] CHANOWITZ 02 studies the impact for the prediction of the Higgs mass of two 3σ anomalies in the SM fits to electroweak data. It argues that the Higgs mass limit should not be trusted whether the anomalies originate from new physics or from systematic effects.

[7] ABBIENDI 01A make Standard Model fits to OPAL's measurements of Z-lineshape parameters and lepton forward-backward asymmetries, using m_t=174.3 ± 5.1 GeV and $1/\alpha(m_Z) = 128.90 \pm 0.09$. The fit also yields $\alpha_s(m_Z)$=0.127 ± 0.005. If the external value of $\alpha_s(m_Z)$=0.1184 ± 0.0031 is added to the fit, the result changes to $m_{H^0}=190^{+335}_{-165}$ GeV.

[8] CHANOWITZ 99 studies LEP/SLD data on 9 observables related $\sin^2\theta^\ell_{eff}$, available in the Spring of 1998. A scale factor method is introduced to perform a global fit, in view of the conflicting data. m_H as large as 750 GeV is allowed at 95% CL.

[9] D'AGOSTINI 99 use m_t, m_W, and effective $\sin^2\theta_W$ from LEP/SLD available in the Fall 1998 and combine with direct Higgs search constraints from LEP2 at E_{cm}=183 GeV. $\alpha(m_Z)$ given by DAVIER 98.

[10] FIELD 99 studies the data on b asymmetries from $Z^0 \rightarrow b\overline{b}$ decays at LEP and SLD (from LEP 99). The limit uses $1/\alpha(M_Z)$= 128.90 $\pm$ 0.09, the variation in the fitted top quark mass, m_t=171.2$^{+3.7}_{-3.8}$ GeV, and excludes b-asymmetry data. It is argued that exclusion of these data, which deviate from the Standard Model expectation, from the electroweak fits reduces significantly the upper limit on m_H. Including the b-asymmetry data gives instead the 95%CL limit m_H < 284 GeV. See also FIELD 00.

[11] CHANOWITZ 98 fits LEP and SLD Z-decay-asymmetry data (as reported in ABBANEO 97), and explores the sensitivity of the fit to the weight ascribed to measurements that are individually in significant contradiction with the direct-search limits. Various prescriptions are discussed, and significant variations of the 95%CL Higgs-mass upper limits are found. The Higgs-mass central value varies from 100 to 250 GeV and the 95%CL upper limit from 340 GeV to the TeV scale.

[12] HAGIWARA 98B fit to LEP, SLD, W mass, and neutrino scattering data as reported in ALCARAZ 96, with m_t = 175 $\pm$ 6 GeV, $1/\alpha(m_Z)$= 128.90 $\pm$ 0.09 and $\alpha_s(m_Z)$= 0.118 $\pm$ 0.003. Strong dependence on m_t is found.

[13] DEBOER 97B fit to LEP and SLD data (as reported in ALCARAZ 96), as well as m_W and m_t from CDF/DØ and CLEO $b \rightarrow s\gamma$ data (ALAM 95). $1/\alpha(m_Z)$ = 128.90 $\pm$ 0.09 and $\alpha_s(m_Z)$ = 0.120 $\pm$ 0.003 are used. Exclusion of SLC data yields m_H=241$^{+218}_{-123}$ GeV. $\sin^2\theta_{\rm eff}$ from SLC (0.23061 $\pm$ 0.00047) would give m_H=16$^{+16}_{-9}$ GeV.

[14] DEGRASSI 97 is a two-loop calculation of M_W and $\sin^2\theta^{\rm lept}_{\rm eff}$ as a function of m_H, using $\sin^2\theta^{\rm lept}_{\rm eff}$ 0.23165(24) as reported in ALCARAZ 96, m_t = 175 $\pm$ 6 GeV, and $1/\alpha(m_Z)$=128.90 $\pm$ 0.09.

[15] DITTMAIER 97 fit to m_W and LEP/SLC data as reported in ALCARAZ 96, with m_t = 175 $\pm$ 6 GeV, $1/\alpha(m_Z^2)$ = 128.89 $\pm$ 0.09. Exclusion of the SLD data gives m_H = 261$^{+224}_{-128}$ GeV. Taking only the data on m_t, m_W, $\sin^2\theta^{\rm lept}_{\rm eff}$, and $\Gamma^{\rm lept}_Z$, the authors get m_H = 190$^{+174}_{-102}$ GeV and m_H = 296$^{+243}_{-143}$ GeV, with and without SLD data, respectively. The 95% CL upper limit is given by 550 GeV (800 GeV removing the SLD data).

[16] RENTON 97 fit to LEP and SLD data (as reported in ALCARAZ 96), as well as m_W and m_t from $p\overline{p}$, and low-energy νN data available in early 1997. $1/\alpha(m_Z)$ = 128.90 $\pm$ 0.09 is used.

[17] ELLIS 96C fit to LEP, SLD, m_W, neutral-current data available in the summer of 1996, plus m_t = 175 $\pm$ 6 GeV from CDF/DØ . The fit yields m_t = 172 $\pm$ 6 GeV.

[18] GURTU 96 studies the effect of the mutually incompatible SLD and LEP asymmetry data on the determination of m_H. Use is made of data available in the Summer of 1996. The quoted value is obtained by increasing the errors *à la* PDG. A fit ignoring the SLD data yields 267$^{+242}_{-135}$ GeV.

MASS LIMITS FOR NEUTRAL HIGGS BOSONS IN SUPERSYMMETRIC MODELS

The minimal supersymmetric model has two complex doublets of Higgs bosons. The resulting physical states are two scalars [H^0_1 and H^0_2, where we define $m_{H^0_1} < m_{H^0_2}$], a pseudoscalar (A^0), and a charged Higgs pair ($H^{\pm}$). H^0_1 and H^0_2 are also called h and H in the literature. There are two free parameters in the theory which can be chosen to be m_{A^0} and $\tan\beta = v_2/v_1$, the ratio of vacuum expectation values of the two Higgs doublets. Tree-level Higgs masses are constrained by the model to be $m_{H^0_1} \leq m_Z$, $m_{H^0_2} \geq m_Z$, $m_{A^0} \geq m_{H^0_1}$, and $m_{H^{\pm}} \geq m_W$. However, as described in the Review on Supersymmetry in this Volume these relations are violated by radiative corrections.

Unless otherwise noted, the experiments in e^+e^- collisions search for the processes $e^+e^- \rightarrow H^0_1 Z^0$ in the channels used for the Standard Model Higgs searches and $e^+e^- \rightarrow H^0_1 A^0$ in the final states $b\overline{b}b\overline{b}$ and $b\overline{b}\tau^+\tau^-$. Limits on the A^0 mass arise from these direct searches, as well as from the relations valid in the minimal supersymmetric model between m_{A^0} and $m_{H^0_1}$. As discussed in the minireview on Supersymmetry, in this volume, these relations depend on the masses of the t quark and $\tilde{t}$ squark. The limits are weaker for larger t and $\tilde{t}$ masses, while they increase with the inclusion of two-loop radiative corrections. To include the radiative corrections to the Higgs masses, unless otherwise stated, the listed papers use the two-loop results with m_t = 175 GeV, the universal scalar mass of 1 TeV, SU(2) gaugino mass of 200 GeV, and the Higgsino mass parameter μ = −200 GeV, and examine the two scenarios of no scalar top mixing and 'maximal' stop mixing (which maximizes the effect of the radiative correction).

The mass region $m_{H^0_1} \lesssim$ 45 GeV has been by now entirely ruled out by measurements at the Z pole. The relative limits, as well as other by now obsolete limits from different techniques, have been removed from this compilation, and can be found in earlier editions of this Review. Unless otherwise stated, the following results assume no invisible H^0_1 or A^0 decays.

H^0_1 (Higgs Boson) MASS LIMITS in Supersymmetric Models

VALUE (GeV)	CL%	DOCUMENT ID		TECN	COMMENT
> 89.7	95	[19,20] ABDALLAH	04	DLPH	$E_{cm} \leq$ 209 GeV, $\tan\beta > 0.4$
> 86.0	95	[19,21] ACHARD	02H	L3	$E_{cm} \leq$ 209 GeV, $\tan\beta > 0.4$
> 89.8	95	[19,22] HEISTER	02	ALEP	$E_{cm} \leq$ 209 GeV, $\tan\beta > 0.5$
>100	95	[23] AFFOLDER	01D	CDF	$p\overline{p} \rightarrow b\overline{b}H^0_1$, $\tan\beta \gtrsim 55$
> 74.8	95	[24] ABBIENDI	00F	OPAL	$E_{cm} \leq$ 189 GeV, $\tan\beta > 1$
• • • We do not use the following data for averages, fits, limits, etc. • • •					
		[25] ABBIENDI	03G	OPAL	$H^0_1 \rightarrow A^0 A^0$

[19] Search for $e^+e^- \rightarrow H^0_1 A^0$ in the final states $b\overline{b}b\overline{b}$ and $b\overline{b}\tau^+\tau^-$, and $e^+e^- \rightarrow H^0_1 Z$. Universal scalar mass of 1 TeV, SU(2) gaugino mass of 200 GeV, and μ= −200 GeV are assumed, and two-loop radiative corrections incorporated. The limits hold for m_t=175 GeV, and for the so-called "m_h-max scenario" (CARENA 99B).

[20] This limit applies also in the no-mixing scenario. Furthermore, ABDALLAH 04 excludes the range 0.54 < $\tan\beta$ < 2.36. The limit improves in the region $\tan\beta$ < 6 (see Fig. 28). Limits for μ = 1 TeV are given in Fig. 30.

[21] ACHARD 02H also search for the final state $H^0_1 Z \rightarrow 2A^0 q\overline{q}$, $A^0 \rightarrow q\overline{q}$. In addition, the MSSM parameter set in the "large-μ" and "no-mixing" scenarios are examined.

[22] HEISTER 02 excludes the range 0.7 <$\tan\beta$ < 2.3. A wider range is excluded with different stop mixing assumptions. Updates BARATE 01C.

[23] AFFOLDER 01D search for final states with 3 or more b-tagged jets. See Figs. 2 and 3 for Higgs mass limits as a function of $\tan\beta$, and for different stop mixing scenarios. Stronger limits are obtained at larger $\tan\beta$ values.

[24] ABBIENDI 00F search for $e^+e^- \rightarrow H^0_1 A^0$ in the final states $b\overline{b}b\overline{b}$, $b\overline{b}\tau^+\tau^-$, and $A^0A^0A^0 \rightarrow b\overline{b}b\overline{b}b\overline{b}$, and $e^+e^- \rightarrow H^0_1 Z$. Universal scalar mass of 1 TeV, SU(2) gaugino mass of 1.63 TeV and Higgsino mass parameter μ=−0.1 TeV are assumed. m_t=175 GeV is used. The cases of maximal and no-stop mixing are examined. Limits obtained from scans of the Supersymmetric parameter space can be found in the paper. Updates the results of ABBIENDI 99E.

[25] ABBIENDI 03G search for $e^+e^- \rightarrow H^0_1 Z$ followed by $H^0_1 \rightarrow A^0A^0$, $A^0 \rightarrow c\overline{c}, gg$, or $\tau^+\tau^-$. In the no-mixing scenario, the region $m_{H^0_1}$ = 45-85 GeV and m_{A^0} = 2-9.5 GeV is excluded at 95% CL.

A^0 (Pseudoscalar Higgs Boson) MASS LIMITS in Supersymmetric Models

VALUE (GeV)	CL%	DOCUMENT ID		TECN	COMMENT
> 90.4	95	[26,27] ABDALLAH	04	DLPH	$E_{cm} \leq$ 209 GeV, $\tan\beta > 0.4$
> 86.5	95	[26,28] ACHARD	02H	L3	$E_{cm} \leq$ 209 GeV, $\tan\beta > 0.4$
> 90.1	95	[26,29] HEISTER	02	ALEP	$E_{cm} \leq$ 209 GeV, $\tan\beta > 0.5$
>100	95	[30] AFFOLDER	01D	CDF	$p\overline{p} \rightarrow b\overline{b}A^0$, $\tan\beta \gtrsim 55$
> 76.5	95	[31] ABBIENDI	00F	OPAL	$E_{cm} \leq$ 189 GeV, $\tan\beta > 1$
• • • We do not use the following data for averages, fits, limits, etc. • • •					
		[32] ABBIENDI	03G	OPAL	$H^0_1 \rightarrow A^0 A^0$
		[33] AKEROYD	02	RVUE	

[26] Search for $e^+e^- \rightarrow H^0_1 A^0$ in the final states $b\overline{b}b\overline{b}$ and $b\overline{b}\tau^+\tau^-$, and $e^+e^- \rightarrow H^0_1 Z$. Universal scalar mass of 1 TeV, SU(2) gaugino mass of 200 GeV, and μ= −200 GeV are assumed, and two-loop radiative corrections incorporated. The limits hold for m_t=175 GeV, and for the so-called "m_h-max scenario" (CARENA 99B).

[27] This limit applies also in the no-mixing scenario. Furthermore, ABDALLAH 04 excludes the range 0.54 < $\tan\beta$ < 2.36. The limit improves in the region $\tan\beta$ < 6 (see Fig. 28). Limits for μ = 1 TeV are given in Fig. 30.

[28] ACHARD 02H also search for the final state $H^0_1 Z \rightarrow 2A^0 q\overline{q}$, $A^0 \rightarrow q\overline{q}$. In addition, the MSSM parameter set in the "large-μ" and "no-mixing" scenarios are examined.

[29] HEISTER 02 excludes the range 0.7 <$\tan\beta$ < 2.3. A wider range is excluded with different stop mixing assumptions. Updates BARATE 01C.

[30] AFFOLDER 01D search for final states with 3 or more b-tagged jets. See Figs. 2 and 3 for Higgs mass limits as a function of $\tan\beta$, and for different stop mixing scenarios. Stronger limits are obtained at larger $\tan\beta$ values.

[31] ABBIENDI 00F search for $e^+e^- \rightarrow H^0_1 A^0$ in the final states $b\overline{b}b\overline{b}$, $b\overline{b}\tau^+\tau^-$, and $A^0A^0A^0 \rightarrow b\overline{b}b\overline{b}b\overline{b}$, and $e^+e^- \rightarrow H^0_1 Z$. Universal scalar mass of 1 TeV, SU(2) gaugino mass of 1.63 TeV and Higgsino mass parameter μ=−0.1 TeV are assumed. m_t=175 GeV is used. The cases of maximal and no-stop mixing are examined. Limits obtained from scans of the Supersymmetric parameter space can be found in the paper. Updates the results of ABBIENDI 99E.

[32] ABBIENDI 03G search for $e^+e^- \rightarrow H^0_1 Z$ followed by $H^0_1 \rightarrow A^0A^0$, $A^0 \rightarrow c\overline{c}, gg$, or $\tau^+\tau^-$. In the no-mixing scenario, the region $m_{H^0_1}$ = 45-85 GeV and m_{A^0} = 2-9.5 GeV is excluded at 95% CL.

[33] AKEROYD 02 examine the possibility of a light A^0 with $\tan\beta$ <1. Electroweak measurements are found to be inconsistent with such a scenario.

H^0 (Higgs Boson) MASS LIMITS in Extended Higgs Models

This Section covers models which do not fit into either the Standard Model or its simplest minimal Supersymmetric extension (MSSM), leading to anomalous production rates, or nonstandard final states and branching ratios. In particular, this Section covers limits which may apply to generic two-Higgs-doublet models (2HDM), or to special regions of the MSSM parameter space where decays to invisible particles or to photon pairs are dominant (see the Note on 'Searches for Higgs Bosons' at the beginning of this Chapter). See the footnotes or the comment lines for details on the nature of the models to which the limits apply.

VALUE (GeV)	CL%	DOCUMENT ID		TECN	COMMENT
• • • We do not use the following data for averages, fits, limits, etc. • • •					
		[34] ABDALLAH	04	DLPH	H^0VV couplings
		[35] ABBIENDI	03F	OPAL	$e^+e^- \rightarrow H^0 Z$, $H^0 \rightarrow$ any
		[36] ABBIENDI	03G	OPAL	$H^0_1 \rightarrow A^0 A^0$

>107	95	[37] ACHARD	03C	L3	$H^0 \rightarrow WW^*, ZZ^*, \gamma\gamma$
		[38] ABBIENDI	02D	OPAL	$e^+e^- \rightarrow b\overline{b}H$
>105.5	95	[39,40] ABBIENDI	02F	OPAL	$H_1^0 \rightarrow \gamma\gamma$
>105.4	95	[41] ACHARD	02C	L3	$H_1^0 \rightarrow \gamma\gamma$
>114.1	95	[42] HEISTER	02	ALEP	Invisible H^0, $E_{cm} \leq 209$ GeV
>105.4	95	[39,43] HEISTER	02L	ALEP	$H_1^0 \rightarrow \gamma\gamma$
>109.1	95	[44] HEISTER	02M	ALEP	$H^0 \rightarrow$ 2 jets or $\tau^+\tau^-$
none 1–44	95	[45] ABBIENDI	01E	OPAL	H_1^0, Type-II model
none 12–56	95	[45] ABBIENDI	01E	OPAL	A^0, Type-II model
>107	95	[46] ABREU	01F	DLPH	$H_1^0 \rightarrow \gamma\gamma$
>98	95	[47] AFFOLDER	01H	CDF	$p\overline{p} \rightarrow H^0 W/Z$, $H^0 \rightarrow \gamma\gamma$
>106.4	95	[42] BARATE	01C	ALEP	Invisible H^0, $E_{cm} \leq 202$ GeV
>89.2	95	[48] ACCIARRI	00M	L3	Invisible H^0
		[49] ACCIARRI	00R	L3	$e^+e^- \rightarrow H^0\gamma$ and/or $H^0 \rightarrow \gamma\gamma$
		[50] ACCIARRI	00R	L3	$e^+e^- \rightarrow e^+e^- H^0$
>94.9	95	[51] ACCIARRI	00S	L3	$e^+e^- \rightarrow H^0 Z$, $H^0 \rightarrow \gamma\gamma$
>100.7	95	[52] BARATE	00L	ALEP	$e^+e^- \rightarrow H^0 Z$, $H^0 \rightarrow \gamma\gamma$
>68.0	95	[53] ABBIENDI	99E	OPAL	$\tan\beta > 1$
>96.2	95	[54] ABBIENDI	99O	OPAL	$e^+e^- \rightarrow H^0 Z$, $H^0 \rightarrow \gamma\gamma$
>78.5	95	[55] ABBOTT	99B	D0	$p\overline{p} \rightarrow H^0 W/Z$, $H^0 \rightarrow \gamma\gamma$
		[56] ABREU	99P	DLPH	$e^+e^- \rightarrow H^0\gamma$ and/or $H^0 \rightarrow \gamma\gamma$
>76.1	95	[57] ABREU	99Q	DLPH	Invisible H^0
		[58] GONZALEZ-G..	98B	RVUE	Anomalous coupling
		[59] KRAWCZYK	97	RVUE	$(g-2)_\mu$
		[60] ALEXANDER	96H	OPAL	$Z \rightarrow H^0\gamma$
		[61] ABREU	95H	DLPH	$Z \rightarrow H^0 Z^*$, $H^0 A^0$
		[62] PICH	92	RVUE	Very light Higgs

[34] ABDALLAH 04 consider the full combined LEP and LEP2 datasets to set limits on the Higgs coupling to W or Z bosons, assuming SM decays of the Higgs. Results in Fig. 26.

[35] ABBIENDI 03F search for $H^0 \rightarrow$ anything in $e^+e^- \rightarrow H^0 Z$, using the recoil mass spectrum of $Z \rightarrow e^+e^-$ or $\mu^+\mu^-$. In addition, it searched for $Z \rightarrow \nu\overline{\nu}$ and $H^0 \rightarrow e^+e^-$ or photons. Scenarios with large width or continuum H^0 mass distribution are considered. See their Figs. 11–14 for the results.

[36] ABBIENDI 03G search for $e^+e^- \rightarrow H_1^0 Z$ followed by $H_1^0 \rightarrow A^0 A^0$, $A^0 \rightarrow c\overline{c}, gg$, or $\tau^+\tau^-$ in the region $m_{H_1^0}$ = 45-86 GeV and m_{A^0} = 2-11 GeV. See their Fig. 7 for the limits.

[37] ACHARD 03C search for $e^+e^- \rightarrow ZH^0$ followed by $H^0 \rightarrow WW^*$ or ZZ^* at E_{cm}= 200-209 GeV and combine with the ACHARD 02C result. The limit is for a H^0 with SM production cross section and B($H^0 \rightarrow f\overline{f}$) = 0 for all f. For B($H^0 \rightarrow WW^*$) + B($H^0 \rightarrow ZZ^*$) = 1, m_{H^0} > 108.1 GeV is obtained. See fig. 6 for the limits under different BR assumptions.

[38] ABBIENDI 02D search for $Z \rightarrow b\overline{b}H_1^0$ and $b\overline{b}A^0$ with $H_1^0/A^0 \rightarrow \tau^+\tau^-$, in the range $4 < m_H < 12$ GeV. See their Fig. 8 for limits on the Yukawa coupling.

[39] Search for associated production of a $\gamma\gamma$ resonance with a Z boson, followed by $Z \rightarrow q\overline{q}$, $\ell^+\ell^-$, or $\nu\overline{\nu}$, at $E_{cm} \leq 209$ GeV. The limit is for a H^0 with SM production cross section and B($H^0 \rightarrow f\overline{f}$)=0 for all fermions f.

[40] For B($H^0 \rightarrow \gamma\gamma$)=1, $m_{H^0} > 117$ GeV is obtained.

[41] ACHARD 02C search for associated production of a $\gamma\gamma$ resonance with a Z boson, followed by $Z \rightarrow q\overline{q}$, $\ell^+\ell^-$, or $\nu\overline{\nu}$, at $E_{cm} \leq 209$ GeV. The limit is for a H^0 with SM production cross section and B($H^0 \rightarrow f\overline{f}$)=0 for all fermions f. For B($H^0 \rightarrow \gamma\gamma$)=1, $m_{H^0} > 114$ GeV is obtained.

[42] HEISTER 02 and BARATE 01C search for $e^+e^- \rightarrow H^0 Z$ with H^0 decaying invisibly. The limit assumes SM production cross section and B($H^0 \rightarrow$ invisible) = 1.

[43] For B($H^0 \rightarrow \gamma\gamma$)=1, $m_{H^0} > 113.1$ GeV is obtained.

[44] HEISTER 02M search for $e^+e^- \rightarrow H^0 Z$, assuming that H^0 decays to $q\overline{q}$, gg, or $\tau^+\tau^-$ only. The limit assumes SM production cross section.

[45] ABBIENDI 01E search for neutral Higgs bosons in general Type-II two-doublet models, at $E_{cm} \leq 189$ GeV. In addition to usual final states, the decays H_1^0, $A^0 \rightarrow q\overline{q}$, gg are searched for. See their Figs. 15,16 for excluded regions.

[46] ABREU 01F search for neutral, fermiophobic Higgs bosons in Type-I two-doublet models, at $E_{cm} \leq 202$ GeV. The limit is from $e^+e^- \rightarrow H^0 Z$ with the SM cross section and B($H^0 \rightarrow \gamma\gamma$)=1. The process $e^+e^- \rightarrow H^0 A^0$ with $H^0 \rightarrow \gamma\gamma$ is also searched for in the modes $A^0 \rightarrow b\overline{b}$, $H^0 Z$ and long-lived A^0. See their Figs. 4–6 for the excluded regions.

[47] AFFOLDER 01H search for associated production of a $\gamma\gamma$ resonance and a W or Z (tagged by two jets, an isolated lepton, or missing E_T). The limit assumes Standard Model values for the production cross section and for the couplings of the H^0 to W and Z bosons. See their Fig. 11 for limits with B($H^0 \rightarrow \gamma\gamma$)< 1.

[48] ACCIARRI 00M search for $e^+e^- \rightarrow ZH^0$ with H^0 decaying invisibly at E_{cm}=183–189 GeV. The limit assumes SM production cross section and B($H^0 \rightarrow$ invisible)=1. See their Fig. 6 for limits for smaller branching ratios.

[49] ACCIARRI 00R search for $e^+e^- \rightarrow H^0\gamma$ with $H^0 \rightarrow b\overline{b}$, $Z\gamma$, or $\gamma\gamma$. See their Fig. 3 for limits on $\sigma \cdot$B. Explicit limits within an effective interaction framework are also given, for which the Standard Model Higgs search results are used in addition.

[50] ACCIARRI 00R search for the two-photon type processes $e^+e^- \rightarrow e^+e^- H^0$ with $H^0 \rightarrow b\overline{b}$ or $\gamma\gamma$. See their Fig. 4 for limits on $\Gamma(H^0 \rightarrow \gamma\gamma)\cdot$B($H^0 \rightarrow \gamma\gamma$or $b\overline{b}$) for m_{H^0}=70–170 GeV.

[51] ACCIARRI 00S search for associated production of a $\gamma\gamma$ resonance with a $q\overline{q}$, $\nu\overline{\nu}$, or $\ell^+\ell^-$ pair in e^+e^- collisions at E_{cm}= 189 GeV. The limit is for a H^0 with SM production cross section and B($H^0 \rightarrow f\overline{f}$)=0 for all fermions f. For B($H^0 \rightarrow \gamma\gamma$)=1, $m_{H^0} > 98$ GeV is obtained. See their Fig. 5 for limits on B($H \rightarrow \gamma\gamma$)$\cdot\sigma(e^+e^- \rightarrow Hf\overline{f})/\sigma(e^+e^- \rightarrow Hf\overline{f})$ (SM).

[52] BARATE 00L search for associated production of a $\gamma\gamma$ resonance with a $q\overline{q}$, $\nu\overline{\nu}$, or $\ell^+\ell^-$ pair in e^+e^- collisions at E_{cm}= 88–202 GeV. The limit is for a H^0 with SM production cross section and B($H^0 \rightarrow f\overline{f}$)=0 for all fermions f. For B($H^0 \rightarrow \gamma\gamma$)=1, $m_{H^0} > 109$ GeV is obtained. See their Fig. 3 for limits on B($H \rightarrow \gamma\gamma$)$\cdot\sigma(e^+e^- \rightarrow Hf\overline{f})/\sigma(e^+e^- \rightarrow Hf\overline{f})$ (SM).

[53] ABBIENDI 99E search for $e^+e^- \rightarrow H^0 A^0$ and $H^0 Z$ at E_{cm} = 183 GeV. The limit is with m_H=m_A in general two Higgs-doublet models. See their Fig. 18 for the exclusion limit in the m_H–m_A plane. Updates the results of ACKERSTAFF 98S.

[54] ABBIENDI 99O search for associated production of a $\gamma\gamma$ resonance with a $q\overline{q}$, $\nu\overline{\nu}$, or $\ell^+\ell^-$ pair in e^+e^- collisions at 189 GeV. The limit is for a H^0 with SM production cross section and B($H^0 \rightarrow f\overline{f}$)=0, for all fermions f. See their Fig. 4 for limits on $\sigma(e^+e^- \rightarrow H^0 Z^0)\times$B($H^0 \rightarrow \gamma\gamma$)$\times$B($X^0 \rightarrow f\overline{f}$) for various masses. Updates the results of ACKERSTAFF 98Y.

[55] ABBOTT 99B search for associated production of a $\gamma\gamma$ resonance and a dijet pair. The limit assumes Standard Model values for the production cross section and for the couplings of the H^0 to W and Z bosons. Limits in the range of $\sigma(H^0+Z/W)\cdot$B($H^0 \rightarrow \gamma\gamma$)= 0.80–0.34 pb are obtained in the mass range m_{H^0}= 65–150 GeV.

[56] ABREU 99P search for $e^+e^- \rightarrow H^0\gamma$ with $H^0 \rightarrow b\overline{b}$ or $\gamma\gamma$, and $e^+e^- \rightarrow H^0 q\overline{q}$ with $H^0 \rightarrow \gamma\gamma$. See their Fig. 4 for limits on $\sigma\times$B. Explicit limits within an effective interaction framework are also given.

[57] ABREU 99Q search for $e^+e^- \rightarrow H^0 Z$ with H^0 decaying invisibly at E_{cm} between 161 and 183 GeV. The limit assumes SM production cross section, and holds for any B($H^0 \rightarrow$ invisible). In the case of invisible decays in the MSSM, the excluded region of the (M_2, $\tan\beta$) plane overlaps the exclusion region from direct searches for charginos and neutralinos (ABREU 99E in the Supersymmetry Listings). See their Fig. 6(d) for limits on a Majoron model.

[58] GONZALEZ-GARCIA 98B use DØ limit for $\gamma\gamma$ events with missing E_T in $p\overline{p}$ collisions (ABBOTT 98) to constrain possible ZH or WH production followed by unconventional $H \rightarrow \gamma\gamma$ decay which is induced by higher-dimensional operators. See their Figs. 1 and 2 for limits on the anomalous couplings.

[59] KRAWCZYK 97 analyse the muon anomalous magnetic moment in a two-doublet Higgs model (with type II Yukawa couplings) assuming no $H_1^0 ZZ$ coupling and obtain $m_{H_1^0} \gtrsim 5$ GeV or $m_{A^0} \gtrsim 5$ GeV for $\tan\beta > 50$. Other Higgs bosons are assumed to be much heavier.

[60] ALEXANDER 96H give B($Z \rightarrow H^0\gamma$)$\times$B($H^0 \rightarrow q\overline{q}$) < 1–4×10^{-5} (95%CL) and B($Z \rightarrow H^0\gamma$)$\times$B($H^0 \rightarrow b\overline{b}$) < 0.7–2×10^{-5} (95%CL) in the range $20 < m_{H^0} < 80$ GeV.

[61] See Fig. 4 of ABREU 95H for the excluded region in the $m_{H^0} - m_{A^0}$ plane for general two-doublet models. For $\tan\beta > 1$, the region $m_{H^0}+m_{A^0} \lesssim 87$ GeV, $m_{H^0} < 47$ GeV is excluded at 95% CL.

[62] PICH 92 analyse H^0 with $m_{H^0} < 2m_\mu$ in general two-doublet models. Excluded regions in the space of mass-mixing angles from LEP, beam dump, and $\pi^{\pm}$, η rare decays are shown in Figs. 3,4. The considered mass region is not totally excluded.

$H^{\pm}$ (Charged Higgs) MASS LIMITS

Unless otherwise stated, the limits below assume B($H^+ \rightarrow \tau^+\nu$)+B($H^+ \rightarrow c\overline{s}$)=1, and hold for all values of B($H^+ \rightarrow \tau^+\nu_\tau$), and assume H^+ weak isospin of T_3=+1/2. In the following, $\tan\beta$ is the ratio of the two vacuum expectation values in two-doublet models (2HDM).

The limits are also applicable to point-like technipions. For a discussion of technipar-ticles, see the Review of Dynamical Electroweak Symmetry Breaking in this Review.

For limits obtained in hadronic collisions before the observation of the top quark, and based on the top mass values inconsistent with the current measurements, see the 1996 (Physical Review **D54** 1 (1996)) Edition of this Review.

Searches in e^+e^- collisions at and above the Z pole have conclusively ruled out the existence of a charged Higgs in the region $m_{H^+} \lesssim 45$ GeV, and are now superseded by the most recent searches in higher energy e^+e^- collisions at LEP. Results by now obsolete are therefore not included in this compilation, and can be found in the previous Edition (The European Physical Journal **C15** 1 (2000)) of this Review.

In the following, and unless otherwise stated, results from the LEP experiments (ALEPH, DELPHI, L3, and OPAL) are assumed to derive from the study of the $e^+e^- \rightarrow H^+H^-$ process. Limits from $b \rightarrow s\gamma$ decays are usually stronger in generic 2HDM models than in Supersymmetric models.

A recent combination (LEP 00B) of preliminary, unpublished results relative to data taken at LEP in the Summer of 1999 at energies up to 202 GeV gives the limit $m_{H_1^{\pm}} > 78.6$ GeV.

VALUE (GeV)	*CL%*	*DOCUMENT ID*		*TECN*	*COMMENT*
>71.5	95	ABDALLAH	02	DLPH	$E_{cm} \leq 202$ GeV
>79.3	95	HEISTER	02P	ALEP	$E_{cm} \leq 209$ GeV
>67.4	95	ACCIARRI	00W	L3	$E_{cm} \leq 202$ GeV
>59.5	95	ABBIENDI	99E	OPAL	$E_{cm} \leq 183$ GeV
• • • We do not use the following data for averages, fits, limits, etc. • • •					
		[63] ABBIENDI	03	OPAL	$\tau \rightarrow \mu\overline{\nu}\nu$, $e\overline{\nu}\nu$
		[64] ABAZOV	02B	D0	$t \rightarrow bH^+$, $H \rightarrow \tau\nu$
		[65] BORZUMATI	02	RVUE	
		[66] ABBIENDI	01Q	OPAL	$B \rightarrow \tau\nu_\tau X$
		[67] BARATE	01E	ALEP	$B \rightarrow \tau\nu_\tau$
>315	99	[68] GAMBINO	01	RVUE	$b \rightarrow s\gamma$
>82.8	95	ABBIENDI	00G	OPAL	$E_{cm} \leq 189$ GeV, B($\tau\nu$) = 1
		[69] AFFOLDER	00I	CDF	$t \rightarrow bH^+$, $H \rightarrow \tau\nu$
		[70] ABBOTT	99E	D0	$t \rightarrow bH^+$

>56.3	95	ABREU	99R	DLPH	$E_{cm} \leq 183$ GeV
		[71] ACKERSTAFF	99D	OPAL	$\tau \rightarrow e\nu\nu, \mu\nu\nu$
		[72] ACCIARRI	97F	L3	$B \rightarrow \tau\nu_\tau$
		[73] AMMAR	97B	CLEO	$\tau \rightarrow \mu\nu\nu$
		[74] COARASA	97	RVUE	$B \rightarrow \tau\nu_\tau X$
		[75] GUCHAIT	97	RVUE	$t \rightarrow bH^+$, $H \rightarrow \tau\nu$
		[76] MANGANO	97	RVUE	$B_{u(c)} \rightarrow \tau\nu_\tau$
		[77] STAHL	97	RVUE	$\tau \rightarrow \mu\nu\nu$
>244	95	[78] ALAM	95	CLE2	$b \rightarrow s\gamma$
		[79] BUSKULIC	95	ALEP	$b \rightarrow \tau\nu_\tau X$

[63] ABBIENDI 03 give a limit $m_{H^+} > 1.28\tan\beta$ GeV (95%CL) in Type II two-doublet models.

[64] ABAZOV 02B search for a charged Higgs boson in top decays with $H^+ \rightarrow \tau^+\nu$ at E_{cm}=1.8 TeV. For m_{H^+}=75 GeV, the region $\tan\beta > 32.0$ is excluded at 95%CL. The excluded mass region extends to over 140 GeV for $\tan\beta$ values above 100.

[65] BORZUMATI 02 point out that the decay modes such as $b\overline{b}W$, $A^0 W$, and supersymmetric ones can have substantial branching fractions in the mass range explored at LEP II and Tevatron.

[66] ABBIENDI 01Q give a limit $\tan\beta/m_{H^+} < 0.53$ GeV^{-1} (95%CL) in Type II two-doublet models.

[67] BARATE 01E give a limit $\tan\beta/m_{H^+} < 0.40$ GeV^{-1} (90%CL) in Type II two-doublet models. An independent measurement of $B \rightarrow \tau\nu_\tau X$ gives $\tan\beta/m_{H^+} < 0.49$ GeV^{-1} (90%CL).

[68] GAMBINO 01 use the world average data in the summer of 2001 B($b \rightarrow s\gamma$)= $(3.23 \pm 0.42) \times 10^{-4}$. The limit applies for Type-II two-doublet models.

[69] AFFOLDER 00I search for a charged Higgs boson in top decays with $H^+ \rightarrow \tau^+\nu$ in $p\overline{p}$ collisions at E_{cm}=1.8 TeV. The excluded mass region extends to over 120 GeV for $\tan\beta$ values above 100 and B($\tau\nu$)=1. If B($t \rightarrow bH^+$)$\gtrsim$0.6, m_{H^+} up to 160 GeV is excluded. Updates ABE 97L.

[70] ABBOTT 99E search for a charged Higgs boson in top decays in $p\overline{p}$ collisions at E_{cm}=1.8 TeV, by comparing the observed $t\overline{t}$ cross section (extracted from the data assuming the dominant decay $t \rightarrow bW^+$) with theoretical expectation. The search is sensitive to regions of the domains $\tan\beta \lesssim 1$, $50 < m_{H^+}$(GeV) $\lesssim 120$ and $\tan\beta \gtrsim 40$, $50 < m_{H^+}$ (GeV) $\lesssim 160$. See Fig. 3 for the details of the excluded region.

[71] ACKERSTAFF 99D measure the Michel parameters ρ, ξ, η, and $\xi\delta$ in leptonic τ decays from $Z \rightarrow \tau\tau$. Assuming e-μ universality, the limit $m_{H^+} > 0.97\tan\beta$ GeV (95%CL) is obtained for two-doublet models in which only one doublet couples to leptons.

[72] ACCIARRI 97F give a limit $m_{H^+} > 2.6\tan\beta$ GeV (90%CL) from their limit on the exclusive $B \rightarrow \tau\nu_\tau$ branching ratio.

[73] AMMAR 97B measure the Michel parameter ρ from $\tau \rightarrow e\nu\nu$ decays and assumes e/μ universality to extract the Michel η parameter from $\tau \rightarrow \mu\nu\nu$ decays. The measurement is translated to a lower limit on m_{H^+} in a two-doublet model $m_{H^+} > 0.97\tan\beta$ GeV (90% CL).

[74] COARASA 97 reanalyzed the constraint on the ($m_{H^\pm}$,$\tan\beta$) plane derived from the inclusive $B \rightarrow \tau\nu_\tau X$ branching ratio in GROSSMAN 95B and BUSKULIC 95. They show that the constraint is quite sensitive to supersymmetric one-loop effects.

[75] GUCHAIT 97 studies the constraints on m_{H^+} set by Tevatron data on $\ell\tau$ final states in $t\overline{t} \rightarrow (Wb)(Hb)$, $W \rightarrow \ell\nu$, $H \rightarrow \tau\nu_\tau$. See Fig. 2 for the excluded region.

[76] MANGANO 97 reconsiders the limit in ACCIARRI 97F including the effect of the potentially large $B_c \rightarrow \tau\nu_\tau$ background to $B_u \rightarrow \tau\nu_\tau$ decays. Stronger limits are obtained.

[77] STAHL 97 fit τ lifetime, leptonic branching ratios, and the Michel parameters and derive limit $m_{H^+} > 1.5\tan\beta$ GeV (90% CL) for a two-doublet model. See also STAHL 94.

[78] ALAM 95 measure the inclusive $b \rightarrow s\gamma$ branching ratio at $\Upsilon(4S)$ and give B($b \rightarrow s\gamma$)$< 4.2 \times 10^{-4}$ (95% CL), which translates to the limit $m_{H^+} > [244 + 63/(\tan\beta)^{1.3}]$ GeV in the Type II two-doublet model. Light supersymmetric particles can invalidate this bound.

[79] BUSKULIC 95 give a limit $m_{H^+} > 1.9\tan\beta$ GeV (90%CL) for Type-II models from $b \rightarrow \tau\nu_\tau X$ branching ratio, as proposed in GROSSMAN 94.

MASS LIMITS for $H^{\pm\pm}$ (doubly-charged Higgs boson)

VALUE (GeV)	CL%	DOCUMENT ID		TECN	COMMENT
>97.3	95	[80] ABDALLAH	03	DLPH	$E_{cm} \leq 209$ GeV
>98.5	95	[81] ABBIENDI	02C	OPAL	$E_{cm} \leq 209$ GeV
• • • We do not use the following data for averages, fits, limits, etc. • • •					
		[82] ABBIENDI	03Q	OPAL	$E_{cm} \leq 209$ GeV, single $H^{\pm\pm}$
		[83] GORDEEV	97	SPEC	muonium conversion
		[84] ASAKA	95	THEO	
>45.6	95	[85] ACTON	92M	OPAL	
>30.4	95	[86] ACTON	92M	OPAL	$T_3(H^{++})= +1$
>25.5	95	[86] ACTON	92M	OPAL	$T_3(H^{++})= 0$
none 6.5–36.6	95	[87] SWARTZ	90	MRK2	$T_3(H^{++}) = +1$
none 7.3–34.3	95	[87] SWARTZ	90	MRK2	$T_3(H^{++}) = 0$

[80] ABDALLAH 03 search for $H^{++}H^{--}$ pair production either followed by $H^{++} \rightarrow \tau^+\tau^+$, or decaying outside the detector. The limit is for weak single H^{++}. The limit for weak triplet is 98.1 GeV.

[81] ABBIENDI 02C searches for pair production of $H^{++}H^{--}$, with $H^{\pm\pm} \rightarrow \ell^\pm\ell^\pm$ (ℓ,ℓ' = e,μ,τ). the limit holds for ℓ=ℓ'=τ, and becomes stronger for other combinations of leptonic final states. To ensure the decay within the detector, the limit only applies for $g(H\ell\ell) \gtrsim 10^{-7}$.

[82] ABBIENDI 03Q searches for single $H^{\pm\pm}$ via direct production in $e^+e^- \rightarrow e^\pm e^\pm H^{\mp\mp}$, and via t-channel exchange in $e^+e^- \rightarrow e^+e^-$. In the direct case, and assuming B($H^{\pm\pm} \rightarrow \ell^\pm\ell^\pm$) = 1, a 95% CL limit on $h_{ee} < 0.071$ is set for $m_{H^{\pm\pm}} < 160$ GeV (see Fig. 6). In the second case, indirect limits on h_{ee} are set for $m_{H^{\pm\pm}} < 2$ TeV (see Fig. 8).

[83] GORDEEV 97 search for muonium-antimuonium conversion and find $G_{M\overline{M}}/G_F < 0.14$ (90% CL), where $G_{M\overline{M}}$ is the lepton-flavor violating effective four-fermion coupling. This limit may be converted to $m_{H^{++}} > 210$ GeV if the Yukawa couplings of H^{++} to ee and $\mu\mu$ are as large as the weak gauge coupling. For similar limits on muonium-antimuonium conversion, see the muon Particle Listings.

[84] ASAKA 95 point out that H^{++} decays dominantly to four fermions in a large region of parameter space where the limit of ACTON 92M from the search of dilepton modes does not apply.

[85] ACTON 92M limit assumes $H^{\pm\pm} \rightarrow \ell^\pm\ell^\pm$ or $H^{\pm\pm}$ does not decay in the detector. Thus the region $g_{\ell\ell} \approx 10^{-7}$ is not excluded.

[86] ACTON 92M from $\Delta\Gamma_Z < 40$ MeV.

[87] SWARTZ 90 assume $H^{\pm\pm} \rightarrow \ell^\pm\ell^\pm$ (any flavor). The limits are valid for the Higgs-lepton coupling g($H\ell\ell$) $\gtrsim 7.4 \times 10^{-7}/[m_H/\text{GeV}]^{1/2}$. The limits improve somewhat for ee and $\mu\mu$ decay modes.

H^0 and $H^\pm$ REFERENCES

ABDALLAH 04 EPJ C32 145 J. Abdallah *et al.* (DELPHI Collab.)
ABBIENDI 03 PL B551 35 G. Abbiendi *et al.* (OPAL Collab.)
ABBIENDI 03B EPJ C26 479 G. Abbiendi *et al.* (OPAL Collab.)
ABBIENDI 03F EPJ C27 311 G. Abbiendi *et al.* (OPAL Collab.)
ABBIENDI 03G EPJ C27 483 G. Abbiendi *et al.* (OPAL Collab.)
ABBIENDI 03Q PL B577 93 G. Abbiendi *et al.* (OPAL Collab.)
ABDALLAH 03 PL B552 127 J. Abdallah *et al.* (DELPHI Collab.)
ACHARD 03C PL B568 191 P. Achard *et al.* (L3 Collab.)
HEISTER 03D PL B565 61 A. Heister *et al.* (ALEPH, DELPHI, L3+)
ALEPH, DELPHI, L3, OPAL, LEP Higgs Working Group
ABAZOV 02B PRL 88 151803 V.M. Abazov *et al.* (D0 Collab.)
ABBIENDI 02C PL B526 221 G. Abbiendi *et al.* (OPAL Collab.)
ABBIENDI 02D EPJ C23 397 G. Abbiendi *et al.* (OPAL Collab.)
ABBIENDI 02F PL B544 44 G. Abbiendi *et al.* (OPAL Collab.)
ABDALLAH 02 PL B525 17 J. Abdallah *et al.* (DELPHI Collab.)
ACHARD 02C PL B534 28 P. Achard *et al.* (L3 Collab.)
ACHARD 02H PL B545 30 P. Achard *et al.* (L3 Collab.)
AKEROYD 02 PR D66 037702 A.G. Akeroyd *et al.*
BORZUMATI 02 PL B549 170 F.M. Borzumati, A. Djouadi
CHANOWITZ 02 PR D66 073002 M.S. Chanowitz
HEISTER 02 PL B526 191 A. Heister *et al.* (ALEPH Collab.)
HEISTER 02L PL B544 16 A. Heister *et al.* (ALEPH Collab.)
HEISTER 02M PL B544 25 A. Heister *et al.* (ALEPH Collab.)
HEISTER 02P PL B543 1 A. Heister *et al.* (ALEPH Collab.)
LEP 02 CERN-EP/2002-091 LEP Collabs.
ALEPH, DELPHI, L3, OPAL, the LEP Electroweak Working Group, and the SLD Heavy Flavor Group
ABAZOV 01E PRL 87 231801 V.M. Abazov *et al.* (D0 Collab.)
ABBIENDI 01A EPJ C19 587 G. Abbiendi *et al.* (OPAL Collab.)
ABBIENDI 01E EPJ C18 425 G. Abbiendi *et al.* (OPAL Collab.)
ABBIENDI 01Q PL B520 1 G. Abbiendi *et al.* (OPAL Collab.)
ABREU 01F PL B507 89 P. Abreu *et al.* (DELPHI Collab.)
ACHARD 01C PL B517 319 P. Achard *et al.* (L3 Collab.)
AFFOLDER 01D PRL 86 4472 T. Affolder *et al.* (CDF Collab.)
AFFOLDER 01H PR D64 092002 T. Affolder *et al.* (CDF Collab.)
BARATE 01C PL B499 53 R. Barate *et al.* (ALEPH Collab.)
BARATE 01E EPJ C19 213 R. Barate *et al.* (ALEPH Collab.)
GAMBINO 01 NP B611 338 P. Gambino, M. Misiak
ABBIENDI 00F EPJ C12 567 G. Abbiendi *et al.* (OPAL Collab.)
ABBIENDI 00G EPJ C14 51 G. Abbiendi *et al.* (OPAL Collab.)
ACCIARRI 00M PL B485 85 M. Acciarri *et al.* (L3 Collab.)
ACCIARRI 00R PL B489 102 M. Acciarri *et al.* (L3 Collab.)
ACCIARRI 00S PL B489 115 M. Acciarri *et al.* (L3 Collab.)
ACCIARRI 00W PL B496 34 M. Acciarri *et al.* (L3 Collab.)
AFFOLDER 00I PR D62 012004 T. Affolder *et al.* (CDF Collab.)
BARATE 00L PL B487 241 R. Barate *et al.* (ALEPH Collab.)
FIELD 00 PR D61 013010 J.H. Field
LEP 00B CERN-EP-2000-055 LEP Collabs.
PDG 00 EPJ C15 1 D.E. Groom *et al.*
ABBIENDI 99E EPJ C7 407 G. Abbiendi *et al.* (OPAL Collab.)
ABBIENDI 99O PL B464 311 G. Abbiendi *et al.* (OPAL Collab.)
ABBOTT 99B PRL 82 2244 B. Abbott *et al.* (D0 Collab.)
ABBOTT 99E PRL 82 4975 B. Abbott *et al.* (D0 Collab.)
ABREU 99E PL B446 75 P. Abreu *et al.* (DELPHI Collab.)
Also 99N PL B451 447 (erratum) P. Abreu *et al.* (DELPHI Collab.)
ABREU 99P PL B458 431 P. Abreu *et al.* (DELPHI Collab.)
ABREU 99Q PL B459 367 P. Abreu *et al.* (DELPHI Collab.)
ABREU 99R PL B460 484 P. Abreu *et al.* (DELPHI Collab.)
ACKERSTAFF 99D EPJ C8 3 K. Ackerstaff *et al.* (OPAL Collab.)
CARENA 99B hep-ph/9912223 M. Carena *et al.*
CERN-TH/99-374
CHANOWITZ 99 PR D59 073005 M.S. Chanowitz
D'AGOSTINI 99 EPJ C10 663 G. D'Agostini, G. Degrassi
FIELD 99 MPL A14 1815 J.H. Field
LEP 99 CERN-EP/99-015 LEP Collabs. (ALEPH, DELPHI, L3, OPAL, LEP EWWG+)
ABBOTT 98 PRL 80 442 B. Abbott *et al.* (D0 Collab.)
ABE 98T PRL 81 5748 F. Abe *et al.* (CDF Collab.)
ACKERSTAFF 98S EPJ C5 19 K. Ackerstaff *et al.* (OPAL Collab.)
ACKERSTAFF 98Y PL B437 218 K. Ackerstaff *et al.* (OPAL Collab.)
CHANOWITZ 98 PRL 80 2521 M. Chanowitz
DAVIER 98 PL B435 427 M. Davier, A. Hoecker
GONZALEZ-G... 98B PR D57 7045 M.C. Gonzalez-Garcia, S.M. Lietti, S.F. Novaes
HAGIWARA 98B EPJ C2 95 K. Hagiwara, D. Haidt, S. Matsumoto
PDG 98 EPJ C3 1 C. Caso *et al.*
ABBANEO 97 CERN-PPE/97-154 D. Abbaneo *et al.*
ALEPH, DELPHI, L3, OPAL, and SLD Collaborations, and the LEP Electroweak Working Group.
ABE 97L PRL 79 357 F. Abe *et al.* (CDF Collab.)
ABE 97W PRL 79 3819 F. Abe *et al.* (CDF Collab.)
ACCIARRI 97F PL B396 327 M. Acciarri *et al.* (L3 Collab.)
AMMAR 97B PRL 78 4686 R. Ammar *et al.* (CLEO Collab.)
COARASA 97 PL B406 337 J.A. Coarasa, R.A. Jimenez, J. Sola
DEBOER 97B ZPHY C75 627 W. de Boer *et al.*
DEGRASSI 97 PL B394 188 G. Degrassi, P. Gambino, A. Sirlin (MPIM, NYU)
DITTMAIER 97 PL B391 420 S. Dittmaier, D. Schildknecht (BIEL)
GORDEEV 97 PAN 60 1164 V.A. Gordeev *et al.* (PNPI)
Translated from YAF 60 1291.
GUCHAIT 97 PR D55 7263 M. Guchait, D.P. Roy (TATA)
KRAWCZYK 97 PR D55 6968 M. Krawczyk, J. Zochowski (WARS)
MANGANO 97 PL B410 299 M. Mangano, S. Slabospitsky
RENTON 97 IJMP A12 4109 P.B. Renton
STAHL 97 ZPHY C74 73 A. Stahl, H. Voss (BONN)
ALCARAZ 96 CERN-PPE/96-183 J. Alcaraz *et al.*
The ALEPH, DELPHI, L3, OPAL, and SLD Collaborations and the LEP Electroweak Working Group
ALEXANDER 96H ZPHY C71 1 G. Alexander *et al.* (OPAL Collab.)
ELLIS 96C PL B389 321 J. Ellis, G.L. Fogli, E. Lisi (CERN, BARI)
GURTU 96 PL B385 415 A. Gurtu (TATA)
PDG 96 PR D54 1 R. M. Barnett *et al.*
ABREU 95H ZPHY C67 69 P. Abreu *et al.* (DELPHI Collab.)
ALAM 95 PRL 74 2885 M.S. Alam *et al.* (CLEO Collab.)

ASAKA	95	PL B345 36	T. Asaka, K.I. Hikasa	(TOHOK)
BUSKULIC	95	PL B343 444	D. Buskulic *et al.*	(ALEPH Collab.)
GROSSMAN	95B	PL B357 630	Y. Grossman, H. Haber, Y. Nir	
GROSSMAN	94	PL B332 373	Y. Grossman, Z. Ligeti	
STAHL	94	PL B324 121	A. Stahl	(BONN)
ACTON	92M	PL B295 347	P.D. Acton *et al.*	(OPAL Collab.)
PICH	92	NP B388 31	A. Pich, J. Prades, P. Yepes	(CERN, CPPM)
SWARTZ	90	PRL 64 2877	M.L. Swartz *et al.*	(Mark II Collab.)

Heavy Bosons Other Than Higgs Bosons, Searches for

We list here various limits on charged and neutral heavy vector bosons (other than W's and Z's), heavy scalar bosons (other than Higgs bosons), vector or scalar leptoquarks, and axigluons.

THE W' SEARCHES

Written October 1997 by K.S. Babu (Oklahoma State University), C. Kolda (Notre Dame University), and J. March-Russell (CERN).

Any electrically charged gauge boson outside of the Standard Model is generically denoted W'. A W' always couples to two different flavors of fermions, similar to the W boson. In particular, if a W' couples quarks to leptons it is a leptoquark gauge boson.

The most attractive candidate for W' is the W_R gauge boson associated with the left-right symmetric models [1]. These models seek to provide a spontaneous origin for parity violation in weak interactions. Here the gauge group is extended to $\mathrm{SU}(3)_C \times \mathrm{SU}(2)_L \times \mathrm{SU}(2)_R \times \mathrm{U}(1)_{B-L}$ with the Standard Model hypercharge identified as $Y = T_{3R} + (B\text{–}L)/2$, T_{3R} being the third component of $\mathrm{SU}(2)_R$. The fermions transform under the gauge group in a left-right symmetric fashion: $q_L(3,2,1,1/3) + q_R(3,1,2,1/3)$ for quarks and $\ell_L(1,2,1,-1) + \ell_R(1,1,2,-1)$ for leptons. Note that the model requires the introduction of right-handed neutrinos, which can facilitate the see-saw mechanism for explaining the smallness of the ordinary neutrino masses. A Higgs bidoublet $\Phi(1,2,2,0)$ is usually employed to generate quark and lepton masses and to participate in the electroweak symmetry breaking. Under left-right (or parity) symmetry, $q_L \leftrightarrow q_R$, $\ell_L \leftrightarrow \ell_R$, $W_L \leftrightarrow W_R$ and $\Phi \leftrightarrow \Phi^\dagger$.

After spontaneous symmetry breaking, the two W bosons of the model, W_L and W_R, will mix. The physical mass eigenstates are denoted as

$$W_1 = \cos\zeta\, W_L + \sin\zeta\, W_R, \qquad W_2 = -\sin\zeta\, W_L + \cos\zeta\, W_R \quad (1)$$

with W_1 identified as the observed W boson. The most general Lagrangian that describes the interactions of the $W_{1,2}$ with the quarks can be written as [2]

$$\mathcal{L} = -\frac{1}{\sqrt{2}}\overline{u}\gamma_\mu \Big[\Big(g_L \cos\zeta\, V^L P_L - g_R e^{i\omega} \sin\zeta\, V^R P_R \Big) W_1^\mu + \Big(g_L \sin\zeta\, V^L P_L + g_R e^{i\omega}\cos\zeta\, V^R P_R \Big) W_2^\mu \Big] d + h.c. \quad (2)$$

where $g_{L,R}$ are the $\mathrm{SU}(2)_{L,R}$ gauge couplings, $P_{L,R} = (1 \mp \gamma_5)/2$ and $V^{L,R}$ are the left- and right-handed CKM matrices in the quark sector. The phase ω reflects a possible complex mixing parameter in the W_L–W_R mass-squared matrix. Note that there is CP violation in the model arising from the right-handed currents even with only two generations. The Lagrangian for leptons is identical to that for quarks, with the replacements $u \to \nu$, $d \to e$ and the identification of $V^{L,R}$ with the CKM matrices in the leptonic sector.

If parity invariance is imposed on the Lagrangian, then $g_L = g_R$. Furthermore, the Yukawa coupling matrices that arise from coupling to the Higgs bidoublet Φ will be Hermitian. If in addition the vacuum expectation values of Φ are assumed to be real, the quark and lepton mass matrices will also be Hermitian, leading to the relation $V^L = V^R$. Such models are called *manifest* left-right symmetric models and are approximately realized with a minimal Higgs sector [3]. If instead parity and CP are both imposed on the Lagrangian, then the Yukawa coupling matrices will be real symmetric and, after spontaneous CP violation, the mass matrices will be complex symmetric. In this case, which is known in the literature as *pseudo-manifest* left-right symmetry, $V^L = (V^R)^*$.

Indirect constraints: In minimal version of manifest or pseudo-manifest left-right symmetric models with $\omega = 0$ or π, there are only two free parameters, ζ and M_{W_2}, and they can be constrained from low energy processes. In the large M_{W_2} limit, stringent bounds on the angle ζ arise from three processes. (i) Nonleptonic K decays: The decays $K \to 3\pi$ and $K \to 2\pi$ are sensitive to small admixtures of right-handed currents. Assuming the validity of PCAC relations in the Standard Model it has been argued in Ref. 4 that the success in the $K \to 3\pi$ prediction will be spoiled unless $|\zeta| \le 4 \times 10^{-3}$. (ii) $b \to s\gamma$: The amplitude for this process has an enhancement factor m_t/m_b relative to the Standard Model and thus can be used to constrain ζ yielding the limit $-0.01 \le \zeta \le 0.003$ [5]. (iii) Universality in weak decays: If the right-handed neutrinos are heavy, the right-handed admixture in the charged current will contribute to β decay and K decay, but not to the μ decay. This will modify the extracted values of V^L_{ud} and V^L_{us}. Demanding that the difference not upset the three generation unitarity of the CKM matrix, a bound $|\zeta| \le 10^{-3}$ has been derived [6].

If the ν_R are heavy, leptonic and semileptonic processes do not constrain ζ since the emission of ν_R will not be kinematically allowed. However, if the ν_R is light enough to be emitted in μ decay and β decay, stringent limits on ζ do arise. For example, $|\zeta| \le 0.039$ can be obtained from polarized μ decay [7] in the large M_{W_2} limit of the manifest left-right model. Alternatively, in the $\zeta = 0$ limit, there is a constraint $M_{W_2} \ge 484$ GeV from direct W_2 exchange. For the constraint on the case in which M_{W_2} is not taken to be heavy, see Ref. 2. There are also cosmological and astrophysical constraints on M_{W_2} and ζ in scenarios with a light ν_R. During nucleosynthesis the process $e^+e^- \to \nu_R\overline{\nu}_R$, proceeding via W_2 exchange, will keep the ν_R in equilibrium leading to an overproduction of ^{4}He unless M_{W_2} is greater than about 1 TeV [8]. Likewise the ν_{eR} produced via $e^-_R p \to n\nu_R$ inside a supernova must not drain too much of its energy, leading to limits $M_{W_2} > 16$ TeV and $|\zeta| \le 3 \times 10^{-5}$ [9]. Note that models with light ν_R do not have a see-saw mechanism for explaining the smallness of the neutrino masses, though other mechanisms may arise in variant models [10].

The mass of W_2 is severely constrained (independent of the value of ζ) from K_L–K_S mass-splitting. The box diagram with exchange of one W_L and one W_R has an anomalous enhancement and yields the bound $M_{W_2} \geq 1.6$ TeV [11] for the case of manifest or pseudo-manifest left-right symmetry. If the ν_R have Majorana masses, another constraint arises from neutrinoless double β decay. Combining the experimental limit from ^{76}Ge decay with arguments of vacuum stability, a limit of $M_{W_2} \geq 1.1$ TeV has been obtained [12].

Direct search limits: Limits on M_{W_2} from direct searches depend on the available decay channels of W_2. If ν_R is heavier than W_2, the decay $W_2^+ \to \ell_R^+ \nu_R$ will be forbidden kinematically. Assuming that ζ is small, the dominant decay of W_2 will be into dijets. UA2 [13] has excluded a W_2 in the mass range of 100 to 251 GeV in this channel. DØ excludes the mass range of 340 to 680 GeV [14], while CDF excludes the mass range of 300 to 420 GeV for such a W_2 [15]. If ν_R is lighter than W_2, the decay $W_2^+ \to e_R^+ \nu_R$ is allowed. The ν_R can then decay into $e_R W_R^*$, leading to an $eejj$ signature. DØ has a limit of $M_{W_2} > 720$ GeV if $m_{\nu_R} \ll M_{W_2}$; the bound weakens, for example, to 650 GeV for $m_{\nu_R} = M_{W_2}/2$ [16]. CDF finds $M_{W_2} > 652$ GeV if ν_R is stable and much lighter than W_2 [17]. All of these limits assume manifest or pseudo-manifest left-right symmetry. See [16] for some variations in the limits if the assumption of left-right symmetry is relaxed.

Alternative models: W' gauge bosons can also arise in other models. We shall briefly mention some such popular models, but for details we refer the reader to the original literature. The *alternate* left-right model [18] is based on the same gauge group as the left-right model, but arises in the following way: In E_6 unification, there is an option to identify the right-handed down quarks as $\mathrm{SU}(2)_R$ singlets or doublets. If they are $\mathrm{SU}(2)_R$ doublets, one recovers the conventional left-right model; if they are singlets it leads to the alternate left-right model. A similar ambiguity exists in the assignment of left-handed leptons; the alternate left-right model assigns them to a $(1, 2, 2, 0)$ multiplet. As a consequence, the ordinary neutrino remains exactly massless in the model. One important difference from the usual left-right model is that the limit from the K_L–K_S mass difference is no longer applicable, since the d_R do not couple to the W_R. There is also no limit from polarized μ decay, since the $\mathrm{SU}(2)_R$ partner of e_R can receive a large Majorana mass. Other W' models include the un-unified Standard Model of Ref. 19 where there are two different SU(2) gauge groups, one each for the quarks and leptons; models with separate SU(2) gauge factors for each generation [20]; and the $\mathrm{SU}(3)_C \times \mathrm{SU}(3)_L \times \mathrm{U}(1)$ model of Ref. 21.

Leptoquark gauge bosons: The $\mathrm{SU}(3)_C \times \mathrm{U}(1)_{B-L}$ part of the gauge symmetry discussed above can be embedded into a simple $\mathrm{SU}(4)_C$ gauge group [22]. The model then will contain leptoquark gauge boson as well, with couplings of the type $\{(\overline{e}_L \gamma_\mu d_L + \overline{\nu}_L \gamma_\mu u_L) W'^\mu + (L \to R)\}$. The best limit on such leptoquark W' comes from nonobservation of $K_L \to \mu e$, which requires $M_{W'} \geq 1400$ TeV; for the corresponding limits on less conventional leptoquark flavor structures, see Ref. 23. Thus such a W' is inaccessible to direct searches with present machines which are sensitive to vector leptoquark masses of order 300 GeV only.

References

1. J.C. Pati and A. Salam, Phys. Rev. **D10**, 275 (1974);
R.N. Mohapatra and J.C. Pati, Phys. Rev. **D11**, 566 (1975); *ibid.* Phys. Rev. **D11**, 2558 (1975);
G. Senjanovic and R.N. Mohapatra, Phys. Rev. **D12**, 1502 (1975).
2. P. Langacker and S. Uma Sankar, Phys. Rev. **D40**, 1569 (1989).
3. A. Masiero, R.N. Mohapatra, and R. Peccei, Nucl. Phys. **B192**, 66 (1981);
J. Basecq, *et al.*, Nucl. Phys. **B272**, 145 (1986).
4. J. Donoghue and B. Holstein, Phys. Lett. **113B**, 383 (1982).
5. K.S. Babu, K. Fujikawa, and A. Yamada, Phys. Lett. **B333**, 196 (1994);
P. Cho and M. Misiak, Phys. Rev. **D49**, 5894 (1994);
T.G. Rizzo, Phys. Rev. **D50**, 3303 (1994).
6. L. Wolfenstein, Phys. Rev. **D29**, 2130 (1984).
7. P. Herczeg, Phys. Rev. **D34**, 3449 (1986).
8. G. Steigman, K.A. Olive, and D. Schramm, Nucl. Phys. **B180**, 497 (1981).
9. R. Barbieri and R.N. Mohapatra, Phys. Rev. **D39**, 1229 (1989);
G. Raffelt and D. Seckel, Phys. Rev. Lett. **60**, 1793 (1988).
10. D. Chang and R.N. Mohapatra, Phys. Rev. Lett. **58**, 1600 (1987);
K.S. Babu and X.G. He, Mod. Phys. Lett. **A4**, 61 (1989).
11. G. Beall, M. Bender, and A. Soni, Phys. Rev. Lett. **48**, 848 (1982).
12. R.N. Mohapatra, Phys. Rev. **D34**, 909 (1986).
13. J. Alitti, *et al.* (UA2 Collaboration), Nucl. Phys. **B400**, 3 (1993).
14. B. Abbott, *et al.* (DØ Collaboration), International Europhysics Conference on High Energy Physics, August 19-26, 1997, Jerusalem, Israel.
15. F. Abe, *et al.* (CDF Collaboration), Phys. Rev. **D55**, R5263 (1997).
16. S. Abachi, *et al.* (DØ Collaboration), Phys. Rev. Lett. **76**, 3271 (1996).
17. F. Abe, *et al.* (CDF Collaboration), Phys. Rev. Lett. **74**, 2900 (1995).
18. E. Ma, Phys. Rev. **D36**, 274 (1987);
K.S. Babu, X-G. He and E. Ma, Phys. Rev. **D36**, 878 (1987).
19. H. Georgi and E. Jenkins, Phys. Rev. Lett. **62**, 2789 (1989);
Nucl. Phys. **B331**, 541 (1990).
20. X. Li and E. Ma, Phys. Rev. Lett. **47**, 1788 (1981);
R.S. Chivukula, E.H. Simmons, and J. Terning, Phys. Lett. **B331**, 383 (1994);
D.J. Muller and S. Nandi, Phys. Lett. **B383**, 345 (1996).

21. F. Pisano, V. Pleitez, Phys. Rev. **D46**, 410 (1992); P. Frampton, Phys. Rev. Lett. **69**, 2889 (1992).

22. J.C. Pati and A. Salam, Phys. Rev. **D10**, 275 (1974).

23. A. Kuznetsov and N. Mikheev, Phys. Lett. **B329**, 295 (1994); G. Valencia and S. Willenbrock, Phys. Rev. **D50**, 6843 (1994).

MASS LIMITS for W' (Heavy Charged Vector Boson Other Than W) in Hadron Collider Experiments

Couplings of W' to quarks and leptons are taken to be identical with those of W. The following limits are obtained from $p\overline{p} \rightarrow W' X$ with W' decaying to the mode indicated in the comments. New decay channels (*e.g.*, $W' \rightarrow WZ$) are assumed to be suppressed. UA1 and UA2 experiments assume that the $t\overline{b}$ channel is not open.

VALUE (GeV)	CL%	DOCUMENT ID		TECN	COMMENT
>786	95	[1] AFFOLDER	01I	CDF	$W' \rightarrow e\nu, \mu\nu$
• • • We do not use the following data for averages, fits, limits, etc. • • •					
225–536	95	[2] ACOSTA	03B	CDF	$W' \rightarrow tb$
none 200–480	95	[3] AFFOLDER	02C	CDF	$W' \rightarrow WZ$
>660	95	[4] ABE	00	CDF	$W' \rightarrow \mu\nu$
none 300–420	95	[5] ABE	97G	CDF	$W' \rightarrow q\overline{q}$
>720	95	[6] ABACHI	96C	D0	$W' \rightarrow e\nu$
>610	95	[7] ABACHI	95E	D0	$W' \rightarrow e\nu, \tau\nu$
>652	95	[8] ABE	95M	CDF	$W' \rightarrow e\nu$
>251	90	[9] ALITTI	93	UA2	$W' \rightarrow q\overline{q}$
none 260–600	95	[10] RIZZO	93	RVUE	$W' \rightarrow q\overline{q}$
>220	90	[11] ALBAJAR	89	UA1	$W' \rightarrow e\nu$
>209	90	[12] ANSARI	87D	UA2	$W' \rightarrow e\nu$

[1] AFFOLDER 01I combine a new bound on $W' \rightarrow e\nu$ of 754 GeV with the bound of ABE 00 on $W' \rightarrow \mu\nu$ to obtain quoted bound.

[2] The ACOSTA 03B quoted limit is for $M_{W'} \gg M_{\nu_R}$. For $M_{W'} < M_{\nu_R}$, $M_{W'}$ between 225 and 566 GeV is excluded.

[3] The quoted limit is obtained assuming $W'WZ$ coupling strength is the same as the ordinary WWZ coupling strength in the Standard Model. See their Fig. 2 for the limits on the production cross sections as a function of the W' width.

[4] ABE 00 assume that the neutrino from W' decay is stable and has a mass significantly less than $m_{W'}$.

[5] ABE 97G search for new particle decaying to dijets.

[6] For bounds on W_R with nonzero right-handed mass, see Fig. 5 from ABACHI 96C.

[7] ABACHI 95E assume that the decay $W' \rightarrow WZ$ is suppressed and that the neutrino from W' decay is stable and has a mass significantly less $m_{W'}$.

[8] ABE 95M assume that the decay $W' \rightarrow WZ$ is suppressed and the (right-handed) neutrino is light, noninteracting, and stable. If m_ν=60 GeV, for example, the effect on the mass limit is negligible.

[9] ALITTI 93 search for resonances in the two-jet invariant mass. The limit assumes $\Gamma(W')/m_{W'} = \Gamma(W)/m_W$ and $B(W' \rightarrow jj) = 2/3$. This corresponds to W_R with $m_{\nu_R} > m_{W_R}$ (no leptonic decay) and $W_R \rightarrow t\overline{b}$ allowed. See their Fig. 4 for limits in the $m_{W'}$–$B(q\overline{q})$ plane.

[10] RIZZO 93 analyses CDF limit on possible two-jet resonances. The limit is sensitive to the inclusion of the assumed K factor.

[11] ALBAJAR 89 cross section limit at 630 GeV is $\sigma(W')\, B(e\nu) <$ 4.1 pb (90% CL).

[12] See Fig. 5 of ANSARI 87D for the excluded region in the $m_{W'}$–$[(g_{W'q})^2\, B(W' \rightarrow e\overline{\nu})]$ plane. Note that the quantity $(g_{W'q})^2\, B(W' \rightarrow e\overline{\nu})$ is normalized to unity for the standard W couplings.

W_R (Right-Handed W Boson) MASS LIMITS

Assuming a light right-handed neutrino, except for BEALL 82, LANGACKER 89B, and COLANGELO 91. $g_R = g_L$ assumed. [Limits in the section MASS LIMITS for W' below are also valid for W_R if $m_{\nu_R} \ll m_{W_R}$.] Some limits assume manifest left-right symmetry, *i.e.*, the equality of left- and right Cabibbo-Kobayashi-Maskawa matrices. For a comprehensive review, see LANGACKER 89B. Limits on the W_L-W_R mixing angle ζ are found in the next section. Values in brackets are from cosmological and astrophysical considerations and assume a light right-handed neutrino.

VALUE (GeV)	CL%	DOCUMENT ID		TECN	COMMENT
> 715	90	[13] CZAKON	99	RVUE	Electroweak
• • • We do not use the following data for averages, fits, limits, etc. • • •					
> 310	90	[14] THOMAS	01	CNTR	β^+ decay
> 137	95	[15] ACKERSTAFF	99D	OPAL	τ decay
>1400	68	[16] BARENBOIM	98	RVUE	Electroweak, Z-Z' mixing
> 549	68	[17] BARENBOIM	97	RVUE	μ decay
> 220	95	[18] STAHL	97	RVUE	τ decay
> 220	90	[19] ALLET	96	CNTR	β^+ decay
> 281	90	[20] KUZNETSOV	95	CNTR	Polarized neutron decay
> 282	90	[21] KUZNETSOV	94B	CNTR	Polarized neutron decay
> 439	90	[22] BHATTACH...	93	RVUE	Z-Z' mixing
> 250	90	[23] SEVERIJNS	93	CNTR	β^+ decay
		[24] IMAZATO	92	CNTR	K^+ decay
> 475	90	[25] POLAK	92B	RVUE	μ decay
> 240	90	[26] AQUINO	91	RVUE	Neutron decay
> 496	90	[26] AQUINO	91	RVUE	Neutron and muon decay
> 700		[27] COLANGELO	91	THEO	$m_{K^0_L} - m_{K^0_S}$
> 477	90	[28] POLAK	91	RVUE	μ decay
[none 540–23000]		[29] BARBIERI	89B	ASTR	SN 1987A; light ν_R
> 300	90	[30] LANGACKER	89B	RVUE	General
> 160	90	[31] BALKE	88	CNTR	$\mu \rightarrow e\nu\overline{\nu}$
> 406	90	[32] JODIDIO	86	ELEC	Any ζ
> 482	90	[32] JODIDIO	86	ELEC	$\zeta = 0$
> 800		MOHAPATRA	86	RVUE	$SU(2)_L \times SU(2)_R \times U(1)$
> 400	95	[33] STOKER	85	ELEC	Any ζ
> 475	95	[33] STOKER	85	ELEC	ζ <0.041
		[34] BERGSMA	83	CHRM	$\nu_\mu e \rightarrow \mu\nu_e$
> 380	90	[35] CARR	83	ELEC	μ^+ decay
>1600		[36] BEALL	82	THEO	$m_{K^0_L} - m_{K^0_S}$
[> 4000]		STEIGMAN	79	COSM	Nucleosynthesis; light ν_R

[13] CZAKON 99 perform a simultaneous fit to charged and neutral sectors.

[14] THOMAS 01 limit is from measurement of β^+ polarization in decay of polarized ^{12}N. The listed limit assumes no mixing.

[15] ACKERSTAFF 99D limit is from τ decay parameters. Limit increase to 145 GeV for zero mixing.

[16] BARENBOIM 98 assumes minimal left-right model with Higgs of $SU(2)_R$ in $SU(2)_L$ doublet. For Higgs in $SU(2)_L$ triplet, m_{W_R} >1100 GeV. Bound calculated from effect of corresponding Z_{LR} on electroweak data through Z–Z_{LR} mixing.

[17] The quoted limit is from μ decay parameters. BARENBOIM 97 also evaluate limit from K_L-K_S mass difference.

[18] STAHL 97 limit is from fit to τ-decay parameters.

[19] ALLET 96 measured polarization-asymmetry correlation in ^{12}Nβ^+ decay. The listed limit assumes zero L-R mixing.

[20] KUZNETSOV 95 limit is from measurements of the asymmetry $\langle \overline{p}_\nu \cdot \sigma_n \rangle$ in the β decay of polarized neutrons. Zero mixing assumed. See also KUZNETSOV 94B.

[21] KUZNETSOV 94B limit is from measurements of the asymmetry $\langle \overline{p}_\nu \cdot \sigma_n \rangle$ in the β decay of polarized neutrons. Zero mixing assumed.

[22] BHATTACHARYYA 93 uses Z-Z' mixing limit from LEP '90 data, assuming a specific Higgs sector of $SU(2)_L \times SU(2)_R \times U(1)$ gauge model. The limit is for m_t=200 GeV and slightly improves for smaller m_t.

[23] SEVERIJNS 93 measured polarization-asymmetry correlation in ^{107}Inβ^+ decay. The listed limit assumes zero L-R mixing. Value quoted here is from SEVERIJNS 94 erratum.

[24] IMAZATO 92 measure positron asymmetry in $K^+ \rightarrow \mu^+\nu_\mu$ decay and obtain $\xi P_\mu >$ 0.990 (90%CL). If W_R couples to $u\overline{s}$ with full weak strength (V^R_{us}=1), the result corresponds to m_{W_R} >653 GeV. See their Fig. 4 for m_{W_R} limits for general $|V^R_{us}|^2 = 1 - |V^R_{ud}|^2$.

[25] POLAK 92B limit is from fit to muon decay parameters and is essentially determined by JODIDIO 86 data assuming ζ=0. Supersedes POLAK 91.

[26] AQUINO 91 limits obtained from neutron lifetime and asymmetries together with unitarity of the CKM matrix. Manifest left-right symmetry assumed. Stronger of the two limits also includes muon decay results.

[27] COLANGELO 91 limit uses hadronic matrix elements evaluated by QCD sum rule and is less restrictive than BEALL 82 limit which uses vacuum saturation approximation. Manifest left-right symmetry assumed.

[28] POLAK 91 limit is from fit to muon decay parameters and is essentially determined by JODIDIO 86 data assuming ζ=0. Superseded by POLAK 92B.

[29] BARBIERI 89B limit holds for $m_{\nu_R} \leq$ 10 MeV.

[30] LANGACKER 89B limit is for any ν_R mass (either Dirac or Majorana) and for a general class of right-handed quark mixing matrices.

[31] BALKE 88 limit is for $m_{\nu_{eR}} = 0$ and $m_{\nu_{\mu R}} \leq$ 50 MeV. Limits come from precise measurements of the muon decay asymmetry as a function of the positron energy.

[32] JODIDIO 86 is the same TRIUMF experiment as STOKER 85 (and CARR 83); however, it uses a different technique. The results given here are combined results of the two techniques. The technique here involves precise measurement of the end-point e^+ spectrum in the decay of the highly polarized μ^+.

[33] STOKER 85 is same TRIUMF experiment as CARR 83. Here they measure the decay e^+ spectrum asymmetry above 46 MeV/c using a muon-spin-rotation technique. Assumed a light right-handed neutrino. Quoted limits are from combining with CARR 83.

[34] BERGSMA 83 set limit m_{W_2}/m_{W_1} >1.9 at CL = 90%.

[35] CARR 83 is TRIUMF experiment with a highly polarized μ^+ beam. Looked for deviation from $V-A$ at the high momentum end of the decay e^+ energy spectrum. Limit from previous world-average muon polarization parameter is m_{W_R} >240 GeV. Assumes a light right-handed neutrino.

[36] BEALL 82 limit is obtained assuming that W_R contribution to K^0_L–K^0_S mass difference is smaller than the standard one, neglecting the top quark contributions. Manifest left-right symmetry assumed.

Limit on W_L-W_R Mixing Angle ζ

Lighter mass eigenstate $W_1 = W_L\cos\zeta - W_R\sin\zeta$. Light ν_R assumed unless noted. Values in brackets are from cosmological and astrophysical considerations.

VALUE	CL%	DOCUMENT ID		TECN	COMMENT
• • • We do not use the following data for averages, fits, limits, etc. • • •					
< 0.12	95	[37] ACKERSTAFF	99D	OPAL	τ decay
< 0.013	90	[38] CZAKON	99	RVUE	Electroweak
< 0.0333		[39] BARENBOIM	97	RVUE	μ decay
< 0.04	90	[40] MISHRA	92	CCFR	νN scattering
−0.0006 to 0.0028	90	[41] AQUINO	91	RVUE	
[none 0.00001–0.02]		[42] BARBIERI	89B	ASTR	SN 1987A
< 0.040	90	[43] JODIDIO	86	ELEC	μ decay
−0.056 to 0.040	90	[43] JODIDIO	86	ELEC	μ decay

[37] ACKERSTAFF 99D limit is from τ decay parameters.

[38] CZAKON 99 perform a simultaneous fit to charged and neutral sectors.

[39] The quoted limit is from μ decay parameters. BARENBOIM 97 also evaluate limit from K_L-K_S mass difference.

[40] MISHRA 92 limit is from the absence of extra large-x, large-y $\overline{\nu}_\mu N \rightarrow \overline{\nu}_\mu X$ events at Tevatron, assuming left-handed ν and right-handed $\overline{\nu}$ in the neutrino beam. The result gives $\zeta^2(1-2m^2_{W_1}/m^2_{W_2}) < 0.0015$. The limit is independent of ν_R mass.

[41] AQUINO 91 limits obtained from neutron lifetime and asymmetries together with unitarity of the CKM matrix. Manifest left-right asymmetry is assumed.

[42] BARBIERI 89B limit holds for $m_{\nu_R} \leq 10$ MeV.

[43] First JODIDIO 86 result assumes $m_{W_R}=\infty$, second is for unconstrained m_{W_R}.

THE Z' SEARCHES

Revised March 2002 by K.S. Babu (Oklahoma State University) and C. Kolda (Notre Dame University).

New massive and electrically neutral gauge bosons are a common feature of physics beyond the Standard Model. They are present in most extensions of the Standard Model gauge group, including models in which the Standard Model is embedded into a unifying group. They can also arise in certain classes of theories with extra dimensions. Whatever the source, such a gauge boson is called a Z'. While current theories suggest that there may be a multitude of such states at or just below the Planck scale, there exist many models in which the Z' sits at or near the weak scale. Models with extra neutral gauge bosons often contain charged gauge bosons as well; these are discussed in the review of W' physics.

The Lagrangian describing a single Z' and its interactions with the fields of the Standard Model is [1,2,3]:

$$\begin{aligned}\mathcal{L}_{Z'} = &-\frac{1}{4}F'_{\mu\nu}F'^{\mu\nu} - \frac{\sin\chi}{2}F'_{\mu\nu}F^{\mu\nu} + M^2_{Z'}Z'_\mu Z'^\mu \\ &+ \delta M^2\, Z'_\mu Z^\mu - \frac{e}{2c_W s_W}\sum_i \overline{\psi}_i\gamma^\mu(f^i_V - f^i_A\gamma^5)\psi_i Z'_\mu\end{aligned} \tag{1}$$

where c_W, s_W are the cosine and sine of the weak angle, $F_{\mu\nu}$, $F'_{\mu\nu}$ are the field strength tensors for the hypercharge and the Z' gauge bosons respectively, ψ_i are the matter fields with Z' vector and axial charges f^i_V and f^i_A, and Z_μ is the electroweak Z-boson. (The overall Z' coupling strength has been normalized to that of the usual Z.) The mass terms are assumed to come from spontaneous symmetry breaking via scalar expectation values; the δM^2 term is generated by Higgs bosons that are charged under both the Standard Model and the extra gauge symmetry, and can have either sign. The above Lagrangian is general to all abelian and non-abelian extensions; however, for the non-abelian case, $F'_{\mu\nu}$ is not gauge invariant and so the kinetic mixing parameter $\chi = 0$. Most analyses take $\chi = 0$, even for the abelian case, and so we do likewise here; see Ref. 3 for a discussion of observables with $\chi \neq 0$.

Strictly speaking, the Z' defined in the Lagrangian above is not a mass eigenstate since it can mix with the usual Z boson. The mixing angle is given by

$$\xi \simeq \frac{\delta M^2}{M^2_Z - M^2_{Z'}}\,. \tag{2}$$

This mixing can alter a large number of the Z-pole observables, including the T-parameter which receives a contribution

$$\alpha T_{\rm new} = \xi^2\left(\frac{M^2_{Z'}}{M^2_Z} - 1\right) \tag{3}$$

to leading order in small ξ. (For $\chi \neq 0$, both S and T receive additional contributions [4,3].) However, the oblique parameters do not encode all the effects generated by $Z-Z'$ mixing; the mixing also alters the couplings of the Z itself, shifting its vector and axial couplings to $T^i_3 - 2Q^i s^2_W + \xi f^i_V$ and $T^i_3 + \xi f^i_A$ respectively.

If the Z' charges are generation-dependent, tree-level flavor-changing neutral currents will generically arise. There exist severe constraints in the first two generations coming from precision measurements such as the $K_L - K_S$ mass splitting and $B(\mu \rightarrow 3e)$; constraints on a Z' which couples differently only to the third generation are somewhat weaker. If the Z' interactions commute with the Standard Model gauge group, then per generation, there are only five independent $Z'\bar{\psi}\psi$ couplings; one can choose them to be $f^u_V, f^u_A, f^d_V, f^e_V, f^e_A$. All other couplings can be determined in terms of these, *e.g.*, $f^\nu_V = (f^e_V + f^e_A)/2$.

Experimental Constraints: There are four primary sets of constraints on the existence of a Z' which will be considered here: precision measurements of neutral current processes at low energies, Z-pole constraints on $Z-Z'$ mixing, indirect constraints from precision electroweak measurements off the Z-pole, and direct search constraints from production at very high energies. In principle, one should expect other new states to appear at the same scale as the Z', including its symmetry-breaking sector and any additional fermions necessary for anomaly cancellation. Because these states are highly model-dependent, searches for these states, or for Z' decays into them, are not included in the Listings.

Low-energy Constraints: After the gauge symmetry of the Z' and the electroweak symmetry are both broken, the Z of the Standard Model can mix with the Z', with mixing angle ξ defined above. As already discussed, this $Z-Z'$ mixing implies a shift in the usual oblique parameters. Current bounds on T (and S) translate into stringent constraints on the mixing angle, ξ, requiring $\xi \ll 1$; similar constraints on ξ arise from the LEP Z-pole data. Thus, we will only consider the small-ξ limit henceforth.

Whether or not the new gauge interactions are parity violating, stringent constraints can arise from atomic parity violation (APV) and polarized electron-nucleon scattering experiments [5]. At low energies, the effective neutral current Lagrangian is conventionally written:

$$\mathcal{L}_{\rm NC} = \frac{G_F}{\sqrt{2}}\sum_{q=u,d}\left\{C_{1q}(\bar{e}\gamma_\mu\gamma^5 e)(\bar{q}\gamma^\mu q) + C_{2q}(\bar{e}\gamma_\mu e)(\bar{q}\gamma^\mu\gamma^5 q)\right\}. \tag{4}$$

APV experiments are sensitive only to C_{1u} and C_{1d} through the "weak charge" $Q_W = -2\,[C_{1u}(2Z+N) + C_{1d}(Z+2N)]$, where

$$C_{1q} = 2(1+\alpha T)(g_A^e + \xi f_A^e)(g_V^q + \xi f_V^q) + 2r(f_A^e f_V^q) \quad (5)$$

with $r = M_Z^2/M_{Z'}^2$. (Terms $\mathcal{O}(r\xi)$ are dropped.) The r-dependent terms arise from Z' exchange and can interfere constructively or destructively with the Z contribution. In the limit $\xi = r = 0$, this reduces to the Standard Model expression. Polarized electron scattering is sensitive to both the C_{1q} and C_{2q} couplings, again as discussed in the Standard Model review. The C_{2q} can be derived from the expression for C_{1q} with the complete interchange $V \leftrightarrow A$.

Stringent limits also arise from neutrino-hadron scattering. One usually expresses experimental results in terms of the effective 4-fermion operators $(\bar\nu\gamma_\mu\nu)(\bar q_{L,R}\gamma^\mu q_{L,R})$ with coefficients $(2\sqrt{2}G_F)\epsilon_{L,R}(q)$. (Again, see the Standard Model review.) In the presence of the Z and Z', the $\epsilon_{L,R}(q)$ are given by:

$$\epsilon_{L,R}(q) = \frac{1+\alpha T}{2}\left\{(g_V^q \pm g_A^q)[1+\xi(f_V^\nu \pm f_A^\nu)] + \xi(f_V^q \pm f_A^q)\right\} + \frac{r}{2}(f_V^q \pm f_A^q)(f_V^\nu \pm f_A^\nu)\,. \quad (6)$$

Again, the r-dependent terms arise from Z'-exchange.

Z-pole Constraints: Electroweak measurements made at LEP and SLC while sitting on the Z-resonance are generally sensitive to Z' physics only through the mixing with the Z, unless the Z and Z' are very nearly degenerate. Constraints on the allowed mixing angle and Z' couplings arise by fitting all data simultaneously to the *ansatz* of $Z - Z'$ mixing. A number of such fits are included in the Listings. If the listed analysis uses data only from the Z resonance, it is marked with a comment "Z parameters" while it is commented as "Electroweak" if low-energy data is also included in the fits. Both types of fits place simultaneous limits on the Z' mass and on ξ.

High-energy Indirect Constraints: At $\sqrt{s} < M_{Z'}$, but off the Z-pole, strong constraints on new Z' physics arise by comparing measurements of asymmetries and leptonic and hadronic cross-sections with their Standard Model predictions. These processes are sensitive not only to $Z - Z'$ mixing, but also to direct Z' exchange primarily through $\gamma - Z'$ and $Z - Z'$ interference; therefore, information on the Z' couplings and mass can be extracted that is not accessible via $Z - Z'$ mixing alone.

Far below the Z' mass scale, experiments at a given $\sqrt{s}$ are only sensitive to the scaled Z' couplings $\sqrt{s}f_{V,A}^i/M_{Z'}$. However, the Z' mass and overall magnitude of the couplings can be separately extracted if measurements are made at more than one energy. As $\sqrt{s}$ approaches $M_{Z'}$ the Z' exchange can no longer be approximated by a contact interaction and the mass and couplings can be simultaneously extracted.

Z' studies done before LEP relied heavily on this approach; see, for example, Ref. 6. LEP has also done similar work using data collected above the Z-peak; see, for example, Ref. 7. For indirect Z' searches at future facilities, see, for example, Refs. 8,9. At a hadron collider the possibility of measuring leptonic forward-backward asymmetries has been suggested [10] and used [11] in searches for a Z' below its threshold.

Direct Search Constraints: Finally, high-energy experiments have searched for on-shell Z' production and decay. Searches can be classified by the initial state off of which the Z' is produced, and the final state into which the Z' decays; exotic decays of a Z' are not included in the listings. Experiments to date have been sensitive to Z' production via their coupling to quarks ($p\bar p$ colliders), to electrons (e^+e^-), or to both (ep).

For a heavy Z' ($M_{Z'} \gg M_Z$), the best limits come from $p\bar p$ machines via Drell-Yan production and subsequent decay to charged leptons. For $M_{Z'} > 600$ GeV, CDF [12] quotes limits on $\sigma(p\bar p \to Z'X)\cdot B(Z' \to \ell^+\ell^-) < 0.04$ pb at 95% C.L. for $\ell = e+\mu$ combined; DØ [13] quotes $\sigma \cdot B < 0.06$ pb for $\ell = e$ and $M_{Z'} > 500$ GeV. For smaller masses, the bounds can be found in the original literature. For studies of the search capabilities of future facilities, see, for example, Ref. 8.

If the Z' has suppressed, or no, couplings to leptons (*i.e.*, it is leptophobic), then experimental sensitivities are much weaker. Searches for a Z' via hadronic decays at CDF [14] are unable to rule out a Z' with quark couplings identical to those of the Z in any mass region. UA2 [15] does find $\sigma \cdot B(Z' \to jj) < 11.7$ pb at 90% C.L. for $M_{Z'} > 200$ GeV, with more complicated bounds in the range 130 GeV $< M_{Z'} <$ 200 GeV.

For a light Z' ($M_{Z'} < M_Z$), direct searches in e^+e^- colliders have ruled out any Z', unless it has extremely weak couplings to leptons. For a combined analysis of the various pre-LEP experiments see Ref. 6.

Canonical Models: One of the prime motivations for an additional Z' has come from string theory, in which certain compactifications lead naturally to an E_6 gauge group, or one of its subgroups. E_6 contains two U(1) factors beyond the Standard Model, a basis for which is formed by the two groups $\mathrm{U}(1)_\chi$ and $\mathrm{U}(1)_\psi$, defined via the decompositions $E_6 \to \mathrm{SO}(10)\times\mathrm{U}(1)_\psi$ and $\mathrm{SO}(10) \to \mathrm{SU}(5)\times\mathrm{U}(1)_\chi$; one special case often encountered is $\mathrm{U}(1)_\eta$, where $Q_\eta = \sqrt{\frac{3}{8}}Q_\chi - \sqrt{\frac{5}{8}}Q_\psi$. The charges of the SM fermions under these U(1)'s can be found in Table 1, and a discussion of their experimental signatures can be found in Ref. 16. A separate listing appears for each of the canonical models, with direct and indirect constraints combined.

It is also common to express experimental bounds in terms of a toy Z', usually denoted Z'_{SM}. This Z'_{SM}, of arbitrary mass, couples to the SM fermions identically to the usual Z. Almost all analyses of Z' physics have worked with one of these canonical models and have assumed zero kinetic mixing at the weak scale.

Extra Dimensions: A new motivation for Z' searches comes from recent work on extensions of the Standard Model into extra

Table 1: Charges of Standard Model fermions in canonical Z' models.

	Y	T_{3R}	$B-L$	$\sqrt{24}Q_\chi$	$\sqrt{\frac{72}{5}}Q_\psi$	Q_η
ν_L, e_L	$-\frac{1}{2}$	0	-1	$+3$	$+1$	$+\frac{1}{6}$
ν_R	0	$+\frac{1}{2}$	-1	$+5$	-1	$+\frac{5}{6}$
e_R	-1	$-\frac{1}{2}$	-1	$+1$	-1	$+\frac{1}{3}$
u_L, d_L	$+\frac{1}{6}$	0	$+\frac{1}{3}$	-1	$+1$	$-\frac{1}{3}$
u_R	$+\frac{2}{3}$	$+\frac{1}{2}$	$+\frac{1}{3}$	$+1$	-1	$+\frac{1}{3}$
d_R	$-\frac{1}{3}$	$-\frac{1}{2}$	$+\frac{1}{3}$	-3	-1	$-\frac{1}{6}$

dimensions. (See the "Review of Extra Dimensions" for many details not included here.) In some classes of these models, the gauge bosons of the Standard Model can inhabit these new directions [17]. When compactified down to the usual (3+1) dimensions, the extra degrees of freedom that were present in the higher-dimensional theory (associated with propagation in the extra dimensions) appear as a tower of massive gauge bosons, called Kaluza-Klein (KK) states. The simplest case is the compactification of a $(4+d)$-dimensional space on a d-torus (T^d) of uniform radius R in all d directions. Then a tower of massive gauge bosons are present with masses

$$M^2_{V_{\vec{n}}} = M^2_{V_{\vec{0}}} + \frac{\vec{n}\cdot\vec{n}}{R^2}\,, \tag{7}$$

where V represents any of the gauge fields of the Standard Model and $\vec{n}$ is a d-vector whose components are semi-positive integers; the vector $\vec{n}=(0,0,\dots 0)$ corresponds to the "zero-mode" gauge boson, which is nothing more than the usual gauge boson of the Standard Model, with mass $M_{V_{\vec{0}}}=M_V$. Compactifications on either non-factorizable or asymmetric manifolds can significantly alter the KK mass formula, but a tower of states will nonetheless persist. All bounds cited in the Listings assume the maximally symmetric spectrum given above for simplicity.

The KK mass formula, coupled with the absence of any observational evidence for W' or Z' states below the weak scale, implies that the extra dimensions in which gauge bosons can propagate must have inverse radii greater than at least a few hundred GeV. If any extra dimensions are larger than this, gravity alone may propagate in them.

Though the gauge principle guarantees that the usual Standard Model gauge fields couple with universal strength (or gauge coupling) to all charged matter, the coupling of KK bosons to ordinary matter is highly model-dependent. In the simplest case, all Standard Model fields are localized at the same point in the d-dimensional subspace; in the parlance of the field, they all live on the same 3-brane. Then the couplings of KK bosons are identical to those of the usual gauge fields, but enhanced: $g_{KK}=\sqrt{2}\,g$. However, in many models, particularly those which naturally suppress proton decay [18], it is common to find ordinary fermions living on different, parallel branes in the extra dimensions. In such cases, different fermions experience very different coupling strengths for the KK states; the effective coupling varies fermion by fermion, and also KK mode by KK mode. In the particular case that fermions of different generations with identical quantum numbers are placed on different branes, large flavor-changing neutral currents can occur unless the mass scale of the KK states is very heavy: $R^{-1}\gtrsim 1000\,\text{TeV}$ [19]. In the Listings, all bounds assume that Standard Model fermions live on a single 3-brane. (The case of the Higgs field is again complicated; see the footnotes on the individual listings.)

In some sense, searches for KK bosons are no different than searches for any other Z' or W'; in fact, bounds on the artificially defined $Z'_{\rm SM}$ are almost precisely bounds on the first KK mode of the Z^0, modulo the $\sqrt{2}$ enhancement in the coupling strength. To date, no experiment has examined direct production of KK Z^0 bosons, but an approximate bound of 820 GeV [20] can be inferred from the CDF bound on Z'_{SM} [12].

Indirect bounds have a very different behavior for KK gauge bosons than for canonical Z' bosons; a number of indirect bounds are given in the Listings. Indirect bounds arise from virtual boson exchange and require a summation over the entire tower of KK states. For $d>1$, this summation diverges, a remnant of the non-renormalizability of the underlying $(4+d)$-dimensional field theory. In a fully consistent theory, such as a string theory, the summation would be regularized and finite. However, this procedure cannot be uniquely defined within the confines of our present knowledge, and so most authors choose to terminate the sum with an explicit cut-off, Λ_{KK}, set equal to the "Planck scale" of the D-dimensional theory, M_D [21]. Reasonable arguments exist that this cut-off could be very different and could vary by process, and so these bounds should be regarded merely as indicative [22].

References

1. B. Holdom, Phys. Lett. **166B**, 196 (1986).
2. F. del Aguila, Acta Phys. Polon. **B25**, 1317 (1994); F. del Aguila, M. Cvetič, and P. Langacker, Phys. Rev. **D52**, 37 (1995).
3. K.S. Babu, C. Kolda, and J. March-Russell, Phys. Rev. **D54**, 4635 (1996); *ibid.*, **D57**, 6788 (1998).
4. B. Holdom, Phys. Lett. **B259**, 329 (1991).
5. J. Kim *et al.*, Rev. Mod. Phys. **53**, 211 (1981); U. Amaldi *et al.*, Phys. Rev. **D36**, 1385 (1987); W. Marciano and J. Rosner, Phys. Rev. Lett. **65**, 2963 (1990) (*Erratum:* **68**, 898 (1992)); K. Mahanthappa and P. Mohapatra, Phys. Rev. **D43**, 3093 (1991) (*Erratum:* **D44**, 1616 (1991)); P. Langacker and M. Luo, Phys. Rev. **D45**, 278 (1992); P. Langacker, M. Luo, and A. Mann, Rev. Mod. Phys. **64**, 87 (1992).
6. L. Durkin and P. Langacker, Phys. Lett. **166B**, 436 (1986).
7. P. Abreu *et al.*, (DELPHI Collaboration), Eur. Phys. J. **C11**, 383 (1999); R. Barate *et al.*, (ALEPH Collaboration) Eur. Phys. J. **C12**, 183 (1999).

8. M. Cvetiĉ and S. Godfrey, in *Electroweak Symmetry Breaking and New Physics at the TeV Scale*, eds. T. Barklow *et al.*, (World Scientific 1996), p. 383 [hep-ph/9504216].
9. T. Rizzo, Phys. Rev. **D55**, 5483 (1997).
10. J. L. Rosner, Phys. Rev. **D54**, 1078 (1996).
11. T. Affolder *et al.*, (CDF Collaboration), Phys. Rev. Lett. **87**, 131802 (2001).
12. F. Abe *et al.*, (CDF Collaboration), Phys. Rev. Lett. **79**, 2191 (1997).
13. V. Abazov *et al.*, (D0 Collaboration), Phys. Rev. Lett. **87**, 061802 (2001).
14. F. Abe *et al.*, (CDF Collaboration), Phys. Rev. **D55**, 5263R (1997) and Phys. Rev. Lett. **82**, 2038 (1999).
15. J. Alitti *et al.*, (UA2 Collaboration), Nucl. Phys. **B400**, 3 (1993).
16. J. Hewett and T. Rizzo, Phys. Rept. **183**, 193 (1989).
17. I. Antoniadis, Phys. Lett. **B246**, 377 (1990);
I. Antoniadis, K. Benakli, and M. Quiros, Phys. Lett. **B331**, 313 (1994);
K. Dienes, E. Dudas, and T. Gherghetta, Phys. Lett. B **436**, 55 (1998);
A. Pomarol and M. Quiros, Phys. Lett. **B438**, 255 (1998).
18. N. Arkani-Hamed and M. Schmaltz, Phys. Rev. **D61**, 033005 (2000).
19. A. Delgado, A. Pomarol, and M. Quiros, JHEP **0001**, 030 (2000).
20. M. Masip and A. Pomarol, Phys. Rev. **D60**, 096005 (1999).
21. G. Giudice, R. Rattazzi, and J. Wells, Nucl. Phys. **B544**, 3 (1999);
T. Han, J. Lykken, and R. Zhang, Phys. Rev. **D59**, 105006 (1999);
J. Hewett, Phys. Rev. Lett. **82**, 4765 (1999).
22. See for example: M. Bando *et al.*, Phys. Rev. Lett. **83**, 3601 (1999);
T. Rizzo and J. Wells, Phys. Rev. **D61**, 016007 (2000);
S. Cullen, M. Perelstein, and M. Peskin, Phys. Rev. **D62**, 055012 (2000).

MASS LIMITS for Z' (Heavy Neutral Vector Boson Other Than Z)

Limits for Z'_{SM}

Z'_{SM} is assumed to have couplings with quarks and leptons which are identical to those of Z, and decays only to known fermions.

VALUE (GeV)	*CL%*	*DOCUMENT ID*	*TECN*	*COMMENT*
>1500	95	[44] CHEUNG 01B	RVUE	Electroweak
> 690	95	[45] ABE 97S	CDF	$p\overline{p}$; $Z'_{SM} \rightarrow e^+e^-$, $\mu^+\mu^-$
• • • We do not use the following data for averages, fits, limits, etc. • • •				
> 670	95	[46] ABAZOV 01B	D0	$p\overline{p}$, $Z'_{SM} \rightarrow e^+e^-$
> 710	95	[47] ABREU 00S	DLPH	e^+e^-
> 898	95	[48] BARATE 00I	ALEP	e^+e^-
> 809	95	[49] ERLER 99	RVUE	Electroweak
> 490	95	ABACHI 96D	D0	$p\overline{p}$; $Z'_{SM} \rightarrow e^+e^-$
> 398	95	[50] VILAIN 94B	CHM2	$\nu_\mu e \rightarrow \nu_\mu e$ and $\overline{\nu}_\mu e \rightarrow \overline{\nu}_\mu e$
> 237	90	[51] ALITTI 93	UA2	$p\overline{p}$; $Z'_{SM} \rightarrow q\overline{q}$
none 260–600	95	[52] RIZZO 93	RVUE	$p\overline{p}$; $Z'_{SM} \rightarrow q\overline{q}$
> 426	90	[53] ABE 90F	VNS	e^+e^-

[44] CHEUNG 01B limit is derived from bounds on contact interactions in a global electroweak analysis.

[45] ABE 97S find $\sigma(Z')\times$B$(e^+e^-,\mu^+\mu^-)<$ 40 fb for $m_{Z'} >$ 600 GeV at $\sqrt{s}$= 1.8 TeV.

[46] ABAZOV 01B search for resonances in $p\overline{p} \rightarrow e^+e^-$ at $\sqrt{s}$=1.8 TeV. They find $\sigma\cdot$B$(Z' \rightarrow ee)<$ 0.06 pb for $M_{Z'} >$ 500 GeV.

[47] ABREU 00S uses LEP data at $\sqrt{s}$=90 to 189 GeV.

[48] BARATE 00I search for deviations in cross section and asymmetries in $e^+e^- \rightarrow$ fermions at $\sqrt{s}$=90 to 183 GeV. Assume θ=0. Bounds in the mass-mixing plane are shown in their Figure 18.

[49] ERLER 99 give 90%CL limit on the Z-Z' mixing $-0.0041 < \theta < 0.0003$. ρ_0=1 is assumed.

[50] VILAIN 94B assume m_t = 150 GeV.

[51] ALITTI 93 search for resonances in the two-jet invariant mass. The limit assumes B$(Z' \rightarrow q\overline{q})$=0.7. See their Fig. 5 for limits in the $m_{Z'}$–B$(q\overline{q})$ plane.

[52] RIZZO 93 analyses CDF limit on possible two-jet resonances.

[53] ABE 90F use data for R, $R_{\ell\ell}$, and $A_{\ell\ell}$. They fix m_W = 80.49 ± 0.43 ± 0.24 GeV and m_Z = 91.13 ± 0.03 GeV.

Limits for Z_{LR}

Z_{LR} is the extra neutral boson in left-right symmetric models. $g_L = g_R$ is assumed unless noted. Values in parentheses assume stronger constraint on the Higgs sector, usually motivated by specific left-right symmetric models (see the Note on the W'). Values in brackets are from cosmological and astrophysical considerations and assume a light right-handed neutrino. Direct search bounds assume decays to Standard Model fermions only, unless noted.

VALUE (GeV)	*CL%*	*DOCUMENT ID*	*TECN*	*COMMENT*
>860	95	[54] CHEUNG 01B	RVUE	Electroweak
>630	95	[55] ABE 97S	CDF	$p\overline{p}$; $Z'_{LR} \rightarrow e^+e^-$, $\mu^+\mu^-$
• • • We do not use the following data for averages, fits, limits, etc. • • •				
>380	95	[56] ABREU 00S	DLPH	e^+e^-
>436	95	[57] BARATE 00I	ALEP	e^+e^-
>550	95	[58] CHAY 00	RVUE	Electroweak
		[59] ERLER 00	RVUE	Cs
		[60] CASALBUONI 99	RVUE	Cs
(> 1205)	90	[61] CZAKON 99	RVUE	Electroweak
>564	95	[62] ERLER 99	RVUE	Electroweak
(> 1673)	95	[63] ERLER 99	RVUE	Electroweak
(> 1700)	68	[64] BARENBOIM 98	RVUE	Electroweak
>244	95	[65] CONRAD 98	RVUE	$\nu_\mu N$ scattering
>253	95	[66] VILAIN 94B	CHM2	$\nu_\mu e \rightarrow \nu_\mu e$ and $\overline{\nu}_\mu e \rightarrow \overline{\nu}_\mu e$
none 200–600	95	[67] RIZZO 93	RVUE	$p\overline{p}$; $Z_{LR} \rightarrow q\overline{q}$
[> 2000]		WALKER 91	COSM	Nucleosynthesis; light ν_R
none 200–500		[68] GRIFOLS 90	ASTR	SN 1987A; light ν_R
none 350–2400		[69] BARBIERI 89B	ASTR	SN 1987A; light ν_R

[54] CHEUNG 01B limit is derived from bounds on contact interactions in a global electroweak analysis.

[55] ABE 97S find $\sigma(Z')\times$B$(e^+e^-,\mu^+\mu^-)<$ 40 fb for $m_{Z'} >$ 600 GeV at $\sqrt{s}$= 1.8 TeV.

[56] ABREU 00S give 95%CL limit on Z-Z' mixing $|\theta| <$ 0.0018. See their Fig. 6 for the limit contour in the mass-mixing plane. $\sqrt{s}$=90 to 189 GeV.

[57] BARATE 00I search for deviations in cross section and asymmetries in $e^+e^- \rightarrow$ fermions at $\sqrt{s}$=90 to 183 GeV. Assume θ=0. Bounds in the mass-mixing plane are shown in their Figure 18.

[58] CHAY 00 also find $-0.0003 < \theta < 0.0019$. For g_R free, $m_{Z'} >$ 430 GeV.

[59] ERLER 00 discuss the possibility that a discrepancy between the observed and predicted values of Q_W(Cs) is due to the exchange of Z'. The data are better described in a certain class of the Z' models including Z_{LR} and Z_χ.

[60] CASALBUONI 99 discuss the discrepancy between the observed and predicted values of Q_W(Cs). It is shown that the data are better described in a class of models including the Z_{LR} model.

[61] CZAKON 99 perform a simultaneous fit to charged and neutral sectors. Assumes manifest left-right symmetric model. Finds $|\theta| <$ 0.0042.

[62] ERLER 99 give 90%CL limit on the Z-Z' mixing $-0.0009 < \theta < 0.0017$.

[63] ERLER 99 assumes 2 Higgs doublets, transforming as 10 of SO(10), embedded in E_6.

[64] BARENBOIM 98 also gives 68% CL limits on the Z-Z' mixing $-0.0005 < \theta < 0.0033$. Assumes Higgs sector of minimal left-right model.

[65] CONRAD 98 limit is from measurements at CCFR, assuming no Z-Z' mixing.

[66] VILAIN 94B assume m_t = 150 GeV and θ=0. See Fig. 2 for limit contours in the mass-mixing plane.

[67] RIZZO 93 analyses CDF limit on possible two-jet resonances.

[68] GRIFOLS 90 limit holds for $m_{\nu_R} \lesssim$ 1 MeV. A specific Higgs sector is assumed. See also GRIFOLS 90D, RIZZO 91.

[69] BARBIERI 89B limit holds for $m_{\nu_R} \leq$ 10 MeV. Bounds depend on assumed supernova core temperature.

Limits for Z_χ

Z_χ is the extra neutral boson in SO(10) $\rightarrow$ SU(5) × U(1)$_\chi$. $g_\chi = e/\cos\theta_W$ is assumed unless otherwise stated. We list limits with the assumption $\rho = 1$ but with no further constraints on the Higgs sector. Values in parentheses assume stronger constraint on the Higgs sector motivated by superstring models. Values in brackets are from cosmological and astrophysical considerations and assume a light right-handed neutrino.

VALUE (GeV)	*CL%*	*DOCUMENT ID*	*TECN*	*COMMENT*
> 680	95	[70] CHEUNG 01B	RVUE	Electroweak
> 595	95	[71] ABE 97S	CDF	$p\overline{p}$; $Z'_\chi \rightarrow e^+e^-$, $\mu^+\mu^-$
• • • We do not use the following data for averages, fits, limits, etc. • • •				
>2100		[72] BARGER 03B	COSM	Nucleosynthesis; light ν_R
> 440	95	[73] ABREU 00S	DLPH	e^+e^-
> 533	95	[74] BARATE 00I	ALEP	e^+e^-
> 554	95	[75] CHO 00	RVUE	Electroweak
		[76] ERLER 00	RVUE	Cs
		[77] ROSNER 00	RVUE	Cs
> 545	95	[78] ERLER 99	RVUE	Electroweak
(> 1368)	95	[79] ERLER 99	RVUE	Electroweak

>215	95	[80] CONRAD	98	RVUE	$\nu_\mu N$ scattering
>190	95	[81] ARIMA	97	VNS	Bhabha scattering
>262	95	[82] VILAIN	94B	CHM2	$\nu_\mu e \rightarrow \nu_\mu e$ and $\overline{\nu}_\mu e \rightarrow \overline{\nu}_\mu e$
[>1470]		[83] FARAGGI	91	COSM	Nucleosynthesis; light ν_R
>231	90	[84] ABE	90F	VNS	e^+e^-
[>1140]		[85] GONZALEZ-G..	90D	COSM	Nucleosynthesis; light ν_R
[>2100]		[86] GRIFOLS	90	ASTR	SN 1987A; light ν_R

[70] CHEUNG 01B limit is derived from bounds on contact interactions in a global electroweak analysis.

[71] ABE 97S find $\sigma(Z')\times$B$(e^+e^-,\mu^+\mu^-)<$ 40 fb for $m_{Z'} > 600$ GeV at $\sqrt{s}$= 1.8 TeV.

[72] BARGER 03B limit is from the nucleosynthesis bound on the effective number of light neutrino $\delta N_\nu < 1$. The quark-hadron transition temperature T_c=150 MeV is assumed. The limit with T_c=400 MeV is $>$4300 GeV.

[73] ABREU 00S give 95%CL limit on Z-Z' mixing $|\theta| < 0.0017$. See their Fig. 6 for the limit contour in the mass-mixing plane. $\sqrt{s}$=90 to 189 GeV.

[74] BARATE 00I search for deviations in cross section and asymmetries in $e^+e^- \rightarrow$ fermions at $\sqrt{s}$=90 to 183 GeV. Assume θ=0. Bounds in the mass-mixing plane are shown in their Figure 18.

[75] CHO 00 use various electroweak data to constrain Z' models assuming m_H=100 GeV. See Fig. 3 for limits in the mass-mixing plane.

[76] ERLER 00 discuss the possibility that a discrepancy between the observed and predicted values of Q_W(Cs) is due to the exchange of Z'. The data are better described in a certain class of the Z' models including Z_{LR} and Z_χ.

[77] ROSNER 00 discusses the possibility that a discrepancy between the observed and predicted values of Q_W(Cs) is due to the exchange of Z'. The data are better described in a certain class of the Z' models including Z_χ.

[78] ERLER 99 give 90%CL limit on the Z-Z' mixing $-0.0020 < \theta < 0.0015$.

[79] ERLER 99 assumes 2 Higgs doublets, transforming as 10 of SO(10), embedded in E_6.

[80] CONRAD 98 limit is from measurements at CCFR, assuming no Z-Z' mixing.

[81] Z-Z' mixing is assumed to be zero. $\sqrt{s}$= 57.77 GeV.

[82] VILAIN 94B assume m_t = 150 GeV and θ=0. See Fig. 2 for limit contours in the mass-mixing plane.

[83] FARAGGI 91 limit assumes the nucleosynthesis bound on the effective number of neutrinos $\Delta N_\nu < 0.5$ and is valid for $m_{\nu_R} < 1$ MeV.

[84] ABE 90F use data for R, $R_{\ell\ell}$, and $A_{\ell\ell}$. ABE 90F fix m_W = 80.49 $\pm$ 0.43 $\pm$ 0.24 GeV and m_Z = 91.13 $\pm$ 0.03 GeV.

[85] Assumes the nucleosynthesis bound on the effective number of light neutrinos ($\delta N_\nu < 1$) and that ν_R is light ($\lesssim$ 1 MeV).

[86] GRIFOLS 90 limit holds for $m_{\nu_R} \lesssim$ 1 MeV. See also GRIFOLS 90D, RIZZO 91.

Limits for Z_ψ

Z_ψ is the extra neutral boson in $E_6 \rightarrow$ SO(10) $\times$ U(1)$_\psi$. $g_\psi = e/\cos\theta_W$ is assumed unless otherwise stated. We list limits with the assumption $\rho = 1$ but with no further constraints on the Higgs sector. Values in brackets are from cosmological and astrophysical considerations and assume a light right-handed neutrino.

VALUE (GeV)	*CL%*	*DOCUMENT ID*		*TECN*	*COMMENT*
>350	95	[87] ABREU	00S	DLPH	e^+e^-
>590	95	[88] ABE	97S	CDF	$p\overline{p}$; $Z'_\psi \rightarrow e^+e^-$, $\mu^+\mu^-$
• • • We do not use the following data for averages, fits, limits, etc. • • •					
>600		[89] BARGER	03B	COSM	Nucleosynthesis; light ν_R
>294	95	[90] BARATE	00I	ALEP	e^+e^-
>137	95	[91] CHO	00	RVUE	Electroweak
>146	95	[92] ERLER	99	RVUE	Electroweak
>54	95	[93] CONRAD	98	RVUE	$\nu_\mu N$ scattering
>135	95	[94] VILAIN	94B	CHM2	$\nu_\mu e \rightarrow \nu_\mu e$ and $\overline{\nu}_\mu e \rightarrow \overline{\nu}_\mu e$
>105	90	[95] ABE	90F	VNS	e^+e^-
[>160]		[96] GONZALEZ-G..	90D	COSM	Nucleosynthesis; light ν_R
[>2000]		[97] GRIFOLS	90D	ASTR	SN 1987A; light ν_R

[87] ABREU 00S give 95%CL limit on Z-Z' mixing $|\theta| < 0.0018$. See their Fig. 6 for the limit contour in the mass-mixing plane. $\sqrt{s}$=90 to 189 GeV.

[88] ABE 97S find $\sigma(Z')\times$B$(e^+e^-,\mu^+\mu^-)<$ 40 fb for $m_{Z'} > 600$ GeV at $\sqrt{s}$= 1.8 TeV.

[89] BARGER 03B limit is from the nucleosynthesis bound on the effective number of light neutrino $\delta N_\nu < 1$. The quark-hadron transition temperature T_c=150 MeV is assumed. The limit with T_c=400 MeV is $>$1100 GeV.

[90] BARATE 00I search for deviations in cross section and asymmetries in $e^+e^- \rightarrow$ fermions at $\sqrt{s}$=90 to 183 GeV. Assume θ=0. Bounds in the mass-mixing plane are shown in their Figure 18.

[91] CHO 00 use various electroweak data to constrain Z' models assuming m_H=100 GeV. See Fig. 3 for limits in the mass-mixing plane.

[92] ERLER 99 give 90%CL limit on the Z-Z' mixing $-0.0013 < \theta < 0.0024$.

[93] CONRAD 98 limit is from measurements at CCFR, assuming no Z-Z' mixing.

[94] VILAIN 94B assume m_t = 150 GeV and θ=0. See Fig. 2 for limit contours in the mass-mixing plane.

[95] ABE 90F use data for R, $R_{\ell\ell}$, and $A_{\ell\ell}$. ABE 90F fix m_W = 80.49 $\pm$ 0.43 $\pm$ 0.24 GeV and m_Z = 91.13 $\pm$ 0.03 GeV.

[96] Assumes the nucleosynthesis bound on the effective number of light neutrinos ($\delta N_\nu < 1$) and that ν_R is light ($\lesssim$ 1 MeV).

[97] GRIFOLS 90D limit holds for $m_{\nu_R} \lesssim$ 1 MeV. See also RIZZO 91.

Limits for Z_η

Z_η is the extra neutral boson in E_6 models, corresponding to $Q_\eta = \sqrt{3/8}\, Q_\chi - \sqrt{5/8}\, Q_\psi$. $g_\eta = e/\cos\theta_W$ is assumed unless otherwise stated. We list limits with the assumption $\rho = 1$ but with no further constraints on the Higgs sector. Values in parentheses assume stronger constraint on the Higgs sector motivated by superstring models. Values in brackets are from cosmological and astrophysical considerations and assume a light right-handed neutrino.

VALUE (GeV)	*CL%*	*DOCUMENT ID*		*TECN*	*COMMENT*
> 619	95	[98] CHO	00	RVUE	Electroweak
> 620	95	[99] ABE	97S	CDF	$p\overline{p}$; $Z'_\eta \rightarrow e^+e^-$, $\mu^+\mu^-$
• • • We do not use the following data for averages, fits, limits, etc. • • •					
>1600		[100] BARGER	03B	COSM	Nucleosynthesis; light ν_R
>310	95	[101] ABREU	00S	DLPH	e^+e^-
>329	95	[102] BARATE	00I	ALEP	e^+e^-
>365	95	[103] ERLER	99	RVUE	Electroweak
>87	95	[104] CONRAD	98	RVUE	$\nu_\mu N$ scattering
>100	95	[105] VILAIN	94B	CHM2	$\nu_\mu e \rightarrow \nu_\mu e$ and $\overline{\nu}_\mu e \rightarrow \overline{\nu}_\mu e$
>125	90	[106] ABE	90F	VNS	e^+e^-
[>820]		[107] GONZALEZ-G..	90D	COSM	Nucleosynthesis; light ν_R
[>3300]		[108] GRIFOLS	90	ASTR	SN 1987A; light ν_R
[>1040]		[107] LOPEZ	90	COSM	Nucleosynthesis; light ν_R

[98] CHO 00 use various electroweak data to constrain Z' models assuming m_H=100 GeV. See Fig. 3 for limits in the mass-mixing plane.

[99] ABE 97S find $\sigma(Z')\times$B$(e^+e^-,\mu^+\mu^-)<$ 40 fb for $m_{Z'} > 600$ GeV at $\sqrt{s}$= 1.8 TeV.

[100] BARGER 03B limit is from the nucleosynthesis bound on the effective number of light neutrino $\delta N_\nu < 1$. The quark-hadron transition temperature T_c=150 MeV is assumed. The limit with T_c=400 MeV is $>$3300 GeV.

[101] ABREU 00S give 95%CL limit on Z-Z' mixing $|\theta| < 0.0024$. See their Fig. 6 for the limit contour in the mass-mixing plane. $\sqrt{s}$=90 to 189 GeV.

[102] BARATE 00I search for deviations in cross section and asymmetries in $e^+e^- \rightarrow$ fermions at $\sqrt{s}$=90 to 183 GeV. Assume θ=0. Bounds in the mass-mixing plane are shown in their Figure 18.

[103] ERLER 99 give 90%CL limit on the Z-Z' mixing $-0.0062 < \theta < 0.0011$.

[104] CONRAD 98 limit is from measurements at CCFR, assuming no Z-Z' mixing.

[105] VILAIN 94B assume m_t = 150 GeV and θ=0. See Fig. 2 for limit contours in the mass-mixing plane.

[106] ABE 90F use data for R, $R_{\ell\ell}$, and $A_{\ell\ell}$. ABE 90F fix m_W = 80.49 $\pm$ 0.43 $\pm$ 0.24 GeV and m_Z = 91.13 $\pm$ 0.03 GeV.

[107] These authors claim that the nucleosynthesis bound on the effective number of light neutrinos ($\delta N_\nu < 1$) constrains Z' masses if ν_R is light ($\lesssim$ 1 MeV).

[108] GRIFOLS 90 limit holds for $m_{\nu_R} \lesssim$ 1 MeV. See also GRIFOLS 90D, RIZZO 91.

Limits for other Z'

VALUE (GeV)	*DOCUMENT ID*		*TECN*	*COMMENT*
• • • We do not use the following data for averages, fits, limits, etc. • • •				
	[109] BARGER	03B	COSM	Nucleosynthesis; light ν_R
	[110] CHO	00	RVUE	E_6-motivated
	[111] CHO	98	RVUE	E_6-motivated
	[112] ABE	97G	CDF	$Z' \rightarrow \overline{q}q$

[109] BARGER 03B use the nucleosynthesis bound on the effective number of light neutrino δN_ν. See their Figs. 4–5 for limits in general E_6 motivated models.

[110] CHO 00 use various electroweak data to constrain Z' models assuming m_H=100 GeV. See Fig. 2 for limits in general E_6-motivated models.

[111] CHO 98 study constraints on four-Fermi contact interactions obtained from low-energy electroweak experiments, assuming no Z-Z' mixing.

[112] Search for Z' decaying to dijets at $\sqrt{s}$=1.8 TeV. For Z' with electromagnetic strength coupling, no bound is obtained.

Indirect Constraints on Kaluza-Klein Gauge Bosons

Bounds on a Kaluza-Klein excitation of the Z boson or photon in d=1 extra dimension. These bounds can also be interpreted as a lower bound on $1/R$, the size of the extra dimension. Unless otherwise stated, bounds assume all fermions live on a single brane and all gauge fields occupy the 4+d-dimensional bulk. See also the section on "Extra Dimensions" in the "Searches" Listings in this *Review*.

VALUE (TeV)	*CL%*	*DOCUMENT ID*		*TECN*	*COMMENT*
• • • We do not use the following data for averages, fits, limits, etc. • • •					
>4.7		[113] MUECK	02	RVUE	Electroweak
>3.3	95	[114] CORNET	00	RVUE	$e\nu qq'$
>5000		[115] DELGADO	00	RVUE	ϵ_K
>2.6	95	[116] DELGADO	00	RVUE	Electroweak
>3.3	95	[117] RIZZO	00	RVUE	Electroweak
>2.9	95	[118] MARCIANO	99	RVUE	Electroweak
>2.5	95	[119] MASIP	99	RVUE	Electroweak
>1.6	90	[120] NATH	99	RVUE	Electroweak
>3.4	95	[121] STRUMIA	99	RVUE	Electroweak

[113] MUECK 02 limit is 2σ and is from global electroweak fit ignoring correlations among observables. Higgs is assumed to be confined on the brane and its mass is fixed. For scenarios of bulk Higgs, of brane-$SU(2)_L$, bulk-$U(1)_Y$, and of bulk-$SU(2)_L$, brane-$U(1)_Y$, the corresponding limits are > 4.6 TeV, > 4.3 TeV and > 3.0 TeV, respectively.
[114] Bound is derived from limits on $e\nu q q'$ contact interaction, using data from HERA and the Tevatron.
[115] Bound holds only if first two generations of quarks lives on separate branes. If quark mixing is not complex, then bound lowers to 400 TeV from Δm_K.
[116] See Figs. 1 and 2 of DELGADO 00 for several model variations. Special boundary conditions can be found which permit KK states down to 950 GeV and that agree with the measurement of Q_W(Cs). Quoted bound assumes all Higgs bosons confined to brane; placing one Higgs doublet in the bulk lowers bound to 2.3 TeV.
[117] Bound is derived from global electroweak analysis assuming the Higgs field is trapped on the matter brane. If the Higgs propagates in the bulk, the bound increases to 3.8 TeV.
[118] Bound is derived from global electroweak analysis but considering only presence of the KK W bosons.
[119] Global electroweak analysis used to obtain bound independent of position of Higgs on brane or in bulk.
[120] Bounds from effect of KK states on G_F, α, M_W, and M_Z. Hard cutoff at string scale determined using gauge coupling unification. Limits for d=2,3,4 rise to 3.5, 5.7, and 7.8 TeV.
[121] Bound obtained for Higgs confined to the matter brane with m_H=500 GeV. For Higgs in the bulk, the bound increases to 3.5 TeV.

LEPTOQUARK QUANTUM NUMBERS

Revised September 2001 by M. Tanabashi (Tohoku University).

Leptoquarks are particles carrying both baryon number (B) and lepton number (L). They are expected to exist in various extensions of the Standard Model (SM). The possible quantum numbers of leptoquark states can be restricted by assuming that their direct interactions with the ordinary SM fermions are dimensionless and invariant under the SM gauge group. Table 1 shows the list of all possible quantum numbers with this assumption [1]. The columns of $SU(3)_C$, $SU(2)_W$, and $U(1)_Y$ in Table 1 indicate the QCD representation, the weak isospin representation, and the weak hypercharge, respectively. The spin of a leptoquark state is taken to be 1 (vector leptoquark) or 0 (scalar leptoquark).

Table 1: Possible leptoquarks and their quantum numbers.

Spin	$3B+L$	$SU(3)_c$	$SU(2)_W$	$U(1)_Y$	Allowed coupling
0	−2	$\bar{3}$	1	1/3	$\bar{q}^c_L \ell_L$ or $\bar{u}^c_R e_R$
0	−2	$\bar{3}$	1	4/3	$\bar{d}^c_R e_R$
0	−2	$\bar{3}$	3	1/3	$\bar{q}^c_L \ell_L$
1	−2	$\bar{3}$	2	5/6	$\bar{q}^c_L \gamma^\mu e_R$ or $\bar{d}^c_R \gamma^\mu \ell_L$
1	−2	$\bar{3}$	2	−1/6	$\bar{u}^c_R \gamma^\mu \ell_L$
0	0	3	2	7/6	$\bar{q}_L e_R$ or $\bar{u}_R \ell_L$
0	0	3	2	1/6	$\bar{d}_R \ell_L$
1	0	3	1	2/3	$\bar{q}_L \gamma^\mu \ell_L$ or $\bar{d}_R \gamma^\mu e_R$
1	0	3	1	5/3	$\bar{u}_R \gamma^\mu e_R$
1	0	3	3	2/3	$\bar{q}_L \gamma^\mu \ell_L$

If we do not require leptoquark states to couple directly with SM fermions, different assignments of quantum numbers become possible.

The Pati-Salam model [2] is an example predicting the existence of a leptoquark state. In this model a vector leptoquark appears at the scale where the Pati-Salam SU(4) "color" gauge group breaks into the familiar QCD $SU(3)_C$ group (or $SU(3)_C \times U(1)_{B-L}$). The Pati-Salam leptoquark is a weak isosinglet and its hypercharge is 2/3. The coupling strength of the Pati-Salam leptoquark is given by the QCD coupling at the Pati-Salam symmetry breaking scale.

Bounds on leptoquark states are obtained both directly and indirectly. Direct limits are from their production cross sections at colliders, while indirect limits are calculated from the bounds on the leptoquark induced four-fermion interactions which are obtained from low energy experiments.

The pair production cross sections of leptoquarks are evaluated from their interactions with gauge bosons. The gauge couplings of a scalar leptoquark are determined uniquely according to its quantum numbers in Table 1. The magnetic-dipole-type and the electric-quadrupole-type interactions of a vector leptoquark are, however, not determined even if we fix its gauge quantum numbers as listed in the table [3]. We need extra assumptions about these interactions to evaluate the pair production cross section for a vector leptoquark.

If a leptoquark couples to fermions of more than a single generation in the mass eigenbasis of the SM fermions, it can induce four-fermion interactions causing flavor-changing-neutral-currents and lepton-family-number violations. Non-chiral leptoquarks, which couple simultaneously to both left- and right-handed quarks, cause four-fermion interactions affecting the $(\pi \to e\nu)/(\pi \to \mu\nu)$ ratio [4]. Indirect limits provide stringent constraints on these leptoquarks. Since the Pati-Salam leptoquark has non-chiral coupling with both e and μ, indirect limits from the bounds on $K_L \to \mu e$ lead to severe bounds on the Pati-Salam leptoquark mass. For detailed bounds obtained in this way, see the Boson Particle Listings for "Indirect Limits for Leptoquarks" and its references.

It is therefore often assumed that a leptoquark state couples only to a single generation in a chiral interaction, where indirect limits become much weaker. This assumption gives strong constraints on concrete models of leptoquarks, however. Leptoquark states which couple only to left- or right-handed quarks are called chiral leptoquarks. Leptoquark states which couple only to the first (second, third) generation are referred as the first (second, third) generation leptoquarks in this section.

Reference

1. W. Buchmüller, R. Rückl, and D. Wyler, Phys. Lett. **B191**, 442 (1987).
2. J.C. Pati and A. Salam, Phys. Rev. **D10**, 275 (1974).
3. J. Blümlein, E. Boos, and A. Kryukov, Z. Phys. **C76**, 137 (1997).
4. O. Shanker, Nucl. Phys. **B204**, 375 (1982).

MASS LIMITS for Leptoquarks from Pair Production

These limits rely only on the color or electroweak charge of the leptoquark.

VALUE (GeV)	CL%	EVTS	DOCUMENT ID		TECN	COMMENT
>200	95		[122] ABBOTT	00C	D0	Second generation
>148	95		[123] AFFOLDER	00K	CDF	Third generation
>202	95		[124] ABE	98S	CDF	Second generation
>242	95		[125] GROSS-PILCH...	98		First generation

• • • We do not use the following data for averages, fits, limits, etc. • • •

> 98	95		[126] ABAZOV	02 D0	All generatrions
>225	95		[127] ABAZOV	01D D0	First generation
> 85.8	95		[128] ABBIENDI	00M OPAL	First generation
> 85.5	95		[128] ABBIENDI	00M OPAL	Second generation
> 82.7	95		[128] ABBIENDI	00M OPAL	Third generation
>123	95		[129] AFFOLDER	00K CDF	Second generation
>160	95		[130] ABBOTT	99J D0	Second generation
>225	95		[131] ABBOTT	98E D0	First generation
> 94	95		[132] ABBOTT	98J D0	Third generation
> 99	95		[133] ABE	97F CDF	Third generation
>213	95		[134] ABE	97X CDF	First generation
> 45.5	95		[135,136] ABREU	93J DLPH	First + second generation
> 44.4	95		[137] ADRIANI	93M L3	First generation
> 44.5	95		[137] ADRIANI	93M L3	Second generation
> 45	95		[137] DECAMP	92 ALEP	Third generation
none 8.9–22.6	95		[138] KIM	90 AMY	First generation
none 10.2–23.2	95		[138] KIM	90 AMY	Second generation
none 5–20.8	95		[139] BARTEL	87B JADE	
none 7–20.5	95	2	[140] BEHREND	86B CELL	

[122] ABBOTT 00C search for scalar leptoquarks using $\mu\mu jj$, $\mu\nu jj$, and $\nu\nu jj$ events in $p\overline{p}$ collisions at $E_{\rm cm}$=1.8 TeV. The limit above assumes B(μq)=1. For B(μq)=0.5 and 0, the bound becomes 180 and 79 GeV respectively. Bounds for vector leptoquarks are also given.

[123] AFFOLDER 00K search for scalar leptoquark using $\nu\nu bb$ events in $p\overline{p}$ collisions at $E_{\rm cm}$=1.8 TeV. The quoted limit assumes B(νb)=1. Bounds for vector leptoquarks are also given.

[124] ABE 98S search for scalar leptoquarks using $\mu\mu jj$ events in $p\overline{p}$ collisions at $E_{\rm cm}$= 1.8 TeV. The limit is for B(μq)= 1. For B(μq)=B(νq)=0.5, the limit is > 160 GeV.

[125] GROSS-PILCHER 98 is the combined limit of the CDF and DØ Collaborations as determined by a joint CDF/DØ working group and reported in this FNAL Technical Memo. Original data published in ABE 97X and ABBOTT 98E.

[126] ABAZOV 02 search for scalar leptoquarks using $\nu\nu jj$ events in $\overline{p}p$ collisions at $E_{\rm cm}$=1.8 TeV. The bound holds for all leptoquark generations. Vector leptoquarks are likewise constrained to lie above 200 GeV.

[127] ABAZOV 01D search for scalar leptoquarks using $e\nu jj$, $eejj$, and $\nu\nu jj$ events in $p\overline{p}$ collisions at $E_{\rm cm}$=1.8 TeV. The limit above assumes B(eq)=1. For B(eq)=0.5 and 0, the bound becomes 204 and 79 GeV, respectively. Bounds for vector leptoquarks are also given. Supersedes ABBOTT 98E.

[128] ABBIENDI 00M search for scalar/vector leptoquarks in e^+e^- collisions at $\sqrt{s}$=183 GeV. The quoted limits are for charge $-4/3$ isospin 0 scalar-leptoquarks with B(ℓq)=1. See their Table 8 and Figs. 6–9 for other cases.

[129] AFFOLDER 00K search for scalar leptoquark using $\nu\nu cc$ events in $p\overline{p}$ collisions at $E_{\rm cm}$=1.8 TeV. The quoted limit assumes B(νc)=1. Bounds for vector leptoquarks are also given.

[130] ABBOTT 99J search for leptoquarks using $\mu\nu jj$ events in $p\overline{p}$ collisions at $E_{\rm cm}$= 1.8TeV. The quoted limit is for a scalar leptoquark with B(μq) = B(νq) = 0.5. Limits on vector leptoquarks range from 240 to 290 GeV.

[131] ABBOTT 98E search for scalar leptoquarks using $e\nu jj$, $eejj$, and $\nu\nu jj$ events in $p\overline{p}$ collisions at $E_{\rm cm}$=1.8 TeV. The limit above assumes B(eq)=1. For B(eq)=0.5 and 0, the bound becomes 204 and 79 GeV, respectively.

[132] ABBOTT 98J search for charge $-1/3$ third generation scalar and vector leptoquarks in $p\overline{p}$ collisions at $E_{\rm cm}$= 1.8 TeV. The quoted limit is for scalar leptoquark with B(νb)=1.

[133] ABE 97F search for third generation scalar and vector leptoquarks in $p\overline{p}$ collisions at $E_{\rm cm}$ = 1.8 TeV. The quoted limit is for scalar leptoquark with B(τb) = 1.

[134] ABE 97X search for scalar leptoquarks using $eejj$ events in $p\overline{p}$ collisions at $E_{\rm cm}$=1.8 TeV. The limit is for B(eq)=1.

[135] Limit is for charge $-1/3$ isospin-0 leptoquark with B(ℓq) = 2/3.

[136] First and second generation leptoquarks are assumed to be degenerate. The limit is slightly lower for each generation.

[137] Limits are for charge $-1/3$, isospin-0 scalar leptoquarks decaying to $\ell^- q$ or νq with any branching ratio. See paper for limits for other charge-isospin assignments of leptoquarks.

[138] KIM 90 assume pair production of charge 2/3 scalar-leptoquark via photon exchange. The decay of the first (second) generation leptoquark is assumed to be any mixture of de^+ and $u\overline{\nu}$ ($s\mu^+$ and $c\overline{\nu}$). See paper for limits for specific branching ratios.

[139] BARTEL 87B limit is valid when a pair of charge 2/3 spinless leptoquarks X is produced with point coupling, and when they decay under the constraint B(X $\rightarrow$ $c\overline{\nu}_\mu$) + B(X $\rightarrow$ $s\mu^+$) = 1.

[140] BEHREND 86B assumed that a charge 2/3 spinless leptoquark, χ, decays either into $s\mu^+$ or $c\overline{\nu}$: B($\chi \rightarrow s\mu^+$) + B($\chi \rightarrow c\overline{\nu}$) = 1.

MASS LIMITS for Leptoquarks from Single Production

These limits depend on the q-ℓ-leptoquark coupling g_{LQ}. It is often assumed that $g^2_{LQ}/4\pi$=1/137. Limits shown are for a scalar, weak isoscalar, charge $-1/3$ leptoquark.

VALUE (GeV)	*CL%*	*DOCUMENT ID*	*TECN*	*COMMENT*
• • • We do not use the following data for averages, fits, limits, etc. • • •				
>298	95	[141] CHEKANOV	03B ZEUS	First generation
>197	95	[142] ABBIENDI	02B OPAL	First generation
		[143] CHEKANOV	02 ZEUS	Lepton-flavor violation
>290	95	[144] ADLOFF	01C H1	First generation
>204	95	[145] BREITWEG	01 ZEUS	First generation
		[146] BREITWEG	00E ZEUS	First generation
>161	95	[147] ABREU	99G DLPH	First generation
>200	95	[148] ADLOFF	99 H1	First generation
		[149] DERRICK	97 ZEUS	Lepton-flavor violation
> 73	95	[150] ABREU	93J DLPH	Second generation
>168	95	[151] DERRICK	93 ZEUS	First generation

[141] CHEKANOV 03B limit is for a scalar, weak isoscalar, charge $-1/3$ leptoquark coupled with e_R. See their Figs. 11–12 and Table 5 for limits on states with different quantum numbers.

[142] For limits on states with different quantum numbers and the limits in the mass-coupling plane, see their Fig. 4 and Fig. 5.

[143] CHEKANOV 02 search for various leptoquarks with lepton-flavor violating couplings. See their Figs. 6–7 and Tables 5–6 for detailed limits.

[144] For limits on states with different quantum numbers and the limits in the mass-coupling plane, see their Fig. 3.

[145] See their Fig. 14 for limits in the mass-coupling plane.

[146] BREITWEG 00E search for F=0 leptoquarks in e^+p collisions. For limits in mass-coupling plane, see their Fig. 11.

[147] ABREU 99G limit obtained from process $e\gamma \rightarrow LQ+q$. For limits on vector and scalar states with different quantum numbers and the limits in the coupling-mass plane, see their Fig. 4 and Table 2.

[148] For limits on states with different quantum numbers and the limits in the mass-coupling plane, see their Fig. 13 and Fig. 14. ADLOFF 99 also search for leptoquarks with lepton-flavor violating couplings. ADLOFF 99 supersedes AID 96B.

[149] DERRICK 97 search for various leptoquarks with lepton-flavor violating couplings. See their Figs. 5–8 and Table 1 for detailed limits.

[150] Limit from single production in Z decay. The limit is for a leptoquark coupling of electromagnetic strength and assumes B(ℓq) = 2/3. The limit is 77 GeV if first and second leptoquarks are degenerate.

[151] DERRICK 93 search for single leptoquark production in ep collisions with the decay eq and νq. The limit is for leptoquark coupling of electromagnetic strength and assumes B(eq) = B(νq) = 1/2. The limit for B(eq) = 1 is 176 GeV. For limits on states with different quantum numbers, see their Table 3.

Indirect Limits for Leptoquarks

VALUE (TeV)	*CL%*	*DOCUMENT ID*	*TECN*	*COMMENT*
• • • We do not use the following data for averages, fits, limits, etc. • • •				
> 1.7	96	[152] ADLOFF	03 H1	First generation
		[153] CHEKANOV	02 ZEUS	Lepton-flavor violation
> 1.7	95	[154] CHEUNG	01B RVUE	First generation
> 0.39	95	[155] ACCIARRI	00P L3	$e^+e^- \rightarrow qq$
> 1.5	95	[156] ADLOFF	00 H1	First generation
> 0.2	95	[157] BARATE	00I ALEP	e^+e^-
		[158] BARGER	00 RVUE	Cs
		[159] GABRIELLI	00 RVUE	Lepton flavor violation
> 0.74	95	[160] ZARNECKI	00 RVUE	S_1 leptoquark
		[161] ABBIENDI	99 OPAL	
> 19.3	95	[162] ABE	98V CDF	$B_s \rightarrow e^\pm\mu^\mp$, Pati-Salam type
		[163] ACCIARRI	98J L3	$e^+e^- \rightarrow q\overline{q}$
		[164] ACKERSTAFF	98V OPAL	$e^+e^- \rightarrow q\overline{q}$, $e^+e^- \rightarrow b\overline{b}$
> 0.76	95	[165] DEANDREA	97 RVUE	$\tilde{R}_2$ leptoquark
		[166] DERRICK	97 ZEUS	Lepton-flavor violation
		[167] GROSSMAN	97 RVUE	$B \rightarrow \tau^+\tau^-$(X)
		[168] JADACH	97 RVUE	$e^+e^- \rightarrow q\overline{q}$
>1200		[169] KUZNETSOV	95B RVUE	Pati-Salam type
		[170] MIZUKOSHI	95 RVUE	Third generation scalar leptoquark
> 0.3	95	[171] BHATTACH...	94 RVUE	Spin-0 leptoquark coupled to $\overline{e}_R t_L$
		[172] DAVIDSON	94 RVUE	
> 18		[173] KUZNETSOV	94 RVUE	Pati-Salam type
> 0.43	95	[174] LEURER	94 RVUE	First generation spin-1 leptoquark
> 0.44	95	[174] LEURER	94B RVUE	First generation spin-0 leptoquark
		[175] MAHANTA	94 RVUE	P and T violation
> 1		[176] SHANKER	82 RVUE	Nonchiral spin-0 leptoquark
> 125		[176] SHANKER	82 RVUE	Nonchiral spin-1 leptoquark

[152] ADLOFF 03 limit is for the weak isotriplet spin-0 leptoquark at strong coupling $\lambda=\sqrt{4\pi}$. For the limits of leptoquarks with different quantum numbers, see their Table 3. Limits are derived from bounds on $e^\pm q$ contact interactions.

[153] CHEKANOV 02 search for lepton-flavor violation in ep collisions. See their Tables 1–4 for limits on lepton-flavor violating and four-fermion interactions induced by various leptoquarks.

[154] CHEUNG 01B quoted limit is for a scalar, weak isoscalar, charge $-1/3$ leptoquark with a coupling of electromagnetic strength. The limit is derived from bounds on contact interactions in a global electroweak analysis. For the limits of leptoquarks with different quantum numbers, see Table 5.

[155] ACCIARRI 00P limit is for the weak isoscalar spin-0 leptoquark with the coupling of electromagnetic strength. For the limits of leptoquarks with different quantum numbers, see their Table 4.

[156] ADLOFF 00 limit is for the weak isotriplet spin-0 leptoquark at strong coupling, $\lambda=\sqrt{4\pi}$. For the limits of leptoquarks with different quantum numbers, see their Table 2. ADLOFF 00 limits are from the Q^2 spectrum measurement of $e^+p \rightarrow e^+X$.

[157] BARATE 00I search for deviations in cross section and jet-charge asymmetry in $e^+e^- \rightarrow \overline{q}q$ due to t-channel exchange of a leptoquark at $\sqrt{s}$=130 to 183 GeV. Limits for other scalar and vector leptoquarks are also given in their Table 22.

[158] BARGER 00 explain the deviation of atomic parity violation in cesium atoms from prediction is explained by scalar leptoquark exchange.

[159] GABRIELLI 00 calculate various process with lepton flavor violation in leptoquark models.

[160] ZARNECKI 00 limit is derived from data of HERA, LEP, and Tevatron and from various low-energy data including atomic parity violation. Leptoquark coupling with electromagnetic strength is assumed.

[161] ABBIENDI 99 limits are from $e^+e^- \rightarrow q\overline{q}$ cross section at 130–136, 161–172, 183 GeV. See their Fig. 8 and Fig. 9 for limits in mass-coupling plane.

[162] ABE 98V quoted limit is from $B(B_s \rightarrow e^\pm\mu^\mp) < 8.2 \times 10^{-6}$. ABE 98V also obtain a similar limit on $M_{LQ} > 20.4$ TeV from $B(B_d \rightarrow e^\pm\mu^\mp) < 4.5 \times 10^{-6}$. Both bounds assume the non-canonical association of the b quark with electrons or muons under SU(4).

[163] ACCIARRI 98J limit is from $e^+e^- \rightarrow q\overline{q}$ cross section at $\sqrt{s}$= 130–172 GeV which can be affected by the t- and u-channel exchanges of leptoquarks. See their Fig. 4 and Fig. 5 for limits in the mass-coupling plane.

[164] ACKERSTAFF 98V limits are from $e^+e^- \rightarrow q\overline{q}$ and $e^+e^- \rightarrow b\overline{b}$ cross sections at $\sqrt{s}$ = 130–172 GeV, which can be affected by the t- and u-channel exchanges of leptoquarks. See their Fig. 21 and Fig. 22 for limits of leptoquarks in mass-coupling plane.

[165] DEANDREA 97 limit is for $\widetilde{R}_2$ leptoquark obtained from atomic parity violation (APV). The coupling of leptoquark is assumed to be electromagnetic strength. See Table 2 for limits of the four-fermion interactions induced by various scalar leptoquark exchange. DEANDREA 97 combines APV limit and limits from Tevatron and HERA. See Fig. 1–4 for combined limits of leptoquark in mass-coupling plane.

[166] DERRICK 97 search for lepton-flavor violation in ep collision. See their Tables 2–5 for limits on lepton-flavor violating four-fermion interactions induced by various leptoquarks.

[167] GROSSMAN 97 estimate the upper bounds on the branching fraction $B \rightarrow \tau^+\tau^-(X)$ from the absence of the B decay with large missing energy. These bounds can be used to constrain leptoquark induced four-fermion interactions.

[168] JADACH 97 limit is from $e^+e^- \rightarrow q\overline{q}$ cross section at $\sqrt{s}$=172.3 GeV which can be affected by the t- and u-channel exchanges of leptoquarks. See their Fig. 1 for limits on vector leptoquarks in mass-coupling plane.

[169] KUZNETSOV 95B use π, K, B, τ decays and μe conversion and give a list of bounds on the leptoquark mass and the fermion mixing matrix in the Pati-Salam model. The quoted limit is from $K_L \rightarrow \mu e$ decay assuming zero mixing.

[170] MIZUKOSHI 95 calculate the one-loop radiative correction to the Z-physics parameters in various scalar leptoquark models. See their Fig. 4 for the exclusion plot of third generation leptoquark models in mass-coupling plane.

[171] BHATTACHARYYA 94 limit is from one-loop radiative correction to the leptonic decay width of the Z. m_H=250 GeV, $\alpha_s(m_Z)$=0.12, m_t=180 GeV, and the electroweak strength of leptoquark coupling are assumed. For leptoquark coupled to $\overline{e}_L t_R$, $\overline{\mu}t$, and $\overline{\tau}t$, see Fig. 2 in BHATTACHARYYA 94B erratum and Fig. 3.

[172] DAVIDSON 94 gives an extensive list of the bounds on leptoquark-induced four-fermion interactions from π, K, D, B, μ, τ decays and meson mixings, *etc.* See Table 15 of DAVIDSON 94 for detail.

[173] KUZNETSOV 94 gives mixing independent bound of the Pati-Salam leptoquark from the cosmological limit on $\pi^0 \rightarrow \overline{\nu}\nu$.

[174] LEURER 94, LEURER 94B limits are obtained from atomic parity violation and apply to any chiral leptoquark which couples to the first generation with electromagnetic strength. For a nonchiral leptoquark, universality in $\pi_{\ell 2}$ decay provides a much more stringent bound.

[175] MAHANTA 94 gives bounds of P- and T-violating scalar-leptoquark couplings from atomic and molecular experiments.

[176] From $(\pi \rightarrow e\nu)/(\pi \rightarrow \mu\nu)$ ratio. SHANKER 82 assumes the leptoquark induced four-fermion coupling $4g^2/M^2$ $(\overline{\nu}_{eL}\, u_R)$ $(\overline{d}_L\, e_R)$with g=0.004 for spin-0 leptoquark and g^2/M^2 $(\overline{\nu}_{eL}\, \gamma_\mu u_L)$ $(\overline{d}_R\, \gamma^\mu e_R)$ with $g \simeq$ 0.6 for spin-1 leptoquark.

MASS LIMITS for Diquarks

VALUE (GeV)	CL%	DOCUMENT ID		TECN	COMMENT
• • • We do not use the following data for averages, fits, limits, etc. • • •					
none 290–420	95	[177] ABE	97G	CDF	E_6 diquark
none 15–31.7	95	[178] ABREU	94O	DLPH	SUSY E_6 diquark

[177] ABE 97G search for new particle decaying to dijets.

[178] ABREU 94O limit is from $e^+e^- \rightarrow \overline{c}s\overline{c}s$. Range extends up to 43 GeV if diquarks are degenerate in mass.

MASS LIMITS for g_A (axigluon)

Axigluons are massive color-octet gauge bosons in chiral color models and have axial-vector coupling to quarks with the same coupling strength as gluons.

VALUE (GeV)	CL%	DOCUMENT ID		TECN	COMMENT
• • • We do not use the following data for averages, fits, limits, etc. • • •					
>365	95	[179] DONCHESKI	98	RVUE	$\Gamma(Z \rightarrow$ hadron)
none 200–980	95	[180] ABE	97G	CDF	$p\overline{p} \rightarrow g_A$X, X $\rightarrow$ 2 jets
none 200–870	95	[181] ABE	95N	CDF	$p\overline{p} \rightarrow g_A$X, $g_A \rightarrow q\overline{q}$
none 240–640	95	[182] ABE	93G	CDF	$p\overline{p} \rightarrow g_A$X, $g_A \rightarrow$ 2jets
> 50	95	[183] CUYPERS	91	RVUE	$\sigma(e^+e^- \rightarrow$ hadrons)
none 120–210	95	[184] ABE	90H	CDF	$p\overline{p} \rightarrow g_A$X, $g_A \rightarrow$ 2jets
> 29		[185] ROBINETT	89	THEO	Partial-wave unitarity
none 150–310	95	[186] ALBAJAR	88B	UA1	$p\overline{p} \rightarrow g_A$X, $g_A \rightarrow$ 2jets
> 20		BERGSTROM	88	RVUE	$p\overline{p} \rightarrow \Upsilon$X via $g_A g$
> 9		[187] CUYPERS	88	RVUE	Υ decay
> 25		[188] DONCHESKI	88B	RVUE	Υ decay

[179] DONCHESKI 98 compare α_s derived from low-energy data and that from $\Gamma(Z \rightarrow$ hadrons)/$\Gamma(Z \rightarrow$ leptons).

[180] ABE 97G search for new particle decaying to dijets.

[181] ABE 95N assume axigluons decaying to quarks in the Standard Model only.

[182] ABE 93G assume $\Gamma(g_A) = N\alpha_s m_{g_A}/6$ with $N = 10$.

[183] CUYPERS 91 compare α_s measured in Υ decay and that from R at PEP/PETRA energies.

[184] ABE 90H assumes $\Gamma(g_A) = N\alpha_s m_{g_A}/6$ with $N = 5$ ($\Gamma(g_A) = 0.09 m_{g_A}$). For $N = 10$, the excluded region is reduced to 120–150 GeV.

[185] ROBINETT 89 result demands partial-wave unitarity of $J = 0$ $t\overline{t} \rightarrow t\overline{t}$ scattering amplitude and derives a limit $m_{g_A} > 0.5\, m_t$. Assumes $m_t > 56$ GeV.

[186] ALBAJAR 88B result is from the nonobservation of a peak in two-jet invariant mass distribution. $\Gamma(g_A) < 0.4\, m_{g_A}$ assumed. See also BAGGER 88.

[187] CUYPERS 88 requires $\Gamma(\Upsilon \rightarrow g g_A) < \Gamma(\Upsilon \rightarrow ggg)$. A similar result is obtained by DONCHESKI 88.

[188] DONCHESKI 88B requires $\Gamma(\Upsilon \rightarrow g q\overline{q})/\Gamma(\Upsilon \rightarrow ggg) < 0.25$, where the former decay proceeds via axigluon exchange. A more conservative estimate of $<$ 0.5 leads to $m_{g_A} > 21$ GeV.

X^0 (Heavy Boson) Searches in Z Decays

Searches for radiative transition of Z to a lighter spin-0 state X^0 decaying to hadrons, a lepton pair, a photon pair, or invisible particles as shown in the comments. The limits are for the product of branching ratios.

VALUE	CL%	DOCUMENT ID		TECN	COMMENT
• • • We do not use the following data for averages, fits, limits, etc. • • •					
		[189] BARATE	98U	ALEP	$X^0 \rightarrow \ell\overline{\ell}$, $q\overline{q}$, gg, $\gamma\gamma$, $\nu\overline{\nu}$
		[190] ACCIARRI	97Q	L3	$X^0 \rightarrow$ invisible particle(s)
		[191] ACTON	93E	OPAL	$X^0 \rightarrow \gamma\gamma$
		[192] ABREU	92D	DLPH	$X^0 \rightarrow$ hadrons
		[193] ADRIANI	92F	L3	$X^0 \rightarrow$ hadrons
		[194] ACTON	91	OPAL	$X^0 \rightarrow$ anything
$<1.1 \times 10^{-4}$	95	[195] ACTON	91B	OPAL	$X^0 \rightarrow e^+e^-$
$<9 \times 10^{-5}$	95	[195] ACTON	91B	OPAL	$X^0 \rightarrow \mu^+\mu^-$
$<1.1 \times 10^{-4}$	95	[195] ACTON	91B	OPAL	$X^0 \rightarrow \tau^+\tau^-$
$<2.8 \times 10^{-4}$	95	[196] ADEVA	91D	L3	$X^0 \rightarrow e^+e^-$
$<2.3 \times 10^{-4}$	95	[196] ADEVA	91D	L3	$X^0 \rightarrow \mu^+\mu^-$
$<4.7 \times 10^{-4}$	95	[197] ADEVA	91D	L3	$X^0 \rightarrow$ hadrons
$<8 \times 10^{-4}$	95	[198] AKRAWY	90J	OPAL	$X^0 \rightarrow$ hadrons

[189] BARATE 98U obtain limits on $B(Z \rightarrow \gamma X^0)B(X^0 \rightarrow \ell\overline{\ell}$, $q\overline{q}$, gg, $\gamma\gamma$, $\nu\overline{\nu}$). See their Fig. 17.

[190] See Fig. 4 of ACCIARRI 97Q for the upper limit on $B(Z \rightarrow \gamma X^0;\ E_\gamma > E_{\mathrm{min}})$ as a function of E_{min}.

[191] ACTON 93E give $\sigma(e^+e^- \rightarrow X^0\gamma)\cdot B(X^0 \rightarrow \gamma\gamma) <$ 0.4 pb (95%CL) for m_{X^0}=60 ± 2.5 GeV. If the process occurs via s-channel γ exchange, the limit translates to $\Gamma(X^0)\cdot B(X^0 \rightarrow \gamma\gamma)^2 <$20 MeV for m_{X^0} = 60 ± 1 GeV.

[192] ABREU 92D give $\sigma_Z \cdot B(Z \rightarrow \gamma X^0) \cdot B(X^0 \rightarrow$ hadrons) <(3–10) pb for m_{X^0} = 10–78 GeV. A very similar limit is obtained for spin-1 X^0.

[193] ADRIANI 92F search for isolated γ in hadronic Z decays. The limit $\sigma_Z \cdot B(Z \rightarrow \gamma X^0) \cdot B(X^0 \rightarrow$ hadrons) <(2–10) pb (95%CL) is given for m_{X^0} = 25–85 GeV.

[194] ACTON 91 searches for $Z \rightarrow Z^* X^0$, $Z^* \rightarrow e^+e^-$, $\mu^+\mu^-$, or $\nu\overline{\nu}$. Excludes any new scalar X^0 with $m_{X^0} <$ 9.5 GeV/c if it has the same coupling to ZZ^* as the MSM Higgs boson.

[195] ACTON 91B limits are for m_{X^0} = 60–85 GeV.

[196] ADEVA 91D limits are for m_{X^0} = 30–89 GeV.

[197] ADEVA 91D limits are for m_{X^0} = 30–86 GeV.

[198] AKRAWY 90J give $\Gamma(Z \rightarrow \gamma X^0)\cdot B(X^0 \rightarrow$ hadrons) < 1.9 MeV (95%CL) for m_{X^0} = 32–80 GeV. We divide by $\Gamma(Z)$ = 2.5 GeV to get product of branching ratios. For nonresonant transitions, the limit is $B(Z \rightarrow \gamma q\overline{q}) <$ 8.2 MeV assuming three-body phase space distribution.

MASS LIMITS for a Heavy Neutral Boson Coupling to e^+e^-

VALUE (GeV)	CL%	DOCUMENT ID		TECN	COMMENT
• • • We do not use the following data for averages, fits, limits, etc. • • •					
none 55–61		[199] ODAKA	89	VNS	$\Gamma(X^0 \rightarrow e^+e^-) \cdot B(X^0 \rightarrow$ hadrons) $\gtrsim$ 0.2 MeV
>45	95	[200] DERRICK	86	HRS	$\Gamma(X^0 \rightarrow e^+e^-)$=6 MeV
>46.6	95	[201] ADEVA	85	MRKJ	$\Gamma(X^0 \rightarrow e^+e^-)$=10 keV
>48	95	[201] ADEVA	85	MRKJ	$\Gamma(X^0 \rightarrow e^+e^-)$=4 MeV
		[202] BERGER	85B	PLUT	
none 39.8–45.5		[203] ADEVA	84	MRKJ	$\Gamma(X^0 \rightarrow e^+e^-)$=10 keV
>47.8	95	[203] ADEVA	84	MRKJ	$\Gamma(X^0 \rightarrow e^+e^-)$=4 MeV
none 39.8–45.2		[203] BEHREND	84C	CELL	
>47	95	[203] BEHREND	84C	CELL	$\Gamma(X^0 \rightarrow e^+e^-)$=4 MeV

[199] ODAKA 89 looked for a narrow or wide scalar resonance in $e^+e^- \rightarrow$ hadrons at E_{cm} = 55.0–60.8 GeV.

[200] DERRICK 86 found no deviation from the Standard Model Bhabha scattering at E_{cm}= 29 GeV and set limits on the possible scalar boson e^+e^- coupling. See their figure 4 for excluded region in the $\Gamma(X^0 \rightarrow e^+e^-)$-$m_{X^0}$ plane. Electronic chiral invariance requires a parity doublet of X^0, in which case the limit applies for $\Gamma(X^0 \rightarrow e^+e^-)$ = 3 MeV.

[201] ADEVA 85 first limit is from 2γ, $\mu^+\mu^-$, hadrons assuming X^0 is a scalar. Second limit is from e^+e^- channel. E_{cm} = 40–47 GeV. Supersedes ADEVA 84.

[202] BERGER 85B looked for effect of spin-0 boson exchange in $e^+e^- \rightarrow e^+e^-$ and $\mu^+\mu^-$ at E_{cm} = 34.7 GeV. See Fig. 5 for excluded region in the $m_{X^0} - \Gamma(X^0)$ plane.

[203] ADEVA 84 and BEHREND 84C have E_{cm} = 39.8–45.5 GeV. MARK-J searched X^0 in $e^+e^- \rightarrow$ hadrons, 2γ, $\mu^+\mu^-$, e^+e^- and CELLO in the same channels plus τ pair. No narrow or broad X^0 is found in the energy range. They also searched for the effect of

X^0 with $m_X > E_{\mathrm{cm}}$. The second limits are from Bhabha data and for spin-0 singlet. The same limits apply for $\Gamma(X^0 \to e^+e^-) = 2$ MeV if X^0 is a spin-0 doublet. The second limit of BEHREND 84C was read off from their figure 2. The original papers also list limits in other channels.

Search for X^0 Resonance in e^+e^- Collisions

The limit is for $\Gamma(X^0 \to e^+e^-) \cdot B(X^0 \to f)$, where f is the specified final state. Spin 0 is assumed for X^0.

VALUE (keV)	CL%	DOCUMENT ID		TECN	COMMENT
• • • We do not use the following data for averages, fits, limits, etc. • • •					
$<10^3$	95	[204] ABE	93C	VNS	$\Gamma(ee)$
$<(0.4\text{–}10)$	95	[205] ABE	93C	VNS	$f = \gamma\gamma$
$<(0.3\text{–}5)$	95	[206,207] ABE	93D	TOPZ	$f = \gamma\gamma$
$<(2\text{–}12)$	95	[206,207] ABE	93D	TOPZ	$f =$ hadrons
$<(4\text{–}200)$	95	[207,208] ABE	93D	TOPZ	$f = ee$
$<(0.1\text{–}6)$	95	[207,208] ABE	93D	TOPZ	$f = \mu\mu$
$<(0.5\text{–}8)$	90	[209] STERNER	93	AMY	$f = \gamma\gamma$

[204] Limit is for $\Gamma(X^0 \to e^+e^-)$ $m_{X^0} = 56\text{–}63.5$ GeV for $\Gamma(X^0) = 0.5$ GeV.

[205] Limit is for $m_{X^0} = 56\text{–}61.5$ GeV and is valid for $\Gamma(X^0) \ll 100$ MeV. See their Fig. 5 for limits for $\Gamma = 1{,}2$ GeV.

[206] Limit is for $m_{X^0} = 57.2\text{–}60$ GeV.

[207] Limit is valid for $\Gamma(X^0) \ll 100$ MeV. See paper for limits for $\Gamma = 1$ GeV and those for $J = 2$ resonances.

[208] Limit is for $m_{X^0} = 56.6\text{–}60$ GeV.

[209] STERNER 93 limit is for $m_{X^0} = 57\text{–}59.6$ GeV and is valid for $\Gamma(X^0) < 100$ MeV. See their Fig. 2 for limits for $\Gamma = 1{,}3$ GeV.

Search for X^0 Resonance in ep Collisions

VALUE	DOCUMENT ID		TECN	COMMENT
• • • We do not use the following data for averages, fits, limits, etc. • • •				
	[210] CHEKANOV	02B	ZEUS	$X \to jj$

[210] CHEKANOV 02B search for photoproduction of X decaying into dijets in ep collisions. See their Fig. 5 for the limit on the photoproduction cross section.

Search for X^0 Resonance in Two-Photon Process

The limit is for $\Gamma(X^0) \cdot B(X^0 \to \gamma\gamma)^2$. Spin 0 is assumed for X^0.

VALUE (MeV)	CL%	DOCUMENT ID		TECN	COMMENT
• • • We do not use the following data for averages, fits, limits, etc. • • •					
<2.6	95	[211] ACTON	93E	OPAL	$m_{X^0}=60 \pm 1$ GeV
<2.9	95	BUSKULIC	93F	ALEP	$m_{X^0} \sim 60$ GeV

[211] ACTON 93E limit for a $J = 2$ resonance is 0.8 MeV.

Search for X^0 Resonance in $e^+e^- \to X^0\gamma$

VALUE (GeV)	DOCUMENT ID		TECN	COMMENT
• • • We do not use the following data for averages, fits, limits, etc. • • •				
	[212] ABBIENDI	03D	OPAL	$X^0 \to \gamma\gamma$
	[213] ABREU	00Z	DLPH	X^0 decaying invisibly
	[214] ADAM	96C	DLPH	X^0 decaying invisibly

[212] ABBIENDI 03D measure the $e^+e^- \to \gamma\gamma\gamma$ cross section at $\sqrt{s}$=181–209 GeV. The upper bound on the production cross section, $\sigma(e^+e^- \to X^0\gamma)$ times the branching ratio for $X^0 \to \gamma\gamma$, is less than 0.03 pb at 95%CL for X^0 masses between 20 and 180 GeV. See their Fig. 9b for the limits in the mass-cross section plane.

[213] ABREU 00Z is from the single photon cross section at $\sqrt{s}$=183, 189 GeV. The production cross section upper limit is less than 0.3 pb for X^0 mass between 40 and 160 GeV. See their Fig. 4 for the limit in mass-cross section plane.

[214] ADAM 96C is from the single photon production cross at $\sqrt{s}$=130, 136 GeV. The upper bound is less than 3 pb for X^0 masses between 60 and 130 GeV. See their Fig. 5 for the exact bound on the cross section $\sigma(e^+e^- \to \gamma X^0)$.

Search for X^0 Resonance in $Z \to f\overline{f}X^0$

The limit is for $B(Z \to f\overline{f}X^0) \cdot B(X^0 \to F)$ where f is a fermion and F is the specified final state. Spin 0 is assumed for X^0.

VALUE	CL%	DOCUMENT ID		TECN	COMMENT
• • • We do not use the following data for averages, fits, limits, etc. • • •					
		[215] ABREU	96T	DLPH	f=e,μ,τ; F=$\gamma\gamma$
$<3.7 \times 10^{-6}$	95	[216] ABREU	96T	DLPH	f=ν; F=$\gamma\gamma$
		[217] ABREU	96T	DLPH	f=q; F=$\gamma\gamma$
$<6.8 \times 10^{-6}$	95	[216] ACTON	93E	OPAL	f=e,μ,τ; F=$\gamma\gamma$
$<5.5 \times 10^{-6}$	95	[216] ACTON	93E	OPAL	f=q; F=$\gamma\gamma$
$<3.1 \times 10^{-6}$	95	[216] ACTON	93E	OPAL	f=ν; F=$\gamma\gamma$
$<6.5 \times 10^{-6}$	95	[216] ACTON	93E	OPAL	f=e,μ; F=$\ell\overline{\ell}$, $q\overline{q}$, $\nu\overline{\nu}$
$<7.1 \times 10^{-6}$	95	[216] BUSKULIC	93F	ALEP	f=e,μ; F=$\ell\overline{\ell}$, $q\overline{q}$, $\nu\overline{\nu}$
		[218] ADRIANI	92F	L3	f=q; F=$\gamma\gamma$

[215] ABREU 96T obtain limit as a function of m_{X^0}. See their Fig. 6.

[216] Limit is for m_{X^0} around 60 GeV.

[217] ABREU 96T obtain limit as a function of m_{X^0}. See their Fig. 15.

[218] ADRIANI 92F give $\sigma_Z \cdot B(Z \to q\overline{q}X^0) \cdot B(X^0 \to \gamma\gamma) < (0.75\text{–}1.5)$ pb (95%CL) for $m_{X^0} = 10\text{–}70$ GeV. The limit is 1 pb at 60 GeV.

Search for X^0 Resonance in $p\overline{p} \to WX^0$

VALUE (MeV)	DOCUMENT ID		TECN	COMMENT
• • • We do not use the following data for averages, fits, limits, etc. • • •				
	[219] ABE	97W	CDF	$X^0 \to b\overline{b}$

[219] ABE 97W search for X^0 production associated with W in $p\overline{p}$ collisions at E_{cm}=1.8 TeV. The 95%CL upper limit on the production cross section times the branching ratio for $X^0 \to b\overline{b}$ ranges from 14 to 19 pb for X^0 mass between 70 and 120 GeV. See their Fig. 3 for upper limits of the production cross section as a function of m_{X^0}.

Heavy Particle Production in Quarkonium Decays

Limits are for branching ratios to modes shown.

VALUE	CL%	DOCUMENT ID		TECN	COMMENT
• • • We do not use the following data for averages, fits, limits, etc. • • •					
$<1.5 \times 10^{-5}$	90	[220] BALEST	95	CLE2	$\Upsilon(1S) \to X^0\gamma$, $m_{X^0} < 5$ GeV
$< 3 \times 10^{-5}\text{–}6 \times 10^{-3}$	90	[221] BALEST	95	CLE2	$\Upsilon(1S) \to X^0\overline{X}^0\gamma$, $m_{X^0} < 3.9$ GeV
$<5.6 \times 10^{-5}$	90	[222] ANTREASYAN	90C	CBAL	$\Upsilon(1S) \to X^0\gamma$, $m_{X^0} < 7.2$ GeV
		[223] ALBRECHT	89	ARG	

[220] BALEST 95 two-body limit is for pseudoscalar X^0. The limit becomes $< 10^{-4}$ for $m_{X^0} < 7.7$ GeV.

[221] BALEST 95 three-body limit is for phase-space photon energy distribution and angular distribution same as for $\Upsilon \to gg\gamma$.

[222] ANTREASYAN 90C assume that X^0 does not decay in the detector.

[223] ALBRECHT 89 give limits for $B(\Upsilon(1S), \Upsilon(2S) \to X^0\gamma) \cdot B(X^0 \to \pi^+\pi^-, K^+K^-, p\overline{p})$ for $m_{X^0} < 3.5$ GeV.

REFERENCES FOR Searches for Heavy Bosons Other Than Higgs Bosons

ABBIENDI	03D	EPJ C26 331	G. Abbiendi *et al.*	(OPAL Collab.)
ACOSTA	03B	PRL 90 081802	D. Acosta *et al.*	(CDF Collab.)
ADLOFF	03	PL B568 35	C. Adloff *et al.*	(H1 Collab.)
BARGER	03B	PR D67 075009	V. Barger, P. Langacker, H. Lee	
CHEKANOV	03B	PR D68 052004	S. Chekanov *et al.*	(ZEUS Collab.)
ABAZOV	02	PRL 88 191801	V.M. Abazov *et al.*	(D0 Collab.)
ABBIENDI	02B	PL B526 233	G. Abbiendi *et al.*	(OPAL Collab.)
AFFOLDER	02C	PRL 88 071806	T. Affolder *et al.*	(CDF Collab.)
CHEKANOV	02	PR D65 092004	S. Chekanov *et al.*	(ZEUS Collab.)
CHEKANOV	02B	PL B531 9	S. Chekanov *et al.*	(ZEUS Collab.)
MUECK	02	PR D65 085037	A. Mueck, A. Pilaftsis, R. Rueckl	
ABAZOV	01B	PRL 87 061802	V.M. Abazov *et al.*	(D0 Collab.)
ABAZOV	01D	PR D64 092004	V.M. Abazov *et al.*	(D0 Collab.)
ADLOFF	01C	PL B523 234	C. Adloff *et al.*	(H1 Collab.)
AFFOLDER	01I	PRL 87 231803	T. Affolder *et al.*	(CDF Collab.)
BREITWEG	01	PR D63 052002	J. Breitweg *et al.*	(ZEUS Collab.)
CHEUNG	01B	PL B517 167	K. Cheung	
THOMAS	01	NP A694 559	E. Thomas *et al.*	
ABBIENDI	00M	EPJ C13 15	G. Abbiendi *et al.*	(OPAL Collab.)
ABBOTT	00C	PRL 84 2088	B. Abbott *et al.*	(D0 Collab.)
ABE	00	PRL 84 5716	F. Abe *et al.*	(CDF Collab.)
ABREU	00S	PL B485 45	P. Abreu *et al.*	(DELPHI Collab.)
ABREU	00Z	EPJ C17 53	P. Abreu *et al.*	(DELPHI Collab.)
ACCIARRI	00P	PL B489 81	M. Acciarri *et al.*	(L3 Collab.)
ADLOFF	00	PL B479 358	C. Adloff *et al.*	(H1 Collab.)
AFFOLDER	00K	PRL 85 2056	T. Affolder *et al.*	(CDF Collab.)
BARATE	00I	EPJ C12 183	R. Barate *et al.*	(ALEPH Collab.)
BARGER	00	PL B480 149	V. Barger, K. Cheung	
BREITWEG	00E	EPJ C16 253	J. Breitweg *et al.*	(ZEUS Collab.)
CHAY	00	PR D61 035002	J. Chay, K.Y. Lee, S. Nam	
CHO	00	MPL A15 311	G. Cho	
CORNET	00	PR D61 037701	F. Cornet, M. Relano, J. Rico	
DELGADO	00	JHEP 0001 030	A. Delgado, A. Pomarol, M. Quiros	
ERLER	00	PRL 84 212	J. Erler, P. Langacker	
GABRIELLI	00	PR D62 055009	E. Gabrielli	
RIZZO	00	PR D61 016007	T.G. Rizzo, J.D. Wells	
ROSNER	00	PR D61 016006	J.L. Rosner	
ZARNECKI	00	EPJ C17 695	A. Zarnecki	
ABBIENDI	99	EPJ C6 1	G. Abbiendi *et al.*	(OPAL Collab.)
ABBOTT	99J	PRL 83 2896	B. Abbott *et al.*	(D0 Collab.)
ABREU	99G	PL B446 62	P. Abreu *et al.*	(DELPHI Collab.)
ACKERSTAFF	99D	EPJ C8 3	K. Ackerstaff *et al.*	(OPAL Collab.)
ADLOFF	99	EPJ C11 447	C. Adloff *et al.*	(H1 Collab.)
Also	00C	EPJ C14 553 errata	C. Adloff *et al.*	(H1 Collab.)
CASALBUONI	99	PL B460 135	R. Casalbuoni *et al.*	
CZAKON	99	PL B458 355	M. Czakon, J. Gluza, M. Zralek	
ERLER	99	PL B456 68	J. Erler, P. Langacker	
MARCIANO	99	PR D60 093006	W. Marciano	
MASIP	99	PR D60 096005	M. Masip, A. Pomarol	
NATH	99	PR D60 116004	P. Nath, M. Yamaguchi	
STRUMIA	99	PL B466 107	A. Strumia	
ABBOTT	98E	PRL 80 2051	B. Abbott *et al.*	(D0 Collab.)
ABBOTT	98J	PRL 81 38	B. Abbott *et al.*	(D0 Collab.)
ABE	98S	PRL 81 4806	F. Abe *et al.*	(CDF Collab.)
ABE	98V	PRL 81 5742	F. Abe *et al.*	(CDF Collab.)
ACCIARRI	98J	PL B433 163	M. Acciarri *et al.*	(L3 Collab.)
ACKERSTAFF	98V	EPJ C2 441	K. Ackerstaff *et al.*	(OPAL Collab.)
BARATE	98U	EPJ C4 571	R. Barate *et al.*	(ALEPH Collab.)
BARENBOIM	98	EPJ C1 369	G. Barenboim	
CHO	98	EPJ C5 155	G. Cho, K. Hagiwara, S. Matsumoto	
CONRAD	98	RMP 70 1341	J.M. Conrad, M.H. Shaevitz, T. Bolton	
DONCHESKI	98	PR D58 097702	M.A. Doncheski, R.W. Robinett	
GROSS-PILCH...	98	hep-ex/9810015	C. Grosso-Pilcher, G. Landsberg, M. Paterno	
ABE	97F	PRL 78 2906	F. Abe *et al.*	(CDF Collab.)
ABE	97G	PR D55 R5263	F. Abe *et al.*	(CDF Collab.)

ABE 97S PRL 79 2192 F. Abe *et al.* (CDF Collab.)
ABE 97W PRL 79 3819 F. Abe *et al.* (CDF Collab.)
ABE 97X PRL 79 4327 F. Abe *et al.* (CDF Collab.)
ACCIARRI 97Q PL B412 201 M. Acciarri *et al.* (L3 Collab.)
ARIMA 97 PR D55 19 T. Arima *et al.* (VENUS Collab.)
BARENBOIM 97 PR D55 4213 G. Barenboim *et al.* (VALE, IFIC)
DEANDREA 97 PL B409 277 A. Deandrea (MARS)
DERRICK 97 ZPHY C73 613 M. Derrick *et al.* (ZEUS Collab.)
GROSSMAN 97 PR D55 2768 Y. Grossman, Z. Ligeti, E. Nardi (REHO, CIT)
JADACH 97 PL B408 281 S. Jadach, B.F.L. Ward, Z. Was (CERN, INPK+)
STAHL 97 ZPHY C74 73 A. Stahl, H. Voss (BONN)
ABACHI 96C PRL 76 3271 S. Abachi *et al.* (D0 Collab.)
ABACHI 96D PL B385 471 S. Abachi *et al.* (D0 Collab.)
ABREU 96T ZPHY C72 179 P. Abreu *et al.* (DELPHI Collab.)
ADAM 96C PL B380 471 W. Adam *et al.* (DELPHI Collab.)
AID 96B PL B369 173 S. Aid *et al.* (H1 Collab.)
ALLET 96 PL B383 139 M. Allet *et al.* (VILL, LEUV, LOUV, WISC)
ABACHI 95E PL B358 405 S. Abachi *et al.* (D0 Collab.)
ABE 95M PRL 74 2900 F. Abe *et al.* (CDF Collab.)
ABE 95N PRL 74 3538 F. Abe *et al.* (CDF Collab.)
BALEST 95 PR D51 2053 R. Balest *et al.* (CLEO Collab.)
KUZNETSOV 95 PRL 75 794 I.A. Kuznetsov *et al.* (PNPI, KIAE, HARV+)
KUZNETSOV 95B PAN 58 2113 A.V. Kuznetsov, N.V. Mikheev (YARO)
Translated from YAF 58 2228.
MIZUKOSHI 95 NP B443 20 J.K. Mizukoshi, O.J.P. Eboli, M.C. Gonzalez-Garcia
ABREU 94O ZPHY C64 183 P. Abreu *et al.* (DELPHI Collab.)
BHATTACH... 94 PL B336 100 G. Bhattacharyya, J. Ellis, K. Sridhar (CERN)
Also 94B PL B338 522 (erratum) G. Bhattacharyya, J. Ellis, K. Sridhar (CERN)
BHATTACH... 94B PL B338 522 (erratum) G. Bhattacharyya, J. Ellis, K. Sridhar (CERN)
DAVIDSON 94 ZPHY C61 613 S. Davidson, D. Bailey, B.A. Campbell (CFPA+)
KUZNETSOV 94 PL B329 295 A.V. Kuznetsov, N.V. Mikheev (YARO)
KUZNETSOV 94B JETPL 60 315 I.A. Kuznetsov *et al.* (PNPI, KIAE, HARV+)
Translated from ZETFP 60 311.
LEURER 94 PR D50 536 M. Leurer (REHO)
LEURER 94B PR D49 333 M. Leurer (REHO)
Also 93 PRL 71 1324 M. Leurer (REHO)
MAHANTA 94 PL B337 128 U. Mahanta (MEHTA)
SEVERIJNS 94 PRL 73 611 (erratum) N. Severijns *et al.* (LOUV, WISC, LEUV+)
VILAIN 94B PL B332 465 P. Vilain *et al.* (CHARM II Collab.)
ABE 93C PL B302 119 K. Abe *et al.* (VENUS Collab.)
ABE 93D PL B304 373 T. Abe *et al.* (TOPAZ Collab.)
ABE 93G PRL 71 2542 F. Abe *et al.* (CDF Collab.)
ABREU 93J PL B316 620 P. Abreu *et al.* (DELPHI Collab.)
ACTON 93E PL B311 391 P.D. Acton *et al.* (OPAL Collab.)
ADRIANI 93M PRPL 236 1 O. Adriani *et al.* (L3 Collab.)
ALITTI 93 NP B400 3 J. Alitti *et al.* (UA2 Collab.)
BHATTACH... 93 PR D47 R3693 G. Bhattacharyya *et al.* (CALC, JADA, ICTP+)
BUSKULIC 93F PL B308 425 D. Buskulic *et al.* (ALEPH Collab.)
DERRICK 93 PL B306 173 M. Derrick *et al.* (ZEUS Collab.)
RIZZO 93 PR D48 4470 T.G. Rizzo (ANL)
SEVERIJNS 93 PRL 70 4047 N. Severijns *et al.* (LOUV, WISC, LEUV+)
Also 94 PRL 73 611 (erratum) N. Severijns *et al.* (LOUV, WISC, LEUV+)
STERNER 93 PL B303 385 K.L. Sterner *et al.* (AMY Collab.)
ABREU 92D ZPHY C53 555 P. Abreu *et al.* (DELPHI Collab.)
ADRIANI 92F PL B292 472 O. Adriani *et al.* (L3 Collab.)
DECAMP 92 PRPL 216 253 D. Decamp *et al.* (ALEPH Collab.)
IMAZATO 92 PRL 69 877 J. Imazato *et al.* (KEK, INUS, TOKY+)
MISHRA 92 PRL 68 3499 S.R. Mishra *et al.* (COLU, CHIC, FNAL+)
POLAK 92B PR D46 3871 J. Polak, M. Zralek (SILES)
ACTON 91 PL B268 122 D.P. Acton *et al.* (OPAL Collab.)
ACTON 91B PL B273 338 D.P. Acton *et al.* (OPAL Collab.)
ADEVA 91D PL B262 155 B. Adeva *et al.* (L3 Collab.)
AQUINO 91 PL B261 280 M. Aquino, A. Fernandez, A. Garcia (CINV, PUEB)
COLANGELO 91 PL B253 154 P. Colangelo, G. Nardulli (BARI)
CUYPERS 91 PL B259 173 F. Cuypers, A.F. Falk, P.H. Frampton (DURH, HARV+)
FARAGGI 91 MPL A6 61 A.E. Faraggi, D.V. Nanopoulos (TAMU)
POLAK 91 NP B363 385 J. Polak, M. Zralek (SILES)
RIZZO 91 PR D44 202 T.G. Rizzo (WISC, ISU)
WALKER 91 APJ 376 51 T.P. Walker *et al.* (HSCA, OSU, CHIC+)
ABE 90F PL B246 297 K. Abe *et al.* (VENUS Collab.)
ABE 90H PR D41 1722 F. Abe *et al.* (CDF Collab.)
AKRAWY 90J PL B246 285 M.Z. Akrawy *et al.* (OPAL Collab.)
ANTREASYAN 90C PL B251 204 D. Antreasyan *et al.* (Crystal Ball Collab.)
GONZALEZ-G... 90D PL B240 163 M.C. Gonzalez-Garcia, J.W.F. Valle (VALE)
GRIFOLS 90 NP B331 244 J.A. Grifols, E. Masso (BARC)
GRIFOLS 90D PR D42 3293 J.A. Grifols, E. Masso, T.G. Rizzo (BARC, CERN+)
KIM 90 PL B240 243 G.N. Kim *et al.* (AMY Collab.)
LOPEZ 90 PL B241 392 J.L. Lopez, D.V. Nanopoulos (TAMU)
ALBAJAR 89 ZPHY C44 15 C. Albajar *et al.* (UA1 Collab.)
ALBRECHT 89 ZPHY C42 349 H. Albrecht *et al.* (ARGUS Collab.)
BARBIERI 89B PR D39 1229 R. Barbieri, R.N. Mohapatra (PISA, UMD)
LANGACKER 89B PR D40 1569 P. Langacker, S. Uma Sankar (PENN)
ODAKA 89 JPSJ 58 3037 S. Odaka *et al.* (VENUS Collab.)
ROBINETT 89 PR D39 834 R.W. Robinett (PSU)
ALBAJAR 88B PL B209 127 C. Albajar *et al.* (UA1 Collab.)
BAGGER 88 PR D37 1188 J. Bagger, C. Schmidt, S. King (HARV, BOST)
BALKE 88 PR D37 587 B. Balke *et al.* (LBL, UCB, COLO, NWES+)
BERGSTROM 88 PL B212 386 L. Bergstrom (STOH)
CUYPERS 88 PRL 60 1237 F. Cuypers, P.H. Frampton (UNCCH)
DONCHESKI 88 PL B206 137 M.A. Doncheski, H. Grotch, R. Robinett (PSU)
DONCHESKI 88B PR D38 412 M.A. Doncheski, H. Grotch, R.W. Robinett (PSU)
ANSARI 87D PL B195 613 R. Ansari *et al.* (UA2 Collab.)
BARTEL 87B ZPHY C36 15 W. Bartel *et al.* (JADE Collab.)
BEHREND 86B PL B178 452 H.J. Behrend *et al.* (CELLO Collab.)
DERRICK 86 PL 166B 463 M. Derrick *et al.* (HRS Collab.)
Also 86B PR D34 3286 M. Derrick *et al.* (HRS Collab.)
JODIDIO 86 PR D34 1967 A. Jodidio *et al.* (LBL, NWES, TRIU)
Also 88 PR D37 237 erratum A. Jodidio *et al.* (LBL, NWES, TRIU)
MOHAPATRA 86 PR D34 909 R.N. Mohapatra (UMD)
ADEVA 85 PL 152B 439 B. Adeva *et al.* (Mark-J Collab.)
BERGER 85B ZPHY C27 341 C. Berger *et al.* (PLUTO Collab.)
STOKER 85 PRL 54 1887 D.P. Stoker *et al.* (LBL, NWES, TRIU)
ADEVA 84 PRL 53 134 B. Adeva *et al.* (Mark-J Collab.)
BEHREND 84C PL 140B 130 H.J. Behrend *et al.* (CELLO Collab.)
BERGSMA 83 PL 122B 465 F. Bergsma *et al.* (CHARM Collab.)
CARR 83 PRL 51 627 J. Carr *et al.* (LBL, NWES, TRIU)
BEALL 82 PRL 48 848 G. Beall, M. Bander, A. Soni (UCI, UCLA)
SHANKER 82 NP B204 375 O. Shanker (TRIU)
STEIGMAN 79 PRL 43 239 G. Steigman, K.A. Olive, D.N. Schramm (BART+)

Axions (A^0) and Other Very Light Bosons, Searches for

AXIONS AND OTHER VERY LIGHT BOSONS

Written October 1997 by H. Murayama (University of California, Berkeley) Part I; April 1998 by G. Raffelt (Max-Planck Institute, München) Part II; and April 1998 by C. Hagmann, K. van Bibber (Lawrence Livermore National Laboratory), and L.J. Rosenberg (Massachusetts Institute of Technology) Part III.

This review is divided into three parts:

Part I (Theory)

Part II (Astrophysical Constraints)

Part III (Experimental Limits)

AXIONS AND OTHER VERY LIGHT BOSONS, PART I (THEORY)

(by H. Murayama)

In this section we list limits for very light neutral (pseudo) scalar bosons that couple weakly to stable matter. They arise if there is a global continuous symmetry in the theory that is spontaneously broken in the vacuum. If the symmetry is exact, it results in a massless Nambu–Goldstone (NG) boson. If there is a small explicit breaking of the symmetry, either already in the Lagrangian or due to quantum mechanical effects such as anomalies, the would-be NG boson acquires a finite mass; then it is called a pseudo-NG boson. Typical examples are axions (A^0) [1], familons [2], and Majorons [3,4], associated, respectively, with spontaneously broken Peccei-Quinn [5], family, and lepton-number symmetries. This Review provides brief descriptions of each of them and their motivations.

One common characteristic for all these particles is that their coupling to the Standard Model particles are suppressed by the energy scale of symmetry breaking, *i.e.* the decay constant f, where the interaction is described by the Lagrangian

$$\mathcal{L} = \frac{1}{f}(\partial_\mu \phi) J^\mu, \tag{1}$$

where J^μ is the Noether current of the spontaneously broken global symmetry.

An axion gives a natural solution to the strong CP problem: why the effective θ-parameter in the QCD Lagrangian $\mathcal{L}_\theta = \theta_{eff} \frac{\alpha_s}{8\pi} F^{\mu\nu a} \widetilde{F}^a_{\mu\nu}$ is so small ($\theta_{eff} \lesssim 10^{-9}$) as required by the current limits on the neutron electric dipole moment, even though $\theta_{eff} \sim O(1)$ is perfectly allowed by the QCD gauge invariance. Here, θ_{eff} is the effective θ parameter after the diagonalization of the quark masses, and $F^{\mu\nu a}$ is the gluon field strength and $\widetilde{F}^a_{\mu\nu} = \frac{1}{2}\epsilon_{\mu\nu\rho\sigma} F^{\rho\sigma a}$. An axion is a pseudo-NG boson of a spontaneously broken Peccei–Quinn symmetry, which is an exact symmetry at the classical level, but is broken quantum mechanically due to the triangle anomaly with the gluons. The definition of the Peccei–Quinn symmetry is model dependent. As a result of the triangle anomaly, the axion acquires an effective coupling to gluons

$$\mathcal{L} = \left(\theta_{eff} - \frac{\phi_A}{f_A}\right) \frac{\alpha_s}{8\pi} F^{\mu\nu a} \widetilde{F}^a_{\mu\nu}\,, \tag{2}$$

where ϕ_A is the axion field. It is often convenient to *define* the axion decay constant f_A with this Lagrangian [6]. The QCD nonperturbative effect induces a potential for ϕ_A whose minimum is at $\phi_A = \theta_{eff} f_A$ cancelling θ_{eff} and solving the strong CP problem. The mass of the axion is inversely proportional to f_A as

$$m_A = 0.62 \times 10^{-3}\text{eV} \ \times (10^{10}\text{GeV}/f_A) \ . \qquad (3)$$

The original axion model [1,5] assumes $f_A \sim v$, where $v = (\sqrt{2}G_F)^{-1/2} = 247$ GeV is the scale of the electroweak symmetry breaking, and has two Higgs doublets as minimal ingredients. By requiring tree-level flavor conservation, the axion mass and its couplings are completely fixed in terms of one parameter ($\tan\beta$): the ratio of the vacuum expectation values of two Higgs fields. This model is excluded after extensive experimental searches for such an axion [7]. Observation of a narrow-peak structure in positron spectra from heavy ion collisions [8] suggested a particle of mass 1.8 MeV that decays into e^+e^-. Variants of the original axion model, which keep $f_A \sim v$, but drop the constraints of tree-level flavor conservation, were proposed [9]. Extensive searches for this particle, A^0(1.8 MeV), ended up with another negative result [10].

The popular way to save the Peccei-Quinn idea is to introduce a new scale $f_A \gg v$. Then the A^0 coupling becomes weaker, thus one can easily avoid all the existing experimental limits; such models are called invisible axion models [11,12]. Two classes of models are discussed commonly in the literature. One introduces new heavy quarks which carry Peccei–Quinn charge while the usual quarks and leptons do not (KSVZ axion or "hadronic axion") [11]. The other does not need additional quarks but requires two Higgs doublets, and all quarks and leptons carry Peccei–Quinn charges (DFSZ axion or "GUT-axion") [12]. All models contain at least one electroweak singlet scalar boson which acquires an expectation value and breaks Peccei–Quinn symmetry. The invisible axion with a large decay constant $f_A \sim 10^{12}$ GeV was found to be a good candidate of the cold dark matter component of the Universe [13](see Dark Matter review). The energy density is stored in the low-momentum modes of the axion field which are highly occupied and thus represent essentially classical field oscillations.

The constraints on the invisible axion from astrophysics are derived from interactions of the axion with either photons, electrons or nucleons. The strengths of the interactions are model dependent (*i.e.*, not a function of f_A only), and hence one needs to specify a model in order to place lower bounds on f_A. Such constraints will be discussed in Part II. Serious experimental searches for an invisible axion are underway; they typically rely on axion-photon coupling, and some of them assume that the axion is the dominant component of our galactic halo density. Part III will discuss experimental techniques and limits.

Familons arise when there is a global family symmetry broken spontaneously. A family symmetry interchanges generations or acts on different generations differently. Such a symmetry may explain the structure of quark and lepton masses and their mixings. A familon could be either a scalar or a pseudoscalar. For instance, an SU(3) family symmetry among three generations is non-anomalous and hence the familons are exactly massless. In this case, familons are scalars. If one has larger family symmetries with separate groups of left-handed and right-handed fields, one also has pseudoscalar familons. Some of them have flavor-off-diagonal couplings such as $\partial_\mu \phi_F \bar{d}\gamma^\mu s/F_{ds}$ or $\partial_\mu \phi_F \bar{e}\gamma^\mu \mu/F_{\mu e}$, and the decay constant F can be different for individual operators. The decay constants have lower bounds constrained by flavor-changing processes. For instance, $\text{B}(K^+ \to \pi^+\phi_F) < 3 \times 10^{-10}$ [14] gives $F_{ds} > 3.4 \times 10^{11}$ GeV [15]. The constraints on familons primarily coupled to third generation are quite weak [15].

If there is a global lepton-number symmetry and if it breaks spontaneously, there is a Majoron. The triplet Majoron model [4] has a weak-triplet Higgs boson, and Majoron couples to Z. It is now excluded by the Z invisible-decay width. The model is viable if there is an additional singlet Higgs boson and if the Majoron is mainly a singlet [16]. In the singlet Majoron model [3], lepton-number symmetry is broken by a weak-singlet scalar field, and there are right-handed neutrinos which acquire Majorana masses. The left-handed neutrino masses are generated by a "seesaw" mechanism [17]. The scale of lepton number breaking can be much higher than the electroweak scale in this case. Astrophysical constraints require the decay constant to be $\gtrsim 10^9$ GeV [18].

There is revived interest in a long-lived neutrino, to improve Big-Bang Nucleosynthesis [19] or large scale structure formation theories [20]. Since a decay of neutrinos into electrons or photons is severely constrained, these scenarios require a familon (Majoron) mode $\nu_1 \to \nu_2\phi_F$ (see, *e.g.*, Ref. 15 and references therein).

Other light bosons (scalar, pseudoscalar, or vector) are constrained by "fifth force" experiments. For a compilation of constraints, see Ref. 21.

It has been widely argued that a fundamental theory will not possess global symmetries; gravity, for example, is expected to violate them. Global symmetries such as baryon number arise by accident, typically as a consequence of gauge symmetries. It has been noted [22] that the Peccei-Quinn symmetry, from this perspective, must also arise by accident and must hold to an extraordinary degree of accuracy in order to solve the strong CP problem. Possible resolutions to this problem, however, have been discussed [22,23]. String theory also provides sufficiently good symmetries, especially using a large compactification radius motivated by recent developments in M-theory [24].

References

1. S. Weinberg, Phys. Rev. Lett. **40**, 223 (1978);

F. Wilczek, Phys. Rev. Lett. **40**, 279 (1978).
2. F. Wilczek, Phys. Rev. Lett. **49**, 1549 (1982).
3. Y. Chikashige, R.N. Mohapatra, and R.D. Peccei, Phys. Lett. **98B**, 265 (1981).
4. G.B. Gelmini and M. Roncadelli, Phys. Lett. **99B**, 411 (1981).
5. R.D. Peccei and H. Quinn, Phys. Rev. Lett. **38**, 1440 (1977); also Phys. Rev. **D16**, 1791 (1977).
6. Our normalization here is the same as f_a used in G.G. Raffelt, Phys. Reports **198**, 1 (1990). See this *Review* for the relation to other conventions in the literature.
7. T.W. Donnelly *et al.*, Phys. Rev. **D18**, 1607 (1978);
S. Barshay *et al.*, Phys. Rev. Lett. **46**, 1361 (1981);
A. Barroso and N.C. Mukhopadhyay, Phys. Lett. **106B**, 91 (1981);
R.D. Peccei, in *Proceedings of Neutrino '81*, Honolulu, Hawaii, Vol. 1, p. 149 (1981);
L.M. Krauss and F. Wilczek, Phys. Lett. **B173**, 189 (1986).
8. J. Schweppe *et al.*, Phys. Rev. Lett. **51**, 2261 (1983);
T. Cowan *et al.*, Phys. Rev. Lett. **54**, 1761 (1985).
9. R.D. Peccei, T.T. Wu, and T. Yanagida, Phys. Lett. **B172**, 435 (1986).
10. W.A. Bardeen, R.D. Peccei, and T. Yanagida, Nucl. Phys. **B279**, 401 (1987).
11. J.E. Kim, Phys. Rev. Lett. **43**, 103 (1979);
M.A. Shifman, A.I. Vainstein, and V.I. Zakharov, Nucl. Phys. **B166**, 493 (1980).
12. A.R. Zhitnitsky, Sov. J. Nucl. Phys. **31**, 260 (1980);
M. Dine and W. Fischler, Phys. Lett. **120B**, 137 (1983).
13. J. Preskill, M. Wise, F. Wilczek, Phys. Lett. **120B**, 127 (1983);
L. Abbott and P. Sikivie, Phys. Lett. **120B**, 133 (1983);
M. Dine and W. Fischler, Phys. Lett. **120B**, 137 (1983);
M.S. Turner, Phys. Rev. **D33**, 889 (1986).
14. S. Adler *et al.*, Phys. Rev. Lett. **79**, 2204 (1997).
15. J. Feng, T. Moroi, H. Murayama, and E. Schnapka, UCB-PTH-97/47.
16. K. Choi and A. Santamaria, Phys. Lett. **B267**, 504 (1991).
17. T. Yanagida, in *Proceedings of Workshop on the Unified Theory and the Baryon Number in the Universe*, Tsukuba, Japan, 1979, edited by A. Sawada and A. Sugamoto (KEK, Tsukuba, 1979), p. 95;
M. Gell-Mann, P. Ramond, and R. Slansky, in *Supergravity*, Proceedings of the Workshop, Stony Brook, New York, 1979, edited by P. Van Nieuwenhuizen and D.Z. Freedman (North-Holland, Amsterdam, 1979), p. 315.
18. For a recent analysis of the astrophysical bound on axion-electron coupling, see G. Raffelt and A. Weiss, Phys. Rev. **D51**, 1495 (1995). A bound on Majoron decay constant can be inferred from the same analysis..
19. M. Kawasaki, P. Kernan, H.-S. Kang, R.J. Scherrer, G. Steigman, and T.P. Walker, Nucl. Phys. **B419**, 105 (1994);
S. Dodelson, G. Gyuk, and M.S. Turner, Phys. Rev. **D49**, 5068 (1994);
J.R. Rehm, G. Raffelt, and A. Weiss, Astron. Astrophys. **327**, 443 (1997);
M. Kawasaki, K. Kohri, and K. Sato, Phys. Lett. **B430**, 132 (1998).
20. M. White, G. Gelmini, and J. Silk, Phys. Rev. **D51**, 2669 (1995);
S. Bharadwaj and S.K. Kethi, Astrophys. J. Supp. **114**, 37 (1998).
21. E.G. Adelberger, B.R. Heckel, C.W. Stubbs, and W.F. Rogers, Ann. Rev. Nucl. and Part. Sci. **41**, 269 (1991).
22. M. Kamionkowski and J. March-Russell, Phys. Lett. **B282**, 137 (1992);
R. Holman *et al.*, Phys. Lett. **B282**, 132 (1992).
23. R. Kallosh, A. Linde, D. Linde, and L. Susskind, Phys. Rev. **D52**, 912 (1995).
24. See, for instance, T. Banks and M. Dine, Nucl. Phys. **B479**, 173 (1996); Nucl. Phys. **B505**, 445 (1997).

AXIONS AND OTHER VERY LIGHT BOSONS: PART II (ASTROPHYSICAL CONSTRAINTS)

(by G.G. Raffelt)

Low-mass weakly-interacting particles (neutrinos, gravitons, axions, baryonic or leptonic gauge bosons, *etc.*) are produced in hot plasmas and thus represent an energy-loss channel for stars. The strength of the interaction with photons, electrons, and nucleons can be constrained from the requirement that stellar-evolution time scales are not modified beyond observational limits. For detailed reviews see Refs. [1,2].

The energy-loss rates are steeply increasing functions of temperature T and density ρ. Because the new channel has to compete with the standard neutrino losses which tend to increase even faster, the best limits arise from low-mass stars, notably from horizontal-branch (HB) stars which have a helium-burning core of about 0.5 solar masses at $\langle\rho\rangle \approx 0.6\times10^4\,\mathrm{g\,cm^{-3}}$ and $\langle T\rangle \approx 0.7\times10^8\,\mathrm{K}$. The new energy-loss rate must not exceed about $10\,\mathrm{ergs\,g^{-1}\,s^{-1}}$ to avoid a conflict with the observed number ratio of HB stars in globular clusters. Likewise the ignition of helium in the degenerate cores of the preceding red-giant phase is delayed too much unless the same constraint holds at $\langle\rho\rangle \approx 2\times10^5\,\mathrm{g\,cm^{-3}}$ and $\langle T\rangle \approx 1\times10^8\,\mathrm{K}$. The white-dwarf luminosity function also yields useful bounds.

The new bosons X^0 interact with electrons and nucleons with a dimensionless strength g. For scalars it is a Yukawa coupling, for new gauge bosons (*e.g.*, from a baryonic or leptonic gauge symmetry) a gauge coupling. Axion-like pseudoscalars couple derivatively as $f^{-1}\bar\psi\gamma_\mu\gamma_5\psi\,\partial^\mu\phi_X$ with f an energy scale. Usually this is equivalent to $(2m/f)\bar\psi\gamma_5\psi\,\phi_X$ with m the mass of the fermion ψ so that $g = 2m/f$. For the coupling to electrons, globular-cluster stars yield the constraint

$$g_{Xe} \lesssim \begin{cases} 0.5\times10^{-12} & \text{for pseudoscalars [3]} \;, \\ 1.3\times10^{-14} & \text{for scalars [4]} \;, \end{cases} \tag{1}$$

if $m_X \lesssim 10\,\mathrm{keV}$. The Compton process $\gamma + {}^4\mathrm{He} \to {}^4\mathrm{He} + X^0$ limits the coupling to nucleons to $g_{XN} \lesssim 0.4\times10^{-10}$ [4].

Scalar and vector bosons mediate long-range forces which are severely constrained by "fifth-force" experiments [5]. In the massless case the best limits come from tests of the equivalence principle in the solar system, leading to

$$g_{B,L} \lesssim 10^{-23} \tag{2}$$

for a baryonic or leptonic gauge coupling [6].

In analogy to neutral pions, axions A^0 couple to photons as $g_{A\gamma}\mathbf{E}\cdot\mathbf{B}\,\phi_A$ which allows for the Primakoff conversion $\gamma \leftrightarrow A^0$ in external electromagnetic fields. The most restrictive limit arises from globular-cluster stars [2]

$$g_{A\gamma} \lesssim 0.6 \times 10^{-10}\,\mathrm{GeV}^{-1}\ . \tag{3}$$

The often-quoted "red-giant limit" [7] is slightly weaker.

The duration of the SN 1987A neutrino signal of a few seconds proves that the newborn neutron star cooled mostly by neutrinos rather than through an "invisible channel" such as right-handed (sterile) neutrinos or axions [8]. Therefore,

$$3 \times 10^{-10} \lesssim g_{AN} \lesssim 3 \times 10^{-7} \tag{4}$$

is excluded for the pseudoscalar Yukawa coupling to nucleons [2]. The "strong" coupling side is allowed because axions then escape only by diffusion, quenching their efficiency as an energy-loss channel [9]. Even then the range

$$10^{-6} \lesssim g_{AN} \lesssim 10^{-3} \tag{5}$$

is excluded to avoid excess counts in the water Cherenkov detectors which registered the SN 1987A neutrino signal [11].

In terms of the Peccei-Quinn scale f_A, the axion couplings to nucleons and photons are $g_{AN} = C_N m_N/f_A$ ($N = n$ or p) and $g_{A\gamma} = (\alpha/2\pi f_A)\,(E/N - 1.92)$ where C_N and E/N are model-dependent numerical parameters of order unity. With $m_A = 0.62\,\mathrm{eV}\,(10^7\,\mathrm{GeV}/f_A)$, Eq. (3) yields $m_A \lesssim 0.4\,\mathrm{eV}$ for $E/N = 8/3$ as in GUT models or the DFSZ model. The SN 1987A limit is $m_A \lesssim 0.008\,\mathrm{eV}$ for KSVZ axions while it varies between about 0.004 and 0.012 eV for DFSZ axions, depending on the angle β which measures the ratio of two Higgs vacuum expectation values [10]. In view of the large uncertainties it is good enough to remember $m_A \lesssim 0.01$ eV as a generic limit (Fig. 1).

In the early universe, axions come into thermal equilibrium only if $f_A \lesssim 10^8$ GeV [12]. Some fraction of the relic axions end up in galaxies and galaxy clusters. Their decay $a \to 2\gamma$ contributes to the cosmic extragalactic background light and to line emissions from galactic dark-matter haloes and galaxy clusters. An unsuccessful "telescope search" for such features yields $m_a < 3.5\,\mathrm{eV}$ [13]. For $m_a \gtrsim 30\,\mathrm{eV}$, the axion lifetime is shorter than the age of the universe.

For $f_A \gtrsim 10^8$ GeV cosmic axions are produced nonthermally. If inflation occurred after the Peccei-Quinn symmetry breaking or if $T_{\mathrm{reheat}} < f_A$, the "misalignment mechanism" [14] leads to a contribution to the cosmic critical density of

$$\Omega_A h^2 \approx 1.9 \times 3^{\pm1}\,(1\,\mu\mathrm{eV}/m_A)^{1.175}\,\Theta_{\mathrm{i}}^2 F(\Theta_{\mathrm{i}}) \tag{6}$$

where h is the Hubble constant in units of $100\,\mathrm{km\,s^{-1}\,Mpc^{-1}}$. The stated range reflects recognized uncertainties of the cosmic conditions at the QCD phase transition and of the temperature-dependent axion mass. The function $F(\Theta)$ with $F(0) = 1$ and $F(\pi) = \infty$ accounts for anharmonic corrections to the axion potential. Because the initial misalignment angle Θ_{i} can be very small or very close to π, there is no real prediction for the mass of dark-matter axions even though one would expect $\Theta_{\mathrm{i}}^2 F(\Theta_{\mathrm{i}}) \sim 1$ to avoid fine-tuning the initial conditions.

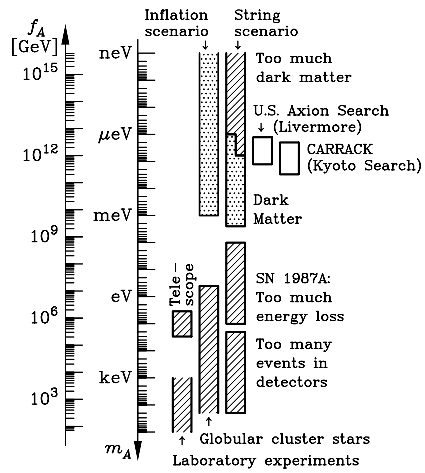

Figure 1: Astrophysical and cosmological exclusion regions (hatched) for the axion mass m_A or equivalently, the Peccei-Quinn scale f_A. An "open end" of an exclusion bar means that it represents a rough estimate; its exact location has not been established or it depends on detailed model assumptions. The globular cluster limit depends on the axion-photon coupling; it was assumed that $E/N = 8/3$ as in GUT models or the DFSZ model. The SN 1987A limits depend on the axion-nucleon couplings; the shown case corresponds to the KSVZ model and approximately to the DFSZ model. The dotted "inclusion regions" indicate where axions could plausibly be the cosmic dark matter. Most of the allowed range in the inflation scenario requires fine-tuned initial conditions. In the string scenario the plausible dark-matter range is controversial as indicated by the step in the low-mass end of the "inclusion bar" (see main text for a discussion). Also shown is the projected sensitivity range of the search experiments for galactic dark-matter axions.

A possible fine-tuning of Θ_{i} is limited by inflation-induced quantum fluctuations which in turn lead to temperature fluctuations of the cosmic microwave background [15,16]. In a broad class of inflationary models one thus finds an upper limit to m_A where axions could be the dark matter. According to the most recent discussion [16] it is about 10^{-3} eV (Fig. 1).

If inflation did not occur at all or if it occurred before the Peccei-Quinn symmetry breaking with $T_{\mathrm{reheat}} > f_A$, cosmic axion strings form by the Kibble mechanism [17]. Their motion is damped primarily by axion emission rather than gravitational waves. After axions acquire a mass at the QCD phase transition they quickly become nonrelativistic and thus form a cold dark matter component. Battye and Shellard [18] found that the dominant source of axion radiation are string loops rather than long strings. At a cosmic time t the average loop creation size is parametrized as $\langle \ell \rangle = \alpha t$ while the radiation power is $P = \kappa\mu$ with μ the renormalized string tension. The loop contribution to the cosmic axion density is [18]

$$\Omega_A h^2 \approx 88 \times 3^{\pm 1} \left[(1+\alpha/\kappa)^{3/2} - 1 \right] \, (1\,\mu\text{eV}/m_A)^{1.175} \, , \quad (7)$$

where the stated nominal uncertainty has the same source as in Eq. (6). The values of α and κ are not known, but probably $0.1 < \alpha/\kappa < 1.0$ [18], taking the expression in square brackets to 0.15–1.83. If axions are the dark matter, we have

$$0.05 \lesssim \Omega_A h^2 \lesssim 0.50 \, , \quad (8)$$

where it was assumed that the universe is older than 10 Gyr, that the dark-matter density is dominated by axions with $\Omega_A \gtrsim 0.2$, and that $h \gtrsim 0.5$. This implies m_A = 6–2500 μeV for the plausible mass range of dark-matter axions (Fig. 1).

Contrary to Ref. 18, Sikivie *et al.* [19] find that the motion of global strings is strongly damped, leading to a flat axion spectrum. In Battye and Shellard's treatment the axion radiation is strongly peaked at wavelengths of order the loop size. In Sikivie *et al.*'s picture more of the string radiation goes into kinetic axion energy which is redshifted so that ultimately there are fewer axions. In this scenario the contributions from string decay and vacuum realignment are of the same order of magnitude; they are both given by Eq. (6) with Θ_i of order one. As a consequence, Sikivie *et al.* allow for a plausible range of dark-matter axions which reaches to smaller masses as indicated in Fig. 1.

The work of both groups implies that the low-mass end of the plausible mass interval in the string scenario overlaps with the projected sensitivity range of the U.S. search experiment for galactic dark-matter axions (Livermore) [20] and of the Kyoto search experiment CARRACK [21] as indicated in Fig. 1. (See also Part III of this Review by Hagmann, van Bibber, and Rosenberg.)

In summary, a variety of robust astrophysical arguments and laboratory experiments (Fig. 1) indicate that $m_A \lesssim 10^{-2}$ eV. The exact value of this limit may change with a more sophisticated treatment of supernova physics and/or the observation of the neutrino signal from a future galactic supernova, but a dramatic modification is not expected unless someone puts forth a completely new argument. The stellar-evolution limits shown in Fig. 1 depend on the axion couplings to various particles and thus can be irrelevant in fine-tuned models where, for example, the axion-photon coupling strictly vanishes. For nearly any m_A in the range generically allowed by stellar evolution, axions could be the cosmic dark matter, depending on the cosmological scenario realized in nature. It appears that our only practical chance to discover these "invisible" particles rests with the ongoing or future search experiments for galactic dark-matter.

References

1. M.S. Turner, Phys. Reports **197**, 67 (1990); G.G. Raffelt, Phys. Reports **198**, 1 (1990).
2. G.G. Raffelt, Stars as Laboratories for Fundamental Physics (Univ. of Chicago Press, Chicago, 1996).
3. D.A. Dicus, E.W. Kolb, V.L. Teplitz, and R.V. Wagoner, Phys. Rev. **D18**, 1829 (1978); G.G. Raffelt and A. Weiss, Phys. Rev. **D51**, 1495 (1995).
4. J.A. Grifols and E. Massó, Phys. Lett. **B173**, 237 (1986); J.A. Grifols, E. Massó, and S. Peris, Mod. Phys. Lett. **A4**, 311 (1989).
5. E. Fischbach and C. Talmadge, Nature **356**, 207 (1992).
6. L.B. Okun, Yad. Fiz. **10**, 358 (1969) [Sov. J. Nucl. Phys. **10**, 206 (1969)]; S.I. Blinnikov *et al.*, Nucl. Phys. **B458**, 52 (1996).
7. G.G. Raffelt, Phys. Rev. **D33**, 897 (1986); G.G. Raffelt and D. Dearborn, *ibid.* **36**, 2211 (1987).
8. J. Ellis and K.A. Olive, Phys. Lett. **B193**, 525 (1987); G.G. Raffelt and D. Seckel, Phys. Rev. Lett. **60**, 1793 (1988).
9. M.S. Turner, Phys. Rev. Lett. **60**, 1797 (1988); A. Burrows, T. Ressel, and M. Turner, Phys. Rev. **D42**, 3297 (1990).
10. H.-T. Janka, W. Keil, G. Raffelt, and D. Seckel, Phys. Rev. Lett. **76**, 2621 (1996); W. Keil *et al.*, Phys. Rev. **D56**, 2419 (1997).
11. J. Engel, D. Seckel, and A.C. Hayes, Phys. Rev. Lett. **65**, 960 (1990).
12. M.S. Turner, Phys. Rev. Lett. **59**, 2489 (1987).
13. M.A. Bershady, M.T. Ressell, and M.S. Turner, Phys. Rev. Lett. **66**, 1398 (1991); M.T. Ressell, Phys. Rev. **D44**, 3001 (1991); J.M. Overduin and P.S. Wesson, Astrophys. J. **414**, 449 (1993).
14. J. Preskill, M. Wise, and F. Wilczek, Phys. Lett. **B120**, 127 (1983); L. Abbott and P. Sikivie, *ibid.* 133; M. Dine and W. Fischler, *ibid.* 137; M.S. Turner, Phys. Rev. **D33**, 889 (1986).
15. D.H. Lyth, Phys. Lett. **B236**, 408 (1990); M.S. Turner and F. Wilczek, Phys. Rev. Lett. **66**, 5 (1991); A. Linde, Phys. Lett. **B259**, 38 (1991).
16. E.P.S. Shellard and R.A. Battye, "Inflationary axion cosmology revisited", in preparation (1998); The main results can be found in: E.P.S. Shellard and R.A. Battye, `astro-ph/9802216`.
17. R.L. Davis, Phys. Lett. **B180**, 225 (1986); R.L. Davis and E.P.S. Shellard, Nucl. Phys. **B324**, 167 (1989).
18. R.A. Battye and E.P.S. Shellard, Nucl. Phys. **B423**, 260 (1994); Phys. Rev. Lett. **73**, 2954 (1994) (E) *ibid.* **76**, 2203 (1996); `astro-ph/9706014`, to be published in: Proceedings Dark Matter 96, Heidelberg, ed. by H.V. Klapdor-Kleingrothaus and Y. Ramacher.
19. D. Harari and P. Sikivie, Phys. Lett. **B195**, 361 (1987); C. Hagmann and P. Sikivie, Nucl. Phys. **B363**, 247 (1991).
20. C. Hagmann *et al.*, Phys. Rev. Lett. **80**, 2043 (1998).
21. I. Ogawa, S. Matsuki, and K. Yamamoto, Phys. Rev. **D53**, R1740 (1996).

AXIONS AND OTHER VERY LIGHT BOSONS, PART III (EXPERIMENTAL LIMITS)

(Revised November 2003 by C. Hagmann, K. van Bibber, and L.J. Rosenberg, LLNL)

In this section we review the experimental methodology and limits on light axions and light pseudoscalars in general. (A comprehensive overview of axion theory is given by H. Murayama in the Part I of this Review, whose notation we follow [1].) Within its scope are purely laboratory experiments, searches where the axion is assumed to be halo dark matter, and searches where the Sun is presumed to be a source of axions. We restrict the discussion to axions of mass $m_A < O(\mathrm{eV})$, as the allowed range for the axion mass is nominally $10^{-6} < m_A < 10^{-2}$ eV. Experimental work in this range predominantly has been through the axion-to-two-photon coupling $g_{A\gamma}$, to which the present review is largely confined. As discussed in Part II of this Review by G. Raffelt, the lower bound to the axion mass derives from a cosmological overclosure argument, and the upper bound most restrictively from SN1987A [2]. Limits from stellar evolution overlap seamlessly above that, connecting with accelerator-based limits that ruled out the original axion. There, it was assumed that the Peccei-Quinn symmetry-breaking scale was the electroweak scale, *i.e.,* $f_A \sim 250$ GeV, implying axions of mass $m_A \sim O(100\,\mathrm{keV})$. These earlier limits from nuclear transitions, particle decays, *etc.,* while not discussed here, are included in the Listings.

While the axion mass is well-determined by the Peccei-Quinn scale, *i.e.,* $m_A = 0.62\,\mathrm{eV}(10^7\,\mathrm{GeV}/f_A)$, the axion-photon coupling $g_{A\gamma}$ is not: $g_{A\gamma} = (\alpha/\pi f_A)g_\gamma$, with $g_\gamma = (E/N - 1.92)/2$, and where E/N is a model-dependent number. It is noteworthy, however, that quite distinct models lead to axion-photon couplings that are not very different. For example, in the case of axions imbedded in Grand Unified Theories, the DFSZ axion [3], $g_\gamma = 0.37$, whereas in one popular implementation of the "hadronic" class of axions, the KSVZ axion [4], $g_\gamma = -0.96$. Hence, between these two models, rates for axion-photon processes $\sim g^2_{A\gamma}$ differ by less than a factor of 10. The Lagrangian $\mathcal{L} = g_{A\gamma}\mathbf{E}\cdot\mathbf{B}\phi_A$, with ϕ_A the axion field, permits the conversion of an axion into a single real photon in an external electromagnetic field, *i.e.,* a Primakoff interaction. In the case of relativistic axions, $k_\gamma - k_A \sim m_A^2/2\omega$, pertinent to several experiments below, coherent axion-photon mixing in long magnetic fields results in significant conversion probability even for very weakly coupled axions [5]. This mixing of photons and axions has been posited to explain dimming from distant supernovae and the apparent long interstellar attenuation length of the most energetic cosmic rays [6].

Below are discussed several experimental techniques constraining $g_{A\gamma}$, and their results. Also included are recent unpublished results, and projected sensitivities of experiments soon to be upgraded or made operational. Recent reviews describe these experiments in greater detail [7].

III.1. Microwave cavity experiments: Perhaps the most promising avenue to the discovery of the axion presumes that axions constitute a significant fraction of the local dark matter halo in our galaxy. An estimate for the Cold Dark matter (CDM) component of our local galactic halo is $\rho_{\mathrm{CDM}} = 7.5\times10^{-25}\mathrm{g/cm^3}$ $(450\,\mathrm{MeV/cm^3})$ [8]. That the CDM halo is in fact made of axions (rather than, *e.g.,* WIMPs) is in principle an independent assumption. However should very light axions exist, they would almost necessarily be cosmologically abundant [2]. As shown by Sikivie [9] and Krauss *et al.* [10], halo axions may be detected by their resonant conversion into a quasi-monochromatic microwave signal in a high-Q cavity permeated by a strong static magnetic field. The cavity is tunable and the signal is maximum when the frequency $\nu = m_A(1 + O(10^{-6}))$, the width of the peak representing the virial distribution of thermalized axions in the galactic gravitational potential. The signal may possess finer structure due to axions recently fallen into the galaxy and not yet thermalized [11]. The feasibility of the technique was established in early experiments of small sensitive volume, $V = O(1\,\mathrm{liter})$ [12] with HFET amplifiers, setting limits in the mass range $4.5 < m_A < 16.3$ μeV, but lacking by 2–3 orders of magnitude the sensitivity to detect KSVZ and DFSZ axions (the conversion power $P_{A\to\gamma} \propto g^2_{A\gamma}$). ADMX, a later experiment ($B \sim 7.8$ T, $V \sim 200$ liter) has achieved sensitivity to KSVZ axions over the mass range 1.9–3.3 μeV, and continues to operate [13]. The exclusion regions shown in Figure 1 for Refs. 12,13 are all normalized to the CDM density $\rho_{\mathrm{CDM}} = 7.5\times10^{-25}\mathrm{g/cm^3}$ $(450\,\mathrm{MeV/cm^3})$ and 90% CL. A near quantum-limited low noise DC SQUID amplifier [14] is being installed in the upgraded ADMX experiment. A Rydberg atom single-quantum detector [15] is being commissioned in a new RF cavity axion search [16]. These new technologies promise dramatic improvements in experimental sensitivity, which should enable rapid scanning of the axion mass range at or better than the sensitivity required to detect DFSZ axions. The search region of the microwave cavity experiments is shown in detail in Figure 1.

III.2 Optical and Radio Telescope searches: For axions of mass greater than about 10^{-1} eV, their cosmological abundance is no longer dominated by vacuum misalignment of string radiation mechanisms, but rather by thermal emission. Their contribution to critical density is small $\Omega \sim 0.01(m_A/\mathrm{eV})$. However, the spontaneous-decay lifetime of axions, $\tau(A \to 2\gamma) \sim 10^{25}\mathrm{sec}(m_A/\mathrm{eV})^{-5}$ while irrelevant for μeV axions, is short enough to afford a powerful constraint on such thermally produced axions in the eV mass range, by looking for a quasi-monochromatic photon line from galactic clusters. This line, corrected for Doppler shift, would be at half the axion mass and its width would be consistent with the observed virial motion, typically $\Delta\lambda/\lambda \sim 10^{-2}$. The expected line intensity would be of the order $I_A \sim 10^{-17}(m_A/3\,\mathrm{eV})^7\mathrm{erg\,cm^{-2}arcsec^{-2}\AA^{-1}sec^{-1}}$ for DFSZ axions, comparable to the continuum night emission.

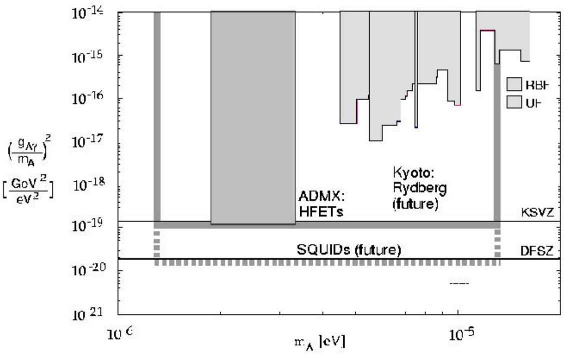

Figure 1: Exclusion region from the microwave cavity experiments, where the plot is flattened by presenting $(g_{A\gamma}/m_A)^2$ versus m_A. The first-generation experiments ("RBF" and "UF" [12]) and in-progress "ADMX" [13] are all HFET-based. Shown also is the full mass range to be covered by the latter experiment (shaded line), and the improved sensitivity when upgraded with DC SQUID amplifiers [14] (shaded dashed line). The expected sensitivity of "CARRACK II" based on a Rydberg single-quantum receiver (dotted line) is also shown in Ref. 16.

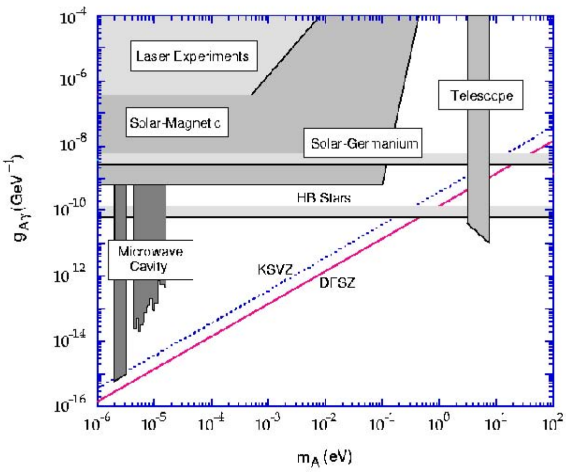

Figure 2: Exclusion region in mass versus axion-photon coupling $(m_A, g_{A\gamma})$ for various experiments. The limit set by globular cluster Horizontal Branch Stars ("HB Stars") is shown in Ref. 2.

The conservative assumption is made that the relative density of thermal axions fallen into the cluster gravitational potential reflects their overall cosmological abundance. A search for thermal axions in three rich Abell clusters was carried out at Kitt Peak National Laboratory [17]; no such line was observed between 3100–8300 Å (m_A = 3–8 eV) after on-off field subtraction of the atmospheric molecular background spectra. A limit everywhere stronger than $g_{A\gamma} < 10^{-10}\text{GeV}^{-1}$ is set, which is seen from Fig. 2 to easily exclude DFSZ axions throughout the mass range.

Similar in principle to the optical telescope search, microwave photons from spontaneous axion decay in halos of astrophysical objects may be searched for with a radio telescope. One group [18] aimed the Haystack radio dish at several nearby dwarf galaxies. The expected signal is a narrow spectral line with the expected virial width, Doppler shift, and intensity distribution about the center of the galaxies. They reported limits of $g_{A\gamma} < 1.0 \times 10^{-9}\text{GeV}^{-1}$ for $m_A \sim$ few×100 μeV. They propose an interferometric radio telescope search with sensitivity near $g_{A\gamma}$ of 10^{-10}GeV^{-1}.

III.3 A search for solar axions: As with the telescope search for thermally produced axions, the search for solar axions was stimulated by the possibility of there being a "1 eV window" for hadronic axions (*i.e.,* axions with no tree-level coupling to leptons), a "window" subsequently closed by an improved understanding of the evolution of globular cluster stars and SN1987A [2]. Hadronic axions would be copiously produced within our Sun's interior by a Primakoff process. Their flux at the Earth of $\sim 10^{12}\text{cm}^{-2}\text{sec}^{-1}(m_A/\text{eV})^2$, which is independent of the details of the solar model, is sufficient for a definitive test via the axion reconversion into photons in a large magnetic field. However, their average energy is $\sim$ 4 keV, implying an oscillation length in the vacuum of $2\pi(m_A^2/2\omega)^{-1} \sim O(\text{mm})$, precluding the mixing from achieving its theoretically maximum value in any practical magnet. It was recognized that one could endow the photon with an effective mass in the gas, $m_\gamma = \omega_{\text{pl}}$, thus permitting the axion and photon dispersion relations to be matched [5]. A first simple implementation of this proposal was carried out using a conventional dipole magnet with a conversion volume of variable-pressure gas and a xenon proportional chamber as the x-ray detector [19]. The magnet was fixed in orientation to take data for $\sim$ 1000 sec/day. Axions were excluded for $g_{A\gamma} < 3.6 \times 10^{-9}\text{GeV}^{-1}$ for $m_A < 0.03$ eV, and $g_{A\gamma} < 7.7 \times 10^{-9}\text{GeV}^{-1}$ for $0.03 < m_A < 0.11$ eV (95% CL). A more sensitive experiment (Tokyo axion helioscope) has been completed, using a superconducting magnet on a telescope mount to track the sun continuously. This gives an exclusion limit of $g_{A\gamma} < 6 \times 10^{-10}\text{GeV}^{-1}$ for $m_A < 0.3$ eV [20]. A new experiment CAST (CERN Axion Solar Telescope), using a decommissioned LHC dipole magnet, is taking first data [21]. The projected sensitivity $g_{A\gamma} < 10^{-10}\text{GeV}^{-1}$ for $m_A < 1$ eV, is about that of the globular cluster bounds.

Other searches for solar axions have been carried out using crystal germanium detectors. These exploit the coherent conversion of axions into photons when their angle of incidence satisfies a Bragg condition with a crystalline plane. Analysis of 1.94 kg-yr of data from a 1 kg germanium detector yields a bound of $g_{A\gamma} < 2.7 \times 10^{-9}\text{GeV}^{-1}$ (95% CL) independent of mass up to $m_A \sim 1$ keV [22]. Analysis of 0.2 kg-yr of data from a 0.234 kg germanium detector yields a bound of $g_{A\gamma} < 2.8 \times 10^{-9}\mathrm{GeV}^{-1}$ (95% CL) [23]. A general study of sensitivities [24] concludes these crystal detectors are unlikely to compete with axion bounds arising from globular clusters [25] or helioseismology [26].

III.4 Photon regeneration ("invisible light shining through walls"): Photons propagating through a transverse field (with $\mathbf{E}\|\mathbf{B}$ may convert into axions. For light axions with $m_A^2 l/2\omega \ll 2\pi$, where l is the length of the magnetic field, the axion beam produced is colinear and coherent with the photon beam, and the conversion probability Π is given by $\Pi \sim (1/4)(g_{A\gamma}Bl)^2$. An ideal implementation for this limit is a laser beam propagating down a long, superconducting dipole magnet like those for high-energy physics accelerators. If another such dipole magnet is set up in line with the first, with an optical barrier interposed between them, then photons may be regenerated from the pure axion beam in the second magnet and detected [27]. The overall probability $P(\gamma \to A \to \gamma) = \Pi^2$. such an experiment has been carried our, utilizing two magnets of length $l = 4.4$ m and $B = 3.7$ T. Axions with mass $m_A < 10^{-3}$ eV, and $g_{A\gamma} > 6.7 \times 10^{-7}\mathrm{GeV}^{-1}$ were excluded at 95% CL [28]. With sufficient effort, limits comparable to those from stellar evolution would be achievable. Due to the $g_{A\gamma}^4$ rate suppression, however, it does not seem feasible to reach standard axion couplings.

III.5 Polarization experiments: The existence of axions can affect the polarization of light propagating through a transverse magnetic field in two ways [29]. First, as the $\mathbf{E}_\|$ component, but not the $\mathbf{E}_\perp$ component will be depleted by the production of real axions, there will be in general a small rotation of the polarization vector of linearly polarized light. This effect will be constant for all sufficiently light m_A such that the oscillation length is much longer than the magnet $m_A^2 l/2\omega \ll 2\pi$. For heavier axions, the effect oscillates and diminishes with increasing m_A, and vanishes for $m_A > \omega$. The second effect is birefringence of the vacuum, again because there could be a mixing of virtual axions in the $\mathbf{E}_\|$ state, but not for the $\mathbf{E}_\perp$ state. This will lead to light that is initially linearly polarized becoming elliptically polarized. Higher-order QED also induces vacuum birefringence, and is much stronger than the contribution due to axions. A search for both polarization-rotation and induced ellipticity has been carried out with the same dipole magnets described above [30]. As in the case of photon regeneration, the observables are boosted linearly by the number of passes of the laser beam in the optical cavity within the magnet. The polarization-rotation resulted in a stronger limit than that from ellipticity, $g_{A\gamma} < 3.6 \times 10^{-7}\mathrm{GeV}^{-1}$ (95% CL) for $m_A < 5 \times 10^{-4}$ eV. The limits from ellipticity are better at higher masses, as they fall off smoothly and do not terminate at m_A. Current experiments with greatly improved sensitivity that, while still far from being able to detect standard axions, have measured the QED "light-by-light" contribution for the first time [31]. The overall envelope for limits from the laser-based experiments is shown schematically in Fig. 2.

III.6 Non-Newtonian monopole-dipole couplings: Axions mediate a CP violating monopole-dipole Yukawa-type gravitational interaction potential ($g_s g_p\, \hat{\sigma} \cdot \hat{r}\, \mathrm{e}^{-r/\lambda}$) between spin and matter [32] where $g_s g_p$ is the product of couplings at the scalar and polarized vertices and λ is the range of the force. Two experiments placed upper limits on the product coupling $g_s g_p$ in a system of magnetized media and test masses. One experiment [33] had peak sensitivity near 100 mm (2 μeV axion mass) another [34] had peak sensitivity near 10 mm (20 μeV axion mass). Both lacked sensitivity by 10 orders of magnitude of the sensitivity required to detect couplings implied by the existing limits on a neutron EDM.

References

1. H. Murayama, Part I (Theory) of this Review.
2. G. Raffelt, Part II (Astrophysical Constraints) of this Review.
3. M. Dine *et al.*, Phys. Lett. **B104**, 199 (1981);
   A. Zhitnitsky, Sov. J. Nucl. Phys. **31**, 260 (1980).
4. J. Kim, Phys. Rev. Lett. **43**, 103 (1979);
   M. Shifman *et al.*, Nucl. Phys. **B166**, 493 (1980).
5. G. Raffelt and L. Stodolsky, Phys. Rev. **D37**, 1237 (1988).
6. See, *e.g.*, C. Csaki, N. Kaloper and J. Terning, Phys. Rev. Lett. **88**, 161302 (2002);
   E. Mörtsell, L. Bergström, and A. Goobar, Phys. Rev. **D66**, 047702 (2002);
   D.S. Gorbunov, G.G. Raffelt, and D.V. Semikoz, Phys. Rev. **D64**, 096005 (2001);
   C. Csaki, N. Kaloper, M. Peloso and J. Terning, JCAP **0305**, 005 (2003).
7. L.J. Rosenberg and K.A. van Bibber, Phys. Reports **325**, 1 (2000);
   R. Bradley *et al.*, Rev. Mod. Phys. **75**, 777 (2003).
8. E. Gates *et al.*, Ap. J. **499**, 123 (1995).
9. P. Sikivie, Phys. Rev. Lett. **51**, 1415 (1983); **52(E)**, 695 (1984); Phys. Rev. **D32**, 2988 (1985).
10. L. Krauss *et al.*, Phys. Rev. Lett. **55**, 1797 (1985).
11. P. Sikivie and J. Ipser, Phys. Lett. **B291**, 288 (1992);
    P. Sikivie *et al.*, Phys. Rev. Lett. **75**, 2911 (1995).
12. S. DePanfilis *et al.*, Phys. Rev. Lett. **59**, 839 (1987);
    W. Wuensch *et al.*, Phys. Rev. **D40**, 3153 (1989);
    C. Hagmann *et al.*, Phys. Rev. **D40**, 3153 (1989).
13. C. Hagmann *et al.*, Phys. Rev. Lett. **80**, 2043 (1998);
    S. J. Asztalos *et al.*, Astrophys. J. **571**, L27 (2002);
    H. Peng at al., Nucl. Instrum. Methods **A444**, 569 (2000);
    S. Asztalos *et al.*, Phys. Rev. **D64**, 092003 (2003).
14. M. Mück, J.B. Kycia, and J. Clarke, Appl. Phys. Lett. **78**, 967 (2001).
15. I. Ogawa, S. Matsuki, and K. Yamamoto, Phys. Rev. **D53**, 1740 (1996).
16. S. Matsuki *et al.*, Nucl. Phys. **51B** (Proc. Suppl.) 213, (1996).
17. M. Bershady *et al.*, Phys. Rev. Lett. **66**, 1398 (1991);
    M. Ressell, Phys. Rev. **D44**, 3001 (1991).
18. B.D. Blout *et al.*, Astrophys. J. **546**, 825 (2001).
19. D. Lazarus *et al.*, Phys. Rev. Lett. **69**, 2333 (1992).

20. S. Moriyama *et al.*, Phys. Lett. **B434**, 147 (1998);
Y. Inoue *et al.*, Phys. Lett. **B536**, 18 (2002).
21. K. Zioutas *et al.*, Nucl. Instrum. Methods **A425**, 480 (1999);
J.I. Collar *et al.*. [CAST Collaboration], "CAST: A search for solar axions at CERN," hep-ex/0304024.
22. F.T. Avignone III *et al.*, Phys. Rev. Lett. **81**, 5068 (1998).
23. I.G. Irastorza *et al.*, Nucl. Phys. **87** (Proc. Suppl.) 111, (2000).
24. S. Cebrián *et al.*, Astropart. Phys. **10**, 397 (1999).
25. G. Raffelt, "Stars as Laboratories for Fundamental Physics," University of Chicago Press, Chicago (1996).
26. H. Schlattl, A. Weiss, and G. Raffelt, Astropart. Phys. **10**, 353 (1999).
27. K. van Bibber *et al.*, Phys. Rev. Lett. **59**, 759 (1987);
A similar proposal has been made for exactly massless pseudoscalars: A. Ansel'm, Sov. J. Nucl. Phys. **42**, 936 (1985).
28. G. Ruoso *et al.*, Z. Phys. **C56**, 505 (1992);
R. Cameron *et al.*, Phys. Rev. **D47**, 3707 (1993).
29. L. Maiani *et al.*, Phys. Lett. **B175**, 359 (1986).
30. See Ref. 28 and Y. Semertzadis *et al.*, Phys. Rev. Lett. **64**, 2988 (1990).
31. D. Bakalov *et al.*, Quantum Semiclass. Opt. **10**, 239(1998).
32. J.E. Moody and F. Wilczek, Phys. Rev. **D30**, 130 (1984).
33. A.N. Youdin *et al.*, Phys. Rev. Lett. **77**, 2170 (1996).
34. Wei-Tou Ni *et al.*, Phys. Rev. Lett. **82**, 2439 (1999).

A^0 (Axion) MASS LIMITS from Astrophysics and Cosmology

These bounds depend on model-dependent assumptions (i.e. — on a combination of axion parameters).

VALUE (MeV)	*DOCUMENT ID*		*TECN*	*COMMENT*
• • • We do not use the following data for averages, fits, limits, etc. • • •				
>0.2	BARROSO	82	ASTR	Standard Axion
>0.25	[1] RAFFELT	82	ASTR	Standard Axion
>0.2	[2] DICUS	78C	ASTR	Standard Axion
	MIKAELIAN	78	ASTR	Stellar emission
>0.3	[2] SATO	78	ASTR	Standard Axion
>0.2	VYSOTSKII	78	ASTR	Standard Axion

[1] Lower bound from 5.5 MeV γ-ray line from the sun.

[2] Lower bound from requiring the red giants' stellar evolution not be disrupted by axion emission.

A^0 (Axion) and Other Light Boson (X^0) Searches in Meson Decays

Limits are for branching ratios.

VALUE	*CL%*	*EVTS*	*DOCUMENT ID*		*TECN*	*COMMENT*
• • • We do not use the following data for averages, fits, limits, etc. • • •						
$<4.5 \times 10^{-11}$	90		[3] ADLER	02C	B787	$K^+ \to \pi^+ A^0$
$<4.9 \times 10^{-5}$	90		AMMAR	01B	CLEO	$B^\pm \to \pi^\pm (K^\pm) X^0$
$<5.3 \times 10^{-5}$	90		AMMAR	01B	CLEO	$B^0 \to K^0_S X^0$
$<1.1 \times 10^{-10}$	90		[4] ADLER	00	B787	$K^+ \to \pi^+ A^0$
$<3.3 \times 10^{-5}$	90		[5] ALTEGOER	98	NOMD	$\pi^0 \to \gamma X^0$, $m_{X^0} < 120$ MeV
$<5.0 \times 10^{-8}$	90		[6] KITCHING	97	B787	$K^+ \to \pi^+ A^0$ $(A^0 \to \gamma\gamma)$
$<5.2 \times 10^{-10}$	90		[7] ADLER	96	B787	$K^+ \to \pi^+ A^0$
$<2.8 \times 10^{-4}$	90		[8] AMSLER	96B	CBAR	$\pi^0 \to \gamma X^0$, $m_{X^0} < 65$ MeV
$<3 \times 10^{-4}$	90		[8] AMSLER	96B	CBAR	$\eta \to \gamma X^0$, $m_{X^0}=$ 50–200 MeV
$<4 \times 10^{-5}$	90		[8] AMSLER	96B	CBAR	$\eta' \to \gamma X^0$, $m_{X^0}=$ 50–925 MeV
$<6 \times 10^{-5}$	90		[8] AMSLER	94B	CBAR	$\pi^0 \to \gamma X^0$, m_{X^0}=65–125 MeV
$<6 \times 10^{-5}$	90		[8] AMSLER	94B	CBAR	$\eta \to \gamma X^0$, m_{X^0}=200–525 MeV
<0.007	90		[9] MEIJERDREES	94	CNTR	$\pi^0 \to \gamma X^0$, m_{X^0}=25 MeV
<0.002	90		[9] MEIJERDREES	94	CNTR	$\pi^0 \to \gamma X^0$, m_{X^0}=100 MeV
$<2 \times 10^{-7}$	90		[10] ATIYA	93B	B787	$K^+ \to \pi^+ A^0$
$<3 \times 10^{-13}$			[11] NG	93	COSM	$\pi^0 \to \gamma X^0$
$<1.1 \times 10^{-8}$	90		[12] ALLIEGRO	92	SPEC	$K^+ \to \pi^+ A^0$ $(A^0 \to e^+ e^-)$
$<5 \times 10^{-4}$	90		[13] ATIYA	92	B787	$\pi^0 \to \gamma X^0$
$<4 \times 10^{-6}$	90		[14] MEIJERDREES	92	SPEC	$\pi^0 \to \gamma X^0$, $X^0 \to e^+ e^-$, $m_{X^0}=$ 100 MeV
$<1 \times 10^{-7}$	90		[15] ATIYA	90B	B787	Sup. by KITCHING 97
$<1.3 \times 10^{-8}$	90		[16] KORENCHE...	87	SPEC	$\pi^+ \to e^+ \nu A^0$ $(A^0 \to e^+ e^-)$
$<1 \times 10^{-9}$	90	0	[17] EICHLER	86	SPEC	Stopped $\pi^+ \to e^+ \nu A^0$
$<2 \times 10^{-5}$	90		[18] YAMAZAKI	84	SPEC	For 160<m<260 MeV
$<(1.5\text{–}4) \times 10^{-6}$	90		[18] YAMAZAKI	84	SPEC	K decay, $m_{A^0} \ll$ 100 MeV
		0	[19] ASANO	82	CNTR	Stopped $K^+ \to \pi^+ A^0$
		0	[20] ASANO	81B	CNTR	Stopped $K^+ \to \pi^+ A^0$
			[21] ZHITNITSKII	79		Heavy axion

[3] ADLER 02C bound is for m_{A^0} <60 MeV. See Fig. 2 for limits at higher masses.

[4] ADLER 00 bound is for massless A^0.

[5] ALTEGOER 98 looked for X^0 from π^0 decay which penetrate the shielding and convert to π^0 in the external Coulomb field of a nucleus.

[6] KITCHING 97 limit is for B($K^+ \to \pi^+ A^0$)·B($A^0 \to \gamma\gamma$) and applies for $m_{A^0} \simeq 50$ MeV, $\tau_{A^0} < 10^{-10}$ s. Limits are provided for $0<m_{A^0} < 100$ MeV, $\tau_{A^0} < 10^{-8}$ s.

[7] ADLER 96 looked for a peak in missing-mass distribution. This work is an update of ATIYA 93. The limit is for massless stable A^0 particles and extends to m_{A^0}=80 MeV at the same level. See paper for dependence on finite lifetime.

[8] AMSLER 94B and AMSLER 96B looked for a peak in missing-mass distribution.

[9] The MEIJERDREES 94 limit is based on inclusive photon spectrum and is independent of X^0 decay modes. It applies to $\tau(X^0) > 10^{-23}$ sec.

[10] ATIYA 93B looked for a peak in missing mass distribution. The bound applies for stable A^0 of m_{A^0}=150–250 MeV, and the limit becomes stronger (10^{-8}) for m_{A^0}=180–240 MeV.

[11] NG 93 studied the production of X^0 via $\gamma\gamma \to \pi^0 \to \gamma X^0$ in the early universe at $T \simeq 1$ MeV. The bound on extra neutrinos from nucleosynthesis $\Delta N_\nu < 0.3$ (WALKER 91) is employed. It applies to $m_{X^0} \ll 1$ MeV in order to be relativistic down to nucleosynthesis temperature. See paper for heavier X^0.

[12] ALLIEGRO 92 limit applies for m_{A^0}=150–340 MeV and is the branching ratio times the decay probability. Limit is $< 1.5 \times 10^{-8}$ at 99%CL.

[13] ATIYA 92 looked for a peak in missing mass distribution. The limit applies to m_{X^0}=0–130 MeV in the narrow resonance limit. See paper for the dependence on lifetime. Covariance requires X^0 to be a vector particle.

[14] MEIJERDREES 92 limit applies for $\tau_{X^0} = 10^{-23}$–10^{-11} sec. Limits between 2×10^{-4} and 4×10^{-6} are obtained for m_{X^0} = 25–120 MeV. Angular momentum conservation requires that X^0 has spin ≥ 1.

[15] ATIYA 90B limit is for B($K^+ \to \pi^+ A^0$)·B($A^0 \to \gamma\gamma$) and applies for $m_{A^0} = 50$ MeV, $\tau_{A^0} < 10^{-10}$ s. Limits are also provided for $0 < m_{A^0} < 100$ MeV, $\tau_{A^0} < 10^{-8}$ s.

[16] KORENCHENKO 87 limit assumes $m_{A^0} = 1.7$ MeV, $\tau_{A^0} \lesssim 10^{-12}$ s, and B($A^0 \to e^+ e^-$) = 1.

[17] EICHLER 86 looked for $\pi^+ \to e^+ \nu A^0$ followed by $A^0 \to e^+ e^-$. Limits on the branching fraction depend on the mass and and lifetime of A^0. The quoted limits are valid when $\tau(A^0) \gtrsim 3. \times 10^{-10}$s if the decays are kinematically allowed.

[18] YAMAZAKI 84 looked for a discrete line in $K^+ \to \pi^+$X. Sensitive to wide mass range (5–300 MeV), independent of whether X decays promptly or not.

[19] ASANO 82 at KEK set limits for B($K^+ \to \pi^+ A^0$) for m_{A^0} <100 MeV as BR $< 4. \times 10^{-8}$ for $\tau(A^0 \to n\gamma\text{'s}) > 1. \times 10^{-9}$ s, BR $< 1.4 \times 10^{-6}$ for $\tau < 1. \times 10^{-9}$s.

[20] ASANO 81B is KEK experiment. Set B($K^+ \to \pi^+ A^0$) $< 3.8 \times 10^{-8}$ at CL = 90%.

[21] ZHITNITSKII 79 argue that a heavy axion predicted by YANG 78 (3 <m <40 MeV) contradicts experimental muon anomalous magnetic moments.

A^0 (Axion) Searches in Quarkonium Decays

Decay or transition of quarkonium. Limits are for branching ratio.

VALUE	*CL%*	*EVTS*	*DOCUMENT ID*		*TECN*	*COMMENT*
• • • We do not use the following data for averages, fits, limits, etc. • • •						
$<1.3 \times 10^{-5}$	90		[22] BALEST	95	CLEO	$\Upsilon(1S) \to A^0 \gamma$
$<4.0 \times 10^{-5}$	90		ANTREASYAN	90C	CBAL	$\Upsilon(1S) \to A^0 \gamma$
			[23] ANTREASYAN	90C	RVUE	
$<5 \times 10^{-5}$	90		[24] DRUZHININ	87	ND	$\phi \to A^0 \gamma$ $(A^0 \to e^+ e^-)$
$<2 \times 10^{-3}$	90		[25] DRUZHININ	87	ND	$\phi \to A^0 \gamma$ $(A^0 \to \gamma\gamma)$
$<7 \times 10^{-6}$	90		[26] DRUZHININ	87	ND	$\phi \to A^0 \gamma$ $(A^0 \to$ missing)
$<3.1 \times 10^{-4}$	90	0	[27] ALBRECHT	86D	ARG	$\Upsilon(1S) \to A^0 \gamma$ $(A^0 \to e^+ e^-)$
$<4 \times 10^{-4}$	90	0	[27] ALBRECHT	86D	ARG	$\Upsilon(1S) \to A^0 \gamma$ $(A^0 \to \mu^+ \mu^-, \pi^+ \pi^-, K^+ K^-)$

$<8 \times 10^{-4}$	90	1	[28] ALBRECHT	86D	ARG	$\Upsilon(1S) \to A^0\gamma$
$<1.3 \times 10^{-3}$	90	0	[29] ALBRECHT	86D	ARG	$\Upsilon(1S) \to A^0\gamma$ ($A^0 \to e^+e^-, \gamma\gamma$)
$<2. \times 10^{-3}$	90		[30] BOWCOCK	86	CLEO	$\Upsilon(2S) \to \Upsilon(1S) \to A^0$
$<5. \times 10^{-3}$	90		[31] MAGERAS	86	CUSB	$\Upsilon(1S) \to A^0\gamma$
$<3. \times 10^{-4}$	90		[32] ALAM	83	CLEO	$\Upsilon(1S) \to A^0\gamma$
$<9.1 \times 10^{-4}$	90		[33] NICZYPORUK	83	LENA	$\Upsilon(1S) \to A^0\gamma$
$<1.4 \times 10^{-5}$	90		[34] EDWARDS	82	CBAL	$J/\psi \to A^0\gamma$
$<3.5 \times 10^{-4}$	90		[35] SIVERTZ	82	CUSB	$\Upsilon(1S) \to A^0\gamma$
$<1.2 \times 10^{-4}$	90		[35] SIVERTZ	82	CUSB	$\Upsilon(3S) \to A^0\gamma$

[22] BALEST 95 looked for a monochromatic γ from $\Upsilon(1S)$ decay. The bound is for $m_{A^0} <$ 5.0 GeV. See Fig. 7 in the paper for bounds for heavier m_{A^0}. They also quote a bound on branching ratios 10^{-3}–10^{-5} of three-body decay $\gamma X \overline{X}$ for $0 < m_X < 3.1$ GeV.

[23] The combined limit of ANTREASYAN 90C and EDWARDS 82 excludes standard axion with $m_{A^0} < 2m_e$ at 90% CL as long as $C_\Upsilon C_{J/\psi} > 0.09$, where C_V ($V = \Upsilon$, J/ψ) is the reduction factor for $\Gamma(V \to A^0\gamma)$ due to QCD and/or relativistic corrections. The same data excludes $0.02 < x < 260$ (90% CL) if $C_\Upsilon = C_{J/\psi} = 0.5$, and further combining with ALBRECHT 86D result excludes $5 \times 10^{-5} < x < 260$. x is the ratio of the vacuum expectation values of the two Higgs fields. These limits use conventional assumption $\Gamma(A^0 \to ee) \propto x^{-2}$. The alternative assumption $\Gamma(A^0 \to ee) \propto x^2$ gives a somewhat different excluded region $0.00075 < x < 44$.

[24] The first DRUZHININ 87 limit is valid when $\tau_{A^0}/m_{A^0} < 3 \times 10^{-13}$ s/MeV and $m_{A^0} < 20$ MeV.

[25] The second DRUZHININ 87 limit is valid when $\tau_{A^0}/m_{A^0} < 5 \times 10^{-13}$ s/MeV and $m_{A^0} < 20$ MeV.

[26] The third DRUZHININ 87 limit is valid when $\tau_{A^0}/m_{A^0} > 7 \times 10^{-12}$ s/MeV and $m_{A^0} < 200$ MeV.

[27] $\tau_{A^0} < 1 \times 10^{-13}$s and $m_{A^0} < 1.5$ GeV. Applies for $A^0 \to \gamma\gamma$ when $m_{A^0} < 100$ MeV.

[28] $\tau_{A^0} > 1 \times 10^{-7}$s.

[29] Independent of τ_{A^0}.

[30] BOWCOCK 86 looked for A^0 that decays into e^+e^- in the cascade decay $\Upsilon(2S) \to \Upsilon(1S)\pi^+\pi^-$ followed by $\Upsilon(1S) \to A^0\gamma$. The limit for $B(\Upsilon(1S) \to A^0\gamma)B(A^0 \to e^+e^-)$ depends on m_{A^0} and τ_{A^0}. The quoted limit for m_{A^0}=1.8 MeV is at $\tau_{A^0} \sim 2. \times 10^{-12}$s, where the limit is the worst. The same limit $2. \times 10^{-3}$ applies for all lifetimes for masses $2m_e < m_{A^0} < 2m_\mu$ when the results of this experiment are combined with the results of ALAM 83.

[31] MAGERAS 86 looked for $\Upsilon(1S) \to \gamma A^0$ ($A^0 \to e^+e^-$). The quoted branching fraction limit is for $m_{A^0} = 1.7$ MeV, at $\tau(A^0) \sim 4. \times 10^{-13}$s where the limit is the worst.

[32] ALAM 83 is at CESR. This limit combined with limit for $B(J/\psi \to A^0\gamma)$ (EDWARDS 82) excludes standard axion.

[33] NICZYPORUK 83 is DESY-DORIS experiment. This limit together with lower limit 9.2×10^{-4} of $B(\Upsilon \to A^0\gamma)$ derived from $B(J/\psi(1S) \to A^0\gamma)$ limit (EDWARDS 82) excludes standard axion.

[34] EDWARDS 82 looked for $J/\psi \to \gamma A^0$ decays by looking for events with a single γ [of energy $\sim 1/2$ the $J/\psi(1S)$ mass], plus nothing else in the detector. The limit is inconsistent with the axion interpretation of the FAISSNER 81B result.

[35] SIVERTZ 82 is CESR experiment. Looked for $\Upsilon \to \gamma A^0$, A^0 undetected. Limit for $1S$ ($3S$) is valid for $m_{A^0} <$7 GeV (4 GeV).

A^0 (Axion) Searches in Positronium Decays

Decay or transition of positronium. Limits are for branching ratio.

VALUE	CL%	DOCUMENT ID		TECN	COMMENT
• • • We do not use the following data for averages, fits, limits, etc. • • •					
$<4.4 \times 10^{-5}$	90	[36] BADERT...	02	CNTR	o-Ps $\to \gamma X_1 X_2$, $m_{X_1}+m_{X_2} \leq 900$ keV
$<2 \times 10^{-4}$	90	MAENO	95	CNTR	o-Ps $\to A^0\gamma$ m_{A^0}=850–1013 keV
$<3.0 \times 10^{-3}$	90	[37] ASAI	94	CNTR	o-Ps $\to A^0\gamma$ m_{A^0}=30–500 keV
$<2.8 \times 10^{-5}$	90	[38] AKOPYAN	91	CNTR	o-Ps $\to A^0\gamma$ ($A^0 \to \gamma\gamma$), $m_{A^0} < 30$ keV
$<1.1 \times 10^{-6}$	90	[39] ASAI	91	CNTR	o-Ps $\to A^0\gamma$, $m_{A^0} < 800$ keV
$<3.8 \times 10^{-4}$	90	GNINENKO	90	CNTR	o-Ps $\to A^0\gamma$, $m_{A^0} <$ 30 keV
$<(1–5) \times 10^{-4}$	95	[40] TSUCHIAKI	90	CNTR	o-Ps $\to A^0\gamma$, $m_{A^0} =$ 300–900 keV
$<6.4 \times 10^{-5}$	90	[41] ORITO	89	CNTR	o-Ps $\to A^0\gamma$, $m_{A^0} < 30$ keV
		[42] AMALDI	85	CNTR	Ortho-positronium
		[43] CARBONI	83	CNTR	Ortho-positronium

[36] BADERTSCHER 02 looked for a three-body decay of ortho-positronium into a photon and two penetrating (neutral or milli-charged) particles.

[37] The ASAI 94 limit is based on inclusive photon spectrum and is independent of A^0 decay modes.

[38] The AKOPYAN 91 limit applies for a short-lived A^0 with $\tau_{A^0} < 10^{-13}\, m_{A^0}$ [keV] s.

[39] ASAI 91 limit translates to $g^2_{A^0 e^+ e^-}/4\pi < 1.1 \times 10^{-11}$ (90%CL) for $m_{A^0} < 800$ keV.

[40] The TSUCHIAKI 90 limit is based on inclusive photon spectrum and is independent of A^0 decay modes.

[41] ORITO 89 limit translates to $g^2_{A^0 ee}/4\pi < 6.2 \times 10^{-10}$. Somewhat more sensitive limits are obtained for larger m_{A^0}: $B < 7.6 \times 10^{-6}$ at 100 keV.

[42] AMALDI 85 set limits $B(A^0\gamma)$ / $B(\gamma\gamma\gamma)$ < (1–5) $\times 10^{-6}$ for m_{A^0} = 900–100 keV which are about 1/10 of the CARBONI 83 limits.

[43] CARBONI 83 looked for orthopositronium $\to A^0\gamma$. Set limit for A^0 electron coupling squared, $g(eeA^0)^2/(4\pi) < 6. \times 10^{-10}$–$7. \times 10^{-9}$ for m_{A^0} from 150–900 keV (CL = 99.7%). This is about 1/10 of the bound from g–2 experiments.

A^0 (Axion) Search in Photoproduction

VALUE	DOCUMENT ID		COMMENT
• • • We do not use the following data for averages, fits, limits, etc. • • •			
	[44] BASSOMPIE...	95	$m_{A^0} = 1.8 \pm 0.2$ MeV

[44] BASSOMPIERRE 95 is an extension of BASSOMPIERRE 93. They looked for a peak in the invariant mass of e^+e^- pairs in the region $m_{e^+e^-} = 1.8 \pm 0.2$ MeV. They obtained bounds on the production rate A^0 for $\tau(A^0) = 10^{-18}$–10^{-9} sec. They also found an excess of events in the range $m_{e^+e^-}$ = 2.1–3.5 MeV.

A^0 (Axion) Production in Hadron Collisions

Limits are for $\sigma(A^0)$ / $\sigma(\pi^0)$.

VALUE	CL%	EVTS	DOCUMENT ID		TECN	COMMENT
• • • We do not use the following data for averages, fits, limits, etc. • • •						
			[45] AHMAD	97	SPEC	e^+ production
			[46] LEINBERGER	97	SPEC	$A^0 \to e^+e^-$
			[47] GANZ	96	SPEC	$A^0 \to e^+e^-$
			[48] KAMEL	96	EMUL	^{32}S emulsion, $A^0 \to e^+e^-$
			[49] BLUEMLEIN	92	BDMP	$A^0 N_Z \to \ell^+\ell^- N_Z$
			[50] MEIJERDREES	92	SPEC	$\pi^- p \to nA^0$, $A^0 \to e^+e^-$
			[51] BLUEMLEIN	91	BDMP	$A^0 \to e^+e^-$, 2γ
			[52] FAISSNER	89	OSPK	Beam dump, $A^0 \to e^+e^-$
			[53] DEBOER	88	RVUE	$A^0 \to e^+e^-$
			[54] EL-NADI	88	EMUL	$A^0 \to e^+e^-$
			[55] FAISSNER	88	OSPK	Beam dump, $A^0 \to 2\gamma$
			[56] BADIER	86	BDMP	$A^0 \to e^+e^-$
$<2. \times 10^{-11}$	90	0	[57] BERGSMA	85	CHRM	CERN beam dump
$<1. \times 10^{-13}$	90	0	[57] BERGSMA	85	CHRM	CERN beam dump
		24	[58] FAISSNER	83	OSPK	Beam dump, $A^0 \to 2\gamma$
			[59] FAISSNER	83B	RVUE	LAMPF beam dump
			[60] FRANK	83B	RVUE	LAMPF beam dump
			[61] HOFFMAN	83	CNTR	$\pi p \to nA^0$ ($A^0 \to e^+e^-$)
			[62] FETSCHER	82	RVUE	See FAISSNER 81B
		12	[63] FAISSNER	81	OSPK	CERN PS ν wideband
		15	[64] FAISSNER	81B	OSPK	Beam dump, $A^0 \to 2\gamma$
		8	[65] KIM	81	OSPK	26 GeV $pN \to A^0 X$
		0	[66] FAISSNER	80	OSPK	Beam dump, $A^0 \to e^+e^-$
$<1. \times 10^{-8}$	90		[67] JACQUES	80	HLBC	28 GeV protons
$<1. \times 10^{-14}$	90		[67] JACQUES	80	HLBC	Beam dump
			[68] SOUKAS	80	CALO	28 GeV p beam dump
			[69] BECHIS	79	CNTR	
$<1. \times 10^{-8}$	90		[70] COTEUS	79	OSPK	Beam dump
$<1. \times 10^{-3}$	95		[71] DISHAW	79	CALO	400 GeV pp
$<1. \times 10^{-8}$	90		ALIBRAN	78	HYBR	Beam dump
$<6. \times 10^{-9}$	95		ASRATYAN	78B	CALO	Beam dump
$<1.5 \times 10^{-8}$	90		[72] BELLOTTI	78	HLBC	Beam dump
$<5.4 \times 10^{-14}$	90		[72] BELLOTTI	78	HLBC	m_{A^0}=1.5 MeV
$<4.1 \times 10^{-9}$	90		[72] BELLOTTI	78	HLBC	m_{A^0}=1 MeV
$<1. \times 10^{-8}$	90		[73] BOSETTI	78B	HYBR	Beam dump
			[74] DONNELLY	78		
$<0.5 \times 10^{-8}$	90		HANSL	78D	WIRE	Beam dump
			[75] MICELMAC...	78		
			[76] VYSOTSKII	78		

[45] AHMAD 97 reports a result of APEX Collaboration which studied positron production in ^{238}U+^{232}Ta and ^{238}U+^{181}Ta collisions, without requiring a coincident electron. No narrow lines were found for $250 < E_{e^+} < 750$ keV.

[46] LEINBERGER 97 (ORANGE Collaboration) at GSI looked for a narrow sum-energy e^+e^--line at $\sim$ 635 keV in ^{238}U+^{181}Ta collision. Limits on the production probability for a narrow sum-energy e^+e^- line are set. See their Table 2.

[47] GANZ 96 (EPos II Collaboration) has placed upper bounds on the production cross section of e^+e^- pairs from ^{238}U+^{181}Ta and ^{238}U+^{232}Th collisions at GSI. See Table 2 for limits both for back-to-back and isotropic configurations of e^+e^- pairs. These limits rule out the existence of peaks in the e^+e^- sum-energy distribution, reported by an earlier version of this experiment.

[48] KAMEL 96 looked for e^+e^- pairs from the collision of ^{32}S (200 GeV/nucleon) and emulsion. No evidence of mass peaks is found in the region of sensitivity $m_{ee} >$2 MeV.

[49] BLUEMLEIN 92 is a proton beam dump experiment at Serpukhov with a secondary target to induce Bethe-Heitler production of e^+e^- or $\mu^+\mu^-$ from the produce A^0.

See Fig. 5 for the excluded region in m_{A^0}-x plane. For the standard axion, $0.3 < x < 25$ is excluded at 95% CL. If combined with BLUEMLEIN 91, $0.008 < x < 32$ is excluded.

[50] MEIJERDREES 92 give $\Gamma(\pi^- p \to nA^0)\cdot B(A^0 \to e^+e^-)/\Gamma(\pi^- p \to \text{all}) < 10^{-5}$ (90% CL) for $m_{A^0} = 100$ MeV, $\tau_{A^0} = 10^{-11}$–10^{-23} sec. Limits ranging from 2.5×10^{-3} to 10^{-7} are given for $m_{A^0} = 25$–136 MeV.

[51] BLUEMLEIN 91 is a proton beam dump experiment at Serpukhov. No candidate event for $A^0 \to e^+e^-$, 2γ are found. Fig. 6 gives the excluded region in m_{A^0}-x plane ($x = \tan\beta = v_2/v_1$). Standard axion is excluded for $0.2 < m_{A^0} < 3.2$ MeV for most $x > 1$, 0.2–11 MeV for most $x < 1$.

[52] FAISSNER 89 searched for $A^0 \to e^+e^-$ in a proton beam dump experiment at SIN. No excess of events was observed over the background. A standard axion with mass $2m_e$–20 MeV is excluded. Lower limit on f_{A^0} of $\simeq 10^4$ GeV is given for $m_{A^0} = 2m_e$–20 MeV.

[53] DEBOER 88 reanalyze EL-NADI 88 data and claim evidence for three distinct states with mass ~ 1.1, ~ 2.1, and ~ 9 MeV, lifetimes 10^{-16}–10^{-15} s decaying to e^+e^- and note the similarity of the data with those of a cosmic-ray experiment by Bristol group (B.M. Anand, Proc. of the Royal Society of London, Section A **A22** 183 (1953)). For a criticism see PERKINS 89, who suggests that the events are compatible with π^0 Dalitz decay. DEBOER 89B is a reply which contests the criticism.

[54] EL-NADI 88 claim the existence of a neutral particle decaying into e^+e^- with mass 1.60 ± 0.59 MeV, lifetime $(0.15 \pm 0.01) \times 10^{-14}$ s, which is produced in heavy ion interactions with emulsion nuclei at ~ 4 GeV/c/nucleon.

[55] FAISSNER 88 is a proton beam dump experiment at SIN. They found no candidate event for $A^0 \to \gamma\gamma$. A standard axion decaying to 2γ is excluded except for a region $x \simeq 1$. Lower limit on f_{A^0} of 10^2–10^3 GeV is given for $m_{A^0} = 0.1$–1 MeV.

[56] BADIER 86 did not find long-lived A^0 in 300 GeV π^- Beam Dump Experiment that decays into e^+e^- in the mass range $m_{A^0} = (20$–$200)$ MeV, which excludes the A^0 decay constant $f(A^0)$ in the interval (60–600) GeV. See their figure 6 for excluded region on $f(A^0)$-m_{A^0} plane.

[57] BERGSMA 85 look for $A^0 \to 2\gamma$, e^+e^-, $\mu^+\mu^-$. First limit above is for $m_{A^0} = 1$ MeV; second is for 200 MeV. See their figure 4 for excluded region on $f_{A^0}-m_{A^0}$ plane, where f_{A^0} is A^0 decay constant. For Peccei-Quinn PECCEI 77 A^0, $m_{A^0} < 180$ keV and $\tau > 0.037$ s. (CL = 90%). For the axion of FAISSNER 81B at 250 keV, BERGSMA 85 expect 15 events but observe zero.

[58] FAISSNER 83 observed 19 1-γ and 12 2-γ events where a background of 4.8 and 2.3 respectively is expected. A small-angle peak is observed even if iron wall is set in front of the decay region.

[59] FAISSNER 83B extrapolate SIN γ signal to LAMPF ν experimental condition. Resulting 370 γ's are not at variance with LAMPF upper limit of 450 γ's. Derived from LAMPF limit that $[d\sigma(A^0)/d\omega$ at $90°]m_{A^0}/\tau_{A^0} < 14 \times 10^{-35}$ cm^2 sr^{-1} MeV ms^{-1}. See comment on FRANK 83B.

[60] FRANK 83B stress the importance of LAMPF data bins with negative net signal. By statistical analysis say that LAMPF and SIN-A0 are at variance when extrapolation by phase-space model is done. They find LAMPF upper limit is 248 not 450 γ's. See comment on FAISSNER 83B.

[61] HOFFMAN 83 set CL = 90% limit $d\sigma/dt$ B$(e^+e^-) < 3.5 \times 10^{-32}$ cm^2/GeV^2 for $140 < m_{A^0} < 160$ MeV. Limit assumes $\tau(A^0) < 10^{-9}$ s.

[62] FETSCHER 82 reanalyzes SIN beam-dump data of FAISSNER 81. Claims no evidence for axion since 2-γ peak rate remarkably decreases if iron wall is set in front of the decay region.

[63] FAISSNER 81 see excess μe events. Suggest axion interactions.

[64] FAISSNER 81B is SIN 590 MeV proton beam dump. Observed 14.5 ± 5.0 events of 2γ decay of long-lived neutral penetrating particle with $m_{2\gamma} \lesssim 1$ MeV. Axion interpretation with η-A^0 mixing gives $m_{A^0} = 250 \pm 25$ keV, $\tau_{(2\gamma)} = (7.3 \pm 3.7) \times 10^{-3}$ s from above rate. See critical remarks below in comments of FETSCHER 82, FAISSNER 83, FAISSNER 83B, FRANK 83B, and BERGSMA 85. Also see in the next subsection ALEKSEEV 82, CAVAIGNAC 83, and ANANEV 85.

[65] KIM 81 analyzed 8 candidates for $A^0 \to 2\gamma$ obtained by Aachen-Padova experiment at CERN with 26 GeV protons on Be. Estimated axion mass is about 300 keV and lifetime is $(0.86\sim 5.6) \times 10^{-3}$ s depending on models. Faissner (private communication), says axion production underestimated and mass overestimated. Correct value around 200 keV.

[66] FAISSNER 80 is SIN beam dump experiment with 590 MeV protons looking for $A^0 \to e^+e^-$ decay. Assuming $A^0/\pi^0 = 5.5 \times 10^{-7}$, obtained decay rate limit $20/(A^0$ mass) MeV/s (CL = 90%), which is about 10^{-7} below theory and interpreted as upper limit to $m_{A^0} < 2m_{e^-}$.

[67] JACQUES 80 is a BNL beam dump experiment. First limit above comes from nonobservation of excess neutral-current-type events $[\sigma(\text{production})\sigma(\text{interaction}) < 7. \times 10^{-68}$ cm^4, CL = 90%$]$. Second limit is from nonobservation of axion decays into 2γ's or e^+e^-, and for axion mass a few MeV.

[68] SOUKAS 80 at BNL observed no excess of neutral-current-type events in beam dump.

[69] BECHIS 79 looked for the axion production in low energy electron Bremsstrahlung and the subsequent decay into either 2γ or e^+e^-. No signal found. CL = 90% limits for model parameter(s) are given.

[70] COTEUS 79 is a beam dump experiment at BNL.

[71] DISHAW 79 is a calorimetric experiment and looks for low energy tail of energy distributions due to energy lost to weakly interacting particles.

[72] BELLOTTI 78 first value comes from search for $A^0 \to e^+e^-$. Second value comes from search for $A^0 \to 2\gamma$, assuming mass $< 2m_{e^-}$. For any mass satisfying this, limit is above value×(mass^{-4}). Third value uses data of PL 60B 401 and quotes $\sigma(\text{production})\sigma(\text{interaction}) < 10^{-67}$ cm^4.

[73] BOSETTI 78B quotes $\sigma(\text{production})\sigma(\text{interaction}) < 2. \times 10^{-67}$ cm^4.

[74] DONNELLY 78 examines data from reactor neutrino experiments of REINES 76 and GURR 74 as well as SLAC beam dump experiment. Evidence is negative.

[75] MICELMACHER 78 finds no evidence of axion existence in reactor experiments of REINES 76 and GURR 74. (See reference under DONNELLY 78 below).

[76] VYSOTSKII 78 derived lower limit for the axion mass 25 keV from luminosity of the sun and 200 keV from red supergiants.

A^0 (Axion) Searches in Reactor Experiments

VALUE	DOCUMENT ID		TECN	COMMENT
• • • We do not use the following data for averages, fits, limits, etc. • • •				
	[77] ALTMANN	95	CNTR	Reactor; $A^0 \to e^+e^-$
	[78] KETOV	86	SPEC	Reactor, $A^0 \to \gamma\gamma$
	[79] KOCH	86	SPEC	Reactor; $A^0 \to \gamma\gamma$
	[80] DATAR	82	CNTR	Light water reactor
	[81] VUILLEUMIER	81	CNTR	Reactor, $A^0 \to 2\gamma$

[77] ALTMANN 95 looked for A^0 decaying into e^+e^- from the Bugey 5 nuclear reactor. They obtain an upper limit on the A^0 production rate of $\omega(A^0)/\omega(\gamma) \times B(A^0 \to e^+e^-) < 10^{-16}$ for $m_{A^0} = 1.5$ MeV at 90% CL. The limit is weaker for heavier A^0. In the case of a standard axion, this limit excludes a mass in the range $2m_e < m_{A^0} < 4.8$ MeV at 90% CL. See Fig. 5 of their paper for exclusion limits of axion-like resonances Z^0 in the (m_{X^0}, f_{X^0}) plane.

[78] KETOV 86 searched for A^0 at the Rovno nuclear power plant. They found an upper limit on the A^0 production probability of $0.8\,[100\text{ keV}/m_{A^0}]^6 \times 10^{-6}$ per fission. In the standard axion model, this corresponds to $m_{A^0} > 150$ keV. Not valid for $m_{A^0} \gtrsim 1$ MeV.

[79] KOCH 86 searched for $A^0 \to \gamma\gamma$ at nuclear power reactor Biblis A. They found an upper limit on the A^0 production rate of $\omega(A^0)/\omega(\gamma(M1)) < 1.5 \times 10^{-10}$ (CL=95%). Standard axion with $m_{A^0} = 250$ keV gives 10^{-5} for the ratio. Not valid for $m_{A^0} > 1022$ keV.

[80] DATAR 82 looked for $A^0 \to 2\gamma$ in neutron capture ($np \to dA^0$) at Tarapur 500 MW reactor. Sensitive to sum of $I = 0$ and $I = 1$ amplitudes. With ZEHNDER 81 $[(I = 0) - (I = 1)]$ result, assert nonexistence of standard A^0.

[81] VUILLEUMIER 81 is at Grenoble reactor. Set limit $m_{A^0} < 280$ keV.

A^0 (Axion) and Other Light Boson (X^0) Searches in Nuclear Transitions

Limits are for branching ratio.

VALUE	CL%	EVTS	DOCUMENT ID		TECN	COMMENT
• • • We do not use the following data for averages, fits, limits, etc. • • •						
$< 8.5 \times 10^{-6}$	90		[82] DERBIN	02	CNTR	^{125m}Te decay
			[83] DEBOER	97C	RVUE	M1 transitions
$< 5.5 \times 10^{-10}$	95		[84] TSUNODA	95	CNTR	^{252}Cf fission, $A^0 \to ee$
$< 1.2 \times 10^{-6}$	95		[85] MINOWA	93	CNTR	^{139}La$^* \to {}^{139}$LaA^0
$< 2 \times 10^{-4}$	90		[86] HICKS	92	CNTR	^{35}S decay, $A^0 \to \gamma\gamma$
$< 1.5 \times 10^{-9}$	95		[87] ASANUMA	90	CNTR	^{241}Am decay
$<(0.4$–$10) \times 10^{-3}$	95		[88] DEBOER	90	CNTR	^{8}Be$^* \to {}^8$BeA^0, $A^0 \to e^+e^-$
$<(0.2$–$1) \times 10^{-3}$	90		[89] BINI	89	CNTR	^{16}O$^* \to {}^{16}$OX^0, $X^0 \to e^+e^-$
			[90] AVIGNONE	88	CNTR	Cu$^* \to$ CuA^0 ($A^0 \to 2\gamma$, $A^0 e \to \gamma e$, $A^0 Z \to \gamma Z$)
$< 1.5 \times 10^{-4}$	90		[91] DATAR	88	CNTR	^{12}C$^* \to {}^{12}$CA^0, $A^0 \to e^+e^-$
$< 5 \times 10^{-3}$	90		[92] DEBOER	88C	CNTR	^{16}O$^* \to {}^{16}$OX^0, $X^0 \to e^+e^-$
$< 3.4 \times 10^{-5}$	95		[93] DOEHNER	88	SPEC	^{2}H*, $A^0 \to e^+e^-$
$< 4 \times 10^{-4}$	95		[94] SAVAGE	88	CNTR	Nuclear decay (isovector)
$< 3 \times 10^{-3}$	95		[94] SAVAGE	88	CNTR	Nuclear decay (isoscalar)
< 0.106	90		[95] HALLIN	86	SPEC	^{6}Li isovector decay
<10.8	90		[95] HALLIN	86	SPEC	^{10}B isoscalar decays
< 2.2	90		[95] HALLIN	86	SPEC	^{14}N isoscalar decays
$< 4 \times 10^{-4}$	90	0	[96] SAVAGE	86B	CNTR	^{14}N*
			[97] ANANEV	85	CNTR	Li*, deut* $A^0 \to 2\gamma$
			[98] CAVAIGNAC	83	CNTR	^{97}Nb*, deut* transition $A^0 \to 2\gamma$
			[99] ALEKSEEV	82B	CNTR	Li*, deut* transition $A^0 \to 2\gamma$
			[100] LEHMANN	82	CNTR	Cu$^* \to$ CuA^0 ($A^0 \to 2\gamma$)
		0	[101] ZEHNDER	82	CNTR	Li*, Nb* decay, n-capt.
		0	[102] ZEHNDER	81	CNTR	Ba$^* \to$ BaA^0 ($A^0 \to 2\gamma$)
			[103] CALAPRICE	79		Carbon

[82] DERBIN 02 looked for the axion emission in an M1 transition in ^{125m}Te decay. They looked for a possible presence of a shifted energy spectrum in gamma rays due to the undetected axion.

[83] DEBOER 97C reanalyzed the existent data on Nuclear M1 transitions and find that a 9 MeV boson decaying into e^+e^- would explain the excess of events with large opening angles. See also DEBOER 01 for follow-up experiments.

[84] TSUNODA 95 looked for axion emission when ^{252}Cf undergoes a spontaneous fission, with the axion decaying into e^+e^-. The bound is for m_{A^0}=40 MeV. It improves to 2.5×10^{-5} for m_{A^0}=200 MeV.

[85] MINOWA 93 studied chain process, ^{139}Ce $\to$ ^{139}La* by electron capture and M1 transition of ^{139}La* to the ground state. It does not assume decay modes of A^0. The bound applies for $m_{A^0} < 166$ keV.

[86] HICKS 92 bound is applicable for $\tau_{X^0} < 4 \times 10^{-11}$ sec.

[87] The ASANUMA 90 limit is for the branching fraction of X^0 emission per ^{241}Am α decay and valid for $\tau_{X^0} < 3 \times 10^{-11}$ s.

[88] The DEBOER 90 limit is for the branching ratio ^{8}Be* (18.15 MeV, 1^+) $\to$ ^{8}BeA^0, $A^0 \to e^+e^-$ for the mass range $m_{A^0} = 4$–15 MeV.

[89] The BINI 89 limit is for the branching fraction of $^{16}O^*(6.05\text{ MeV}, 0^+) \rightarrow {}^{16}O X^0$, $X^0 \rightarrow e^+e^-$ for m_X = 1.5–3.1 MeV. $\tau_{X^0} \lesssim 10^{-11}$ s is assumed. The spin-parity of X is restricted to 0^+ or 1^-.

[90] AVIGNONE 88 looked for the 1115 keV transition $C^* \rightarrow Cu\,A^0$, either from $A^0 \rightarrow 2\gamma$ in-flight decay or from the secondary A^0 interactions by Compton and by Primakoff processes. Limits for axion parameters are obtained for $m_{A^0} < 1.1$ MeV.

[91] DATAR 88 rule out light pseudoscalar particle emission through its decay $A^0 \rightarrow e^+e^-$ in the mass range 1.02–2.5 MeV and lifetime range 10^{-13}–10^{-8} s. The above limit is for $\tau = 5 \times 10^{-13}$ s and $m = 1.7$ MeV; see the paper for the τ-m dependence of the limit.

[92] The limit is for the branching fraction of $^{16}O^*(6.05\text{ MeV}, 0^+) \rightarrow {}^{16}O X^0$, $X^0 \rightarrow e^+e^-$ against internal pair conversion for $m_{X^0} = 1.7$ MeV and $\tau_{X^0} < 10^{-11}$ s. Similar limits are obtained for m_{X^0} = 1.3–3.2 MeV. The spin parity of X^0 must be either 0^+ or 1^-. The limit at 1.7 MeV is translated into a limit for the X^0-nucleon coupling constant: $g^2_{X^0NN}/4\pi < 2.3 \times 10^{-9}$.

[93] The DOEHNER 88 limit is for $m_{A^0} = 1.7$ MeV, $\tau(A^0) < 10^{-10}$ s. Limits less than 10^{-4} are obtained for m_{A^0} = 1.2–2.2 MeV.

[94] SAVAGE 88 looked for A^0 that decays into e^+e^- in the decay of the 9.17 MeV $J^P = 2^+$ state in ^{14}N, 17.64 MeV state $J^P = 1^+$ in ^{8}Be, and the 18.15 MeV state $J^P = 1^+$ in ^{8}Be. This experiment constrains the isovector coupling of A^0 to hadrons, if m_{A^0} = (1.1 → 2.2) MeV and the isoscalar coupling of A^0 to hadrons, if m_{A^0} = (1.1 → 2.6) MeV. Both limits are valid only if $\tau(A^0) \lesssim 1 \times 10^{-11}$ s.

[95] Limits are for $\Gamma(A^0(1.8\text{ MeV}))/\Gamma(\pi M1)$; i.e., for 1.8 MeV axion emission normalized to the rate for internal emission of e^+e^- pairs. Valid for $\tau_{A^0} < 2 \times 10^{-11}$s. ^{6}Li isovector decay data strongly disfavor PECCEI 86 model I, whereas the ^{10}B and ^{14}N isoscalar decay data strongly reject PECCEI 86 model II and III.

[96] SAVAGE 86B looked for A^0 that decays into e^+e^- in the decay of the 9.17 MeV $J^P = 2^+$ state in ^{14}N. Limit on the branching fraction is valid if $\tau_{A^0} \lesssim 1. \times 10^{-11}$s for m_{A^0} = (1.1–1.7) MeV. This experiment constrains the iso-vector coupling of A^0 to hadrons.

[97] ANANEV 85 with IBR-2 pulsed reactor exclude standard A^0 at CL = 95% masses below 470 keV (Li* decay) and below $2m_e$ for deuteron* decay.

[98] CAVAIGNAC 83 at Bugey reactor exclude axion at any $m_{^{97}\text{Nb}^*\text{decay}}$ and axion with m_{A^0} between 275 and 288 keV (deuteron* decay).

[99] ALEKSEEV 82 with IBR-2 pulsed reactor exclude standard A^0 at CL = 95% mass-ranges m_{A^0} <400 keV (Li* decay) and 330 keV $< m_{A^0} <$2.2 MeV. (deuteron* decay).

[100] LEHMANN 82 obtained $A^0 \rightarrow 2\gamma$ rate $< 6.2 \times 10^{-5}$/s (CL = 95%) excluding m_{A^0} between 100 and 1000 keV.

[101] ZEHNDER 82 used Goesgen 2.8GW light-water reactor to check A^0 production. No 2γ peak in Li*, Nb* decay (both single p transition) nor in n capture (combined with previous Ba* negative result) rules out standard A^0. Set limit m_{A^0} <60 keV for any A^0.

[102] ZEHNDER 81 looked for $\text{Ba}^* \rightarrow A^0\,\text{Ba}$ transition with $A^0 \rightarrow 2\gamma$. Obtained 2γ coincidence rate $< 2.2 \times 10^{-5}$/s (CL = 95%) excluding m_{A^0} >160 keV (or 200 keV depending on Higgs mixing). However, see BARROSO 81.

[103] CALAPRICE 79 saw no axion emission from excited states of carbon. Sensitive to axion mass between 1 and 15 MeV.

A^0 (Axion) Limits from Its Electron Coupling

Limits are for $\tau(A^0 \rightarrow e^+e^-)$.

VALUE (s)	CL%	DOCUMENT ID		TECN	COMMENT
• • • We do not use the following data for averages, fits, limits, etc. • • •					
none 4×10^{-16}–4.5×10^{-12}	90	[104] BROSS	91	BDMP	$eN \rightarrow eA^0N$ ($A^0 \rightarrow ee$)
		[105] GUO	90	BDMP	$eN \rightarrow eA^0N$ ($A^0 \rightarrow ee$)
		[106] BJORKEN	88	CALO	$A \rightarrow e^+e^-$ or 2γ
		[107] BLINOV	88	MD1	$ee \rightarrow eeA^0$ ($A^0 \rightarrow ee$)
none 1×10^{-14}–1×10^{-10}	90	[108] RIORDAN	87	BDMP	$eN \rightarrow eA^0N$ ($A^0 \rightarrow ee$)
none 1×10^{-14}–1×10^{-11}	90	[109] BROWN	86	BDMP	$eN \rightarrow eA^0N$ ($A^0 \rightarrow ee$)
none 6×10^{-14}–9×10^{-11}	95	[110] DAVIER	86	BDMP	$eN \rightarrow eA^0N$ ($A^0 \rightarrow ee$)
none 3×10^{-13}–1×10^{-7}	90	[111] KONAKA	86	BDMP	$eN \rightarrow eA^0N$ ($A^0 \rightarrow ee$)

[104] The listed BROSS 91 limit is for $m_{A^0} = 1.14$ MeV. $B(A^0 \rightarrow e^+e^-) = 1$ assumed. Excluded domain in the τ_{A^0}–m_{A^0} plane extends up to $m_{A^0} \approx 7$ MeV (see Fig. 5). Combining with electron $g-2$ constraint, axions coupling only to e^+e^- ruled out for $m_{A^0} < 4.8$ MeV (90%CL).

[105] GUO 90 use the same apparatus as BROWN 86 and improve the previous limit in the shorter lifetime region. Combined with $g-2$ constraint, axions coupling only to e^+e^- are ruled out for $m_{A^0} < 2.7$ MeV (90% CL).

[106] BJORKEN 88 reports limits on axion parameters (f_A, m_A, τ_A) for $m_{A^0} < 200$ MeV from electron beam-dump experiment with production via Primakoff photoproduction, bremsstrahlung from electrons, and resonant annihilation of positrons on atomic electrons.

[107] BLINOV 88 assume zero spin, $m = 1.8$ MeV and lifetime $< 5 \times 10^{-12}$ s and find $\Gamma(A^0 \rightarrow \gamma\gamma)B(A^0 \rightarrow e^+e^-) < 2$ eV (CL=90%).

[108] Assumes $A^0\gamma\gamma$ coupling is small and hence Primakoff production is small. Their figure 2 shows limits on axions for $m_{A^0} < 15$ MeV.

[109] Uses electrons in hadronic showers from an incident 800 GeV proton beam. Limits for $m_{A^0} < 15$ MeV are shown in their figure 3.

[110] $m_{A^0} = 1.8$ MeV assumed. The excluded domain in the τ_{A^0}–m_{A^0} plane extends up to $m_{A^0} \approx 14$ MeV, see their figure 4.

[111] The limits are obtained from their figure 3. Also given is the limit on the $A^0\gamma\gamma$–$A^0e^+e^-$ coupling plane by assuming Primakoff production.

Search for A^0 (Axion) Resonance in Bhabha Scattering

The limit is for $\Gamma(A^0)[B(A^0 \rightarrow e^+e^-)]^2$.

VALUE (10^{-3} eV)	CL%	DOCUMENT ID		TECN	COMMENT
• • • We do not use the following data for averages, fits, limits, etc. • • •					
< 1.3	97	[112] HALLIN	92	CNTR	m_{A^0} = 1.75–1.88 MeV
none 0.0016–0.47	90	[113] HENDERSON	92C	CNTR	m_{A^0}= 1.5–1.86 MeV
< 2.0	90	[114] WU	92	CNTR	m_{A^0}= 1.56–1.86 MeV
< 0.013	95	TSERTOS	91	CNTR	m_{A^0} = 1.832 MeV
none 0.19–3.3	95	[115] WIDMANN	91	CNTR	m_{A^0}= 1.78–1.92 MeV
< 5	97	BAUER	90	CNTR	m_{A^0} = 1.832 MeV
none 0.09–1.5	95	[116] JUDGE	90	CNTR	m_{A^0} = 1.832 MeV, elastic
< 1.9	97	[117] TSERTOS	89	CNTR	m_{A^0} = 1.82 MeV
<(10–40)	97	[117] TSERTOS	89	CNTR	m_{A^0} = 1.51–1.65 MeV
<(1–2.5)	97	[117] TSERTOS	89	CNTR	m_{A^0} = 1.80–1.86 MeV
< 31	95	LORENZ	88	CNTR	m_{A^0} = 1.646 MeV
< 94	95	LORENZ	88	CNTR	m_{A^0} = 1.726 MeV
< 23	95	LORENZ	88	CNTR	m_{A^0} = 1.782 MeV
< 19	95	LORENZ	88	CNTR	m_{A^0} = 1.837 MeV
< 3.8	97	[118] TSERTOS	88	CNTR	m_{A^0} = 1.832 MeV
		[119] VANKLINKEN	88	CNTR	
		[120] MAIER	87	CNTR	
<2500	90	MILLS	87	CNTR	m_{A^0} = 1.8 MeV
		[121] VONWIMMER.	87	CNTR	

[112] HALLIN 92 quote limits on lifetime, 8×10^{-14} – 5×10^{-13} sec depending on mass, assuming $B(A^0 \rightarrow e^+e^-) = 100\%$. They say that TSERTOS 91 overstated their sensitivity by a factor of 3.

[113] HENDERSON 92C exclude axion with lifetime $\tau_{A^0} = 1.4 \times 10^{-12}$ – 4.0×10^{-10} s, assuming $B(A^0 \rightarrow e^+e^-)$=100%. HENDERSON 92C also exclude a vector boson with $\tau = 1.4 \times 10^{-12}$ – 6.0×10^{-10} s.

[114] WU 92 quote limits on lifetime $> 3.3 \times 10^{-13}$ s assuming $B(A^0 \rightarrow e^+e^-)$=100%. They say that TSERTOS 89 overestimate the limit by a factor of $\pi/2$. WU 92 also quote a bound for vector boson, $\tau > 8.2 \times 10^{-13}$ s.

[115] WIDMANN 91 bound applies exclusively to the case $B(A^0 \rightarrow e^+e^-)$=1, since the detection efficiency varies substantially as $\Gamma(A^0)_{\text{total}}$ changes. See their Fig. 6.

[116] JUDGE 90 excludes an elastic pseudoscalar e^+e^- resonance for 4.5×10^{-13} s $< \tau(A^0) < 7.5 \times 10^{-12}$ s (95% CL) at $m_{A^0} = 1.832$ MeV. Comparable limits can be set for m_{A^0} = 1.776–1.856 MeV.

[117] See also TSERTOS 88B in references.

[118] The upper limit listed in TSERTOS 88 is too large by a factor of 4. See TSERTOS 88B, footnote 3.

[119] VANKLINKEN 88 looked for relatively long-lived resonance ($\tau = 10^{-10}$–10^{-12} s). The sensitivity is not sufficient to exclude such a narrow resonance.

[120] MAIER 87 obtained limits $R\Gamma \lesssim 60$ eV (100 eV) at $m_{A^0} \simeq 1.64$ MeV (1.83 MeV) for energy resolution $\Delta E_{\text{cm}} \simeq 3$ keV, where R is the resonance cross section normalized to that of Bhabha scattering, and $\Gamma = \Gamma^2_{ee}/\Gamma_{\text{total}}$. For a discussion implying that $\Delta E_{\text{cm}} \simeq 10$ keV, see TSERTOS 89.

[121] VONWIMMERSPERG 87 measured Bhabha scattering for E_{cm} = 1.37–1.86 MeV and found a possible peak at 1.73 with $\int \sigma dE_{\text{cm}} = 14.5 \pm 6.8$ keV·b. For a comment and a reply, see VANKLINKEN 88B and VONWIMMERSPERG 88. Also see CONNELL 88.

Search for A^0 (Axion) Resonance in $e^+e^- \rightarrow \gamma\gamma$

The limit is for $\Gamma(A^0 \rightarrow e^+e^-) \cdot \Gamma(A^0 \rightarrow \gamma\gamma)/\Gamma_{\text{total}}$

VALUE (10^{-3} eV)	CL%	DOCUMENT ID		TECN	COMMENT
• • • We do not use the following data for averages, fits, limits, etc. • • •					
< 0.18	95	VO	94	CNTR	m_{A^0}=1.1 MeV
< 1.5	95	VO	94	CNTR	m_{A^0}=1.4 MeV
<12	95	VO	94	CNTR	m_{A^0}=1.7 MeV
< 6.6	95	[122] TRZASKA	91	CNTR	m_{A^0} = 1.8 MeV
< 4.4	95	WIDMANN	91	CNTR	m_{A^0}= 1.78–1.92 MeV
		[123] FOX	89	CNTR	
< 0.11	95	[124] MINOWA	89	CNTR	m_{A^0} = 1.062 MeV
<33	97	CONNELL	88	CNTR	m_{A^0} = 1.580 MeV
<42	97	CONNELL	88	CNTR	m_{A^0} = 1.642 MeV
<73	97	CONNELL	88	CNTR	m_{A^0} = 1.782 MeV
<79	97	CONNELL	88	CNTR	m_{A^0} = 1.832 MeV

[122] TRZASKA 91 also give limits in the range (6.6–30) $\times 10^{-3}$ eV (95%CL) for m_{A^0} = 1.6–2.0 MeV.
[123] FOX 89 measured positron annihilation with an electron in the source material into two photons and found no signal at 1.062 MeV ($< 9 \times 10^{-5}$ of two-photon annihilation at rest).
[124] Similar limits are obtained for m_{A^0} = 1.045–1.085 MeV.

Search for X^0 (Light Boson) Resonance in $e^+e^- \rightarrow \gamma\gamma\gamma$

The limit is for $\Gamma(X^0 \rightarrow e^+e^-)\cdot\Gamma(X^0 \rightarrow \gamma\gamma\gamma)/\Gamma_{total}$. C invariance forbids spin-0 X^0 coupling to both e^+e^- and $\gamma\gamma\gamma$.

VALUE (10^{-3} eV)	CL%	DOCUMENT ID		TECN	COMMENT
• • • We do not use the following data for averages, fits, limits, etc. • • •					
< 0.2	95	[125] VO	94	CNTR	m_{X^0}=1.1–1.9 MeV
< 1.0	95	[126] VO	94	CNTR	m_{X^0}=1.1 MeV
< 2.5	95	[126] VO	94	CNTR	m_{X^0}=1.4 MeV
<120	95	[126] VO	94	CNTR	m_{X^0}=1.7 MeV
< 3.8	95	[127] SKALSEY	92	CNTR	m_{X^0}= 1.5 MeV

[125] VO 94 looked for $X^0 \rightarrow \gamma\gamma\gamma$ decaying at rest. The precise limits depend on m_{X^0}. See Fig. 2(b) in paper.
[126] VO 94 looked for $X^0 \rightarrow \gamma\gamma\gamma$ decaying in flight.
[127] SKALSEY 92 also give limits 4.3 for m_{X^0} = 1.54 and 7.5 for 1.64 MeV. The spin of X^0 is assumed to be one.

Light Boson (X^0) Search in Nonresonant e^+e^- Annihilation at Rest

Limits are for the ratio of $n\gamma + X^0$ production relative to $\gamma\gamma$.

VALUE (units 10^{-6})	CL%	DOCUMENT ID		TECN	COMMENT
• • • We do not use the following data for averages, fits, limits, etc. • • •					
< 4.2	90	[128] MITSUI	96	CNTR	γX^0
< 4	68	[129] SKALSEY	95	CNTR	γX^0
<40	68	[130] SKALSEY	95	RVUE	γX^0
< 0.18	90	[131] ADACHI	94	CNTR	$\gamma\gamma X^0$, $X^0 \rightarrow \gamma\gamma$
< 0.26	90	[132] ADACHI	94	CNTR	$\gamma\gamma X^0$, $X^0 \rightarrow \gamma\gamma$
< 0.33	90	[133] ADACHI	94	CNTR	γX^0, $X^0 \rightarrow \gamma\gamma\gamma$

[128] MITSUI 96 looked for a monochromatic γ. The bound applies for a vector X^0 with C=−1 and m_{X^0} <200 keV. They derive an upper bound on $ee X^0$ coupling and hence on the branching ratio B(o-Ps $\rightarrow \gamma\gamma X^0$)< 6.2×10^{-6}. The bounds weaken for heavier X^0.
[129] SKALSEY 95 looked for a monochromatic γ without an accompanying γ in e^+e^- annihilation. The bound applies for scalar and vector X^0 with $C = -1$ and m_{X^0} = 100–1000 keV.
[130] SKALSEY 95 reinterpreted the bound on γA^0 decay of o-Ps by ASAI 91 where 3% of delayed annihilations are not from $^3S_1$ states. The bound applies for scalar and vector X^0 with $C = -1$ and m_{X^0} = 0–800 keV.
[131] ADACHI 94 looked for a peak in the $\gamma\gamma$ invariant mass distribution in $\gamma\gamma\gamma\gamma$ production from e^+e^- annihilation. The bound applies for m_{X^0} = 70–800 keV.
[132] ADACHI 94 looked for a peak in the missing-mass mass distribution in $\gamma\gamma$ channel, using $\gamma\gamma\gamma\gamma$ production from e^+e^- annihilation. The bound applies for m_{X^0} <800 keV.
[133] ADACHI 94 looked for a peak in the missing mass distribution in $\gamma\gamma\gamma$ channel, using $\gamma\gamma\gamma\gamma$ production from e^+e^- annihilation. The bound applies for m_{X^0} = 200–900 keV.

Searches for Goldstone Bosons (X^0)

(Including Horizontal Bosons and Majorons.) Limits are for branching ratios.

VALUE	CL%	EVTS	DOCUMENT ID		TECN	COMMENT
• • • We do not use the following data for averages, fits, limits, etc. • • •						
			[134] DIAZ	98	THEO	$H^0 \rightarrow X^0X^0$, $A^0 \rightarrow X^0X^0X^0$, Majoron
			[135] BOBRAKOV	91		Electron quasi-magnetic interaction
$<3.3 \times 10^{-2}$	95		[136] ALBRECHT	90E	ARG	$\tau \rightarrow \mu X^0$. Familon
$<1.8 \times 10^{-2}$	95		[136] ALBRECHT	90E	ARG	$\tau \rightarrow e X^0$. Familon
$<6.4 \times 10^{-9}$	90		[137] ATIYA	90	B787	$K^+ \rightarrow \pi^+ X^0$. Familon
$<1.1 \times 10^{-9}$	90		[138] BOLTON	88	CBOX	$\mu^+ \rightarrow e^+ \gamma X^0$. Familon
			[139] CHANDA	88	ASTR	Sun, Majoron
			[140] CHOI	88	ASTR	Majoron, SN 1987A
$<5 \times 10^{-6}$	90		[141] PICCIOTTO	88	CNTR	$\pi \rightarrow e\nu X^0$, Majoron
$<1.3 \times 10^{-9}$	90		[142] GOLDMAN	87	CNTR	$\mu \rightarrow e\gamma X^0$. Familon
$<3 \times 10^{-4}$	90		[143] BRYMAN	86B	RVUE	$\mu \rightarrow e X^0$. Familon
$<1. \times 10^{-10}$	90	0	[144] EICHLER	86	SPEC	$\mu^+ \rightarrow e^+ X^0$. Familon
$<2.6 \times 10^{-6}$	90		[145] JODIDIO	86	SPEC	$\mu^+ \rightarrow e^+ X^0$. Familon
			[146] BALTRUSAIT...	85	MRK3	$\tau \rightarrow \ell X^0$. Familon
			[147] DICUS	83	COSM	ν(hvy) $\rightarrow \nu$(light)X^0

[134] DIAZ 98 studied models of spontaneously broken lepton number with both singlet and triplet Higgses. They obtain limits on the parameter space from invisible decay $Z \rightarrow H^0A^0 \rightarrow X^0X^0X^0X^0X^0$ and $e^+e^- \rightarrow ZH^0$ with $H^0 \rightarrow X^0X^0$.
[135] BOBRAKOV 91 searched for anomalous magnetic interactions between polarized electrons expected from the exchange of a massless pseudoscalar boson (arion). A limit $x_e^2 < 2 \times 10^{-4}$ (95%CL) is found for the effective anomalous magneton parametrized as $x_e(G_F/8\pi\sqrt{2})^{1/2}$.
[136] ALBRECHT 90E limits are for B($\tau \rightarrow \ell X^0$)/B($\tau \rightarrow \ell\nu\overline{\nu}$). Valid for m_{X^0} < 100 MeV. The limits rise to 7.1% (for μ), 5.0% (for e) for m_{X^0} = 500 MeV.
[137] ATIYA 90 limit is for $m_{X^0} = 0$. The limit B < 1×10^{-8} holds for m_{X^0} < 95 MeV. For the reduction of the limit due to finite lifetime of X^0, see their Fig. 3.
[138] BOLTON 88 limit corresponds to $F > 3.1 \times 10^9$ GeV, which does not depend on the chirality property of the coupling.
[139] CHANDA 88 find v_T < 10 MeV for the weak-triplet Higgs vacuum expectation value in Gelmini-Roncadelli model, and $v_S > 5.8 \times 10^6$ GeV in the singlet Majoron model.
[140] CHOI 88 used the observed neutrino flux from the supernova SN 1987A to exclude the neutrino Majoron Yukawa coupling h in the range $2 \times 10^{-5} < h < 3 \times 10^{-4}$ for the interaction $L_{\text{int}} = \frac{1}{2} i h \overline{\psi}_\nu^c \gamma_5 \psi_\nu \phi_X$. For several families of neutrinos, the limit applies for $(\Sigma h_i^4)^{1/4}$.
[141] PICCIOTTO 88 limit applies when m_{X^0} < 55 MeV and τ_{X^0} > 2ns, and it decreases to 4×10^{-7} at m_{X^0} = 125 MeV, beyond which no limit is obtained.
[142] GOLDMAN 87 limit corresponds to $F > 2.9 \times 10^9$ GeV for the family symmetry breaking scale from the Lagrangian $L_{\text{int}} = (1/F)\overline{\psi}_\mu\gamma^\mu\,(a+b\gamma_5)\,\psi_e\partial_\mu\phi_{X^0}$ with $a^2+b^2 = 1$. This is not as sensitive as the limit $F > 9.9 \times 10^9$ GeV derived from the search for $\mu^+ \rightarrow e^+X^0$ by JODIDIO 86, but does not depend on the chirality property of the coupling.
[143] Limits are for $\Gamma(\mu \rightarrow eX^0)/\Gamma(\mu \rightarrow e\nu\overline{\nu})$. Valid when m_{X^0} = 0–93.4, 98.1–103.5 MeV.
[144] EICHLER 86 looked for $\mu^+ \rightarrow e^+X^0$ followed by $X^0 \rightarrow e^+e^-$. Limits on the branching fraction depend on the mass and and lifetime of X^0. The quoted limits are valid when $\tau_{X^0} \lesssim 3. \times 10^{-10}$ s if the decays are kinematically allowed.
[145] JODIDIO 86 corresponds to $F > 9.9 \times 10^9$ GeV for the family symmetry breaking scale with the parity-conserving effective Lagrangian $L_{\text{int}} = (1/F)\,\overline{\psi}_\mu\gamma^\mu\psi_e\partial^\mu\phi_{X^0}$.
[146] BALTRUSAITIS 85 search for light Goldstone boson(X^0) of broken U(1). CL = 95% limits are B($\tau \rightarrow \mu^+X^0$)/B($\tau \rightarrow \mu^+\nu\nu$) <0.125 and B($\tau \rightarrow e^+X^0$)/B($\tau \rightarrow e^+\nu\nu$) <0.04. Inferred limit for the symmetry breaking scale is m >3000 TeV.
[147] The primordial heavy neutrino must decay into ν and familon, f_A, early so that the red-shifted decay products are below critical density, see their table. In addition, $K \rightarrow \pi f_A$ and $\mu \rightarrow e f_A$ are unseen. Combining these excludes $m_{\text{heavy}\nu}$ between 5×10^{-5} and 5×10^{-4} MeV (μ decay) and $m_{\text{heavy}\nu}$ between 5×10^{-5} and 0.1 MeV (K-decay).

Majoron Searches in Neutrinoless Double β Decay

Limits are for the half-life of neutrinoless $\beta\beta$ decay with a Majoron emission.
No experiment currently claims any such evidence. Only the best or comparable limits for each isotope are reported. Also see the reviews ZUBER 98 and FAESSLER 98B.

$t_{1/2}$(10^{21} yr)	CL%	ISOTOPE	TRANSITION	METHOD	DOCUMENT ID	
>7200	**90**	**^{128}Te**		**CNTR**	[148] BERNATOW...	92
• • • We do not use the following data for averages, fits, limits, etc. • • •						
> 2.2	90	^{130}Te	$0\nu1\chi$	Cryog. det.	[149] ARNABOLDI	03
> 0.9	90	^{130}Te	$0\nu2\chi$	Cryog. det.	[150] ARNABOLDI	03
> 8	90	^{116}Cd	$0\nu1\chi$	$CdWO_4$ scint.	[151] DANEVICH	03
> 0.8	90	^{116}Cd	$0\nu2\chi$	$CdWO_4$ scint.	[152] DANEVICH	03
> 500	90	^{136}Xe	$0\nu\chi$	Liquid Xe Scint.	[153] BERNABEI	02D
> 5.8	90	^{100}Mo	$0\nu\chi$	ELEGANT V	[154] FUSHIMI	02
> 0.32	90	^{100}Mo	$0\nu\chi$	Liq. Ar ioniz.	[155] ASHITKOV	01
> 0.0035	90	^{160}Gd	$0\nu\chi$	$^{160}Gd_2SiO_5$:Ce	[156] DANEVICH	01
> 0.013	90	^{160}Gd	$0\nu2\chi$	$^{160}Gd_2SiO_5$:Ce	[157] DANEVICH	01
> 2.3	90	^{82}Se	$0\nu\chi$	NEMO 2	[158] ARNOLD	00
> 0.31	90	^{96}Zr	$0\nu\chi$	NEMO 2	[159] ARNOLD	00
> 0.63	90	^{82}Se	$0\nu2\chi$	NEMO 2	[160] ARNOLD	00
> 0.063	90	^{96}Zr	$0\nu2\chi$	NEMO 2	[160] ARNOLD	00
> 0.16	90	^{100}Mo	$0\nu2\chi$	NEMO 2	[160] ARNOLD	00
> 2.4	90	^{82}Se	$0\nu\chi$	NEMO 2	[161] ARNOLD	98
> 7.2	90	^{136}Xe	$0\nu2\chi$	TPC	[162] LUESCHER	98
> 7.91	90	^{76}Ge		SPEC	[163] GUENTHER	96
> 17	90	^{76}Ge		CNTR	BECK	93

[148] BERNATOWICZ 92 studied double-β decays of ^{128}Te and ^{130}Te, and found the ratio $\tau(^{130}\text{Te})/\tau(^{128}\text{Te}) = (3.52 \pm 0.11) \times 10^{-4}$ in agreement with relatively stable theoretical predictions. The bound is based on the requirement that Majoron-emitting decay cannot be larger than the observed double-beta rate of ^{128}Te of $(7.7 \pm 0.4) \times 10^{24}$ year. We calculated 90% CL limit as $(7.7\text{–}1.28 \times 0.4{=}7.2) \times 10^{24}$.
[149] Supersedes ALESSANDRELLO 00. Array of TeO_2 crystals in high resolution cryogenic calorimeter. Some enriched in ^{130}Te. Derive $\langle g_{\nu\chi}\rangle$ < 17–33 $\times 10^{-5}$ depending on matrix element.
[150] Supersedes ALESSANDRELLO 00. Cryogenic calorimeter search.
[151] Limit for the $0\nu\chi$ decay with Majoron emission of ^{116}Cd using enriched $CdWO_4$ scintillators. $\langle g_{\nu\chi}\rangle$ < 4.6–8.1 $\times 10^{-5}$ depending on the matrix element. Supersedes DANEVICH 00.
[152] Limit for the $0\nu2\chi$ decay of ^{116}Cd. Supersedes DANEVICH 00.
[153] BERNABEI 02D obtain limit for $0\nu\chi$ decay with Majoron emission of ^{136}Xe using liquid Xe scintillation detector. They derive $\langle g_{\nu\chi}\rangle$ < 2.0–3.0 $\times 10^{-5}$ with several nuclear matrix elements.

[154] Replaces TANAKA 93. FUSHIMI 02 derive half-life limit for the $0\nu\chi$ decay by means of tracking calorimeter ELEGANT V. Considering various matrix element calculations, a range of limits for the Majoron-neutrino coupling is given: $\langle g_{\nu\chi}\rangle <(6.3\text{–}360)\times 10^{-5}$.

[155] ASHITKOV 01 result for $0\nu\chi$ of ^{100}Mo is less stringent than ARNOLD 00.

[156] DANEVICH 01 obtain limit for the $0\nu\chi$ decay with Majoron emission of ^{160}Gd using Gd_2SiO_5:Ce crystal scintillators.

[157] DANEVICH 01 obtain limit for the $0\nu 2\chi$ decay with 2 Majoron emission of ^{160}Gd.

[158] ARNOLD 00 reports limit for the $0\nu\chi$ decay with Majoron emission derived from tracking calorimeter NEMO 2. Using ^{82}Se source: $\langle g_{\nu\chi}\rangle < 1.6\times 10^{-4}$. Matrix element from GUENTHER 96.

[159] Using ^{96}Zr source: $\langle g_{\nu\chi}\rangle < 2.6\times 10^{-4}$. Matrix element from ARNOLD 99.

[160] ARNOLD 00 reports limit for the $0\nu 2\chi$ decay with two Majoron emission derived from tracking calorimeter NEMO 2.

[161] ARNOLD 98 determine the limit for $0\nu_\chi$ decay with Majoron emission of ^{82}Se using the NEMO-2 tracking detector. They derive $\langle g_{\nu_\chi}\rangle < 2.3\text{–}4.3\times 10^{-4}$ with several nuclear matrix elements.

[162] LUESCHER 98 report a limit for the 0ν decay with Majoron emission of ^{136}Xe using Xe TPC. This result is more stringent than BARABASH 89. Using the matrix elements of ENGEL 88, they obtain a limit on $\langle g_{\nu\chi}\rangle$ of 2.0×10^{-4}.

[163] See Table 1 in GUENTHER 96 for limits on the Majoron coupling in different models.

Invisible A^0 (Axion) MASS LIMITS from Astrophysics and Cosmology

$v_1 = v_2$ is usually assumed (v_i = vacuum expectation values). For a review of these limits, see RAFFELT 90C and TURNER 90. In the comment lines below, D and K refer to DFSZ and KSVZ axion types, discussed in the above minireview.

VALUE (eV)	DOCUMENT ID		TECN	COMMENT
• • • We do not use the following data for averages, fits, limits, etc. • • •				
3 to 20	[164] MOROI	98	COSM	K, hot dark matter
< 0.007	[165] BORISOV	97	ASTR	D, neutron star
< 4	[166] KACHELRIESS	97	ASTR	D, neutron star cooling
$<(0.5\text{–}6)\times 10^{-3}$	[167] KEIL	97	ASTR	SN 1987A
< 0.018	[168] RAFFELT	95	ASTR	D, red giant
< 0.010	[169] ALTHERR	94	ASTR	D, red giants, white dwarfs
	[170] CHANG	93	ASTR	K, SN 1987A
< 0.01	WANG	92	ASTR	D, white dwarf
< 0.03	WANG	92C	ASTR	D, C-O burning
none 3–8	[171] BERSHADY	91	ASTR	D, K, intergalactic light
<10	[172] KIM	91C	COSM	D, K, mass density of the universe, supersymmetry
	[173] RAFFELT	91B	ASTR	D,K, SN 1987A
$< 1 \quad \times 10^{-3}$	[174] RESSELL	91	ASTR	K, intergalactic light
none 10^{-3}–3	BURROWS	90	ASTR	D,K, SN 1987A
	[175] ENGEL	90	ASTR	D,K, SN 1987A
< 0.02	[176] RAFFELT	90D	ASTR	D, red giant
$< 1 \quad \times 10^{-3}$	[177] BURROWS	89	ASTR	D,K, SN 1987A
$<(1.4\text{–}10)\times 10^{-3}$	[178] ERICSON	89	ASTR	D,K, SN 1987A
$< 3.6 \quad \times 10^{-4}$	[179] MAYLE	89	ASTR	D,K, SN 1987A
<12	CHANDA	88	ASTR	D, Sun
$< 1 \quad \times 10^{-3}$	RAFFELT	88	ASTR	D,K, SN 1987A
	[180] RAFFELT	88B	ASTR	red giant
< 0.07	FRIEMAN	87	ASTR	D, red giant
< 0.7	[181] RAFFELT	87	ASTR	K, red giant
$< 2\text{–}5$	TURNER	87	COSM	K, thermal production
< 0.01	[182] DEARBORN	86	ASTR	D, red giant
< 0.06	RAFFELT	86	ASTR	D, red giant
< 0.7	[183] RAFFELT	86	ASTR	K, red giant
< 0.03	RAFFELT	86B	ASTR	D, white dwarf
< 1	[184] KAPLAN	85	ASTR	K, red giant
$< 0.003\text{–}0.02$	IWAMOTO	84	ASTR	D, K, neutron star
$> 1 \quad \times 10^{-5}$	ABBOTT	83	COSM	D,K, mass density of the universe
$> 1 \quad \times 10^{-5}$	DINE	83	COSM	D,K, mass density of the universe
< 0.04	ELLIS	83B	ASTR	D, red giant
$> 1 \quad \times 10^{-5}$	PRESKILL	83	COSM	D,K, mass density of the universe
< 0.1	BARROSO	82	ASTR	D, red giant
< 1	[185] FUKUGITA	82	ASTR	D, stellar cooling
< 0.07	FUKUGITA	82B	ASTR	D, red giant

[164] MOROI 98 points out that a KSVZ axion of this mass range (see CHANG 93) can be a viable hot dark matter of Universe, as long as the model-dependent $g_{A\gamma}$ is accidentally small enough as originally emphasized by KAPLAN 85; see Fig. 1.

[165] BORISOV 97 bound is on the axion-electron coupling $g_{ae} < 1\times 10^{-13}$ from the photo-production of axions off of magnetic fields in the outer layers of neutron stars.

[166] KACHELRIESS 97 bound is on the axion-electron coupling $g_{ae} < 1\times 10^{-10}$ from the production of axions in strongly magnetized neutron stars. The authors also quote a stronger limit, $g_{ae} < 9\times 10^{-13}$ which is strongly dependent on the strength of the magnetic field in white dwarfs.

[167] KEIL 97 uses new measurements of the axial-vector coupling strength of nucleons, as well as a reanalysis of many-body effects and pion-emission processes in the core of the neutron star, to update limits on the invisible-axion mass.

[168] RAFFELT 95 reexamined the constraints on axion emission from red giants due to the axion-electron coupling. They improve on DEARBORN 86 by taking into proper account degeneracy effects in the bremsstrahlung rate. The limit comes from requiring the red giant core mass at helium ignition not to exceed its standard value by more than 5% (0.025 solar masses).

[169] ALTHERR 94 bound is on the axion-electron coupling $g_{ae} < 1.5\times 10^{-13}$, from energy loss via axion emission.

[170] CHANG 93 updates ENGEL 90 bound with the Kaplan-Manohar ambiguity in $z = m_u/m_d$ (see the Note on the Quark Masses in the Quark Particle Listings). It leaves the window $f_A = 3\times 10^5$–3×10^6 GeV open. The constraint from Big-Bang Nucleosynthesis is satisfied in this window as well.

[171] BERSHADY 91 searched for a line at wave length from 3100–8300 Å expected from 2γ decays of relic thermal axions in intergalactic light of three rich clusters of galaxies.

[172] KIM 91C argues that the bound from the mass density of the universe will change drastically for the supersymmetric models due to the entropy production of saxion (scalar component in the axionic chiral multiplet) decay. Note that it is an *upperbound* rather than a lowerbound.

[173] RAFFELT 91B argue that previous SN 1987A bounds must be relaxed due to corrections to nucleon bremsstrahlung processes.

[174] RESSELL 91 uses absence of any intracluster line emission to set limit.

[175] ENGEL 90 rule out $10^{-10} \lesssim g_{AN} \lesssim 10^{-3}$, which for a hadronic axion with EMC motivated axion-nucleon couplings corresponds to 2.5×10^{-3} eV $\lesssim m_{A^0} \lesssim 2.5\times 10^4$ eV. The constraint is loose in the middle of the range, i.e. for $g_{AN} \sim 10^{-6}$.

[176] RAFFELT 90D is a re-analysis of DEARBORN 86.

[177] The region $m_{A^0} \gtrsim 2$ eV is also allowed.

[178] ERICSON 89 considered various nuclear corrections to axion emission in a supernova core, and found a reduction of the previous limit (MAYLE 88) by a large factor.

[179] MAYLE 89 limit based on naive quark model couplings of axion to nucleons. Limit based on couplings motivated by EMC measurements is 2–4 times weaker. The limit from axion-electron coupling is weak: see HATSUDA 88B.

[180] RAFFELT 88B derives a limit for the energy generation rate by exotic processes in helium-burning stars $\epsilon < 100$ erg g^{-1} s^{-1}, which gives a firmer basis for the axion limits based on red giant cooling.

[181] RAFFELT 87 also gives a limit $g_{A\gamma} < 1\times 10^{-10}$ GeV^{-1}.

[182] DEARBORN 86 also gives a limit $g_{A\gamma} < 1.4\times 10^{-11}$ GeV^{-1}.

[183] RAFFELT 86 gives a limit $g_{A\gamma} < 1.1\times 10^{-10}$ GeV^{-1} from red giants and $< 2.4\times 10^{-9}$ GeV^{-1} from the sun.

[184] KAPLAN 85 says $m_{A^0} < 23$ eV is allowed for a special choice of model parameters.

[185] FUKUGITA 82 gives a limit $g_{A\gamma} < 2.3\times 10^{-10}$ GeV^{-1}.

Search for Relic Invisible Axions

Limits are for $[G_{A\gamma\gamma}/m_{A^0}]^2 \rho_A$ where $G_{A\gamma\gamma}$ denotes the axion two-photon coupling, $L_{\rm int} = \frac{G_{A\gamma\gamma}}{4}\phi_A F_{\mu\nu}\widetilde{F}^{\mu\nu} = G_{A\gamma\gamma}\phi_A \mathbf{E}\cdot\mathbf{B}$, and ρ_A is the axion energy density near the earth.

VALUE	CL%	DOCUMENT ID		TECN	COMMENT
• • • We do not use the following data for averages, fits, limits, etc. • • •					
$<5.5\times 10^{-43}$	95	[186] HAGMANN	98	CNTR	$m_{A^0} = 2.9\text{–}3.3\times 10^{-6}$ eV
		[187] KIM	98	THEO	
$<2 \quad \times 10^{-41}$		[188] HAGMANN	90	CNTR	$m_{A^0} = (5.4\text{–}5.9)10^{-6}$ eV
$<1.3\times 10^{-42}$	95	[189] WUENSCH	89	CNTR	$m_{A^0} = (4.5\text{–}10.2)10^{-6}$ eV
$<2 \quad \times 10^{-41}$	95	[189] WUENSCH	89	CNTR	$m_{A^0} = (11.3\text{–}16.3)10^{-6}$ eV

[186] Based on the conversion of halo axions to microwave photons. Limit assumes ρ_A=0.45 GeV cm^{-3}. At 90%CL this result excludes a version of KSVZ axions as dark matter in the halo of our Galaxy, for the quoted axion mass range. See ASZTALOS 01 for more details.

[187] KIM 98 calculated the axion-to-photon couplings for various axion models and compared them to the HAGMANN 90 bounds. This analysis demonstrates a strong model dependence of $G_{A\gamma\gamma}$ and hence the bound from relic axion search.

[188] HAGMANN 90 experiment is based on the proposal of SIKIVIE 83.

[189] WUENSCH 89 looks for condensed axions near the earth that could be converted to photons in the presence of an intense electromagnetic field via the Primakoff effect, following the proposal of SIKIVIE 83. The theoretical prediction with $[G_{A\gamma\gamma}/m_{A^0}]^2 = 2\times 10^{-14}$ MeV^{-4} (the three generation DFSZ model) and $\rho_A = 300$ MeV/cm^3 that makes up galactic halos gives $(G_{A\gamma\gamma}/m_{A^0})^2\ \rho_A = 4\times 10^{-44}$. Note that our definition of $G_{A\gamma\gamma}$ is $(1/4\pi)$ smaller than that of WUENSCH 89.

Invisible A^0 (Axion) Limits from Photon Coupling

Limits are for the axion-two-photon coupling $G_{A\gamma\gamma}$ defined by $L = G_{A\gamma\gamma}\phi_A \mathbf{E}\cdot\mathbf{B}$.

Related limits from astrophysics can be found in the "Invisible A^0 (Axion) Mass Limits from Astrophysics and Cosmology" section.

VALUE (GeV^{-1})	CL%	DOCUMENT ID		TECN	COMMENT
• • • We do not use the following data for averages, fits, limits, etc. • • •					
$<1.1 \quad \times 10^{-9}$	95	[190] INOUE	02		$m_{A^0} = 0.05\text{–}0.27$ eV
$<2.78\times 10^{-9}$	95	[191] MORALES	02B		$m_{A^0} <1$ keV
$<1.7 \quad \times 10^{-9}$	90	[192] BERNABEI	01B		$m_{A^0} <100$ eV
$<1.5 \quad \times 10^{-4}$	90	[193] ASTIER	00B	NOMD	$m_{A^0} <40$ eV
		[194] MASSO	00	THEO	induced photon coupling
$<2.7 \quad \times 10^{-9}$	95	[195] AVIGNONE	98	SLAX	$m_{A^0} < 1$ keV
$<6.0 \quad \times 10^{-10}$	95	[196] MORIYAMA	98		$m_{A^0} < 0.03$ eV
$<3.6 \quad \times 10^{-7}$	95	[197] CAMERON	93		$m_{A^0} < 10^{-3}$ eV, optical rotation
$<6.7 \quad \times 10^{-7}$	95	[198] CAMERON	93		$m_{A^0} < 10^{-3}$ eV, photon regeneration
$<3.6 \quad \times 10^{-9}$	99.7	[199] LAZARUS	92		$m_{A^0} < 0.03$ eV
$<7.7 \quad \times 10^{-9}$	99.7	[199] LAZARUS	92		$m_{A^0} = 0.03\text{–}0.11$ eV
$<7.7 \quad \times 10^{-7}$	99	[200] RUOSO	92		$m_{A^0} < 10^{-3}$ eV
$<2.5 \quad \times 10^{-6}$		[201] SEMERTZIDIS	90		$m_{A^0} < 7\times 10^{-4}$ eV

[190] INOUE 02 looked for Primakoff conversion of solar axions in 4T superconducting magnet into X ray.

[191] MORALES 02B looked for the coherent conversion of solar axions to photons via the Primakoff effect in Germanium detector.

[192] BERNABEI 01B looked for Primakoff coherent conversion of solar axions into photons via Bragg scattering in NaI crystal in DAMA dark matter detector.

[193] ASTIER 00B looked for production of axions from the interaction of high-energy photons with the horn magnetic field and their subsequent re-conversion to photons via the interaction with the NOMAD dipole magnetic field.

[194] MASSO 00 studied limits on axion-proton coupling using the induced axion-photon coupling through the proton loop and CAMERON 93 bound on the axion-photon coupling using optical rotation. They obtained the bound $g_p^2/4\pi < 1.7 \times 10^{-9}$ for the coupling $g_p \overline{p} \gamma_5 p \phi_A$.

[195] AVIGNONE 98 result is based on the coherent conversion of solar axions to photons via the Primakoff effect in a single crystal germanium detector.

[196] Based on the conversion of solar axions to *X*-rays in a strong laboratory magnetic field.

[197] Experiment based on proposal by MAIANI 86.

[198] Experiment based on proposal by VANBIBBER 87.

[199] LAZARUS 92 experiment is based on proposal found in VANBIBBER 89.

[200] RUOSO 92 experiment is based on the proposal by VANBIBBER 87.

[201] SEMERTZIDIS 90 experiment is based on the proposal of MAIANI 86. The limit is obtained by taking the noise amplitude as the upper limit. Limits extend to $m_{A^0} = 4 \times 10^{-3}$ where $G_{A\gamma\gamma} < 1 \times 10^{-4}$ GeV^{-1}.

Limit on Invisible A^0 (Axion) Electron Coupling

The limit is for $G_{Aee} \partial_\mu \phi_A \overline{e} \gamma^\mu \gamma_5 e$ in GeV^{-1}, or equivalenty, the dipole-dipole potential $\frac{G_{Aee}^2}{4\pi}\left((\boldsymbol{\sigma}_1 \cdot \boldsymbol{\sigma}_2) - 3(\boldsymbol{\sigma}_1 \cdot \boldsymbol{n})(\boldsymbol{\sigma}_2 \cdot \boldsymbol{n})\right)/r^3$ where $\boldsymbol{n} = \boldsymbol{r}/r$.

The limits below apply to invisible axion of $m_A \leq 10^{-6}$ eV.

VALUE (GeV^{-1})	*CL%*	*DOCUMENT ID*		*TECN*	*COMMENT*
• • • We do not use the following data for averages, fits, limits, etc. • • •					
$<5.3 \times 10^{-5}$	66	[202] NI	94		Induced magnetism
$<6.7 \times 10^{-5}$	66	[202] CHUI	93		Induced magnetism
$<3.6 \times 10^{-4}$	66	[203] PAN	92		Torsion pendulum
$<2.7 \times 10^{-5}$	95	[202] BOBRAKOV	91		Induced magnetism
$<1.9 \times 10^{-3}$	66	[204] WINELAND	91	NMR	
$<8.9 \times 10^{-4}$	66	[203] RITTER	90		Torsion pendulum
$<6.6 \times 10^{-5}$	95	[202] VOROBYOV	88		Induced magnetism

[202] These experiments measured induced magnetization of a bulk material by the spin-dependent potential generated from other bulk material with aligned electron spins, where the magnetic field is shielded with superconductor.

[203] These experiments used a torsion pendulum to measure the potential between two bulk matter objects where the spins are polarized but without a net magnetic field in either of them.

[204] WINELAND 91 looked for an effect of bulk matter with aligned electron spins on atomic hyperfine splitting using nuclear magnetic resonance.

Invisible A^0 (Axion) Limits from Nucleon Coupling

Limits are for the axion mass in eV.

VALUE (eV)	*CL%*	*DOCUMENT ID*		*TECN*	*COMMENT*
• • • We do not use the following data for averages, fits, limits, etc. • • •					
$< 3.2 \times 10^4$	95	[205] KRCMAR	01	CNTR	Solar axion
<745	90	[206] KRCMAR	98	CNTR	Solar axion

[205] KRCMAR 01 looked for solar axions emitted by the M1 transition of ^{7}Li after the electron capture by ^{7}Be and the emission of 384 keV line neutrino, using their resonant capture on ^{7}Li in the laboratory. The mass bound assumes $m_u/m_d = 0.56$ and the flavor-singlet axial-vector matrix element $S = 0.4$.

[206] KRCMAR 98 looked for solar axions emitted by the M1 transition of thermally excited ^{57}Fe nuclei in the Sun, using their possible resonant capture on ^{57}Fe in the laboratory, following MORIYAMA 95B. The mass bound assumes $m_u/m_d = 0.56$ and the flavor-singlet axial-vector matrix element $S = 3F - D \simeq 0.5$.

Axion Limits from *T*-violating Medium-Range Forces

The limit is for the coupling g in a *T*-violating potential between nucleons or nucleon and electron of the form $V = \frac{g\hbar^2}{8\pi m_p}(\boldsymbol{\sigma} \cdot \hat{\boldsymbol{r}})\left(\frac{1}{r^2} + \frac{m_A c}{\hbar r}\right) e^{-m_A c r/\hbar}$

VALUE	*DOCUMENT ID*		*TECN*	*COMMENT*
• • • We do not use the following data for averages, fits, limits, etc. • • •				
	[207] NI	99		paramagnetic Tb F_3
	[208] POSPELOV	98	THEO	neutron EDM
	[209] YOUDIN	96		
	[210] RITTER	93		torsion pendulum
	[211] VENEMA	92		nuclear spin-precession frequencies
	[212] WINELAND	91	NMR	

[207] NI 99 searched for a *T*-violating medium-range force acting on paramagnetic Tb F_3 salt. See their Fig. 1 for the result.

[208] POSPELOV 98 studied the possible contribution of *T*-violating Medium-Range Force to the neutron electric dipole moment, which is possible when axion interactions violate *CP*. The size of the force among nucleons must be smaller than gravity by a factor of 2×10^{-10} $(1\,\text{cm}/\lambda_A)$, where $\lambda_A = \hbar/m_A c$.

[209] YOUDIN 96 compared the precession frequencies of atomic ^{199}Hg and Cs when a large mass is positioned near the cells, relative to an applied magnetic field. See Fig. 3 for their limits.

[210] RITTER 93 used a torsion pendulum to study the influence of bulk mass with polarized electrons on the pendulum.

[211] VENEMA 92 looked for an effect of Earth's gravity on nuclear spin-precession frequencies of ^{199}Hg and ^{201}Hg atoms.

[212] WINELAND 91 looked for an effect of bulk matter with aligned electron spins on atomic hyperfine resonances in stored ^{9}Be$^+$ ions using nuclear magnetic resonance.

REFERENCES FOR Searches for Axions (A^0) and Other Very Light Bosons

ARNABOLDI	03	PL B557 167	C. Arnaboldi *et al.*	
DANEVICH	03	PR C68 035501	F.A. Danevich *et al.*	
ADLER	02C	PL B537 211	S. Adler *et al.*	(BNL E787 Collab.)
BADERT...	02	PL B542 29	A. Badertscher *et al.*	
BERNABEI	02D	PL B546 23	R. Bernabei *et al.*	(DAMA Collab.)
DERBIN	02	PAN 65 1302	A.V. Derbin *et al.*	
		Translated from YAF 65 1335.		
FUSHIMI	02	PL B531 190	K. Fushimi *et al.*	(ELEGANT V Collab.)
INOUE	02	PL B536 18	Y. Inoue *et al.*	
MORALES	02B	ASP 16 325	A. Morales *et al.*	(COSME Collab.)
AMMAR	01B	PRL 87 271801	R. Ammar *et al.*	(CLEO Collab.)
ASHITKOV	01	JETPL 74 529	V.D. Ashitkov *et al.*	
		Translated from ZETFP 74 601.		
ASZTALOS	01	PR D64 092003	S. Asztalos *et al.*	
BERNABEI	01B	PL B515 6	R. Bernabei *et al.*	(DAMA Collab.)
DANEVICH	01	NP A694 375	F.A. Danevich *et al.*	
DEBOER	01	JPG 27 L29	F.W.N. de Boer *et al.*	
KRCMAR	01	PR D64 115016	M. Krcmar *et al.*	
ADLER	00	PRL 84 3768	S. Adler *et al.*	(BNL E787 Collab.)
ALESSAND...	00	PL B486 13	A. Alessandrello *et al.*	
ARNOLD	00	NP A678 341	R. Arnold *et al.*	
ASTIER	00B	PL B479 371	P. Astier *et al.*	(NOMAD Collab.)
DANEVICH	00	PR C62 045501	F.A. Danevich *et al.*	
MASSO	00	PR D61 011701R	E. Masso	
ARNOLD	99	NP A658 299	R. Arnold *et al.*	(NEMO Collab.)
NI	99	PRL 82 2439	W.-T. Ni *et al.*	
ALTEGOER	98	PL B428 197	J. Altegoer *et al.*	
ARNOLD	98	NP A636 209	R. Arnold *et al.*	(NEMO-2 Collab.)
AVIGNONE	98	PRL 81 5068	F.T. Avignone *et al.*	(Solar Axion Experiment)
DIAZ	98	NP B527 44	M.A. Diaz *et al.*	
FAESSLER	98B	JPG 24 2139	A. Faessler, F. Simkovic	
HAGMANN	98	PRL 80 2043	C. Hagmann *et al.*	
KIM	98	PR D58 055006	J.E. Kim	
KRCMAR	98	PL B442 38	M. Krcmar *et al.*	
LUESCHER	98	PL B434 407	R. Luescher *et al.*	
MORIYAMA	98	PL B434 147	S. Moriyama *et al.*	
MOROI	98	PL B440 69	T. Moroi, H. Murayama	
POSPELOV	98	PR D58 097703	M. Pospelov	
ZUBER	98	PRPL 305 295	K. Zuber	
AHMAD	97	PRL 78 618	I. Ahmad *et al.*	(APEX Collab.)
BORISOV	97	JETP 83 868	A.V. Borisov, V.Y. Grishinia	(MOSU)
DEBOER	97C	JPG 23 L85	F.W.N. de Boer *et al.*	
KACHELRIESS	97	PR D56 1313	M. Kachelriess, C. Wilke, G. Wunner	(BOCH)
KEIL	97	PR D56 2419	W. Keil *et al.*	
KITCHING	97	PRL 79 4079	P. Kitching *et al.*	(BNL E787 Collab.)
LEINBERGER	97	PL B394 16	U. Leinberger *et al.*	(ORANGE Collab.)
ADLER	96	PRL 76 1421	S. Adler *et al.*	(BNL E787 Collab.)
AMSLER	96B	ZPHY C70 219	C. Amsler *et al.*	(Crystal Barrel Collab.)
GANZ	96	PL B389 4	R. Ganz *et al.*	(GSI, HEID, FRAN, JAGL+)
GUENTHER	96	PR D54 3641	M. Gunther *et al.*	(MPIH, SASSO)
KAMEL	96	PL B368 291	S. Kamel	(SHAMS)
MITSUI	96	EPL 33 111	T. Mitsui *et al.*	(TOKY)
YOUDIN	96	PRL 77 2170	A.N. Youdin *et al.*	(AMHT, WASH)
ALTMANN	95	ZPHY C68 221	M. Altmann *et al.*	(MUNT, LAPP, CPPM)
BALEST	95	PR D51 2053	R. Balest *et al.*	(CLEO Collab.)
BASSOMPIE...	95	PL B355 584	G. Bassompierre *et al.*	(LAPP, LCGT, LYON)
MAENO	95	PL B351 574	T. Maeno *et al.*	(TOKY)
MORIYAMA	95B	PRL 75 3222	S. Moriyama	
RAFFELT	95	PR D51 1495	G. Raffelt, A. Weiss	(MPIM, MPIA)
SKALSEY	95	PR D51 6292	M. Skalsey, R.S. Conti	(MICH)
TSUNODA	95	EPL 30 273	T. Tsunoda *et al.*	(TOKY)
ADACHI	94	PR A49 3201	S. Adachi *et al.*	(TMU)
ALTHERR	94	ASP 2 175	T. Altherr, E. Petitgirard, T. del Rio Gaztelurrutia	
AMSLER	94B	PL B333 271	C. Amsler *et al.*	(Crystal Barrel Collab.)
ASAI	94	PL B323 90	S. Asai *et al.*	(TOKY)
MEIJERDREES	94	PR D49 4937	M.R. Drees *et al.*	(BRCO, OREG, TRIU)
NI	94	Physica B194 153	W.T. Ni *et al.*	(NTHU)
VO	94	PR C49 1551	D.T. Vo *et al.*	(ISU, LBL, LLNL, UCD)
ATIYA	93	PRL 70 2521	M.S. Atiya *et al.*	(BNL E787 Collab.)
Also	93C	PRL 71 305 (erratum)	M.S. Atiya *et al.*	(BNL E787 Collab.)
ATIYA	93B	PR D48 R1	M.S. Atiya *et al.*	(BNL E787 Collab.)
BASSOMPIE...	93	EPL 22 239	G. Bassompierre *et al.*	(LAPP, TORI, LYON)
BECK	93	PRL 70 2853	M. Beck *et al.*	(MPIH, KIAE, SASSO)
CAMERON	93	PR D47 3707	R.E. Cameron *et al.*	(ROCH, BNL, FNAL+)
CHANG	93	PL B316 51	S. Chang, K. Choi	
CHUI	93	PRL 71 3247	T.C.P. Chui, W.T. Ni	(NTHU)
MINOWA	93	PRL 71 4120	M. Minowa *et al.*	(TOKY)
NG	93	PR D48 2941	K.W. Ng	(AST)
RITTER	93	PRL 70 701	R.C. Ritter *et al.*	
TANAKA	93	PR D48 5412	J. Tanaka, H. Ejiri	(OSAK)
ALLIEGRO	92	PRL 68 278	C. Alliegro *et al.*	(BNL, FNAL, PSI+)
ATIYA	92	PRL 69 733	M.S. Atiya *et al.*	(BNL, LANL, PRIN+)
BERNATOW...	92	PRL 69 2341	T. Bernatowicz *et al.*	(WUSL, TATA)
BLUEMLEIN	92	IJMP A7 3835	J. Blumlein *et al.*	(BERL, BUDA, JINR+)
HALLIN	92	PR D45 3955	A.L. Hallin *et al.*	(PRIN)
HENDERSON	92C	PRL 69 1733	S.D. Henderson *et al.*	(YALE, BNL)
HICKS	92	PL B276 423	K.H. Hicks, D.E. Alburger	(OHIO, BNL)
LAZARUS	92	PRL 69 2333	D.M. Lazarus *et al.*	(BNL, ROCH, FNAL)
MEIJERDREES	92	PRL 68 3845	R. Meijer Drees *et al.*	(SINDRUM I Collab.)
PAN	92	MPL A7 1287	S.S. Pan, W.T. Ni, S.C. Chen	(NTHU)
RUOSO	92	ZPHY C56 505	G. Ruoso *et al.*	(ROCH, BNL, FNAL, TRST)
SKALSEY	92	PRL 68 456	M. Skalsey, J.J. Kolata	(MICH, NDAM)
VENEMA	92	PRL 68 135	B.J. Venema *et al.*	
WANG	92	MPL A7 1497	J. Wang	(ILL)
WANG	92C	PL B291 97	J. Wang	(ILL)
WU	92	PRL 69 1729	X.Y. Wu *et al.*	(BNL, YALE, CUNY)
AKOPYAN	91	PL B272 443	M.V. Akopyan *et al.*	(INRM)
ASAI	91	PRL 66 2440	S. Asai *et al.*	(ICEPP)

BERSHADY 91 PRL 66 1398 M.A. Bershady, M.T. Ressell, M.S. Turner (CHIC+)
BLUEMLEIN 91 ZPHY C51 341 J. Blumlein *et al.* (BERL, BUDA, JINR+)
BOBRAKOV 91 JETPL 53 294 V.F. Bobrakov *et al.* (PNPI)
Translated from ZETFP 53 283.
BROSS 91 PRL 67 2942 A.D. Bross *et al.* (FNAL, ILL)
KIM 91C PRL 67 3465 J.E. Kim (SEOUL)
RAFFELT 91B PRL 67 2605 G. Raffelt, D. Seckel (MPIM, BART)
RESSELL 91 PR D44 3001 M.T. Ressell (CHIC, FNAL)
TRZASKA 91 PL B269 54 W.H. Trzaska *et al.* (TAMU)
TSERTOS 91 PL B266 259 H. Tsertos *et al.* (ILLG, GSI)
WALKER 91 APJ 376 51 T.P. Walker *et al.* (HSCA, OSU, CHIC+)
WIDMANN 91 ZPHY A340 209 E. Widmann *et al.* (STUT, GSI, STUTM)
WINELAND 91 PRL 67 1735 D.J. Wineland *et al.* (NBSB)
ALBRECHT 90E PL B246 278 H. Albrecht *et al.* (ARGUS Collab.)
ANTREASYAN 90C PL B251 204 D. Antreasyan *et al.* (Crystal Ball Collab.)
ASANUMA 90 PL B237 588 T. Asanuma *et al.* (TOKY)
ATIYA 90 PRL 64 21 M.S. Atiya *et al.* (BNL E787 Collab.)
ATIYA 90B PRL 65 1188 M.S. Atiya *et al.* (BNL E787 Collab.)
BAUER 90 NIM B50 300 W. Bauer *et al.* (STUT, VILL, GSI)
BURROWS 90 PR D42 3297 A. Burrows, M.T. Ressell, M.S. Turner (ARIZ+)
DEBOER 90 JPG 16 L1 F.W.N. de Boer, J. Lehmann, J. Steyaert (LOUV)
ENGEL 90 PRL 65 960 J. Engel, D. Seckel, A.C. Hayes (BART, LANL)
GNINENKO 90 PL B237 287 S.N. Gninenko *et al.* (INRM)
GUO 90 PR D41 2924 R. Guo *et al.* (NIU, LANL, FNAL, CASE+)
HAGMANN 90 PR D42 1297 C. Hagmann *et al.* (FLOR)
JUDGE 90 PRL 65 972 S.M. Judge *et al.* (ILLG, GSI)
RAFFELT 90C PRPL 198 1 G.G. Raffelt (MPIM)
RAFFELT 90D PR D41 1324 G.G. Raffelt (MPIM)
RITTER 90 PR D42 977 R.C. Ritter *et al.* (VIRG)
SEMERTZIDIS 90 PRL 64 2988 Y.K. Semertzidis *et al.* (ROCH, BNL, FNAL+)
TSUCHIAKI 90 PL B236 81 M. Tsuchiaki *et al.* (ICEPP)
TURNER 90 PRPL 197 67 M.S. Turner (FNAL)
BARABASH 89 PL B223 273 A.S. Barabash *et al.* (ITEP, INRM)
BINI 89 PL B221 99 M. Bini *et al.* (FIRZ, CERN, AARH)
BURROWS 89 PR D39 1020 A. Burrows, M.S. Turner, R.P. Brinkmann (ARIZ+)
Also 88 PRL 60 1797 M.S. Turner (FNAL, EFI)
DEBOER 89B PRL 62 2639 F.W.N. de Boer, R. van Dantzig (ANIK)
ERICSON 89 PL B219 507 T.E.O. Ericson, J.F. Mathiot (CERN, IPN)
FAISSNER 89 ZPHY C44 557 H. Faissner *et al.* (AACH3, BERL, PSI)
FOX 89 PR C39 288 J.D. Fox *et al.* (FSU)
MAYLE 89 PL B219 515 R. Mayle *et al.* (LLL, CERN, MINN, FNAL+)
Also 88 PL B203 188 R. Mayle *et al.* (LLL, CERN, MINN, FNAL+)
MINOWA 89 PRL 62 1091 H. Minowa *et al.* (ICEPP)
ORITO 89 PRL 63 597 S. Orito *et al.* (ICEPP)
PERKINS 89 PRL 62 2638 D.H. Perkins (OXF)
TSERTOS 89 PR D40 1397 H. Tsertos *et al.* (GSI, ILLG)
VANBIBBER 89 PR D39 2089 K. van Bibber *et al.* (LLL, TAMU, LBL)
WUENSCH 89 PR D40 3153 W.U. Wuensch *et al.* (ROCH, BNL, FNAL)
Also 87 PRL 59 839 S. de Panfilis *et al.* (ROCH, BNL, FNAL)
AVIGNONE 88 PR D37 618 F.T. Avignone *et al.* (PRIN, SCUC, ORNL+)
BJORKEN 88 PR D38 3375 J.D. Bjorken *et al.* (FNAL, SLAC, VPI)
BLINOV 88 SJNP 47 563 A.E. Blinov *et al.* (NOVO)
Translated from YAF 47 889.
BOLTON 88 PR D38 2077 R.D. Bolton *et al.* (LANL, STAN, CHIC+)
Also 86 PRL 56 2461 R.D. Bolton *et al.* (LANL, STAN, CHIC+)
Also 86 PRL 57 3241 D. Grosnick *et al.* (CHIC, LANL, STAN+)
CHANDA 88 PR D37 2714 R. Chanda, J.F. Nieves, P.B. Pal (UMD, UPR+)
CHOI 88 PR D37 3225 K. Choi *et al.* (JHU)
CONNELL 88 PRL 60 2242 S.H. Connell *et al.* (WITW)
DATAR 88 PR C37 250 V.M. Datar *et al.* (IPN)
DEBOER 88 PRL 61 1274 F.W.N. de Boer, R. van Dantzig (ANIK)
Also 89 PRL 62 2644 erratum F.W.N. de Boer, R. van Dantzig (ANIK)
Also 89 PRL 62 2638 D.H. Perkins (OXF)
Also 89B PRL 62 2639 F.W.N. de Boer, R. van Dantzig (ANIK)
DEBOER 88C JPG 14 L131 F.W.N. de Boer *et al.* (LOUV)
DOEHNER 88 PR D38 2722 J. Dohner *et al.* (HEIDP, ANL, ILLG)
EL-NADI 88 PRL 61 1271 M. el Nadi, O.E. Badawy (CAIR)
ENGEL 88 PR C37 731 J. Engel, P. Vogel, M.R. Zirnbauer
FAISSNER 88 ZPHY C37 231 H. Faissner *et al.* (AACH3, BERL, SIN)
HATSUDA 88B PL B203 469 T. Hatsuda, M. Yoshimura (KEK)
LORENZ 88 PL B214 10 E. Lorenz *et al.* (MPIM, PSI)
MAYLE 88 PL B203 188 R. Mayle *et al.* (LLL, CERN, MINN, FNAL+)
PICCIOTTO 88 PR D37 1131 C.E. Picciotto *et al.* (TRIU, CNRC)
RAFFELT 88 PRL 60 1793 G. Raffelt, D. Seckel (UCB, LLL, UCSC)
RAFFELT 88B PR D37 549 G.G. Raffelt, D.S.P. Dearborn (UCB, LLL)
SAVAGE 88 PR D37 1134 M.J. Savage, B.W. Filippone, L.W. Mitchell (CIT)
TSERTOS 88 PL B207 273 A. Tsertos *et al.* (GSI, ILLG)
TSERTOS 88B ZPHY A331 103 A. Tsertos *et al.* (GSI, ILLG)
VANKLINKEN 88 PL B205 223 J. van Klinken *et al.* (GRON, GSI)
VANKLINKEN 88B PRL 60 2442 J. van Klinken (GRON)
VONWIMMER... 88 PRL 60 2443 U. von Wimmersperg (BNL)
VOROBYOV 88 PL B208 146 P.V. Vorobiev, Y.I. Gitarts (NOVO)
DRUZHININ 87 ZPHY C37 1 V.P. Druzhinin *et al.* (NOVO)
FRIEMAN 87 PR D36 2201 J.A. Frieman, S. Dimopoulos, M.S. Turner (SLAC+)
GOLDMAN 87 PR D36 1543 T. Goldman *et al.* (LANL, CHIC, STAN+)
KORENCHE... 87 SJNP 46 192 S.M. Korenchenko *et al.* (JINR)
Translated from YAF 46 313.
MAIER 87 ZPHY A326 527 K. Maier *et al.* (STUT, GSI)
MILLS 87 PR D36 707 A.P. Mills, J. Levy (BELL)
RAFFELT 87 PR D36 2211 G.G. Raffelt, D.S.P. Dearborn (LLL, UCB)
RIORDAN 87 PRL 59 755 E.M. Riordan *et al.* (ROCH, CIT+)
TURNER 87 PRL 59 2489 M.S. Turner (FNAL, EFI)
VANBIBBER 87 PRL 59 759 K. van Bibber *et al.* (LLL, CIT, MIT+)
VONWIMMER... 87 PRL 59 266 U. von Wimmersperg *et al.* (WITW)
ALBRECHT 86D PL B179 403 H. Albrecht *et al.* (ARGUS Collab.)
BADIER 86 ZPHY C31 21 J. Badier *et al.* (NA3 Collab.)
BOWCOCK 86 PRL 56 2676 T.J.V. Bowcock *et al.* (CLEO Collab.)
BROWN 86 PRL 57 2101 C.N. Brown *et al.* (FNAL, WASH, KYOT+)
BRYMAN 86B PRL 57 2787 D.A. Bryman, E.T.H. Clifford (TRIU)
DAVIER 86 PL B180 295 M. Davier, J. Jeanjean, H. Nguyen Ngoc (LALO)
DEARBORN 86 PRL 56 26 D.S.P. Dearborn, D.N. Schramm, G. Steigman (LLL+)
EICHLER 86 PL B175 101 R.A. Eichler *et al.* (SINDRUM Collab.)
HALLIN 86 PRL 57 2105 A.L. Hallin *et al.* (PRIN)
JODIDIO 86 PR D34 1967 A. Jodidio *et al.* (LBL, NWES, TRIU)
Also 88 PR D37 237 erratum A. Jodidio *et al.* (LBL, NWES, TRIU)
KETOV 86 JETPL 44 146 S.N. Ketov *et al.* (KIAE)
Translated from ZETFP 44 114.
KOCH 86 NC 96A 182 H.R. Koch, O.W.B. Schult (JULI)
KONAKA 86 PRL 57 659 A. Konaka *et al.* (KYOT, KEK)
MAGERAS 86 PRL 56 2672 G. Mageras *et al.* (MPIM, COLU, STON)
MAIANI 86 PL B175 359 L. Maiani, R. Petronzio, E. Zavattini (CERN)
PECCEI 86 PL B172 435 R.D. Peccei, T.T. Wu, T. Yanagida (DESY)
RAFFELT 86 PR D33 897 G.G. Raffelt (MPIM)
RAFFELT 86B PL 166B 402 G.G. Raffelt (MPIM)
SAVAGE 86B PRL 57 178 M.J. Savage *et al.* (CIT)
AMALDI 85 PL 153B 444 U. Amaldi *et al.* (CERN)
ANANEV 85 SJNP 41 585 V.D. Ananev *et al.* (JINR)
Translated from YAF 41 912.
BALTRUSAIT... 85 PRL 55 1842 R.M. Baltrusaitis *et al.* (Mark III Collab.)
BERGSMA 85 PL 157B 458 F. Bergsma *et al.* (CHARM Collab.)
KAPLAN 85 NP B260 215 D.B. Kaplan (HARV)
IWAMOTO 84 PRL 53 1198 N. Iwamoto (UCSB, WUSL)
YAMAZAKI 84 PRL 52 1089 T. Yamazaki *et al.* (INUS, KEK)
ABBOTT 83 PL 120B 133 L.F. Abbott, P. Sikivie (BRAN, FLOR)
ALAM 83 PR D27 1665 M.S. Alam *et al.* (VAND, CORN, ITHA, HARV+)
CARBONI 83 PL 123B 349 G. Carboni, W. Dahme (CERN, MUNI)
CAVAIGNAC 83 PL 121B 193 J.F. Cavaignac *et al.* (ISNG, LAPP)
DICUS 83 PR D28 1778 D.A. Dicus, V.L. Teplitz (TEXA, UMD)
DINE 83 PL 120B 137 M. Dine, W. Fischler (IAS, PENN)
ELLIS 83B NP B223 252 J. Ellis, K.A. Olive (CERN)
FAISSNER 83 PR D28 1198 H. Faissner *et al.* (AACH)
FAISSNER 83B PR D28 1787 H. Faissner *et al.* (AACH3)
FRANK 83B PR D28 1790 J.S. Frank *et al.* (LANL, YALE, LBL+)
HOFFMAN 83 PR D28 660 C.M. Hoffman *et al.* (LANL, ARZS)
NICZYPORUK 83 ZPHY C17 197 B. Niczyporuk *et al.* (LENA Collab.)
PRESKILL 83 PL 120B 127 J. Preskill, M.B. Wise, F. Wilczek (HARV, UCSBT)
SIKIVIE 83 PRL 51 1415 P. Sikivie (FLOR)
Also 84 PRL 52 695 erratum P. Sikivie (FLOR)
ALEKSEEV 82 JETP 55 591 E.A. Alekseeva *et al.* (KIAE)
Translated from ZETF 82 1007.
ALEKSEEV 82B JETPL 36 116 G.D. Alekseev *et al.* (MOSU, JINR)
Translated from ZETFP 36 94.
ASANO 82 PL 113B 195 Y. Asano *et al.* (KEK, TOKY, INUS, OSAK)
BARROSO 82 PL 116B 247 A. Barroso, G.C. Branco (LISB)
DATAR 82 PL 114B 63 V.M. Datar *et al.* (BHAB)
EDWARDS 82 PRL 48 903 C. Edwards *et al.* (Crystal Ball Collab.)
FETSCHER 82 JPG 8 L147 W. Fetscher (ETH)
FUKUGITA 82 PRL 48 1522 M. Fukugita, S. Watamura, M. Yoshimura (KEK)
FUKUGITA 82B PR D26 1840 M. Fukugita, S. Watamura, M. Yoshimura (KEK)
LEHMANN 82 PL 115B 270 P. Lehmann *et al.* (SACL)
RAFFELT 82 PL 119B 323 G. Raffelt, L. Stodolsky (MPIM)
SIVERTZ 82 PR D26 717 J.M. Sivertz *et al.* (CUSB Collab.)
ZEHNDER 82 PL 110B 419 A. Zehnder, K. Gabathuler, J.L. Vuilleumier (ETH+)
ASANO 81B PL 107B 159 Y. Asano *et al.* (KEK, TOKY, INUS, OSAK)
BARROSO 81 PL 106B 91 A. Barroso, N.C. Mukhopadhyay (SIN)
FAISSNER 81 ZPHY C10 95 H. Faissner *et al.* (AACH3)
FAISSNER 81B PL 103B 234 H. Faissner *et al.* (AACH3)
KIM 81 PL 105B 55 B.R. Kim, C. Stamm (AACH3)
VUILLEUMIER 81 PL 101B 341 J.L. Vuilleumier *et al.* (CIT, MUNI)
ZEHNDER 81 PL 104B 494 A. Zehnder (ETH)
FAISSNER 80 PL 96B 201 H. Faissner *et al.* (AACH3)
JACQUES 80 PR D21 1206 P.F. Jacques *et al.* (RUTG, STEV, COLU)
SOUKAS 80 PRL 44 564 A. Soukas *et al.* (BNL, HARV, ORNL, PENN)
BECHIS 79 PRL 42 1511 D.J. Bechis *et al.* (UMD, COLU, AFRR)
CALAPRICE 79 PR D20 2708 F.P. Calaprice *et al.* (PRIN)
COTEUS 79 PRL 42 1438 P. Coteus *et al.* (COLU, ILL, BNL)
DISHAW 79 PL 85B 142 J.P. Dishaw *et al.* (SLAC, CIT)
ZHITNITSKII 79 SJNP 29 517 A.R. Zhitnitsky, Y.I. Skovpen (NOVO)
Translated from YAF 29 1001.
ALIBRAN 78 PL 74B 134 P. Alibran *et al.* (Gargamelle Collab.)
ASRATYAN 78B PL 79B 497 A.E. Asratyan *et al.* (ITEP, SERP)
BELLOTTI 78 PL 76B 223 E. Bellotti, E. Fiorini, L. Zanotti (MILA)
BOSETTI 78B PL 74B 143 P.C. Bosetti *et al.* (BEBC Collab.)
DICUS 78C PR D18 1829 D.A. Dicus *et al.* (TEXA, VPI, STAN)
DONNELLY 78 PR D18 1607 T.W. Donnelly *et al.* (STAN)
Also 76 PRL 37 315 F. Reines, H.S. Gurr, H.W. Sobel (UCI)
Also 74 PRL 33 179 H.S. Gurr, F. Reines, H.W. Sobel (UCI)
HANSL 78D PL 74B 139 T. Hansl *et al.* (CDHS Collab.)
MICELMAC... 78 LNC 21 441 G.V. Mitselmakher, B. Pontecorvo (JINR)
MIKAELIAN 78 PR D18 3605 K.O. Mikaelian (FNAL, NWES)
SATO 78 PTP 60 1942 K. Sato (KYOT)
VYSOTSKII 78 JETPL 27 502 M.I. Vysotsky *et al.* (ASCI)
Translated from ZETFP 27 533.
YANG 78 PRL 41 523 T.C. Yang (MASA)
PECCEI 77 PR D16 1791 R.D. Peccei, H.R. Quinn (STAN, SLAC)
Also 77B PRL 38 1440 R.D. Peccei, H.R. Quinn (STAN, SLAC)
REINES 76 PRL 37 315 F. Reines, H.S. Gurr, H.W. Sobel (UCI)
GURR 74 PRL 33 179 H.S. Gurr, F. Reines, H.W. Sobel (UCI)
ANAND 53 PRSL A22 183 B.M. Anand

OTHER RELATED PAPERS

SREDNICKI 85 NP B260 689 M. Srednicki (UCSB)
BARDEEN 78 PL 74B 229 W.A. Bardeen, S.-H.H. Tye (FNAL)